Gasim Hayder Ahmed Salih
Rashid A. Saeed   *Editors*

Sustainability Challenges and Delivering Practical Engineering Solutions

Resources, Materials, Energy, and Buildings

IEREK
RESEARCH & KNOWLEDGE ENRICHMENT

Springer

Advances in Science, Technology & Innovation

IEREK Interdisciplinary Series for Sustainable Development

Advances in Science, Technology & Innovation (ASTI) is a series of peer-reviewed books based on important emerging research that redefines the current disciplinary boundaries in science, technology and innovation (STI) in order to develop integrated concepts for sustainable development. It not only discusses the progress made towards securing more resources, allocating smarter solutions, and rebalancing the relationship between nature and people, but also provides in-depth insights from comprehensive research that addresses the **17 sustainable development goals (SDGs)** as set out by the UN for 2030.

The series draws on the best research papers from various IEREK and other international conferences to promote the creation and development of viable solutions for a **sustainable future and a positive societal** transformation with the help of integrated and innovative science-based approaches. Including interdisciplinary contributions, it presents innovative approaches and highlights how they can best support both economic and sustainable development, through better use of data, more effective institutions, and global, local and individual action, for the welfare of all societies.

The series particularly features conceptual and empirical contributions from various interrelated fields of science, technology and innovation, with an emphasis on digital transformation, that focus on providing practical solutions to **ensure food, water and energy security to achieve the SDGs.** It also presents new case studies offering concrete examples of how to resolve sustainable urbanization and environmental issues in different regions of the world.

The series is intended for professionals in research and teaching, consultancies and industry, and government and international organizations. Published in collaboration with IEREK, the Springer ASTI series will acquaint readers with essential new studies in STI for sustainable development.

ASTI series has now been accepted for Scopus (September 2020). All content published in this series will start appearing on the Scopus site in early 2021.

Gasim Hayder Ahmed Salih •
Rashid A. Saeed

Editors

Sustainability Challenges and Delivering Practical Engineering Solutions

Resources, Materials, Energy, and Buildings

Springer

Editors
Gasim Hayder Ahmed Salih ⓘ
Department of Civil Engineering
College of Engineering
Universiti Tenaga Nasional (UNITEN)
Kajang, Selangor, Malaysia

Rashid A. Saeed ⓘ
Department of Computer Engineering
College of Computers and Information
Technology
Taif University
Taif, Saudi Arabia

About This Book

Advances in science engineering technology and sustainability issues are highlighted in this book of Sustainability Challenges and Engineering Solutions.

Recent advances in science engineering technology and sustainability issues are highlighted in this book of *Sustainability Challenges and Delivering Practical Engineering Solutions: Resources, Materials, Energy, and Buildings*. Trending research is reported in areas related to artificial intelligence, sustainability and new technologies as well as bioremediation and phytoremediation and decision-making applications and computer science from latest research findings by researchers, postgraduate students, professionals and experts from different institutions. The book aims to present about the various interrelated disciplines from the proceedings of the Science Engineering Technology and Sustainability International Conference (SETS2021) which was held virtually during December 23–25, 2021. The discussed issues are related to science, technology and innovation (STI) from various perspectives and around different parts of the world. STI is a key millstone and would play a vital role and drive to the Sustainable Development Goals (SDGs) which would be achieved by research and developing international and national STI collaborations and discussions.

Introduction

This book discusses the issues related to the United Nations' agenda for Sustainable Development Goals (SDGs) by year 2030 that has been approved in the year of 2015 and offers and adopts same vision among UN members for people prosperity and peace and for the whole planet. The 17 SDGs considered as a blueprint, initiative, partnership and strategic roadmap for global, whole nations and countries to take actions. UN recognized and intended for poverty ending, and other global deficiencies should be considered and tackled collaboratively with policies that enhance education and health, outgrowth economic and reduction of inequality. This is including tackling the global warming due to change of climate and preserving natural wealth like forests and oceans.

Science, technology and innovation (STI) are a key millstone and drive to the SDGs, where all continental and the UN nations are prepared their strategies and policies for STI. This includes the start from basic sciences, contributing basic research, developing applied research, creating inventions and finally translating all that to innovation through creativity. The aim of sciences, technology and innovations is to create a potential of culture for utilizing and optimizing the available wealth as much as we can to achieve our end goal of reaching the sustainable developments. This can be achieved by developing international and national STI roadmaps. Undeniably, that sciences, technology and innovations could play a vital role in all 17 SDGs.

This book discusses the issues related to science, technology and innovation (STI) from various perspectives and around different parts of the world. Our aim is to facilitate a platform that the researchers and academia share their experiences, ideas and works in STI. This book presents the selected peer-reviewed papers from the proceedings and the key research presentations that took place during the Science Engineering Technology and Sustainability International Conference (SETS2021), at which SETS organized its first grand conference. The work and discussions also revolved around the theme of the Sustainability Challenges and Delivering Practical Engineering Solutions for Resources, Materials, Energy and Buildings. SETS aimed to become a well-established international forum for the review and discussion of advances, research results and industrial improvements. Researchers from all over the world have met virtually at SETS2021 conference for important topics and research presentations such as fuzzy modeling and decision-making applications in computer science, trending research about bioremediation and phytoremediation. This book will be useful to postgraduate students, researchers and professionals working in the multidisciplinary area of sustainability. Given the range of topics covered and the main three research findings that covers artificial intelligence, sustainability and new technologies, this book will be of interest to the readers.

Contents

About the Editors

Dr. Gasim Hayder Ahmed Salih is a MIET and a chartered engineer (CEng) from the Engineering Council (UK), and he is a senior lecturer at the Civil Engineering Department, College of Engineering, Universiti Tenaga Nasional (UNITEN), where he has been a faculty member since 2013. He teaches, conducts research and provides short courses and consultancy services to industry, especially in the field of water and wastewater assessment and monitoring. He is the head of Water and Environmental Engineering Unit at the Department of Civil Engineering and also served as the head of Unit at the Institute of Energy Infrastructure (IEI); he is also a senior researcher for Sustainable Engineering Group UNITEN. He received his PhD in Civil Engineering from Universiti Teknologi PETRONAS (UTP), Malaysia; MSc in Environmental Engineering from Universiti Putra Malaysia (UPM), Malaysia; and BSc in Civil Engineering from Omdurman Islamic University, Sudan. He has extensive practical engineering, teaching and management experience. He has written several publications, holds patents and has received national and international awards.

Scopus: 56239664100

https://www.scopus.com/authid/detail.uri?authorId=56239664100
https://g.co/kgs/zEBu13

Prof. Dr. Rashid A. Saeed (M'02–SM'07) received his PhD in Communications and Network Engineering, Universiti Putra Malaysia (UPM). Currently, he is a professor in Computer Engineering Department, Taif University. He was also working in Electronics Department, Sudan University of Science and Technology (SUST), since 1999. He was a senior researcher in Telekom Malaysia™ Research and Development (TMRND) and MIMOS. Rashid published more than 150 research papers, books and book chapters on wireless communications and networking in peer-reviewed academic journals and conferences. His areas of research interest include computer network, cognitive computing, computer engineering, wireless broadband and WiMAX Femtocell. He is successfully awarded three US patents in these areas. He supervised more 50 MSc/PhD students. Rashid is a senior member of the IEEE, member in IEM (I.E.M), SigmaXi and SEC.

Scopus: 16022855100

https://www.scopus.com/authid/detail.uri?authorId=16022855100

Macrophytes Cultivation
for Phytoremediation of Wastewater

Hauwa Mohammed Mustafa and Gasim Hayder

Abstract

There is growing interest in phytoremediation, a plant-based wastewater treatment technique that is both environmentally benign and cost-effective. Macrophytes such as water lettuce (*Pistia stratiotes*) and duckweed (*Lemna minor*) were investigated for their efficiency in wastewater treatment for a period of ten days. The untreated and treated samples were subjected to turbidity and chemical oxygen demand (COD) tests at a detention time of 24 h. The findings from the investigations indicated up to 91.9% reduction efficiency for water lettuce-treated effluent, while duckweed-treated effluent achieved 87.2% (turbidity) and 46% (COD) reduction efficiency. Therefore, the overall findings demonstrated that the two plants can be effectively used in the remediation of domestic wastewater.

1 Introduction

In Malaysia, clean water from the environment accounts for the 97% of the country's water consumption (Gasim et al. 2009). However, illegal disposal of waste from industries and manmade activities has led to water pollution (Afroz et al. 2014). As a result, water and wastewater treatment has become essential in decreasing the menace of water pollution. Therefore, environmental pollution can be curtailed using phytoremediation techniques (Raju et al. 2010). Taking advantage of remediation capability of macrophytes (aquatic plants), excess nutrients or pollutants can be removed successfully from wastewater.

Hanafiah et al. (2018) investigated the capability of macrophytes in improving the quality of wastewater. The authors concluded that the macrophytes were capable of reducing the concentration of ammonia and total suspended solids in the wastewater. Additionally, the potentials of water hyacinth, water lettuce and giant salvinia in bioremediation of wastewater were reported by Hayder and Mustafa (2021a). The outcome demonstrated that the plants were effective in decreasing the nitrate, ammonia, turbidity and phosphorous content in the water. Mustafa and Hayder (2020) reported the potentials of macrophytes in wastewater treatment. The findings indicated that the macrophytes were efficient in polishing the wastewater. Furthermore, Mustafa and Hayder (2021b) investigated the efficiency of *S. molesta* plants in bioremediation of wastewater. The nitrate, turbidity, ammonia and phosphate tests of the treated and untreated water samples were conducted using spectrophotometric techniques. The results obtained showed that about 90.6%, 97.7%, 99% and 99% removal was observed for nitrate, turbidity, ammonia and phosphate, respectively. Therefore, this study aimed at examining the potentials of water lettuce (*Pistia stratiotes*) and duckweed (*Lemna minor*) in improving the quality of wastewater for ten days.

2 Methodology

This research was conducted in a campus wastewater treatment plant using constructed ponds of known dimensions for the cultivation of the plants. The inlet and outlet pipes were

H. M. Mustafa (✉)
College of Graduate Studies, Universiti Tenaga Nasional (UNITEN), 43000 Kajang, Selangor Darul Ehsan, Malaysia
e-mail: hauwa.mustafa@uniten.edu.my

Department of Chemistry, Kaduna State University (KASU), Tafawa Balewa Way, P.M.B. 2339, Kaduna, Nigeria

G. Hayder
Department of Civil Engineering, College of Engineering, Universiti Tenaga Nasional (UNITEN), 43000 Kajang, Selangor Darul Ehsan, Malaysia

Institute of Energy Infrastructure (IEI), Universiti Tenaga Nasional (UNITEN), 43000 Kajang, Selangor Darul Ehsan, Malaysia

connected in order to supply and control the inflow and outflow of the water samples into the ponds.

The treated and untreated water samples were collected at 48 h interval at one-day detention time for ten days. Furthermore, the analyses were conducted on the treated and untreated samples using turbidity test as well as chemical oxygen demand (COD). The results obtained are presented in the subsequent section.

3 Results

3.1 Turbidity Test

The efficiency of water lettuce and duckweed plants in bioremediation of the untreated water samples was investigated. Turbidity tests were performed on the treated and untreated water samples, and the results obtained are summarized in Fig. 1.

3.2 Chemical Oxygen Demand (COD) Test

COD test is used in estimating the degree of pollution in wastewater. The outcome of the COD tests is presented in Fig. 2.
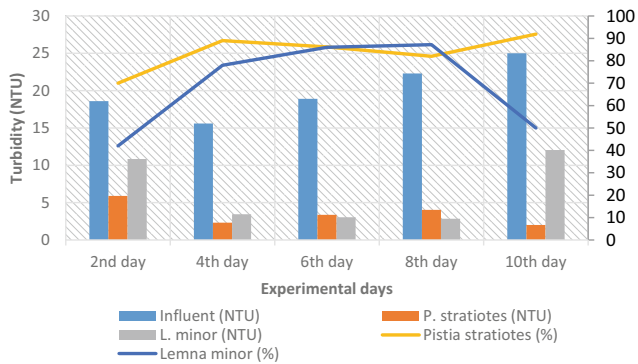
Fig. 1 Graph of turbidity against sampling days
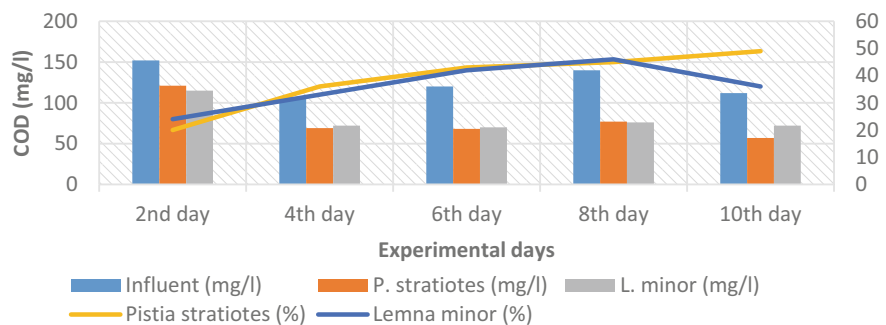
4 Discussion

According to Fig. 1, the trends of the treated water samples demonstrated a remarkable enhancement in decreasing the turbidity compared to the untreated water samples from the beginning to the end of the study. The outcome showed that the water lettuce and duckweed plants decreased the turbidity of the untreated water from 18.6 ± 0.28 NTU to 5.9 ± 1 and 10.8 ± 1.9 NTU, respectively. Furthermore, the turbidity concentration of the untreated samples was reduced from 22.3 ± 0.57 to 4 ± 0.52 (water lettuce) and 2.8 ± 0.95 NTU (duckweed). Similarly, up to 42–91% turbidity reduction was recorded from the two plants during the sampling period. Moreover, water lettuce recorded a minimum and highest removal percentage of 70% and 90%, while duckweed plants achieved the minimum and highest reduction percentage of 42% and 87%, respectively. These outcomes indicated a significant reduction in the turbidity level of the treated samples. However, duckweed plants were observed to be less effective in improving the untreated samples when compared to the water lettuce plants. These findings indicated that the two plants are capable of improving the water quality of the untreated samples to the 5 NTU standard water turbidity level. Additionally, the outcome obtained for water lettuce in this research agrees with the findings reported by Aswathy (2017).

Furthermore, Fig. 2 showed a constant rate of COD removal by the plants. The COD concentration of the treated samples decreased steadily as the sampling days increased. Additionally, a slow COD reduction of the untreated samples from 152 ± 0.5 to 121 ± 0 (water lettuce) and 115 ± 0 mg/L (duckweed) was recorded on the first day of the experiment. However, a maximum percentage reduction efficiency of 49% (water lettuce) and 46% (duckweed) was obtained. The findings indicated that the two were efficient in lowering the COD content of the untreated water samples. Similarly, the results obtained for COD analysis from this research coincide with the outcome reported by Ng and Chan (2017).

Fig. 2 Graph of COD against sampling days

5 Conclusions

The untreated water samples used in this study have passed through primary and secondary phase of domestic wastewater treatment plant. The cultivation of the plants in the untreated water was used as tertiary treatment prior to disposal into the environment. The findings demonstrated that the two plants can be used to effectively improve the quality of the untreated water samples before further use within a short time.

References

R. Afroz, M.M. Masud, R. Akhtar, J.B. Duasa, Water pollution: Challenges and future direction for water resource management policies in malaysia. Environ. Urban. Asia **5**(1), 63–81 (2014)

M. Aswathy, Wastewater treatment using constructed wetland with water lettuce (*Eichornia crasipies*). Int. J. Civ. Eng. Technol. **8**(8), 1413–1421 (2017)

M. Gasim, I. Sahid, E. Toriman, J. Pereira, M. Mokhtar, M.P. Abdullah, Integrated water resource management and pollution sources in Cameron. Am. J. Agric. Environ. Sci. **5**(6), 725–732 (2009)

M.M. Hanafiah, N.H.S. Mohamad, N.I.H. Abd. Aziz, Salvinia molesta dan pistia stratiotes sebagai agen fitoremediasi dalam rawatan air sisa kumbahan. Sains Malaysiana **47**(8), 1625–1634 (2018)

H.M. Mustafa, G. Hayder, Performance of *Pistia stratiotes*, *Salvinia molesta,* and *Eichhornia crassipes* aquatic plants in the tertiary treatment of domestic wastewater with varying retention times. Appl. Sci. **10**(9105), 1–19 (2020)

G. Hayder, H.M. Mustafa, Cultivation of aquatic plants for biofiltration of wastewater. Lett. Appl. Nanobioscience **10**(1), 1919–1924 (2021a)

H.M. Mustafa, G. Hayder, Cultivation of *S. molesta* plants for phytoremediation of secondary treated domestic wastewater. Ain Shams Eng. J. **12**(3), 2585–2592 (2021b)

Y.S. Ng, D.J.C. Chan, Phytoremediation capabilities of *Spirodela polyrhiza, Salvinia molesta* and *Lemna* sp. in synthetic wastewater: A comparative study. Int. J. Phytoremediation **20**(12), 1179–1186 (2017)

A.R. Raju, C.T. Anitha, P.D. Sidhimol, K.J. Rosna, Phytoremediation of domestic wastewater by using a free floating aquatic angiosperm, lemna minor. Nat. Environ. Pollut. Technol. **9**(1), 83–88 (2010)

Comparative Review of Global and Malaysian Green Building Rating Systems: Literature Review

Yousif Mohammed, Gasim Hayder, and Sivadass Thiruchelvam

Abstract

Environmental assessment and carbon footprint have recently become popular research topics due to their significant impact on greenhouse gas (GHG) and building life cycle (BLC), both of which have an impact on human life all over the world. Thus, the issue of developing a more sustainable society through creative methods has opened up a significant research area for officials and environmental specialists to increase building efficiency, cut carbon dioxide CO_2 emissions, and boost human welfare throughout this industrial rapid transition. The goal was to create an environmental rating system that would have a substantial impact on the industry. Comparing international rating systems such as LEED, BREEAM, and CASBEE, as well as local rating systems such as GBI and MyCREST, establishing criteria for the suggested rating system, and conducting a thorough examination. As a result, a new interface might be designed that includes the system's criteria and measurements. Then it may be put to the test and compared to other rating systems. It is expected to have a profound impact on the sustainability dimensions (economy, society, and environment). BIM is associated with tools for collaboration between modeling and extra analysis. Limitations, as well as the future route of a sustainable planet, are highlighted.

Keywords

Sustainable • Carbon footprint • Green building • BLC • BIM

Y. Mohammed (✉)
College of Graduate Studies, Universiti Tenaga Nasional (UNITEN), 43000 Kajang, Selangor Darul Ehsan, Malaysia
e-mail: yousif.suleiman@uniten.edu.my

G. Hayder · S. Thiruchelvam
Department of Civil Engineering, College of Engineering, Universiti Tenaga Nasional (UNITEN), 43000 Kajang, Selangor, Malaysia

1 Introduction

Designation of green building (GB) returns in specific to building designed to be echo efficient during its life service. This involves the whole construction process, from planning to demolition (Liu et al. 2019). This could be accomplished using sustainability indicators or rating systems, which are useful because they summarize trends and correlations in a concise manner (Khanh 2012). Their diversity among countries makes it difficult to grasp for international businesses (Yusoff and Wen 2014), complicated by the fact that few systems are well-known and set a long-term development standard (Nguyen and Altan 2011).

Buildings or the building sector are responsible for 30–40% of worldwide environmental impact (Liu et al. 2019), as well as 30% of raw material utilization, 50% of landfill wastes, around 40% of pollution detected in drinking water, generates around 23% of air pollution, consumes 40% of energy, huge part of it in the operating phase and emits a significant quantity of GHG (CIDB 2018; Khahro et al. 2021). Indeed, because of their high operational energy besides water consumption, raw material employment and land use, buildings have proved to be the largest CO_2 emitters and contribute significantly to world's climate (CIDB 2018). Thus, countries all around the globe have set long-term carbon emission reduction objectives in order to help prevent climate change. Malaysia has actually committed to reducing emissions throughout the country by up to 45% by the year 2030 as part of a worldwide initiative (Abdullah 2017).

According to United States Green Building Council (USGBC), green construction can save 30% on energy, 30–50% on water, 50–90% on construction waste, and 20–35% on GHG (CIDB 2018). As a result, technologies such as sustainability rating systems (SRS) and life cycle assessment (LCA) have been developed. LEED and BREEAM are global Sustainability assessment systems, while Malaysia's GBI and MyCREST are local, both of whch has been

initiated for assessing buildings with its environments in Malaysia. Several research regarding BIM and energy efficiency (EE) has set frame for implementing BIM to minimize energy and emissions of the related buildings (Petri et al. 2017), because of their powerful mechanism to sustainability analyses and project management along construction stage (Khahro et al. 2021; Marrero et al. 2020). It enables designers to create constructive components while also defining their qualities or parameters during the project's current life cycle stage (Marrero et al. 2020).

This research reviewed both global and Malaysian SRS and has selected three international rating systems LEED, BREEAM, and CASBEE together with two Malaysian rating systems GBI and MyCREST as samples to represent as per their data information and assessment tools.

2 Methodology

This research technique, which was conducted by employing global content analysis of materials that were published in the form of articles, procedures, or other guidelines from the SBRS (Yusoff and Wen 2014). A systematic review strategy is required to gain a deeper knowledge of the peculiarities and distinctiveness of each existing Malaysian sustainability rating tool. The review criteria chosen for examining the similarities and differences of sustainability rating tools were inspired by the BRE (2004) study (CIDB 2018). This study is review of the previous literature of the international rating systems based on their influence and the Malaysian rating systems as well. Comparative review among both is highlighted. The methodology flowchart of this study is illustrated in Fig. 1.

3 Review Criteria

3.1 Sustainability Rating System

Due to climate threats besides the current global warming, understanding of sustainability is generally acknowledged (Lu et al. 2019). Actually, resilience of people has urged awareness toward the GB as a result of various negative environmental concerns that have arisen (Yusoff and Wen 2014). Sustainable building design in the construction field is defined by terms such as green design or energy-efficient structures (Wang and Adeli 2014). While the average global temperature has risen by around 2 °F (1.1 °C), this is mostly owing to increased greenhouse gas emissions (GHGs) into the atmosphere (Azharuddin 2019). Buildings utilized 40% of energy sources and resulted in 36% energy-related carbon emissions in developed countries, according to Intergovernmental Panel on Climate Change (Fu et al. 2014). To
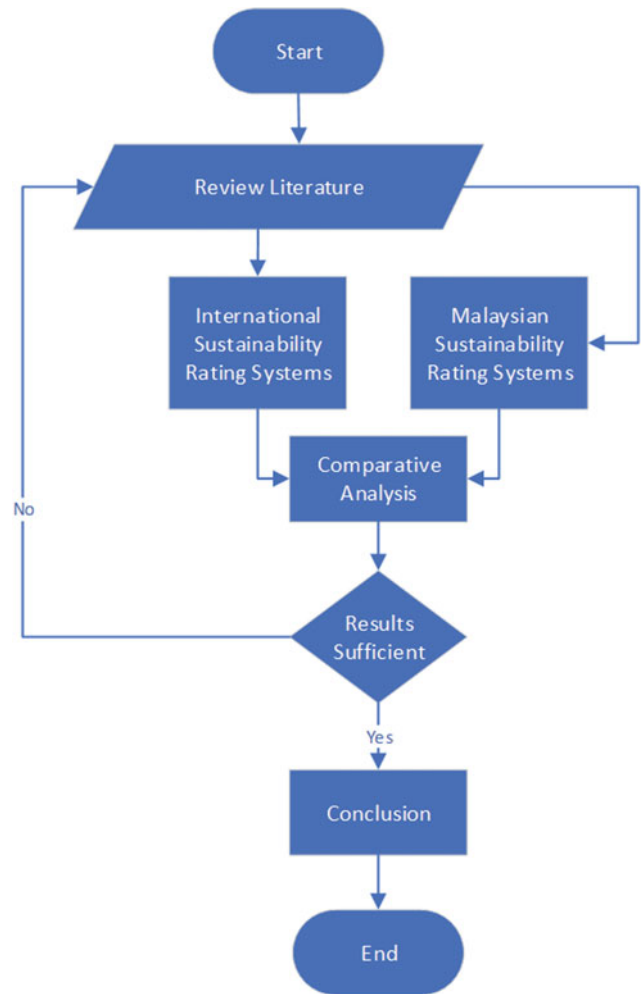
Fig. 1 Study methodology

reduce environmental impacts during the life cycle of a building and to provide people with a suitable living environment, meaningful and significant adjustments are required (Xu and Daskalova Laura Franco Garcia 2018), to assess the effects of buildings, structures, infrastructure, urban-scale efforts, and community program (CIDB 2018). Figure 2 details the building entire life from planning to demolition (B icons 2021).

Rating systems are intended generally to assist projects in becoming more sustainable by offering specific frames that contain criteria that address various aspects of the project's environmental hazards. In 1990, sustainability importance has emerged (CIDB 2018). BREEAM was launched to be the pioneer of the industry, followed by LEED in 1993 and CASBEE in 2001 (CIDB 2018; Xu and Daskalova Laura Franco Garcia 2018). Those tools were followed by numerous of similar types over the world. In fact, other systems used their fundamentals, including their difference, to construct their tools. Thus, the line between "green" and
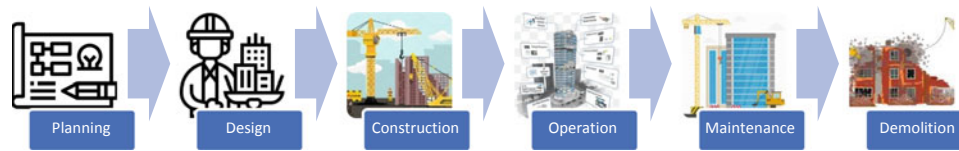
Fig. 2 Building entire life

"sustainable" has become increasingly blurred (Nguyen and Altan 2012). The rating systems listed intelligent system computing, sensor, and lifecycle cost optimization technologies as technologies that might aid in the building environment (Wang and Adeli 2014) and other greater challenges related to buildings sustainability, such as social elements, zero energy, living and regenerative building concepts (CIDB 2018).

3.2 Criteria Based

Majority of world SRS are criteria based. They're organized into categories, sub-categories, and issues. Issues are given points to determine their worth. Later scores are given to evaluate project parameters based on an assessor's satisfaction and the result is in rating levels. There are differences in their allocation points and methods of result presentation, but they share common criteria concept such as site planning and management, energy efficiency (EE), indoor environmental quality (IEQ), materials and resources, and water efficiency (WE), innovation, quality of services, health and comfort, transport, waste, land use and ecology and emissions (Khanh 2012; Yusoff and Wen 2014; CIDB 2018; Nguyen and Altan 2012; Yim et al. 2018).

3.3 Carbon Emission Calculation

Regardless of the reality that many sustainability systems have taken steps to minimize CO_2 from construction activities, there is still a limited amount of comprehensive research and analysis of buildings' (GHG), particularly in densely populated areas (Roh et al. 2018). LCA is a method to assess environmental loads (Lu et al. 2019), of CO_2 and other impacts during a building's entire life span (Roh et al. 2018), when calculating and measuring GHG emissions from buildings, they are frequently defined as building's life cycle (Kaspersen et al. 2016). Although a building can be built to promote sustainability, quantitative evaluation of its performance is required (Wang and Adeli 2014), therefore, carbon dioxide is the predominant greenhouse gas (GHG) produced from a number of different sources including transportation, on-campus stationary sources, purchased energy, refrigerants, and solid waste among

others, that should be quantified (Abdul-Azeez 2018). Estimated CO_2 between 2000 and 2010 increased by 1.0 giga ton annually, compared to 0.4 giga ton per year from 1970 to 2000, and overall anthropogenic GHG peaked at 49.0 giga ton in 2010 (Roh et al. 2018), thus, buildings' sustainability initiators at national and international levels, where they high concern to buildings' impact (Solís-Guzmán et al. 2018). They confirmed that increasing in green construction growth might result in a 35% lowering in carbon emissions (Klufallah et al. 2014). Carbon computation techniques are enhanced by the existing rating systems, such as the current international edition of BREEAM, which rewards points for calculating and lowering embodied CO_2 (Abdullah 2017). While the USGBC recently released an alternative compliance strategy that allows LEED credit measures to include CO_2 metrics (Drew and Quintanilla 2017). MyCREST has introduced carbon emission calculation for the Malaysian rating systems (CIDB 2018).

3.4 Global Environmental Rating System

Disparity in approaches among existing SRS systems like BREEAM (UK), LEED (USA), GBTool (International), and CASBEE (Japan) has perplexed developers and business owners (Nguyen and Altan 2012). That has enforced other countries developing their own system benefiting from the experience of leading tools. A basic introduction of SRS examples can be found in the paragraph below.

Introducing BREEAM, which was founded by the BBRE in 1990, is the pioneer of the SRS (Liu et al. 2019). BREEAM objectives were reducing energy emissions while assuring building safety and comfort (Xu and Daskalova Laura Franco Garcia 2018). Rating levels are Excellent for (70–100)% score, Very Good for (55–69)% score, Good for (40–54)% score, and Pass for (25–39)% score. Management, health, energy, materials, and land were considered at the design and construction phase, while transportation, water, waste and pollutions at the operation. These are the primary assessment criteria that can be evaluated over the course of a building's lifespan (Khanh 2012).

LEED was deployed by USGBC in 1994, and then LEED V1 was launched in 2000. It is highly influencing building assessment over the world, where million plus eight hundred and fifty square feet is the estimated assessed area for a day

(Liu et al. 2019; Xu and Daskalova Laura Franco Garcia 2018; Mohamed 2019). The LEED methodology works for all sorts of buildings, from existing structures to those still in the design and planning stages. Energy efficiency, environmental development, and water conservation have all received recent attention (Liu et al. 2019). Sustainable buildings can save within 24–50% on energy, 30% on CO_2 emissions, 40% on water, and 70% on solid waste, to the USGBC evaluation (Wang and Adeli 2014). LEED rating levels for buildings range within Platinum for (80–100) points score, Gold for (60–79) points score, Silver for (50–59) points score, and certified for (40–49) points score while its assessment criteria range within sustainable sites, water efficiency, energy, and others (Khanh 2012).

CASBEE the official SRS of Japan (Abdullah 2017) was launched by Japan Sustainable Building Consortium (JSBC) (Wang and Adeli 2014). It is designed to assess building with its environment (Wallhagen 2010). In 2003, 2004, and 2005, it was enhanced to include additional capabilities for newly constructed buildings, existing buildings, and renovation projects, respectively (Liu et al. 2019). CASBEE rating levels are; S for score (BEE = 3 − 5), A for score (BEE = 1.5 − 3), B+ for score (BEE = 1 − 1.5), B for score (BEE = 0.5 − 1), and C for score (BEE = 0 − 0.5). Its major assessment criteria range within IEQ, quality of services, site, energy, resources and materials and off-site environment (Khanh 2012).

3.5 Malaysian Environmental Rating System

GB assessment tools began at 2009, when GBI was launched through PAM which is the abbreviation of Pertubuhan Arkitek Malaysia and translated to Malaysian Institute of Architects, together with ACEM that is briefed to Association of Consulting Engineers Malaysia. They were inspired by the sustainability assessment systems that were emerging at that period (Abdullah 2017). Then, other institutions were motivated to build up numerous systems such as GreenRE that was driven to the industry by REHDA, Melaka Green Seal which was deployed by the authority of Melaka. They were intended to assess buildings as well as township. GreenPASS, PHJKR, MyCREST, and CASBEE Iskandar were among the additional systems implemented for the same goal, whereas MyGHI was focused on infrastructure (Kamal et al. 2019). The advantages of having a shared base with LEED and BREEAM could help with the transition to a globally recognized rating system (CIDB 2018). From 2006 through 2010, the whole national energy demand is expected to expand at a rate of 6.3% per year, according to the Ninth Malaysia Plan (Klufallah et al. 2014), that has driven the officials encouraging sustainability projects.

The fact that PAM and ACEM have launched GBI for an environmental evaluation related to structures (Yim et al. 2018; GBI 2009), in addition to developing both structures and towns in order to enhance construction environmental sustainability. Furthermore, it was intended to enhance environmental awareness among construction stakeholders, to ensure a brighter and greener future (Tools 2016). It is influenced by LEED in its assessment approaches. GBI rating levels range within Platinum for (86 +) points score, Gold for (76–85) points score, Silver for (66–75) points score, and Bronze for (50–65) points score. Furthermore, the GBI's key building assessment criteria are energy, indoor, sustainable site, materials and resources and water, while climate, energy and water, ecology, community, transportation and connectivity, building and business are the criteria for a sustainable township (BSI).

In order to promote and manage building project echo systems, CIDB built MyCREST (Kamal et al. 2019), to assist in guiding, quantifying, and thereby eliminating building impact, while considering the performance of the building along its life span (MyCREST 2016). MyCREST rating levels range within 5 Stars for (80–100)% score, 4 Stars for (70–79)% score, 3 Stars for (60–69)% score, 2 Stars for (50–59)% score, and 1 Star for (40–49)% score (CIDB 2018). Pre-design, infrastructure, energy, occupant, embodied carbon, water, social and cultural, demolition and disposal and carbon initiatives are some of the major criteria (CIDB 2018; Tools 2016).

3.6 Comparative Analysis

Throughout existing buildings to those currently under planning and design, based on the examined literature. It was discovered that LEED standards are now frequently used to assess the sustainability of new construction and substantial renovations (Liu et al. 2019). It is used mostly in North America, Brazil, and India (Wang and Adeli 2014), while BREEAM has affected Europe and part of Asia. CASBEE started with building quality and environmental impact evaluation and upgraded to include new buildings and renovation project (Liu et al. 2019; Wallhagen 2010). Both BREEAM and LEED have continued to increase building LCA standards by modifying green building criteria, making LCA a fundamental component rather than an optional item (Roh et al. 2018). The three rating systems reflect the differences in their result presentation, rating levels, and in counter the similarity approach for their targeting assessment. LEED has allocated high scores toward site planning and management, while BREEAM and CASBEE concentrated on EE, as well as they have minimal or even neglected Innovation (Fig. 3).

Fig. 3 International and Malaysian rating scores by categories
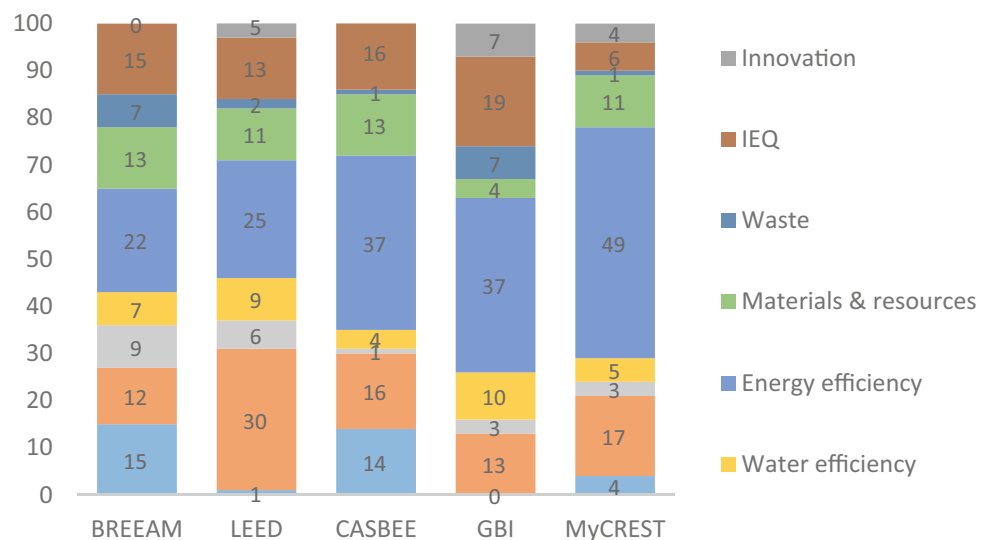
Concerning the local assessment system inside Malaysia, various similarities and differences could be remarked, their general trends can be identified as well. Among the existing rating tools for instance GBI that was launched to assess the buildings together with township. We can see that GreenRE uses the same approach while MyGHI is specialized in addressing highway. PHJKR involves health care while Melaka Green Seal for residential buildings. Also surveying the GB industry, we can realize that other system like Green Pass, CASBEE Iskandar, and LCCF are other progressing assessment tools. MyCREST is last deployed among all systems (CIDB 2018; Kamal et al. 2019). They are criteria checklist base except MyCREST that introduces carbon calculation and criteria checklist. According to a review of the local systems applications, PHJKR, Green Pass, and MyCREST are involved in construction, while SUSDUX and LCCF are used to assess townships. MyGHI is the only tool specialized to infrastructure assessment (CIDB 2018). Both GBI and MyCREST has allocated high score for EE (Fig. 3). GBI is more detailed than MyCREST for target assessment area.

4 Discussion

There is currently minimal public discussion about the requirements for a satisfactory rating system. However, it is widely acknowledged that the success of a voluntary plan is largely determined by how well it is received by profit-seeking building stakeholders (CIDB 2018). Using the LCA approach as part of a bigger plan to urge the building industry to reduce carbon emissions is crucial (Roh et al. 2018). Incorporating BIM-LCA, designers and engineers may get quick and accurate findings concerning a building's environmental performance (Lu et al. 2019). The trend for

energy efficiency is increasing since the initiation of the environmental rating tools by BREEAM to the most recent one MyCREST, demonstrating the need for constant development and system updates to keep up with industry changes. The local rating tools are more competent to assess their environment, but they should be connected to the global to act as integrated system.

5 Conclusions

Observation through the study will end to regularly update the local systems learning from the global ones, to be valid to the industry revolution and maintain the world climate. The regional systems are developed to assess their local parameters, but they should be integrated into the global ones, for maximizing benefits and further research purposes. BIM-LCA should be enforced to have precise quantification and hence enhance building life cycle and reduce carbon footprint. Malaysian rating system could exchange their experience as well as strengthen their scaling to global rating systems, through comprehensive research projects.

References

F. Abdullah, Potentials and challenges of MyCREST: a Malaysian initiative to assess carbon emissions from buildings (2017)

I.A. Abdul-Azeez, Development of carbon dioxide emission assessment tool towards pro-moting sustainability in UTM Malaysia. Open Journal of Energy Efficiency **7**, 53–73 (2018). https://doi.org/10.4236/ojee.2018.72004

M. Azharuddin, Integrated carbon emission management for the United Arab Emirates Construction Industry (2019)

B icons, Construction building icons—Bing images, https://www.bing.com/images/search?q=construction+building+icons&form=HDRSC3&first=1&tsc=ImageBasicHover. Accessed 21 Dec 2021

CIDB, Built-it-green-CIDB [Construction Industry Development Board] (2018)

N. Diyana Nizarudin, I. Tukiman, M. Ramzi Mohd, The application of the green building index (GBI) on sustainable site planning and management for residential new construction: prospects and future benefits architecture for autism view project ICoFA 2017 view project the application of the green building index (GBI) on sustainable site planning and management for residential new construction: prospects and future benefits (2010). [Online] Available: https://www.researchgate.net/publication/280730724

C. Drew, N. Quintanilla, The path to life cycle carbon neutrality in high rise buildings (2017)

F. Fu et al., Development of a carbon emission calculations system for optimizing building plan based on the LCA framework (2014)

GBI, GBI ASSESSmENT cRITERIA (2009). [Online] Available: www.greenbuildingindex.org (info@greenbuildingindex.org)

M.F.M. Kamal et al., Malaysian carbon reduction and environmental sustainability tool (MyCREST) qualified professional training assessment. Journal of Technical Education and Training 11(4), 45–55 (2019). https://doi.org/10.30880/jtet.2019.11.04.006

B. Kaspersen, J. Lohne, R.A. Bohne, Exploring the CO_2-impact for building height; a study on technical building installations (2016)

S.H. Khahro, D. Kumar, F.H. Siddiqui, T.H. Ali, M.S. Raza, A.R. Khoso, Optimizing energy use, cost and carbon emission through building information modelling and a sustainability approach: A case-study of a hospital building. Sustainability (Switzerland) 13(7) (2021). https://doi.org/10.3390/su13073675

B.N. Khanh, Developing a framework for assessing sustainability of tall-building projects volume I (2012)

M.M.A. Klufallah, M. Fadhil Nuruddin, M.F. Khamidi, N. Jamaludin, Assessment of carbon emission reduction for buildings projects in Malaysia—a comparative analysis (2014). https://doi.org/10.1051/e3sconf/20140301016

T.Y. Liu, P.H. Chen, N.N.S. Chou, Comparison of assessment systems for green building and green civil infrastructure. Sustainability 11(7), 2117 (2019). https://doi.org/10.3390/su11072117

K. Lu et al., Development of a carbon emissions analysis framework using building information modeling and life cycle assessment for the construction of hospital projects. Sustainability (Switzerland) 11(22) (2019). https://doi.org/10.3390/su11226274

M. Marrero, M. Wojtasiewicz, A. Martínez-Rocamora, J. Solís-Guzmán, M.D. Alba-Rodríguez, BIM-LCA integration for the environmental impact assessment of the urbanization process. Sustainability (Switzerland) 12(10). MDPI (2020). https://doi.org/10.3390/su12104196

M. Mohamed, Green building rating systems as sustainability assessment tools: case study analysis (2019), [Online] Available: www.intechopen.com

MyCREST, Malaysian carbon reduction & environmental sustainability tool—version 1.0 (2016)

B.K. Nguyen, H. Altan, Comparative review of five sustainable rating systems. Procedia Engineering 21, 376–386 (2011). https://doi.org/10.1016/j.proeng.2011.11.2029

B.K. Nguyen, H. Altan, Tall-building projects sustainability indicator (TPSI): a new design and environmental assessment tool for tall buildings. Buildings 2(2), 43–62 (2012). https://doi.org/10.3390/buildings2020043

I. Petri et al., Optimizing energy efficiency in operating built environment assets through building information modeling a case study (2017)

S. Roh, S. Tae, R. Kim, Developing a green building index (GBI) certification system to effectively reduce carbon emissions in South Korea's building industry. Sustainability (Switzerland) 10(6) (2018). https://doi.org/10.3390/su10061872

J. Solís-Guzmán, C. Rivero-Camacho, D. Alba-Rodríguez, A. Martínez-Rocamora, Carbon footprint estimation tool for residential buildings for non-specialized users: OERCO2 project. Sustainability (Switzerland) 10(5) (2018). https://doi.org/10.3390/su10051359

G. Tools, Includes information on GBI (2016) [Online] Available: www.greenbuildingindex.org

M. Wallhagen, Environmental assessment of buildings and the influence on architectural design (2010)

N. Wang, H. Adeli, Sustainable building design. Journal of Civil Engineering and Management 20(1), 1–10 (2014). https://doi.org/10.3846/13923730.2013.871330

J. Xu, V. Daskalova Laura Franco Garcia, Master thesis proposal research on the resident perception rating for green building through ESGB in China (2018)

S.Y.C. Yim, S.T. Ng, M.U. Hossain, J.M.W. Wong, Comprehensive evaluation of carbon emissions for the development of high-rise residential building. Buildings 8(11) (2018). https://doi.org/10.3390/buildings8110147

W.Z.W. Yusoff, W.R. Wen, Analysis of the international sustainable building rating systems (SBRSs) for sustainable development with special focused on green building index (GBI) Malaysia. Journal of Environmental Conservation Research 2(1), 11 (2014). https://doi.org/10.12966/jecr.02.02.2014

Artificial Intelligence Techniques for Predicting Water Quality Parameters and Management in a Complex River System: A Review

Hadi Aljumaily, Gasim Hayder, Salman Yussof, and Rouwaida Hussein Ali

Abstract

Evaluation of the water quality in the rivers is necessary to enhance the health of humans and ecosystems, but it quite difficult and requires more time and effort due to many parameters affected. Although, the Ringlet River considered the more important rivers in the Cameron Highland, probably it is the most badly affected river with records of incidences where permissible levels of certain parameters such as suspended solids, agrochemicals, and sewage have been contravened and drinking water. Recently, the tourism, agriculture, and industry in that region dramatically increased. This parameter leads to increase the pollution rate in the water of the four rivers that flow into the lake, which changes the quality of the water to the worse level. The nature of the muddy area is a parameter that allows soil erosion on the banks of the rivers especially at the time of floods. Due to these parameters, the dam loses the goal of hydroelectric construction benefit, in addition to protect catchment areas from floods, recently this dam become less useful due to the accumulated amount of mud increasing steadily, therefore, the annual removing mud sediments from the Ringlet reservoir is difficult and expensive. The aim of the study is to find logical, feasible, and economic solutions to mitigate the damage and treat it in the future. The study is concerned to estimate, evaluate, predict, and solve the problems of the Ringlet River and Ringlet reservoir which are located in the north of Malaysia. Numerous intelligent models have been developed to accurately predict and evaluate the quality of the surface water by using conventional methods that may be ineffective, inaccurate, and relatively slow in predicting results. Therefore, the use of artificial intelligence (AI) technology was resorted to predict water quality and sediment volume in the Ringlet Basin to assess its applicability of water quality. ANN method is selected as a statistical method applied to develop an interpretability model for decision-maker. A methodology has been scheduled to include the Ringlet river and Ringlet catchment reservoir. There are many parameters affected the pollution of the Ringlet reservoir such as urban activities, seasonal effects (flood and climate), animal's wastes, agricultural residues, and `soil properties that may cause the erosion of the specified area.

Keywords

ANN approaches • Ringlet river and Ringlet reservoir • Parameters • Water quality • Sedimentation

H. Aljumaily (✉)
College of Graduate Studies, Universiti Tenaga Nasional (UNITEN), 43000 Kajang, Selangor Darul Ehsan, Malaysia
e-mail: hadi.aljumaily@uomustansiriyah.edu.iq

Department of Civil Engineering, College of Engineering, University of Mustansiriyah, Baghdad, Iraq

G. Hayder
Department of Civil Engineering, College of Engineering, Universiti Tenaga Nasional (UNITEN), 43000 Kajang, Selangor Darul Ehsan, Malaysia

S. Yussof
Institute of Informatics and Computing in Energy, Universiti Tenaga Nasional (UNITEN), 43000 Kajang, Selangor Darul Ehsan, Malaysia

R. H. Ali
Department of Civil Engineering, University of Bilad AL-Rafidain, Baghdad, Iraq

1 Introduction

The evaluation of river water quality is vital to improve the health of humans and ecosystems, but it is complicated and time-consuming owing to the many variables involved. Despite the fact that the Ringlet reservoir is one of the more significant reservoirs in the Cameron Highlands, it is also the river with the most accidents, with records of violations of allowable levels of suspended particles, agrochemicals,

sewage, and drinking water. The project's goal is to develop rational, viable, and cost-effective methods to prevent harm and cure it in the future. The study focused on estimating, evaluating, predicting, and alleviating difficulties at the Ringlet reservoir in Malaysia's north. Numerous research have produced models for reliably and intelligently forecasting and assessing water quality, rather than relying on inefficient, incorrect, and slow-to-predict approaches. To examine the applicability of water quality, artificial intelligence (AI) technology was used to estimate water quality and sediment volume in the Ringlet Basin. The ANN approach was chosen as a statistical tool for developing a decision-maker interpretability model. The Ringlet catchment reservoir will be included in a methodology. A collection of criteria selected to meet the requirements of the specified place. Several factors that affect water quality of the rivers such as river's mineral system, soil formation and erodibility, pesticides and fertilizers of cultivation operations, municipal wastewater discharge, waste of landfill regions, and variation of time of year are important to be considered. According to the data acquired using artificial intelligence algorithms, these factors are among the contamination sources that might damage water bodies.

Water quality is one of the most important properties of a river system, and it can be predicted. It is a crucial aspect of water resource management (Sönmez et al. 2018). Every city's drinking water is distributed to the public following a treatment procedure by the local water corporation (Dalle et al. 2020). As a result, drinking water treatment plants (DWTPs) must be efficiently managed to produce safe water at all times, regardless of influent water quality fluctuations (Godo-Pla et al. 2021). The phrase "water quality" refers to the state of water, as well as its chemical, physical, and biological properties (Najah et al. 2013). It is thought to be a significant concern in terms of ecosystem health (Orouji et al. 2013), as well as human life (Dalle et al. 2020). It is also critical to assess river pollution levels and establish environmental indices in river systems. Because of the nonlinear behavior of numerous water quality factors, estimating the water quality of a river at each position is a difficult task (Sarkar and Pandey 2015). Physical, chemical, and biological characteristics, for example, are all interconnected (Mohamed Khalil et al. 2012). Indeed, a greater knowledge of the interrelationships between these factors and the Water Quality Index (WQI) can help anticipate the WQI and hence enhance water resource management (Faridah Othman et al. 2020). Because numerous variables impact water quality, evaluating the water quality in rivers is complicated and time-consuming. As a result, traditional data processing technologies are incapable of addressing this problem (Sönmez et al. 2018). The value of good water quality for human use and consumption cannot be emphasized, and its quality is determined through effective water

quality index monitoring (Hayder et al. 2020). A massive amount of water quality data must be collected, analyzed, and managed. Manual field sampling is still used to collect water quality data, although real-time sensor monitoring is becoming increasingly popular for more efficient data collection (Park et al. 2020). Water quality control management in water resources is critical for delivering clean and safe drinking water to the public (Park et al. 2020). Numerous water quality models have been created to forecast and evaluate water quality precisely and intelligently in order to govern the water quality environment more effectively and intelligently (Chen et al. 2019). To improve the health of individuals and ecosystems, it is vital to evaluate water characteristics in general and water quality in particular. Data-driven models are computational approaches for obtaining various system states without the need of complicated linkages. Prediction and simulation are two types of data-driven modeling that fill in gaps in time series using prior and previous-current data sets (Orouji et al. 2013).

The cornerstone of water environmental planning, assessment, and management is water quality prediction (Huang 2018). Because of the various hydrological and environmental factors that impact river water quality, predicting it efficiently and accurately is a tough task (Noori et al. 2020). A highly nonlinear dynamical system governs river flows. Furthermore, because monthly flows are a random variable, they cannot be predicted precisely in advance. In such instances, reservoir operation is compelled to be carried out at great risk. The correct determination of the operating regulations of water resources, especially during drought periods, will ensure a minimum risk. This may be handled by using state-of-the-art approaches to anticipate monthly river flows as accurately as feasible (Baydaroğlu et al. 2018). Although In the treatment and monitoring of water quality indicators, many methodologies have been used (WQP) (Hayder et al. 2020). Water quality criteria play a vital part in assessing water quality; however, when the worst ranking parameters are compensated by higher ranking characteristics in the overall evaluation process, the findings might be concealed. Adopting appropriate aggregating strategies (Singh et al. 2014) can help to avoid this.

In the examination of any aquatic system, modeling water quality characteristics is critical. Surface water quality prediction is necessary for good river basin management, so that appropriate measures may be performed to keep pollutants below acceptable levels. The lifeblood of effective water resource management is accurate forecasting of future events (Najah et al. 2013). It is crucial for good water resource management (Wang et al. 2020). As a result, dealing with water resource challenges necessitates an awareness of public opinion. In order to manage water resources sustainably, it is critical to establish a communication collaboration between community and government. An opinion poll

is an important step in getting feedback from the local community. However, it invariably results in a vast and complicated dataset that is difficult for decision-makers to analyze. Statistical approaches are used to construct an interpretability model for this problem. An opinion poll is an important step in gathering feedback from the local community. However, it always produces a vast and complicated dataset that is difficult for decision-makers to analyze. Statistical approaches are used to build an interpretability model for decision makers in order to solve this challenge (Tan and Mokhtar 2010). The functioning and resilience of ecosystems, the health of civilizations, and the strength and growth of economies are all influenced by how effectively water is handled (Loucks and Beek 2017).

1.1 Sedimentation

Different sources of contamination such as sediments of rainfall runoff and farming processes (Fig. 1) release different pollutants that could seriously impact natural rivers (Mateo Sagasta et al. 2017). Plenty of models that deal with one-source of pollution were developed to simulate the fate of the contaminants (Adu and Kumarasamy 2020). However, the most effective pollutants are those released from agricultural waste such as pesticides and fertilizers which are used by the farmers to improve the production of the crops.

The water quality will be damaged over a lengthy period of time. As a result, the government should actively lead and strongly encourage green agricultural growth, as well as manage it from the start. From the standpoint of the firm, many heavy industrial companies in the industrial park dump untreated wastewater straight into the adjacent lake entry region, causing the nutrients in the rivers and lakes to grow to a high degree, and hence boosting the breakout of cyanobacteria. As a result, more environmental regulation and punishment of these types of businesses are required. At the same time, it is feasible to improve pollution levels by
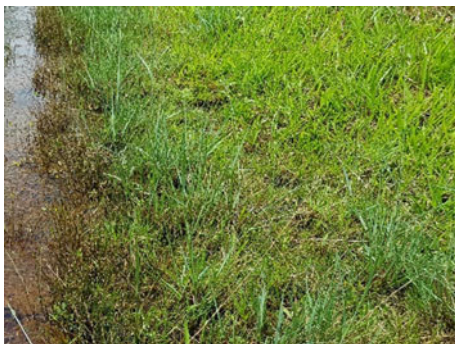
Fig. 1 Water pollution from agriculture

growing water plants and utilizing plants' capacity to filter water bodies (Yang 2019).

Agricultural and industrial growth and the population expansion are resulted in releasing variety of hazardous pollutants into the air, water, and soil of the environment. Some examples of these pollutants are pesticides, copper, lead, gasoline, benzene, phosphorus, and so on. These pollutants have been linked to cancer, cardiovascular illness, gastrointestinal disease, renal disease, liver disease, and neurological disorders. In the case of runoff or floods following precipitation, a considerable portion of these toxins eventually collect in bodies of water such as lakes, rivers, and streams. Outflows from sewage treatment plants, which cause eutrophication, are another source of pollution in these bodies of water (Sibtain et al. 2021).

The more accurate models in simulating water quality the better results to avoid contamination of water system in advance could be obtained (Astuti et al. 2020).

Suspended sediment is one of the most significant characteristics on the contamination of water bodies. Through the suspension movement in the flow, it may transport various contaminants with varying concentrations. As a result, it is critical to monitor or estimate these loads in order to implement an effective sediment reduction plan. The monitoring procedure, on the other hand, is arduous and time-consuming. As a result, modeling is proposed as an alternate strategy (Al-Mukhtar and Al-Yaseen 2019).

Great progress has been made in understanding the process of sediment movement in natural streams during the last several decades. Estimation of sediment transport in rivers and lakes has been extensively studied. The significance of this issue stemmed from its enormous impact on water structures in rivers and lakes such as water treatment and power plant intakes as well as its impact on the system and management of the rivers and lakes. This topic has recently gained popularity due to its environmental implications. Sediments at the bottom of the rivers and lakes can be contaminated with numerous pollutants due to disposing of agricultural and industrial wastes into the water bodies. As a result, as a river's stage changes, the deposits of the pollutants probably transferred to the downstream of the river. The accumulated quantity of the polluted materials is first estimated to predict and recover the quality of the water. Numerous methods for estimating sediment discharge have been proposed. Aggregate quantity of deposits flows to the river can be determined by using several traditional ways. The accumulated deposits to the river may be calculated by summing the functions of the settled and unsettled particles by using the traditional approaches (indirect approaches) which are differ in their functioning modes. On the other hand, a clear differentiation among the modes is difficult to make. The use of those ideas is hypothetically somewhat thorough, yet it may appear time-consuming. Other

approaches, known as direct approaches, compute the overall deposit capacity without distinguishing between the two routes of conveyance (Nagy et al. 2002).

1.2 Ringlet River

Rivers play an important role in meeting freshwater (Parmar et al. 2019), agricultural, and industrial water demands (Hussein et al. 2013). Ringlet River and Ringlet reservoir were used as case study rivers in this study. Figure 2 depicts the Ringlet River as a complicated adaptive system (O'Keefe and Walker 2019).

Ringlet reservoir in Cameron Highlands was developed with a total storage capacity of about 7,000,000 m^3 and an expected life period of eight decades. On the other hand, after using the reservoir for about four decades, the capacity of the reservoir could be reduced to more than 50% (Gasim et al. 2009).

The Ringlet Falls/Sultan Abu Bakar Dam, which rises 40 m tall and is made out of concrete buttresses with four (4) gated spillways, was the scheme's principal feature. The reservoir has a surface area of 60 ha and an elevation of 1070.7 m at full supply level. Water flows into the reservoir from the rivers Sg. Habu, Sg. Bertam, Sg. Ringlet, and other minor tributaries. Ringlet Reservoir was intended for 6,300,000 m^3 of total capacity. Part of the total capacity (4,700,000 m^3) is an active part and 1,600,000 m^3 is dead part. The inactive store was planned to have an usable lifespan of around 80 years, corresponding to 20,000m^3/year of sediment influx (Jaafar et al. 2010).

Different mountain summits which have a minimum height of 1524 m and a maximum height of 2032 m constitute the Cameron Highland drainage region with a total catchment areas of 180 km^2. The total catchment area is divided into Telom region with an area of 110 km^2, and Bertam region with an area of 70 km^2. The Cameron Highlands scheme can be divided into two parts: the upper catchments and the lower catchments (Luis et al. 2012).
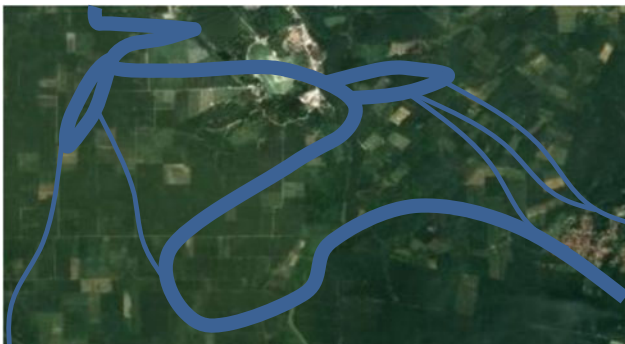
Fig. 2 Illustration of complex adaptive system

1.3 Optimized Intelligence Model Development

Water quality is now determined by laboratory tests, which involve expensive chemicals, expert labor, and time. As a result, finding an alternate way becomes important. Machine learning algorithms have recently been effectively utilized in the observing, approximation, and prediction of WQI of the river to give an alternative to laboratory analytical methods' restrictions (Hayder et al. 2020).

There is a lot of room for innovation in the field of river water quality modeling, and these obstacles will keep people coming up with new ideas (Tiyasha et al. 2020). Artificial intelligence AI models were used to data collected from rivers' continuous water quality monitoring stations, and their application to water quality forecasting was evaluated (Yeon et al. 2008). In the issue area, the integration creates a more intelligent and user-friendly system, potentially closing the gap between numerical modelers and application users. The prototype system illustrates its component reusability as well as its ability to facilitate knowledge acquisition and search (Chau 2007). It is critical to emphasize the importance and utility of multivariate statistical approaches for evaluating and interpreting huge used variables in order to obtain more precise output data related to the quality of the river and construct an observing system for successful water resource controlling. Water-quality monitoring methods create complicated multidimensional data that require multivariate statistical treatment (MST) in order to be analyzed and interpreted. Thus, MST worked as an effective investigative technique in the evaluation and interpretation of complicated data sets of the quality of the water, as well as in comprehending their temporal and geographical fluctuations (Singh et al. 2004). The ability to accurately forecast the quantity of total deposits that settle in rivers can significantly affect the hydraulics of the rivers. The interpretation of the interaction between the sediment and the flow of the river relies on many aspects; therefore, the problem's solution has grown difficult. Traditional approaches do not provide enough precise findings; thus, the use of several regression techniques and AI methods may result in improving the forecasts (Yilmaz et al. 2020). In many nations, river water salinity is a serious problem, and salinity is measured in total dissolved solids (TDS). As a result, one of the key elements affecting water quality is the river's water salinity. As a result, ANN is an effective tool for forecasting the nonlinear equation of salinity in a variety of challenging environmental scenarios along the river (Abbas et al. 2019). Due to their precision, speed, and repeatability (Baseri and Belali-Owsia 2017). In water resource research, this is a common modeling and estimation method. The capacity to combine human information with language phrases into fuzzy rules, as well as the non-linearity and flexibility of these systems,

are the main distinguishing features of artificial intelligence technologies (Jang 1993). The artificial neural network (ANN) is another modeling approach, with the key capability of knowledge by practicing the available information without the necessity of the final outputs (Tashnehlab and Menhaj 2001; Riahi-Madvar et al. 2011). To define the optimal architecture of models, however, designing and performing ANFIS and ANN simulations is running for long time and laborious (Baseri and Belali-Owsia 2017). The hybrid simulations are resulted in approaches which use data to imitate any phenomena in the best possible way. The optimization techniques are frequently utilized to get the optimal ANFIS and ANN parameters (Baseri and Belali-Owsia 2017; Karkevandi-Talkhooncheh et al. 2017; Gupta et al. 2017; Adib and Mahmoodi 2017; Mukerji et al. 2009; Shahlaei et al. 2012; Rezakazemi et al. 2017; Sarkheyli et al. 2015).

2 Research Question (Problem Statement)

The Ringlet River considered the more important rivers in the Cameron Highland, probably it is the most badly affected river with records of incidences where permissible levels of certain parameters such as suspended solids, agrochemicals, sewage and drinking water have been contravened. Recently, the tourism, agriculture, and industry in that region have dramatically increased. This parameter leads to increase the pollution rate in the water of the four rivers that flow into the lake, which change the quality of the water to the worse level. The nature of the muddy area is a parameter that allows soil erosion on the banks of the rivers, especially at the time of floods. Due to these parameters, the dam loses the goal of hydroelectric construction benefit, in addition to protect catchment areas from floods, recently this dam become less useful due to the accumulated amount of mud increasing steadily, therefore, the annual removing mud sediments from the Ringlet reservoir is difficult and expensive.

3 Research Objectives

1. The aim of the study is to deal with the prediction of the sediment volume quantity in the Ringlet reservoir resulting from reasons that lead to increase the sedimentation in the water of the rivers and reservoirs. In addition, to focus on the most important parameters that affect the water quality.
2. Present a new approach using a neural network to estimate the most important causes that lead to increased sedimentation in the basin of rivers and reservoirs.

3. The third aim of the study is to develop methodologies to investigate the sensitivity of a model parameters related to predict or to identify the input parameters that have the greatest effect on forecasting the water quality that causes sedimentation in the complex rivers and reservoirs.
4. The more accurate models in simulating water quality the better results to avoid contamination of water system in advance could be obtained. And enhance logical, feasible, and economic solutions to mitigate the damage and treat it in the future.

4 Research Hypothesis

The research hypothesis can be summarized in the following points:

1. The application of artificial neural networks as a modern method in water resources in Malaysia is considered necessary to ensure successful management. Many responsible authorities and departments feel the need for such a system in managing important and large projects.
2. Poor forecasting of water quality due to the currently available techniques are weak. It is suffer from being traditional, slow and uncertain. Besides the need for new, efficient techniques and more advantages to make it modern, fast, accurate, flexible, easy to use, and has a value.

5 Research the Importance and Justifications

The most important reasons behind adopting the research are:

1. Bad water quality in reservoir Ringlet is under study.
2. The increase in the level and volume of sediments in the reservoir in a way that affects the capacity of the lake basin, as well as the height of the dead storage level and the design storage level.
3. The management of water resources in Malaysia in general needs to establish an effective management tool that uses modern methods of exploiting water resources and preserving them from pollution because they suffer from the absence of systematic rules that can help them achieve this.
4. Knowing the most important reasons that lead to an increase in the percentage of pollutants and sediments in rivers and water reservoirs and its effect on human health, agricultural crops and animals, and its impact on the

waterways and important projects such as dams, reservoirs and rivers.

5. The need for scientific, accurate, easy and fast-to-use methods, and reliable administrative tools to be used in water project management.

6. The importance of water resources in this area is under study due to its tourism, agricultural, industrial, and residential resources.

7. A civilized society cannot survive without potable water, agriculture, industry, and other uses.

8. Water has an esthetic and touristic value, and it is greatly needed by human in all live fields.

9. Good water resource management greatly enhances the value of the land.

6 Comparative Analysis

This study investigates the results value of the previous studies for different rivers and reservoirs in different locations, and compare the analysis declaration of the artificial neural network (ANN) and discuss the input parameters with the output results. Table 1 demonstrates the summary of

Table 1 Summary of previous studies for a comparison predicted values using different types of approaches and parameters

Reference and year	Case study	Type of approach	Parameters	Research findings
Hayder et al. (2021)	Kelantan River basin	Artificial neural network (ANN)	DO, BOD, COD, pH, NH3-NL, S.S	1. The presence of outliers has a detrimental influence on performance, as seen by the low kurtosis values of pH 2. In order to make a decent forecast, the model needed more input values 3. The quantity of data points used in the forecast is critical 4. The prediction of the pH parameter yielded the best results
Khalik et al. (2013)	Bertam River, Cameron Highlands	Analysis of variance (ANOVA)	Nitrogen and phosphorus, the quality of sediment	1. The pH value of Bertam river is constant 2. Water temperatures were relatively constant 3. The measured electrical conductivity was in the range of 38–62 $\mu S\ cm^{-1}$ 4. An accumulation of nutrient contaminant in sediment bed, which become higher 5. The measured concentration of nitrate (NO_3^{-1}) of the river water was ($1.55 \pm 0.09\ mg\ L^{-1}$) which was with the limits of the drinking water determined by the World Health Organization (WHO) and the national drinking water quality standards (NDWQS) 6. The concentration of phosphate (PO_4) in water was ($0.96 \pm 0.20\ mg\ L^{-1}$) which was higher than the maximum limits of the regulations. However, relative accumulation index of NO_3 and PO_4 were (6.27 ± 3.72; $5.03 \pm 3.31\ mg\ L^{-1}$) 7. The levels of the above ions (nitrate and phosphate) in the sediment were much higher than that in water
Li and Gu (2003)	Jingjiang reach of the Yangtze River and Dongting Lake, China	ANN	Water flow and sediment transport simulations are performed using different sets of data due to data availability for flows and sediments. Instream flow (daily discharge) and nonpoint source surface runoff data	1. ANN approach showed reliable results for simulating water and sediment transport in river system 2. A complex system of rivers could be successfully modeled by the application of ANN technique which is considered as the main advantage of this approach 3. Using real data set of a complex system of river to construct ANN approach would decrease the number of iterations for simulating water and sediment transport 4. The combination of data-driven modeling method and fundamental physical principles to construct ANN approach by using real system data is feasible and practical 5. ANN approach showed an efficient performance in describing the behavior of water and sediment transport in a complex system of rivers and lakes 6. ANN technique is effectively applied for the stationary systems such as weather, hydrology, and morphology
		ANN		

(continued)

Table 1 (continued)

Reference and year	Case study	Type of approach	Parameters	Research findings
Nagy et al. (2002)	Rio Grande River, Sacramento River, Mississippi River		Water discharge per unit width, the water depth h, the longitudinal slope, the bed shear stress, the sediment discharge per unit width, the particle's median diameter, the sediment and fluid density, the kinematic viscosity, the acceleration gravity g, and the particle's fall velocity	1. Unlike other developed models which cannot be applied to the sediment transport due to the unpredictable nature and movement of the sediment, ANN can successfully predict the quantity of the sediment 2. The results obtained from ANN model could be more precise by increasing the range of the input patterns and data 3. The number of the input variables of the ANN model has no limit which can be used without ignoring or simplifying these data as be done in other models 4. From their experiences, site engineers have the ability to estimate the sediment quantity by using artificial neural network without returning to the theoretical sediment transport methods
Alp and Cigizoglu (2007)	Juniata Catchment, Juniata River, Pennsylvania, USA	Two different ANN algorithms, the feed-forward back-propagation (FFBP) method and the radial basis functions (RBF), were used for this purpose	The neural networks are trained using rainfall flow and suspended sediment load data	1. The outcomes of the ANN simulation are more reliable compared to the conventional multi-linear regression in terms of the selected performance criteria 2. The trends of the simulated sediment load hydrographs given by this approach are similar to the observed ones 3. The simulation using data of rainfall as the sole input parameter was not adequate to get reliable results of suspended sediment load 4. Estimating of suspended sediment loads is crucial factor in designing water resource projects such as dam construction The efficient application of ANN as a simulation tool for suspended sediment load promises a potential progress solution for this problem

previous studies for a comparison predicted values using different types of approaches and parameters.

7 Conclusions and Discussion

This study addresses the challenge of accurately forecasting the most important causes of increasing sedimentation in river and lake water, as well as shedding light on the most critical elements that impact water quality. In order for the research to represent its arguments and hypotheses in a set of objectives to be met, the following objectives have been adopted:

1. The primary goal of this research, which is based on literary surveys and field investigations, is to emphasize and explain the following items:
   (a) Methods for forecasting the causes of sedimentation in large, complicated lakes and rivers.
   (b) Critical variables (factors) in determining water quality in large lakes and rivers.
   (c) The level of documentation, information preservation, and database quality required for water resource management.
2. The study also intends to propose a novel technique that employs a neural network to predict the most important

reasons of increasing sedimentation in river and lake water, as well as shed light on the most critical elements that impact water quality accurately at an early stage. The following technique justifies this purpose.
   (a) Investigating the use of artificial neural networks (ANNs) in water quality, water resource management, and environmental engineering projects.
   (b) Using cutting-edge approaches, such as forward feeding propagation, to optimize and train neural networks in order to develop an ideal neural network model that accommodates the stated parameter.
   (c) Developing a comprehensive tool (mathematical equation) to predict water quality and the most important causes that lead to sediments in rivers and lakes, using the resulting neural network model.
   (d) Evaluating the performance of the neural network model by comparing the results of the neural network model with the results of other prediction methods described in the literature and previous similar studies.
3. Developing methodologies to study the sensitivity of a developed model to changes in the parameters related to the prediction or to identify the input variables that have the greatest impact on predicting water quality and causes of sedimentation in rivers and lakes and to adapt the model to new project environments.

References

S. Abbas, B. Khudair, M. Jaafar, River water salinity impact on drinking water treatment plant performance using artificial neural network. J. Eng. **25**(8), 149–159 (2019). https://doi.org/10.31026/j.eng.2019.08.10

A. Adib, A. Mahmoodi, Prediction of suspended sediment load using ANN GA conjunction model with Markov chain approach at flood conditions. KSCE J. Civ. Eng. **21**(1), 447–457 (2017). https://doi.org/10.1007/s12205-016-0444-2

J.T. Adu, M.V. Kumarasamy, Development of non-point source hybrid cells in series model for reactive pollutant transport in natural rivers. Polish J. Environ. Stud. **29**(5), 3031–3039, 9p (2020). https://doi.org/10.15244/pjoes/109025

M. Al-Mukhtar, F. Al-Yaseen, Modeling water quality parameters using data-driven models, a case study Abu-Ziriq Marsh in South of Iraq. Hydrology **6**(1), 24 (2019). https://www.mdpi.com/2306-5338/6/1/24#cite

M. Alp, H.K. Cigizoglu, Suspended sediment load simulation by two artificial neural network methods using hydrometeorological data. Environ. Model. Softw. **22**, 2–13 (2007). https://doi.org/10.1016/j.envsoft.2005.09.009

A.D. Astuti, A. Aris, M.R. Salim, S. Azman, S. Salmiati, M.I.M. Said, Artificial intelligence approach to predicting river water quality: a review. J. Environ. Treatment Tech. **8**(3), 1093–1100 (2020)

H. Banjad, M. Kamali, K. Amir Moradi, E. Aliai, Forecasting some of the qualitative parameters of rivers using wavelet artificial neural network hybrid (W-ANN) model) (case of study: Jajroud River of Tehran and Gharaso River of Kermanshah). Iran. J. Health Environ. **6**(3), 277–294, 18 (Language: Persian)

H. Baseri, M. Belali-Owsia, A novel hybrid ICA-ANFIS model for prediction of manufacturing processes performance. Proc. IMechE Part E: J. Process Mech. Eng. **231**(2), 181–190 (2017). https://doi.org/10.1177/0954408915585256

Ö. Baydaroğlu, K. Koçak, K. Duran, River flow prediction using hybrid models of support vector regression with the wavelet transform, singular spectrum analysis and chaotic approach. Meteorol. Atmos. Phys. **130**(3), 349–359, 11 (2018). https://doi.org/10.1007/s00703-017-0518-9

K.W. Chau, An ontology-based knowledge management system for flow and water quality modeling. Adv. Eng. Softw. **38**(3), 172–181 (2007). https://doi.org/10.1016/j.advengsoft.2006.07.003. ISSN 0965-9978

Y. Chen, X. Fang, L. Yang, L. Liu, C. Gong, Y. Di, Artificial neural networks in the prediction and assessment for water quality: a review. J. Phys.: Conf. Ser. **1237**(4) (2019). https://doi.org/10.1088/1742-6596/1237/4/042051

J. Dalle, M.Z. Elfirman, M. Sufyan, Microcontroller based water measurement level prototype using fuzzy logic method. TEM J. **9**(2), 694–701, 8p. https://doi.org/10.18421/tem92-36

M.E. Faridah Othman, M.S. Alaaeldin, A.N. Ahmed, F.Y. Teo, C.M. Fai, H.A. Afan, M. Sherif, A. Sefelnasr, A. El-Shafie, Efficient river water quality index prediction considering minimal number of inputs variables. Eng. Appl. Comput. Fluid Mech. **14**(1), 751–763 (2020). https://doi.org/10.1080/19942060.2020.1760942

M.B. Gasim, S. Surif, M.E. Toriman, S.A. Rahim, R. Elfithri, P.I. Lun, Land-use change and climate-change patterns of the Cameron highlands, Pahang, Malaysia. Arab World Geogr. **12**(1–2), 51–61 (2009). https://doi.org/10.5555/arwg.12.1-2.l2p14j2833g2q4l7

L. Godo-Pla, J.J. Rodríguez, J. Suquet, P. Emiliano, F. Valero, M. Poch, H. Monclús, Control of primary disinfection in a drinking water treatment plant based on a fuzzy inference system. Process Saf. Environ. Protect.: Trans. Inst. Chem. Eng. Part B. **145**, 63–70, 8p (2021). https://doi.org/10.1016/j.psep.2020.07.037

A.K. Gupta, P. Kumar, R.K. Sahoo, A.K. Sahu, S.K. Sarangi, Performance measurement of plate fin heat exchanger by exploration: ANN, ANFIS, GA, and SA. J. Com. Des. Eng. **4**(1), 60–68 (2017). https://doi.org/10.1016/j.jcde.2016.07.002

G. Hayder, I. Kurniawan, H. Mustafa, Implementation of machine learning methods for monitoring and predicting water quality parameters. Biointerface Res. Appl. Chem. **11**, 9285–9295 (2020). https://doi.org/10.33263/BRIAC112.92859295

G. Hayder, I. Kurniawan, H.M. Mustafa, Implementation of machine learning methods for monitoring and predicting water quality parameters. Biointerface Res. Appl. Chem. **11**(2), 9285–9295 (2021). ISSN 2069-5837

M. Huang, D. Tian, H. Liu, C. Zhang, X. Yi, J. Cai, J. Ruan, T. Zhang, S. Kong, G. Ying, A hybrid fuzzy wavelet neural network model with self-adapted fuzzy-means clustering and genetic algorithm for water quality prediction in rivers. Complexity **2018**, Article ID 8241342, 11 (2018). https://doi.org/10.1155/2018/8241342

O. Jaafar, M.E. Toriman, S.A. Sharifah Mastura, M.B. Gazim, P.I. Lun, P. Abdullah, M.K.A. Kamarudin, N.A.A. Aziz, Modeling the impacts of ringlet reservoir on downstream hydraulic capacity of Bertam River using XPSWMM in Cameron highlands, Malaysia. Res. J. Appl. Sci. **5**, 47–53 (2010). https://doi.org/10.3923/rjasci.2010.47.53. https://medwelljournals.com/abstract/?doi=rjasci.2010.47.53

J.S. Jang, ANFIS: adaptive-network-based fuzzy inference system. IEEE Trans. Syst. Man Cybern. **23**(3), 665–685 (1993). https://doi.org/10.1109/21.256541

A. Karkevandi-Talkhooncheh, S. Hajirezaie, A. Hemmati-Sarapardeh, M.M. Husein, K. Karan, M. Sharifi, Application of adaptive neuro fuzzy interface system optimized with evolutionary algorithms for modeling CO_2-crude oil minimum miscibility pressure. Fuel **205**, 34–45 (2017). https://doi.org/10.1016/j.fuel.2017.05.026

W.M.A.W.M. Khalik, M.P. Abdullah, N. Padli, N.A. Amerudin, Assessment on nutrient status in water and sediment quality of Bertam River, Cameron Highlands. Int. J. Chem. Sci. **11**(2), 709–720 (2013). ISSN 0972-768X

Y. Li, R.R. Gu, Modeling flow and sediment transport in a river system using an artificial neural network. Environ. Manage. **31**(1), 122–134 (2003). https://doi.org/10.1007/s00267-002-2862-9

D.P. Loucks, E. van Beek, in *Project Planning: Putting It All Together*. Water Resource Systems Planning and Management (Springer, Cham, 2017). https://doi.org/10.1007/978-3-319-44234-1_13

J. Luis, L.M. Sidek, M.N.B.M. Desa, P.Y. Julien, in *Challenge in running hydropower as source of clean energy: ringlet reservoir, Cameron highlands case study*. Proceedings National Graduate Conference 2012 (NatGrad2012), Universiti Tenaga Nasional, Putrajaya Campus, 8–10 Nov 2012

J. Mateo Sagasta (IWMI), S.M. Zadeh (FAO) and H. Turral with contributions from J. Burke (formerly FAO), Water pollution from agriculture: a global review. Published by the Food and Agriculture Organization of the United Nations Rome, 2017 and the International Water Management Institute on behalf of the Water Land and Ecosystems research program Colombo, 2017. www.fao.org/contact-us/licencerequest. copyright@fao.org. FAO information products are available on the FAO website (www.fao.org/publications) and can be purchased through publications-sales@fao.org© (FAO and IWMI, 2017). Cover photograph: © Jim Holmes/IWMI

B. Mohamed Khalil, A. Georges Awadallah, H. Karaman, A. El-Sayed, Application of artificial neural networks for the prediction of water quality variables in the Nile Delta. J. Water Resour. Protect. **4**(6), 388–394 (2012). https://doi.org/10.4236/jwarp.2012.46044

A. Mukerji, C. Chatterjee, N.S. Raghuwanshi, Flood forecasting using ANN, neuro-fuzzy, and neuro-GA models. J. Hydrol. Eng. **14**(6), 647–652. https://doi.org/10.1061/(ASCE)HE.1943-5584.0000040

H.M. Nagy, K. Watanabe, M. Hirano, Prediction of sediment load concentration in rivers using artificial neural network model. J. Hydraul. Eng. **128**(6), 588–595 (2002). https://doi.org/10.1061/(ASCE)0733-9429(2002)128:6(588). ISSN 0733-9429

A. Najah, A. El-Shafie, O.A. Karim et al., Application of artificial neural networks for water quality prediction. Neural Comput. Appl. **22**, 187–201 (2013). https://doi.org/10.1007/s00521-012-0940-3

N. Noori, L. Kalin, S. Isik, Water quality prediction using SWAT-ANN coupled approach. J. Hydrol. **590**, 125220 (2020). https://doi.org/10.1016/j.jhydrol.2020.125220

J. O'Keefe, K. Walker, Large river ecosystems: a dedication to Bryan Davies. Special Issue **35**(5) (2019)

H. Orouji, O. Bozorg Haddad, E. Fallah-Mehdipour, M.A. Mariño, Modeling of water quality parameters using data-driven model. J. Environ. Eng. **139**(7) (2013). https://doi.org/10.1061/(ASCE)EE.1943-7870.0000706

J. Park, K.T. Kim, W.H. Lee, Recent advances in information and communications technology (ICT) and sensor technology for monitoring water quality. Water **12**(2), 510 (2020). https://doi.org/10.3390/w12020510

K.S. Parmar, S.J.S. Makkhan, S. Kaushal, Neuro-fuzzy-wavelet hybrid approach to estimate the future trends of river water quality. Neural Comput. Appl. **31**(12), 8463–8473, 11 (2019). https://doi.org/10.1007/s00521-019-04560-8

M. Rezakazemi, A. Dashti, M. Asghari, S. Shirazian, H_2-selective mixed matrix membranes modeling using ANFIS, PSO-ANFIS, GA ANFIS. Int. J. Hydrog. Energy **42**(22), 15211–15225 (2017). https://doi.org/10.1016/j.ijhydene.2017.04.044

H. Riahi-Madvar, S.A. Ayyoubzadeh, M.G. Atani, Developing an expert system for predicting alluvial channel geometry using ANN. Expert Syst. Appl. **38**(1), 215–222 (2011). https://doi.org/10.1016/j.eswa.2010.06.047

A. Sarkar, P. Pandey, River water quality modelling using artificial neural network technique. Aquat. Proc. 4, 1070–1077 (2015). ISSN 2214-241X. https://doi.org/10.1016/j.aqpro.2015.02.135

A. Sarkheyli, A.M. Zain, S. Sharif, Robust optimization of ANFIS based on a new modified GA. Neurocomputing **166**, 357–366 (2015). https://doi.org/10.1016/j.neucom.2015.03.060

M. Shahlaei, A. Madadkar-Sobhani, L. Saghaie, A. Fassihi, Application of an expert system based on genetic algorithm–adaptive neuro-fuzzy inference system (GA–ANFIS) in QSAR of cathepsin K inhibitors. Expert Syst. Appl. **39**(6), 6182–6191 (2012). https://doi.org/10.1016/j.eswa.2011.11.106

M. Sibtain, X. Li, M.I. Azam, H. Bashir, Applicability of a three-stage hybrid model by employing a two-stage signal decomposition approach and a deep learning methodology for runoff forecasting at Swat River Catchment, Pakistan. Polish J. Environ. Stud. **30**(1), 369–384, 16 (2021). https://doi.org/10.15244/pjoes/120773

K.P. Singh, A. Malik, D. Mohan, S. Sinha, Multivariate statistical techniques for the evaluation of spatial and temporal variations in water quality of Gomti River (India)—a case study. Water Res. **38**(18), 3980–3992 (2004). https://doi.org/10.1016/j.watres.2004.06.011. ISSN 0043-1354. http://www.sciencedirect.com/science/article/pii/S0043135404003367

A.P. Singh, R. Srinivas, S. Kumar, S. Chakrabarti, Water quality assessment of a River Basin under fuzzy multi-criteria framework. Int. J. Water. 9 (2014). https://doi.org/10.1504/IJW.2015.070364

A. Sönmez, S. Kale, R.C. Ozdemir, A. Kadak, An adaptive neuro-fuzzy inference system (ANFIS) to predict of cadmium (Cd) concentrations in the Filyos River, Turkey. Turk. J. Fish. Aquat. Sci. **18**, 1333–1343 (2018). https://doi.org/10.4194/1303-2712-v18_12_01

K.W. Tan, M.B. Mokhtar, Evaluation of social perception on water issues in cameron highlands (Malaysia) by principle factor analysis, Institute for Environment and Development (LESTARI), University Kebangsaan Malaysia, Selangor 43600, Malaysia. Received: 21 Feb 2010/Accepted: 1 Apr 2010/Published: 20 Apr 2010. J. Environ. Sci. Eng. **4**(4) (Serial No. 29). ISSN 1934-8932, USA

M. Tashnehlab, S. Menhaj, Modeling trip tours using ANFIS, modeling. Univ. College Eng. **31**(3), 361–370 (2001)

Tiyasha, T.M. Tung, Z.M. Yaseen, A survey on river water quality modelling using artificial intelligence models: 2000–2020. J. Hydrol. **585**, 124670 (2020). https://doi.org/10.1016/j.jhydrol.2020.124670. ISSN 0022-1694

Y. Wang, Y. Yuan, Y. Pan, Z. Fan, Modeling daily and monthly water quality indicators in a canal using a hybrid wavelet-based support vector regression structure. Water **12**(5), 1476 (2020). https://doi.org/10.3390/w12051476

L. Yang, Fuzzy evaluation of water quality based on micronucleus technology of *Vicia faba* root tip. Mathe. Prob. Eng. 1–6, 6p (2019). https://doi.org/10.1155/2019/3047362

I.S. Yeon, J.H. Kim, K.W. Jun, Application of artificial intelligence models in water quality forecasting. Environ. Technol. **29**(6), 625–631 (2008). https://doi.org/10.1080/09593330801984456

B. Yilmaz, A.R.A.S. Egemen, M. Kankal, S. Nacar, Sigma: suspended sediment load prediction in rivers by using heuristic regression and hybrid artificial intelligence models. J. Eng. Nat. Sci./Mühendislik Ve Fen Bilimleri Dergisi **38**(2), 703–714, 12 (2020)

Effect of Concrete-Steel Interactions on the Performance of Emended Distributed Optical Fiber Sensor; Review

Ahmad Mazin ALhamad, Yousif Mohammed, and Gasim Hayder

Abstract

Distributed optical fiber sensor (OFS) is a cutting-edge technology that has been introduced to the construction industry as a structural health monitoring system for the structural assessment of existing and newly built structures. The OFS can be attached to the surface of the existing structures or embedded into the newly built structures. Furthermore, the bond stress resistance produces the composite action at the embedded reinforcement and the adjoining concrete interfaces. This study is developed to determine the effects of the interaction at the interfaces and their impact on the performance of the distributed OFS as a monitoring system of the structural health. The strain evolution will be obtained from the previous study and used with different perspectives compared to the original research. Therefore, monotonic loading was applied in terms of displacement control with roller supports to obtain the maximum strain profile of the reinforced concrete beam. The result obtained will be used to develop the relationship of the bond-slip and compare it with Model Code 2010 predicated bond-slip relationship. Therefore, the bond-slip relationship is significant concern to evaluate the impact of the concrete-to-steel interaction on the OFS performance.

Keywords

Distributed optical fiber sensors • Strain evolution • Concrete-steel interactions • Monotonic loading • Structural health monitoring

A. M. ALhamad (✉) · Y. Mohammed
College of Graduate Studies, Universiti Tenaga Nasional (UNITEN), 43000 Kajang, Selangor Darul Ehsan, Malaysia
e-mail: sc23192@student.uniten.edu.my

G. Hayder
Department of Civil Engineering, College of Engineering, Universiti Tenaga Nasional (UNITEN), 43000 Kajang, Selangor Darul Ehsan, Malaysia

1 Introduction

The distributed optical fiber sensor (OFS) is an innovative tool that is used in many industries around the globe. It has been introduced to the construction business as a mean of observation to the structure's health along its life span. It could be imbedded on the newly constructed structure or planted on the existing one. Furthermore, OFSs have the ability to monitor the structural element throughout the entire optical fiber in a fully distributed way (Barrias et al. 2016). By evaluating it in terms of cost, it was found to be low in comparison with the traditional method and more efficient as well. It offers a wide range of applications in the construction industry, such as continuous monitoring of existing or newly built structures (Bado et al. 2020; Barrias et al. 2016). On the other hand, the conventional structural health monitoring method relies heavily on visual inspections carried out by trained engineers (Barrias et al. 2016; Davis et al. 2016).

The OFS is a non-destructive tool that has been used to monitor the serviceability condition of structures to provide proper risk management in order to prevent structural failures through regular maintenance updates. It can be entrenched into the newly built structures or attached to the surface of the existing structures (López-Higuera et al. 2011). Thus, the strain record will commence as soon the temperature is transferred to the fiber and the scattered signal is modulated by strain and temperature (Barrias et al. 2016). Actually, both the strain profile and the interaction between the concrete and steel could be achieved through the embedded optical fiber. The interaction at the interfaces of the embedded reinforcement and surrounded concrete for any sort of structural element is known as the bond zone. This bond zone experiences multi-complex stress actions in the forms of secondary splitting microcracks, local concrete crushing for the member, and shear crack for the concrete member in front of the ribs (Jakubovskis and Kaklauskas 2019).

The distributed OFS relies on bonding at the interfaces between the OFS properties and the surrounding materials to monitor the strain distribution (Ansari and Libo 1998). The extracted strain profile that was generated by the optical fiber, provides strain measurement of the structural materials to determine the composite action between the concrete and steel. However, the output of the strain profile is not fit to be used as representative of strains induced directly as an input to evaluate the bond stress (Ansari and Libo 1998; Bado et al. 2021). The strain field transferred of the structural material is affected by the glass core, glass cladding, and protective silicone coating. On the other hand, the bond stress resistance produces the composite action at the interfaces between the surrounded concrete and the embedded reinforcement (Kankam 1997). At those interfaces, the total bond resistance of the element consists of both bearing and friction resistance (Murcia-Delso and Benson Shing 2015).

The bond-slip relationship models were developed for monotonic and cyclic loading and used in the finite element analysis to simulate concrete member's bond stress at the interfaces of the deformed bars and the surrounding concrete in order to evaluate their ultimate structural capacity at the required period. Some researchers (Eligehausen et al. 1982) have carried out an extensive experimental investigation (Eligehausen et al. 1982) to develop a model for the bond-slip relationship. On the other hand, another bond-slip model, known as Model 2010, was developed by Beverly (2010) based on extensive research and experimental work. Few researchers (Bado et al. 2021; Kaklauskas et al. 2019) have used the stress approach and Model Code 2010 to validate their experimental findings. Therefore, bond-slip models and stress approaches play a significant role in evaluating the performance of the distributed OFS. In this study, the effect of the steel-to-concrete interaction on the performance of OFS is assessed based on the extracted strain profile through an embedded OFS.

2   Proposed Methodology

The goal of this research is to find out how steel–concrete interactions affect the performance of emended distributed OFSs. The data for this study will be gathered through literature reviews of published studies, and the information gathered will be analyzed from other angles than the original study. The OFS's strain profile will be the major source of data collection. The bond-slip relationship could be determined using numerical analysis using the reinforced concrete (RC) beam strain profile extracted and obtained from the previous investigation by distributed OFS. The research methods and approaches employed to reach the study work's goal will be highlighted in this part (Kaklauskas et al. 2019).

The research approach framework for this study as stated by the authors starts by a literature review. The literature review is important since the data gathering will be done through previous studies. The features and uses of the OFS in the construction industry will be examined throughout the literature review. On the other side, past investigations will be used to illustrate the extracted strain profile and numerical formulation of the bond-slip relationship. The focus of this research will be on the bond-slip behavior of RC beams under monotonic load utilizing OFSs, so far to investigate the effect of steel–concrete interactions on the performance of emended distributed OFSs along the structural member. The relationship between the structural behavior of both bond and slip between the concrete element and steel reinforcement bars for the structural element will be compared to the measure of Standard Code 2010 based for slip-bond relationship. OFSs will extract a strain profile, which will be used to construct the bond-slip relationship (Bado et al. 2021).

The strain evolution along the RC beam as derived by the OFS and the Model Code 2010 predicated slip-bond relationship will be the initial step of data gathering in this investigation. The structural behavior of the relationship between bond and slip that were specified for structural elements composing the concrete member will be calculated using the approach of strain evolution to examine the reinforcement steel bar interaction with a concrete element. The prior method that was reported will be used to develop the strain-bond-slip relationship (Bado et al. 2021; Kaklauskas et al. 2019).

2.1   The Geometry of RC Beam

The specimen is made up of RC beams with embedded OFSs and two supports as described by Berrocal et al. (2021). The OFS was implanted into the RC beam and fastened to the reinforcement bar, with a cross-section of 100 mm × 150 mm and a beam span of 800 mm from the center of the supports. The goal of attaching the OFS to the steel bar is to see how steel–concrete interactions affect the performance of the modified distributed OFS. The retrieved strain profile will also be used to build the bond-slip curve as a source of the element strain, due to the OFS was linked to the steel bar (Barrias et al. 2018).

2.2   Test Setup

The specimen that was intended to be tested consists of RC beams with embedded OFSs, hydraulic jack, load cell, and 80 mm × 100 mm loading plate as shown in a study by Berrocal et al. (2021). The beam was subjected to a point

load at the mid-span, and roller support was used to obtain the maximum strain profile using a hydraulic jack. Displacement control for the tested member was applied at the mid-span upon closed-loop feedback system at every 0.5 mm/min displacement measure rate as monotonic loading for the testing sample along the period.

3 Conclusions

This study will be mainly focused on the influence of the steel–concrete interaction on the OFS. The data collection for the study will be obtained from previously existing published articles and other materials with different perspectives. The extracted strain profile or strain evolution will be used to develop the slip-bond relationship and relate it with the Code Model 2010 predicated slip-bond relationship. Based on the comparison of the developed slip-bond relationship and Code Model 2010 predicated slip-bond relationship, which is affecting concrete and steel interactions of the structural member on the emended distributed OFSs performance in the assessed member. Therefore, the slip-bond relation is significant concern to evaluate the impact of the steel-to-concrete interaction on the performance of the OFS.

References

F. Ansari, Y. Libo, Mechanics of bond and interface shear transfer in optical fiber sensors. J. Eng. Mech. **124**(4), 385–394 (1998)

M.F. Bado, J.R. Casas, A. Dey, C.G. Berrocal, Distributed optical fiber sensing bonding techniques performance for embedment inside reinforced concrete structures. Sensors **20**(20), 5788 (2020)

M.F. Bado, J.R. Casas, G. Kaklauskas, Distributed sensing (DOFS) in reinforced concrete members for reinforcement strain monitoring, crack detection and bond-slip calculation. Eng. Struct. **226**, 111385 (2021)

A. Barrias, J.R. Casas, S. Villalba, A review of distributed optical fiber sensors for civil engineering applications. Sensors **16**(5), 748 (2016)

A. Barrias, J.R. Casas, S. Villalba, Embedded distributed optical fiber sensors in reinforced concrete structures—a case study. Sensors (Basel, Switzerland) **18**(4), 980 (2018). https://doi.org/10.3390/s18040980

C.G. Berrocal, I. Fernandez, R. Rempling, Crack monitoring in reinforced concrete beams by distributed optical fiber sensors. Struct. Infrastruct. Eng. **17**(1), 124–139 (2021)

P. Beverly, International Federation for Structural Concrete (eds) (2013) fib model code for concrete structures 2010. Ernst & Sohn, Berlin (2010)

M. Davis, N.A. Hoult, A. Scott, Distributed strain sensing to determine the impact of corrosion on bond performance in reinforced concrete. Constr. Build. Mater. **114**, 481–491 (2016)

R. Eligehausen, E.P. Popov, V.V. Bertero, Local bond stress-slip relationships of deformed bars under generalized excitations (1982)

R. Jakubovskis, G. Kaklauskas, Bond-stress and bar-strain profiles in RC tension members modelled via finite elements. Eng. Struct. **194**, 138–146 (2019)

G. Kaklauskas, A. Sokolov, R. Ramanauskas, R. Jakubovskis, Reinforcement strains in reinforced concrete tensile members recorded by strain gauges and FBG sensors: experimental and numerical analysis. Sensors **19**(1), 200 (2019)

C.K. Kankam, Relationship of bond stress, steel stress, and slip in reinforced concrete. J. Struct. Eng. **123**(1), 79–85 (1997)

J.M. López-Higuera, L.R. Cobo, A.Q. Incera, A. Cobo, Fiber optic sensors in structural health monitoring. J. Lightwave Technol. **29**(4), 587–608 (2011)

J. Murcia-Delso, P. Benson Shing, Bond-slip model for detailed finite-element analysis of reinforced concrete structures. J. Struct. Eng. **141**(4), 04014125 (2015)

River Water Quality Prediction and Analysis–Deep Learning Predictive Models Approach

Nur Najwa Mohd Rizal, Gasim Hayder, and Salman Yussof

Abstract

In depth research about river water qualities are no more outlandish nowadays due to river water pollutions and contaminations. In order to have an accurate and precise measurement taken towards these river water pollution, advanced and new technologies need to be applied rather than old technique of everyday lab testing. Therefore, with the usage of deep learning predictive models approach, the decision makers able to provide immediate response and give precautionary measures to prevent a disastrous event. In the current research, Adaptive Neuro-fuzzy Inference System (ANFIS) has been used to predict six different types of river water quality parameters at Langat River, Malaysia. Root mean square error (RMSE) and determination of coefficient (R^2) were used to assess the performances of the models. The results have been proven that ANFIS able to predict the parameters of river water quality as ANFIS Model 5 has achieved the highest value of R^2 (0.9712). It also obtained the low values of RMSE which were 0.0028, 0.0144 and 0.0924 for training, testing and checking data sets, respectively. Overall, the six ANFIS models have successfully predict six different water quality parameters.

N. N. M. Rizal (✉)
College of Graduate Studies, Universiti Tenaga Nasional (UNITEN), 43000 Kajang, Selangor Darul Ehsan, Malaysia
e-mail: nur.najwa@uniten.edu.my

G. Hayder
Department of Civil Engineering, College of Engineering, Universiti Tenaga Nasional (UNITEN), 43000 Kajang, Selangor Darul Ehsan, Malaysia

S. Yussof
Institute of Informatics and Computing in Energy, Universiti Tenaga Nasional (UNITEN), 43000 Kajang, Selangor Darul Ehsan, Malaysia

1 Introduction

The prediction of river water quality is no more out of the ordinary today especially in the field of hydrology and environmental science. Clean water is extremely important for all. Therefore, there is no living beings including animals, plants and humans can survive in this world without clean water. Besides drinking, numerous sectors of economy, viz. manufacturing and commercial, agriculture, hydroelectric power supply, fisheries and even animal husbandry depends on the clean river water supply. Thus it shows that water, particularly river water plays an important role (Tyagi et al. 2013).

As urbanization and population growth increased, it has caused the needs of fresh water increased to the very great extent over the past several decades (Al-Badaii et al. 2013). As stated by Abba et al. (2020), water pollution is known as the existence of toxic or harmful substances in water that may results in disadvantageous to living beings at a certain level (Abba et al. 2020). The chances of rivers to be polluted by heavy metals and other contaminants that results from human activities are high. Therefore, this has placed the river system at high risk due to the disadvantageous of environment pollution since the river can be effortless accessed for waste disposal and also because of the dynamic nature of the river itself (Ahmed et al. 2019).

These contaminants and pollutions occur in rivers have deteriorated the river water quality. There are two main factors that will affect the water quality which are the natural factors (hydrological, climate and geological factors) and the human factors (Sami et al. 2021). Human factors usually are the contaminants and pollutions that results from rapid

urbanization, agriculture and livestock farming. Thus, a suitable measure need to be done in order to maintain the management of the river water quality from the river water pollution.

Artificial Intelligence (AI) have been widely used by most scientist and investigators from all over the world to predict the parameters of the river water quality. Lafdani et al. (2013) have stated that nowadays, the growth in AI gives a difference in prediction as an estimator used for hydrological phenomenon (Lafdani et al. 2013). When the hydrological data is introduced to the model, it able to learn or discover the system behaviour which gives the main advantage of the AI models.

There are abundance of AI modelling that have been developed to predict river water quality. Adaptive Neuro-fuzzy Inference System (ANFIS), Fuzzy Logic (FL), Support Vector Machine (SVM), Artificial Neural Network (ANN), Radial Basis Neural Network (RBNN) and Multi-layer Perceptron (MLP) are the examples of AI models that able to be applied to predict time series related modelling based on historical data (Rizal 2020). ANFIS on the other hand is a machine learning that has a feed-forward multi-layer neural network composed of fuzzy logic and ANN. In order to produce the input–output relationship with the nonlinear depiction, ANFIS uses ANN and a learning algorithm of fuzzy logic systems (Azad et al. 2019).

Previous study also showed great results when using ANFIS to predict water quality in their research. For example, Abba et al. (2017) have used ANN and ANFIS techniques in order to predict the concentration of dissolved oxygen (DO) in Yamuna River. However, it has shown that ANFIS outperformed ANN in performances. The authors have achieved satisfying results for ANFIS with the value of 0.94 and 0.7 for correlation coefficient (R) and root mean square error (RMSE), respectively, in the calibration phase and the value of 0.81 and 1.38 for R and RMSE, respectively, in the validation phase. Even though ANFIS is better than ANN, the authors concluded that it still can be applied in modelling the DO concentration in the river (Abba et al. 2017). Other previous research that conducted by Abba et al. (2019), Sonmez et al. (2018) and Ranković et al. (2012) also predicted river water quality only by using historical data and have achieved good results in their research (Abba et al. 2019; Sonmez et al. 2018; Ranković et al. 2012). In the current research, ANFIS models have been established for the prediction of six different water quality parameters in Langat River, Malaysia. In the next section, study area and the methods are explained. In Sect. 3, the results of the modellings are presented while the discussion is deliberated in Sect. 4. The conclusion of the study is detailed out in Sect. 5.

2 Study Area and Methods

Langat River, Malaysia is the study area chosen as shown in Fig. 1. The historical data (from 1981 to 2019) of the river water quality parameters have been retrieved from the water quality station (Station No. 2917601) at Department of Irrigation and Drainage (DID), Malaysia. Magnesium, pH, total solid (TS), conductivity, colour, ammonia, nitrate, turbidity, dissolved solid (DS), chloride, solids, alkalinity, fluoride, calcium, hardness, biochemical oxygen demand (BOD$_{5day}$), chemicals, potassium, sodium, manganese, silica, iron, phosphate, total suspended solid (TSS) and sulphate were the parameters of water quality applied as inputs for the modelling. Moreover, only 161 data for all 25 parameters of the water quality were available due to the missing value. A basic statistics of the raw data of the parameters of the water quality in Langat River are shown in Table 1.

The ANFIS models have been developed using Neuro-Fuzzy Designer app in MATLAB 2020b and all of the historical data have been cleaned and pre-processed to avoid errors while running the modelling. The missing values in the historical data have been replaced with a constant value which was a zero value. Furthermore, the historical data have been normalized in the range of [0,1] and have been divided into 3 sets of data namely, training data (70%), testing data (15%) and checking data (15%) sets. While developing the ANFIS models, subtraction clustering method was used due to large input data in the modelling. Backpropagation method and 100 epochs were chosen for the optimization method and the number of training epochs, respectively.
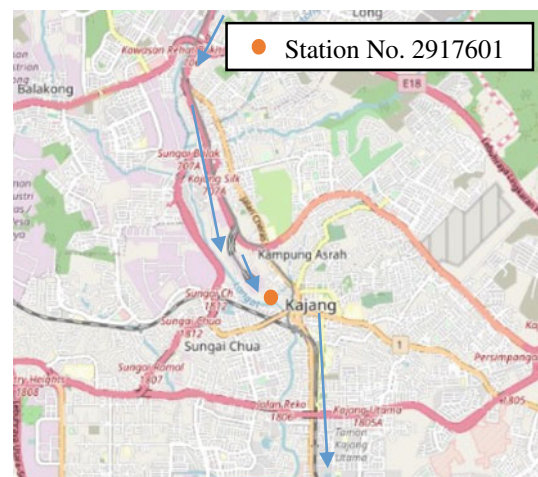
Fig. 1 The study area

Table 1 Basic statistic of the raw data of the parameters of water quality in Langat River

Parameters (unit)	Average	Std. Dev
Alkalinity (mg/L × 100)	3801.43	1661.62
Ammonia (mg/L × 100)	193.18	168.51
BOD5day (mg/L × 100)	7.47	13.37
Calcium (mg/L × 10)	177.68	147.42
Chemical (mg/L × 100)	3207.64	2542.24
Chloride (mg/L × 10)	87.80	49.59
Colour (Hazen)	66.30	89.18
Conductivity (µs/cm)	154.85	68.94
Dissolved solid (mg/L × 100)	1053.99	3818.74
Fluoride (mg/L × 100)	27.19	10.34
Hardness	49.79	54.58
Iron (mg/L × 10)	57.56	86.57
Magnesium (mg/L × 10)	15.95	53.75
Manganese (mg/L × 100)	41.2	150.21
Nitrate (mg/L × 100)	822.98	769.82
pH (pH × 10)	68.91	41.55
Phosphate (mg/L × 100)	51.08	245.42
Potassium (mg/L × 10)	199.54	888.25
Silica (mg/L × 100)	1809.54	1103.56
Sodium (mg/L × 100)	1328.65	5091.28
Solids (mg/L)	264.21	298.22
Sulphate (mg/L × 10)	136.93	93.87
Total solid (mg/L)	360.16	269.97
Total suspended solid (mg/L)	348.27	274.88
Turbidity (Fullers × 10)	1520.68	2336.71

3 Results

In the current research, six models of ANFIS have been established to predict six different water quality parameters, viz. nitrate, phosphate, BOD, TS, DS and TSS. Table 2 shows the results of the ANFIS models according to the respective targets.

Based on Table 2, it has shown that ANFIS Model 5 has achieved the highest value of R^2 with the value of 0.9712. It also obtained low values of RMSE which were 0.0028, 0.0144 and 0.0924 for training, testing and checking data sets, respectively. Compared to ANFIS Model 3 that has been used to predict DS, it has achieved the lowest value of R^2 (0.4662). ANFIS Model 1, 2, 4 and 6 also obtained satisfying outcome by gaining good value of R^2 which were 0.9501, 0.8903, 0.8342 and 0.7588, respectively. However, all of the ANFIS models have obtained low values of RMSE for all data sets. Figure 2 shows the regression plot of ANFIS Model 5 that has been used to predict nitrate.

Table 2 The outcomes of the ANFIS models according to the respective targets

ANFIS model No.	Target	R^2	RMSE		
			Training	Testing	Checking
1	BOD	0.9501	0.0037	0.0103	0.07868
2	TSS	0.8903	0.0045	0.0491	0.1236
3	DS	0.4662	0.0013	0.0110	0.2422
4	TS	0.8342	0.0024	0.1318	0.1119
5	Nitrate	0.9712	0.0028	0.0144	0.0924
6	Phosphate	0.7588	0.0020	0.0899	0.1169
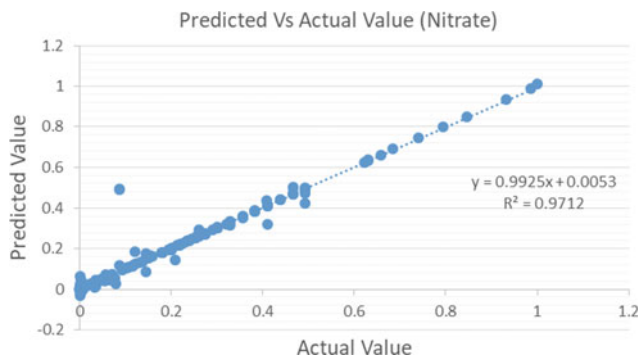
Fig. 2 The regression plot for ANFIS Model 5

4 Discussion

Based on the results in Sect. 3, it has shown that most of ANFIS models have achieved wonderful outcomes. Most of the models also obtained line of best fit in regression plots and achieved high accuracy in prediction. Past researches also have proven that using ANFIS to predict river water quality do obtained good outcome. Ranković et al. (2012) have used ANFIS method to predict dissolved oxygen (DO) in Gruža reservoir in Serbia. Eight parameters of water quality as inputs for the model have been used by the authors. The authors have achieved the respective values for the mean square error (MSE) and the mean absolute error (MAE) for the comparisons of measured and ANFIS predicted values of DO which were 0.6670 and 1.23 for test set while 1.0373 and 2.1831 for training and test set (Ranković et al. 2012). Meanwhile, Sonmez et al. (2018) have applied ANFIS for prediction of cadmium (Cd) concentrations in Fliyos River, Turkey. The performance parameters that have been used were R^2, mean absolute deviation (MAD), mean absolute percentage error (MAPE), MSE and Nash–Sutcliffe efficiency. The results obtained shown that relatively higher correlation value, $R^2 = 0.91$ was found between modelled and observed Cd concentrations. Thus, it indicated that ANFIS model gave good estimations with high degree robustness and accuracy for the concentrations of cadmium (Sonmez et al. 2018). Abba et al. (2019) on the other hand have used ANFIS, auto regressive integrated moving average (ARIMA) and ANN model in modelling WQI at Yamuna River, India and Kinta River, Malaysia. The result has shown that ANFIS-III with 5 input parameters, triangular membrane function and 2 membership function (5, trimf, 2) was the best model in predicting WQI for calibration and verification phase for both Kinta and Agra stations. Thus, ANFIS has proven to be the optimal performance in predicting the water quality index for both regions (Abba et al. 2019). Therefore, ANFIS models have been proven as an excellent approach to predict water quality parameters in

rivers since it able to provide high accuracy prediction with low errors while developing the modelling.

5 Conclusion

Six ANFIS models have been developed successfully for prediction of six different parameters of water quality in Langat River. Five of the ANFIS models have achieved high value of R^2 and low value for RMSE in all three data sets. ANFIS Model 3 is the only model that has obtained poor results and achieved low accuracy to predict the river water quality. For future study, the models can be upgraded to an advance predictive modellings to predict the water quality parameters.

References

S.I. Abba, S.J. Hadi, J. Abdullahi, River water modelling prediction using multi-linear regression, artificial neural network, and adaptive neuro-fuzzy inference system techniques. Procedia Computer Science **120**, 75–82 (2017)

S.I. Abba, A.S. Maihula, M.B. Jibril, A.M. Sunusi, M.A. Ahmad, M.A. Saleh, Application of data driven algorithms for the forecasting of non-linear parameter. International Journal of Recent Engineering Science **6**(2) (2019)

S.I. Abba, S.J. Hadi, S.S. Sammen, S.Q. Salih, R.A. Abdulkadir, Q.B. Pham, Z.M. Yaseen, Evolutionary computational intelligence algorithm coupled with self-tuning predictive model for water quality index determination. J. Hydrol. **587**, 124974 (2020)

A.N. Ahmed, F.B. Othman, H.A. Afan, R.K. Ibrahim, C.M. Fai, M.S. Hossain et al., Machine learning methods for better water quality prediction. Journal of Hydrology **578**, 124084 (2019)

F. Al-Badaii, M. Shuhaimi-Othman, M.B. Gasim, Water quality assessment of the Semenyih river, Selangor, Malaysia. Journal of Chemistry (2013)

A. Azad, H. Karami, S. Farzin, S.F. Mousavi, O. Kisi, Modeling river water quality parameters using modified adaptive neuro fuzzy inference system. Water Science and Engineering **12**(1), 45–54 (2019)

E.K. Lafdani, A.M. Nia, A. Ahmadi, Daily suspended sediment load prediction using artificial neural networks and support vector machines. J. Hydrol. **478**, 50–62 (2013)

V. Ranković, J. Radulović, I. Radojević, A. Ostojić, L. Čomić, Prediction of dissolved oxygen in reservoirs using adaptive network-based fuzzy inference system. J. Hydroinf. **14**(1), 167–179 (2012)

N.N.M. Rizal, River water quality prediction using artificial intelligence approach: literature review. Journal of Energy and Environment (2020)

B.H.Z. Sami, B.F.Z. Sami, C.M. Fai, Y. Essam, A.N. Ahmed, A. El-Shafie, Investigating the reliability of machine learning algorithms as a sustainable tool for total suspended solid prediction. Ain Shams Engineering Journal (2021)

A.Y. Sonmez, S. Kale, R.C. Ozdemir, A.E. Kadak, An adaptive neuro-fuzzy inference system (ANFIS) to predict of cadmium (Cd) concentrations in the Filyos River, Turkey. Turk. J. Fish. Aquat. Sci. **18**(12), 1333–1343 (2018)

S. Tyagi, B. Sharma, P. Singh, R. Dobhal, Water quality assessment in terms of water quality index. American Journal of Water Resources **1**(3), 34–38 (2013)

Engineering-Economic Evaluation of Al-Fashir 5 MWp Mini-Grid Connected Photovoltaic Power Plant

Mahmoud Hassan Onsa and Eptihal Sir Elkhatim Hassan Modwi

Abstract

Sudan's power sector is subject to frequent power discontinuity due fiscal and engineering problems. The Sudan has high solar irradiation eventuality, which is a radical solution to the problem of lack of electricity supply. Mini-grid system solar networks are a wise solution for such a wide country. This paper evaluates the Sudan first large solar photovoltaic (PV) operation (5 MWp) at Al-Fashir, in terms of power, cost, saving, responsibility and dependability. The project commissioned in 2020 for $6.8 M (turnkey price) and since then it is ready to supply a town to assist the 12 MW diesel power stations. The diurnal energy production is 31–28 MWh, this saves 7 tons of the gas-oil normally used by the diesel power plant. For a normal cost of the 1-Ton gas-oil of $600, the station will have a payback period of 3.2 years. From Al-Fashir mini-grid analysis, the five analogous power plants could be erected to assist the diesel plants partially for the daytime base load.

1 Introduction

Frequent electricity break is one of the key power issues in Sudan that attributed to engineering and financial problems. Solar power potential is seen as a great solution to the rapid demand in Sudan, which is a thorough solution to the problem of lack of electricity production. As the country is stretched over a wide area, a mini-grid networks of solar system is a visible and promising solution. Al-Fashir city is in the west region of Sudan at 13° 38′ N 25° 22′ E, at an altitude of 700 m above sea level at a distance of 802 km west of the capital Khartoum, and 195 km northeast to the city of Nyala. This work assesses the large and first application of solar photovoltaic in the Sudan at Al-Fashir city and dictates how much PV to be applied for Al-Fashir to partially assist the old diesel plants for the daytime base load.

The technological advance resulted in reduction in price and increase in the efficiency of the power production and transmission devices. The solar PV took the lion share in this advance (Technical report 2020). Eltayeb and Hamza addressed the using of solar and wind and other renewables to solve part of energy need for Al-Fashir (Eltayeb and Hamza 2018). This paper evaluates the use of the new erected PV power station.

2 Al-Fashir Power Station

The first power station initiated at Al-Fashir was in 1976, large generating units were set in 2000 (1 MW), 4 × 2.5 MW was installed in 2016. Till now there are more Thermal units planned to be installed. At the time of introducing the PV scheme at 2018, almost 20 MW were in operation.

The PV power station started in early 2018, the project commissioned and its operation transferred in 2020 to the Electricity Distribution Company (Fig. 1).

3 Operation of Al-Fashir PV Power Station

Table 1 show the net electricity generated in the first year. A total of 9.8372 GWh was generated in the base year. The monthly generation in the subsequent year is almost the same as the base year, from the tables of the (information

M. H. Onsa (✉) · E. Sir Elkhatim Hassan Modwi
University of Khartoum, Khartoum, Sudan
e-mail: onsa@uofk.edu

Fig. 1 Arial view of Al-Fashir
PV solar power station. *Source*
https://www.google.com/maps/

Area: 89,216 m^2
Border: 1,187 m

Table 1 The 5 MWp station
Monthly power generation
(Technical Report 2020)

	Month	Power generated [GWh]		Month	Power generated [GWh]
1	Jan	0.9028	7	Jul	0.7243
2	Feb	0.8515	8	Aug	0.7328
3	Mar	0.9213	9	Sep	0.7734
4	Apr	0.8394	10	Oct	0.8542
5	May	0.9215	11	Nov	0.8496
6	Jun	0.8394	12	Dec	0.08371

Total = 9.837 GWh in the year 2019

from the operations company). This information was compared with the aid of that from software (SMA Solar Technology 2021), and IRENA report 2020 (IRENA 2020).

The project commissioned in 2020 and connected to Al-Fashir mini-grid. Table 1 shows the base year energy (2019) production. It shows a near steady energy production, similarly Fig. 2 show the diurnal production in the month October 2020. From the record of the subsequent year the production and the connection to the grid goes smoothly almost all the time, thanks to the advance in harmonization between the two energy sources done by the advanced `electronic circuits.
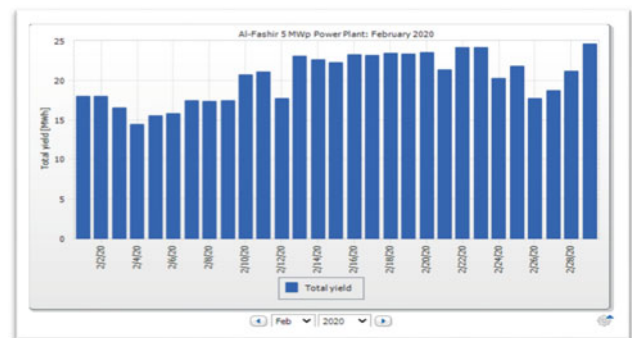
Fig. 2 Total energy yield in October 2020

4 The Economic Analysis

Table 1 shows the net electricity generated 9.837 GWh in the base year; this gives 0.225-capacity or utilization factor. The monthly generation in the subsequent year is almost the same as the base year, as depicted from the performance tables (information from the operations company), see Fig. 2. The power generated from the PV station reduced the diesel oil consumption by 7 t/day. This information from the operator; was supported by the value from textbooks and research papers, (Design review Report 2018; Technical report on the solar power plant in Al Fashir; Kanoglu et al. 2005).

The total cost of this 5 MWp power station is $6.84 M (turnkey price), the price include the location preparation,

securing a water supply source, PV modules, inverters and cable to the grid. Since commissioning, it is ready to supply electricity to the town as in Table 1. This station gives support to the stations (diesel-powered) with 20 MW. The diurnal production of energy is 31–28 MWh, and saves seven tons of the gas-oil normally used by the plant that diesel-powered. Taking the cost of one-Ton gas-oil as $600.00, the payback period of the station will have 3.2 years.

Table 2 demonstrates the parameters used to calculate the leveled cost of electricity. The value of $0.0361/kWh is quite comparable with the world average of $0.057/kWh, and the lowest value in the Saudi Arabia of $0.017/kWh.

Table 2 Parameters for calculating the LCOE

Plant capacity	5 MWp	Life time	25 year
Energy yield	9.837×10^6 kWh	Capacity factor	0.225
Annual O. & M.	$250,000	Initial capital cost	$8,640,000
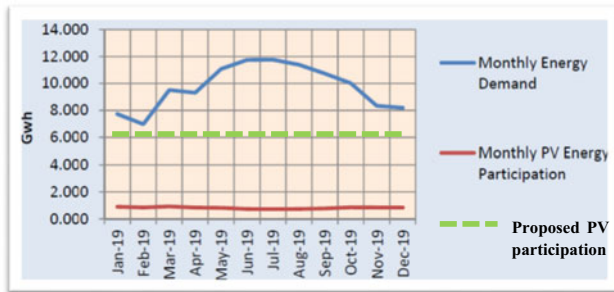
Fig. 3 The current (2019) energy demand and PV participation and the proposed PV participation

5 Upgrading of Al-Fashir Power Generation

Figure 3 shows the energy demand and the participation of PV energy. If 25 MW PV installed it will fulfill the daytime demand and enhance he reduction of fuel consumption a rather good penetration of PV into the existing system.

6 Conclusion

The 5 MWp PV station at Al-Fashir has a payback period of 3.2 year, which is good for a solar energy application this due to lower price of equipment and preparation. The LCOE is also low. Besides that, the environmental benefit is very large. It is highly recommended to go for further addition of PV module to reach a 30 MWp for the current situation. A formula for the share of PV to diesel is derived to assist future expansion of such schemes in the Sudan. Current price of installing such a power plants is getting down. It is recommended to continue in installing such system for remote cities and to set regulations to use PV sublimated diesel power plants, and to study the use of battery assisted PV power plants.

References

Design Review Report 5 MWP photovoltaic for AL fashir and Al Deain power station, 23 July 2018

K.O.H Eltayeb, M.M. Hamza, Utilization of renewable energy resources in Al-Fashir city, in 2018 International Conference on Computer, Control, Electrical, and Electronics Engineering (ICC-CEEE) (2018)

IRENA, renewable power generation cost in 2020. Accessed June 2021. https://www.irena.org/publications/2021/Jun/Renewable-Power-Costs-in-2020

M. Kanoglu, S.K. Işık, A. Abuşoğlu, Performance characteristics of a diesel engine power plant. Energy Convers. Manage. **46**, 1692–1702 (2005)

SMA Solar Technology, Sunny Portal powered by ennexOS. Accessed March 2021

Technical report on the solar power plant in Al Fashir

Technical report on the solar power plant in El Fashir (2020)

Landslide Susceptibility Mapping with Stacking Ensemble Machine Learning

Mahmud Iwan Solihin, Yanto, Gasim Hayder, and Haris Al-Qodri Maarif

Abstract

Landslide susceptibility mapping (LSM) is an important preliminary effort to reduce the risk and harshness of landslide disasters. While numerous methods have been proposed, machine learning (ML) is the most popular approach that has been applied across the globe. One of the prominent methods to improve machine learning accuracy is by using ensemble method which basically employs multiple base models. In this paper, the stacking ensemble method is used to increase the accuracy of the machine learning model for LSM where the base (first-level) learners use five ML algorithms namely decision tree (DT), k-nearest neighbor (KNN), AdaBoost, extreme gradient boosting (XGB) and random forest (RF). The second-level learner uses logistic regression (LR) to aggregate the final prediction output. The landslide data together with its conditioning factors (feature variables) collected from three districts in the Central Java Province, Indonesia, has been used as the case study for the LSM. As the data are extremely imbalanced, Adaptive Synthetic (ADASYN) resampling technique was picked to balance the data between two classes, i.e., landslide and non-landslide. This is because the occurrence of non-slide incidents is much more than the landslide. The evaluation results of the LSM performance show that the proposed stacking ensemble ML improves the overall accuracy of the individual base ML model even when it is compared with RF which is naturally also ensemble ML.

Keywords

Landslide susceptibility mapping • Stacking ensemble • Machine learning algorithms • Imbalanced classification

1 Introduction

A total of 11,033 landslides induced by rainfall have been reported in the period of 2007–2019 globally based on Global Landslide Catalog (GLC). In Indonesia, landslide is always the third rank of natural disaster in term of the number of events with reported annual average of approximately 648 events (https://gis.bnpb.go.id/). Developing landslide susceptibility mapping (LSM) is an initial step for landslide disaster mitigation planning to lessen the risk and severity to humans. Areas prone to landslide need to be mapped accurately.

Landslide occurs when the slope is unstable (Yanto et al. 2021a). The downslope movement in landslide includes soil, rock and organic materials under the driving force of gravity effect (Wu et al. 2020). This occurrence is caused by many factors such as geographical spatial location, soil mechanical characteristics, rainfall. This is called landslide conditioning factors.

There are numerous studies conducted nowadays in developing LSM involving hybrid approaches in computer science using machine learning (ML) and metaheuristic optimization. ML algorithms such as neural networks (NN), decision tree (DT), support vector machine (SVM) and random forest (RF) including deep learning (DL) can be used as standalone predictor in LSM. These can be found in

M. I. Solihin (✉)
Department of Mechanical and Mechatronics Engineering, UCSI University, Kuala Lumpur, Malaysia
e-mail: mahmudis@ucsiuniversity.edu.my

Yanto
Department of Civil Engineering, Jenderal Soedirman University, Purwokerto, Indonesia

G. Hayder
Department of Civil Engineering, College of Engineering, Universiti Tenaga Nasional (UNITEN), 43000 Kajang, Selangor Darul Ehsan, Malaysia

H. A.-Q. Maarif
Computer Science Department, Nusa Putra University, Sukabumi, Indonesia

studies (Wu et al. 2020; Wang et al. 2020a, b). A review paper on this subject has been discussed (Huang and Zhao 2018). In addition, some studies involve metaheuristic optimization algorithms such as particle swarm and gray wolf optimization to optimize the parameters in the machine learning (Ling et al. 2021; Balogun et al. 2021; Jaafari et al. 2019; Zhang et al. 2020; Moayedi et al. 2019). These approaches are basically data-driven method in addition to the two other methods in LSM, namely knowledge-based and physics-based methods (Huang and Zhao 2018).

Ensemble machine learning emerges as an effort of improving prediction accuracy of individual ML model by combining multiples ML model into final prediction output. RF is one of the best ensemble ML that performs well in many applications including LSM. For LSM application, this has been investigated in Goetz et al. (2015) and reviewed in Huang and Zhao (2018). Furthermore in a study by Micheletti et al. (2013), RF and AdaBoost are proven to be more efficient algorithm than adaptive SVM.

This paper further implements another approach of ensemble ML, called stacking ensemble, for LSM application. In the stacking ensemble ML, some ML algorithms will be used as first-level (base) learners, and logistic regression (LR) will be used as the second-level learner to aggregate the outputs of first-level learners and come up with the final prediction output (Nordhausen 2013). The result will further improve the result of LSM using RF previously developed by the authors (Yanto et al. 2021b).

2 Area of Study and Data

For the LSM case study in this paper, the data of landslide and its conditioning factors were collected from three regencies in the Middle Western Central Java, Indonesia, namely Banyumas, Purbalingga and Banjarnegara. The map of these three districts is shown in Fig. 1. This area spreads on 3420 km² surrounded by mountainous border with surface gradient up to 37° and elevation up to 3 km above sea level. Geologically, it is composed by intrusive and extrusive igneous rocks in the high altitude and sedimentary rock in the low altitude that account for 37% and 63%, respectively. Hydrologically, it has a typical of tropical climate with annual rainfall of 1955 mm in lowland and up to 4722 mm in highland.

A total of 10 variables were compiled as landslide conditioning factors that can be classified as topographic data (elevation, aspect, slope, profile curvature, plan curvature and topographic wetness index), soil mechanical data (depth to surface of rupture, cohesion and friction angle) and rainfall data. Several data sources are used in this study including digital elevation method (DEM) from DEMNAS (https://tanahair.indonesia.go.id/demnas/#/), field measurement and laboratory test from the Laboratory of Civil Engineering, Jenderal Soedirman University and station-based precipitation from the Center of Water Resources Research and Development, Ministry of Public Works, Indonesia.

Since the original data collected within the year of 2005 to 2018 have various spatial scale, some interpolation techniques were employed to unify the spatial pixel. Soil mechanical properties data were interpolated using Ordinary Kriging, topographic data were generated using QGIS Point Sampling Tool and rainfall data were assigned on the pixel based on the value produced by Polygon Thiessen method (Yanto et al. 2021a). All data in this study were gridded on 200 m spatial pixel size resulting 83,597 instances of total data with the 10 variables as the ML feature input and the landslide event (ground truth) as the target variable. However, in the target variable, only 218 landslide events (as compared to 83,389 non-landslide) were observed which creates extreme imbalanced dataset for the ML to learn as classification problem. This imbalance will be treated before used in the ML training.

Figure 2 shows the boxplot of the resulting dataset used in this study. As we can see, some variables have clearly distinctive correlation to landslide. For example, the higher median value of slope and rainfall is observed for landslide cases, and this makes sense.

3 Methodology

3.1 Data Treatment and Machine Learning Model Development

As the normal practice in ML model building, the dataset is split into training and testing set with ratio of 75% and 25%, respectively. This is performed by using stratified random sampling to make sure that each class has balanced amount in terms of categorical target variable, i.e., landslide.

Prior to this data splitting, imbalance data treatment has been performed using Adaptive Synthetic (ADASYN) up sampling technique. ADASYN is used to generate more synthetic data for minority class (landslide events) using weighted distribution in order to prevent bias learning introduced to class (categorical) imbalance (He et al. 2008). ADASYN is an improvement of the previously well-known imbalance data treatment method called Synthetic Minority Over-sampling Technique (SMOTE) (Chawla et al. 2002). It finds the n-nearest neighbors in the minority class for each of the samples in the class. Then it draws a line between the neighbors and generates random points on the lines. After creating those samples, ADASYN does minor improvement by adding a random small value to the points thus making it more realistic.

Fig. 1 Geographical map of the study area for LSM
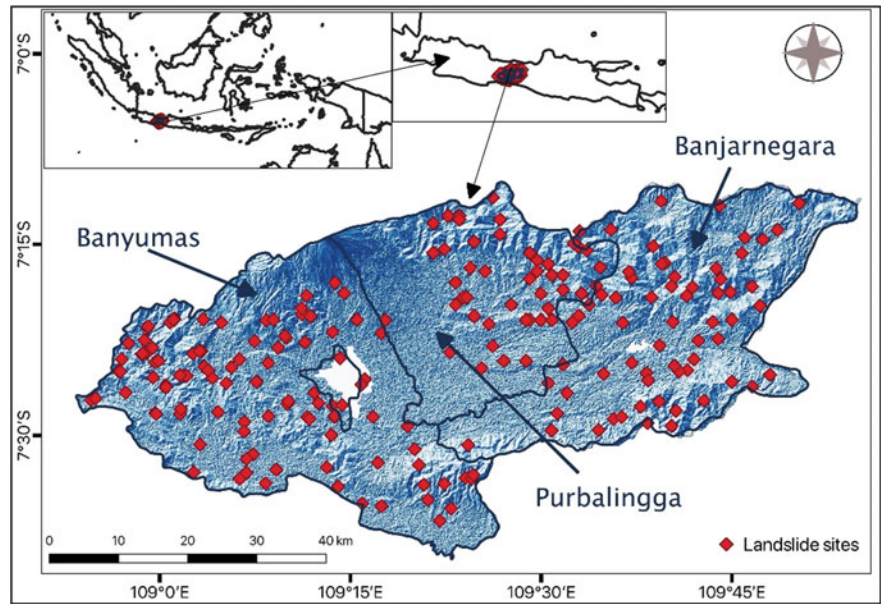
Fig. 2 Box plot of the dataset for LSM
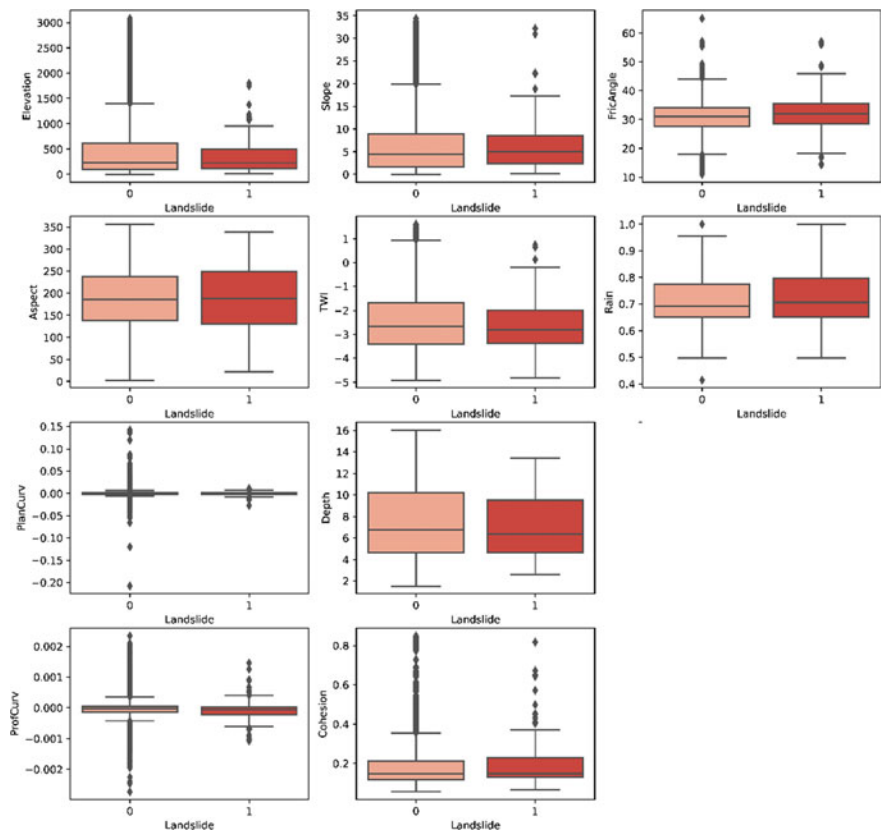
3.2 Stacking Ensemble Machine Learning

The idea of ensemble ML is basically creating multiple ML models and aggregates the final prediction using a certain method to improve the accuracy of each individual base model performance. There are fundamentally three methods of ensemble, namely bagging (bootstrap aggregating), boosting and stacking.

Bagging often entails training each model on a distinct sample of the same training dataset using a single machine learning technique, almost always an unpruned decision tree (DT). The ensemble members' forecasts are then merged

using simple statistics like voting or average (Zhang and Ma 2012). Random forest (RF), which is essentially a bagging ensemble of DT, is a common example of bagging ensemble approach.

Boosting, on the other hand, entails the employment of 'weak learners' which are very simple decision trees that only make one or a few decisions. Simple voting or averaging is used to combine the forecasts of the poor learners, though their contributions are weighed proportionally to their performance or competence. The goal is to create a 'strong learner' from a group of 'weak learners.' Popular boosting ensemble approaches include adaptive boosting (AdaBoost) and Extreme Gradient Boosting (XGB).

Furthermore, we use stacking ensemble ML in this paper. In stacking ensemble, two levels of learning are used where first-level (base) learners can be different ML algorithms, and second-level learner is used to combine the predictions which is normally a logistic regression for classification. Here, the proposed stacking ensemble ML algorithm uses five ML algorithms, namely k-nearest neighbor (KNN), decision tree (DT), AdaBoost, extreme gradient boosting (XGB) and random forest (RF), as first-level learners. The second-level learner uses logistic regression (LR) to aggregate the final output (see Fig. 3 for the diagram). Thus, suppose that $\hat{y}_i$ is the prediction output of the respective first-level learners, the final prediction can be expressed as:

$$\hat{y}_{\text{output}} = \text{logreg}(\hat{y}_{\text{KNN}}, \hat{y}_{\text{DT}}, \hat{y}_{\text{Adaboost}}, \hat{y}_{\text{XGB}}, \hat{y}_{\text{RF}}) \quad (1)$$

The experiment is implemented in Python programming language. Noted that we purposely do not include popular ML algorithm such as neural networks (NN) and support vector machine (SVM) in the first-level learners as these excellent algorithms are computationally expensive and complicated in terms of hyperparameters tuning. We use only those five ML algorithms in the first-level learners which are computationally simple as they are based on DT except for KNN. Those five ML algorithms only involve simple hyperparameters tuning. The hyperparameters setup for these algorithms implementation in the stacking ensemble can be listed in Table 1.
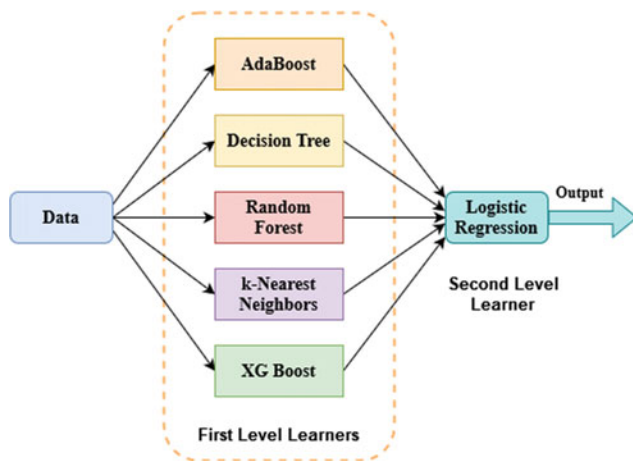
4 Results and Evaluation

The problem in LSM using ML is handled as binary classification problem. Therefore, the performance evaluation of the ML models is mainly based on the confusion matrix. From the confusion matrix, some metrics can be derived as listed in Table 2. The quantitative terms used in Table 2 can be seen from the confusion matrix where TP, TN, FP and FN mean true positive, true negative, false positive and false negative, respectively. For instance, FP reflects the pixels which are non-landslide but predicted as landslide by the ML model.

In this regards, higher value of FP is saver than higher value of FN. Consequently, in LSM application, beside the accuracy and AUC, the model that produces lower FN (higher recall) is preferable than higher precision if these two metrics are disputable. Furthermore, accuracy can be misleading metric especially in the case of extreme imbalance dataset. This is because predicting all outputs as majority class (non-landslide) will give high accuracy despite zero F1 score. AUC provides more reliable metric in this case. After the model training (learning the data), the model performance will be evaluated using the whole set of original data (75% training dataset combined with 25% testing dataset excluding the synthetic data).

The evaluation results of all ML models for LSM tested on full original data are presented as confusion matrix as shown in Table 3. Each base learner is tested individually and compared with the proposed stacking ensemble ML model. As we can see, the advantage of stacking ensemble ML model in LSM is clear where only 38 false predictions (FP + FN) are observed. The only closest competitor is from RF where 62 false predictions (FP + FN) are observed out of 83,597 data instances. This is understandable since RF is naturally also ensemble method, i.e., ensemble of DTs.

Further comparison of the metric (as listed in Table 2) is shown in Table 4. As mentioned earlier, all models can give high accuracy here except for KNN which seems to produce bias result with the lowest $F1$ score, among others. The proposed stacking ensemble ML method can produce very high values of all the metrics. This result again clearly shows the advantage of ensemble ML including RF and stacking ensemble.

Fig. 3 Stacking ensemble ML method proposed

Table 1 Hyperparameter(s) setup for the ML algorithms in the stacking ensemble

First-level learners	ML algorithm	Hyperparameters setup
	KNN	Number of neighbors (k) = 5
	Decision Tree	Tree depth limit = 100
	AdaBoost	Number of estimators = 50, Learning rate = 0.3
	XGBoost	Number of trees = 100, Learning rate = 0.3 (defaults)
	Random Forest	Number of trees = 100
Second-level learner	Logistic regression	Use L1-Lasso regularization

Table 2 Performance metrics generally used in classification problems

Performance metrics	Description	Formula
Accuracy	Ratio of correctly predicted pixels to the total pixels (data instances)	$\frac{TP+TN}{TP+FP+FN+TN}$
Precision	Ratio of correctly predicted Landslide (1) pixels to the total predicted Landslide (1) pixels	$\frac{TP}{TP+FP}$
Recall F1 AUC	Ratio of precisely predicted Landslide (1) pixels to all actual Landslide (1) pixels. Weighted average of precision and recall. How much the model is capable of distinguishing between classes. Higher AUC close to 1 means good separation capability	$\frac{TP}{TP+FN}$ $\frac{2\times Recall\times Precision}{Recall+Precision}$ Calculated as the area under receiver operating characteristic (ROC) curve

Table 3 Confusion matrix comparison for all ML models in LSM

KNN	Predicted: NO	Predicted: YES		DT	Predicted: NO	Predicted: YES	
Actual: NO	TN = 68385	FP = 15004	83389	Actual: NO	TN = 81112	FP = 2277	83389
Actual: YES	FN = 0	TP = 208	208	Actual: YES	FN = 36	TP = 172	208
	68385	15212			81148	2449	
AdaBoost	Predicted: NO	Predicted: YES		XGB	Predicted: NO	Predicted: YES	
Actual: NO	TN = 83105	FP = 284	83389	Actual: NO	TN = 81505	FP = 1884	83389
Actual: YES	FN = 11	TP = 197	208	Actual: YES	FN = 21	TP = 187	208
	83116	481			81526	2071	
RF	Predicted: NO	Predicted: YES		Stack ensemble ML	Predicted: NO	Predicted: YES	
Actual: NO	TN = 83328	FP = 61	83389	Actual: NO	TN = 83355	FP = 34	83389s
Actual: YES	FN = 1	TN= 207	208	Actual: YES	FN = 4	TP = 204	208
	83329	268			83359	238	

Table 4 Metric comparison of all ML models for the LSM

ML model	AUC	Accuracy	Precision	Recall	F1
KNN	0.992	0.821	0.998	0.821	0.899
DT	0.926	0.972	0.997	0.972	0.984
AdaBoost	0.972	0.996	0.998	0.996	0.997
XGB	0.992	0.977	0.997	0.977	0.986
RF	≈1	0.999	≈1	0.999	0.999
Stacking ensemble ML	≈1	≈1	≈1	≈1	≈1

5 Conclusions

As the conclusion, LSM using ensemble machine learning (ML) algorithms has been proposed. The advantage of using ensemble ML including random forest (RF) and stacking ensemble machine learning has been presented. Compared to random forest, the proposed stacking ensemble machine learning provides slightly better where smaller number of false predictions is observed. This study purposely does not include complicated and computationally expensive ML algorithms such as neural networks and support vector machines as they require extensive hyperparameters tuning. Including of these two algorithms in the first-level learners in the stacking ensemble can further improve the result provided that the hyperparameters tuning is performed properly.

References

A.L. Balogun, F. Rezaie, Q.B. Pham, L. Gigović, S. Drobnjak, Y.A. Aina, M. Panahi, S.T. Yekeen, S. Lee, Spatial prediction of landslide susceptibility in western Serbia using hybrid support vector regression (SVR) with GWO, BAT and COA algorithms. Geosci. Front. **12** (2021). https://doi.org/10.1016/j.gsf.2020.10.009

N.V. Chawla, K.W. Bowyer, L.O. Hall, W.P. Kegelmeyer, SMOTE: synthetic minority over-sampling technique. J. Artif. Intell. Res. **16**, 321–357 (2002). https://doi.org/10.1613/JAIR.953

J.N. Goetz, A. Brenning, H. Petschko, P. Leopold, Evaluating machine learning and statistical prediction techniques for landslide susceptibility modeling. Comput. Geosci. **81**, 1–11 (2015). https://doi.org/10.1016/J.CAGEO.2015.04.007

H. He, Y. Bai, E.A. Garcia, S. Li, in *ADASYN: adaptive synthetic sampling approach for imbalanced learning*. Proceedings of the International Joint Conference on Neural Networks, 2008, pp. 1322–1328

Y. Huang, L. Zhao, Review on landslide susceptibility mapping using support vector machines. CATENA **165**, 520–529 (2018). https://doi.org/10.1016/j.catena.2018.03.003

A. Jaafari, M. Panahi, B.T. Pham, H. Shahabi, D.T. Bui, F. Rezaie, S. Lee, Meta optimization of an adaptive neuro-fuzzy inference system with grey wolf optimizer and biogeography-based optimization algorithms for spatial prediction of landslide susceptibility. CATENA **175**, 430–445 (2019). https://doi.org/10.1016/j.catena.2018.12.033

Q. Ling, Q. Zhang, Y. Wei, L. Kong, L. Zhu, Slope reliability evaluation based on multi-objective grey wolf optimization-multi-kernel-based extreme learning machine agent model. Bull. Eng. Geol. Environ. **80**, 2011–2024 (2021). https://doi.org/10.1007/s10064-020-02090-5

N. Micheletti, L. Foresti, S. Robert, M. Leuenberger, A. Pedrazzini, M. Jaboyedoff, M. Kanevski, Machine learning feature selection methods for landslide susceptibility mapping. Math. Geosci. **46**, 33–57 (2013). https://doi.org/10.1007/S11004-013-9511-0

H. Moayedi, M. Mehrabi, M. Mosallanezhad, A.S.A. Rashid, B. Pradhan, Modification of landslide susceptibility mapping using optimized PSO-ANN technique. Eng. Comput. **35**, 967–984 (2019). https://doi.org/10.1007/s00366-018-0644-0

K. Nordhausen, Ensemble methods: foundations and algorithms by Zhi-Hua Zhou. Int. Stat. Rev. **81**, 470–470 (2013). https://doi.org/10.1111/INSR.12042_10

Y. Wang, Z. Fang, M. Wang, L. Peng, H. Hong, Comparative study of landslide susceptibility mapping with different recurrent neural networks. Comput. Geosci. **138**, 104445 (2020a). https://doi.org/10.1016/j.cageo.2020.104445

H. Wang, L. Zhang, K. Yin, H. Luo, J. Li, Landslide identification using machine learning. Geosci. Front. (2020b). https://doi.org/10.1016/j.gsf.2020.02.012

Y. Wu, Y. Ke, Z. Chen, S. Liang, H. Zhao, H. Hong, Application of alternating decision tree with AdaBoost and bagging ensembles for landslide susceptibility mapping. CATENA **187**, 104396 (2020). https://doi.org/10.1016/j.catena.2019.104396

Yanto, A. Apriyono, P.B. Santoso, Sumiyanto landslide susceptible areas identification using IDW and Ordinary Kriging interpolation techniques from hard soil depth at middle western Central Java, Indonesia. Nat. Hazards (2021a). https://doi.org/10.1007/S11069-021-04982-5

Yanto, M.I. Solihin, G. Sugiyanto, in *The effect of spatial scales and imbalanced data treatment on the landslide susceptibility mapping using random forest*. AIP Conference Proceedings **2482**(1), 050006 (2021b). https://doi.org/10.1063/5.0111326

C. Zhang, Y. Ma, Ensemble machine learning : methods and applications. SpringerLink (Online service) **329** (2012)

L. Zhang, X. Chen, Y. Zhang, F. Wu, F. Chen, W. Wang, F. Guo, Application of GWO-ELM model to prediction of caojiatuo landslide displacement in the three gorge reservoir area. Water (Switzerland) **12** (2020). https://doi.org/10.3390/w12071860

Phosphorus Removal from Synthetic Wastewater by Using Palm Oil Clinker as Media in Continuous Activated Sludge

Baker Nasser Saleh Al-dhawi, Shamsul Rahman Mohamed Kutty,
Lavania Baloo, Najib Mohammed Yahya Almahbashi,
Aiban Abdulhakim Saeed Ghaleb, Ahmad Hussaini Jagaba,
Vicky Kumar, and Anwar Ameen Hezam Saeed

Abstract

The presence of large amounts of phosphorus in wastewater is one of the primary causes of eutrophication, which has a detrimental impact on many natural water bodies. Prior to discharge to the stream, wastewater treatment plants should remove phosphorus from the effluent. In this study, (POC) is used as submerged attached growth systems to be introduced into the aeration tank of activated sludge systems which was evaluated for the removal phosphorus PO_4 from synthetic wastewater. The experiments were conducted into different influent flow rates ranging from 5, 10, 15, 20, 25, and 30 L/d. Sampling was conducted every two days from the influent and effluent points. Parameters such as Phosphorus were monitored. Generally, PO_4 was highly removed. The average removal of PO_4 reached 88% for reactor A while 77% for reactor B with flowrate 5L/d. While for the first order kinetic model the substrate removal rate (K_1) was found as 5 and 3.9 per day with a correlation coefficient (R^2) of 0.9721 and 0.9718 for reactor A and B, respectively.

Keywords

Phosphorus • Attach growth media • Kinetic • Synthetic wastewater • Biological processes

1 Introduction

Phosphorus is a vital mineral for plant and animal development. However, phosphorus enrichment in water bodies such as rivers, and, lakes could cause abnormal development of hydrophytes, resulting in degradation of water quality and, eventually, eutrophication (Weihrauch and Weber 2020). Thus, phosphorus should be removed from domestic and industrial wastewater before being discharged into the stream (Bawiec 2019; Ayaz et al. 2012).

These nutrients are clearly in charge of the eutrophication (abnormal development of algae caused by an excess of nutrients in water bodies) of rivers, lakes, and oceans across the world. As a result, wastewater disposal creates a continual danger to the world's fresh water supply (Stewart et al. 2008; Noor et al. 2021).

Before discharge wastewater into bodies of water, phosphorus removal is typically required; but, in many situations, this is not done, resulting in widespread pollution on a global scale (De-Bashan and Bashan 2004). To remove phosphorus from wastewater, many techniques are currently used. While some of them are utilized in large-scale treatment facilities, others are just experimental initiatives, and as a result, are still being utilized on a short scale basis (De-Bashan and Bashan 2004). Phosphorus is eliminated in all situations by transforming the phosphorus ions in wastewater into a solid fraction. This percentage may consist of an insoluble salt precipitate, a microbiological mass in activated sludge, or plant biomass in built wetlands. Because phosphorus is extracted alongside other waste products, some of which are hazardous, these methods do not recycle phosphorus as a really sustainable product (Robles et al. 2020). Non-solubilized phosphates are either buried in landfills following organic waste incineration or utilized as sludge fertilizer if the treatment plant removes human pathogens and hazardous chemicals (Jagaba et al. 2021). In this research, the Palm Oil Clinker by-product, the residue from the steam boiler of the palm oil mill (Al-dhawi et al. 2020),

Baker Nasser Saleh Al-dhawi (✉) · S. R. M. Kutty · L. Baloo ·
Najib Mohammed Y. Almahbashi · Aiban Abdulhakim
Saeed Ghaleb · Ahmad Hussaini Jagaba · V. Kumar ·
Anwar Ameen Hezam Saeed
Universiti Teknologi PETRONAS, 32610 Seri Iskandar,
Perak Darul Ridzuan, Malaysia
e-mail: bakeraldhawi@gmail.com

is to be used as an attached growth system. The POC will be processed before being applied as an attached growth system. The effectiveness and efficiencies of using Palm Oil Clinker as attached growth media in the combined attached growth/conventional system in the removal of Phosphorus will be evaluated.

each reactor. All the reactors were run in suspended mode. Reactor A was act as Palm Oil Clinker submerged media in aeration tank and received the feeding from an influent source. Reactor B was act as control and received the feeding from influent sources. Operating parameters monitored during the study include (PO_4).

2 Methods and Materials

Two parallel continuous flow activated sludge systems treating synthetic domestic wastewater. In Reactor A, POC was used as the submerged attached growth media while Reactor B was used as a control reactor. Aeration and clarifier zones are present in both reactors A and B as shown in Fig. 1.

Continuous activated sludge reactor (CASR), reactors were fed synthetic wastewater until they reached a steady state. The working sludge age was maintained between 15 and 25 days. To realize the required sludge, about 10 mL of (MLSS) was taken every two days from the aeration tank for

3 Results and Discussion

3.1 Experimental Results for Removal of Phosphorus PO_4

Phosphorus removal in the experimental operation was shown in the Fig. 2. The experimental approach evaluated the impact of flow rate on phosphorus removal. The flowrate was varied in the range of 5, 10, 15, 20, 25, and 30 L/d, respectively. The average influent PO_4 was at 9 and 11 mg/L at various. The average effluent PO_4 was at 1.1, 1.7, 2.3, 2.7, 3, and 3.4 mg/L and 2, 2.5, 3, 3.5, 4, and 4.5 mg/L for reactor A and B, respectively.

Fig. 1 Process flow schematic (CASR)
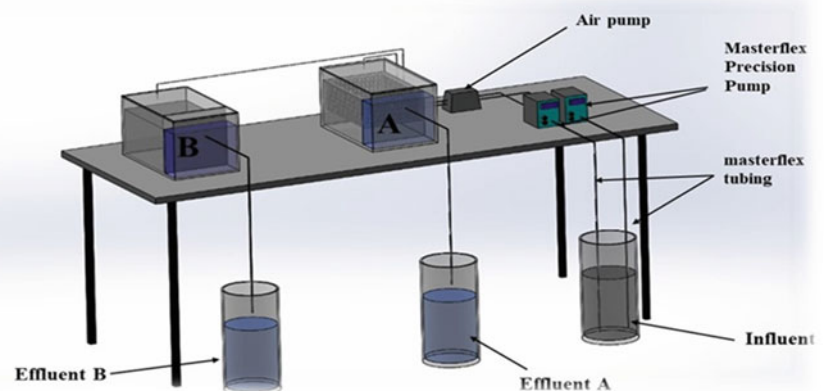
Fig. 2 Influent and effluent phosphorus versus sampling days
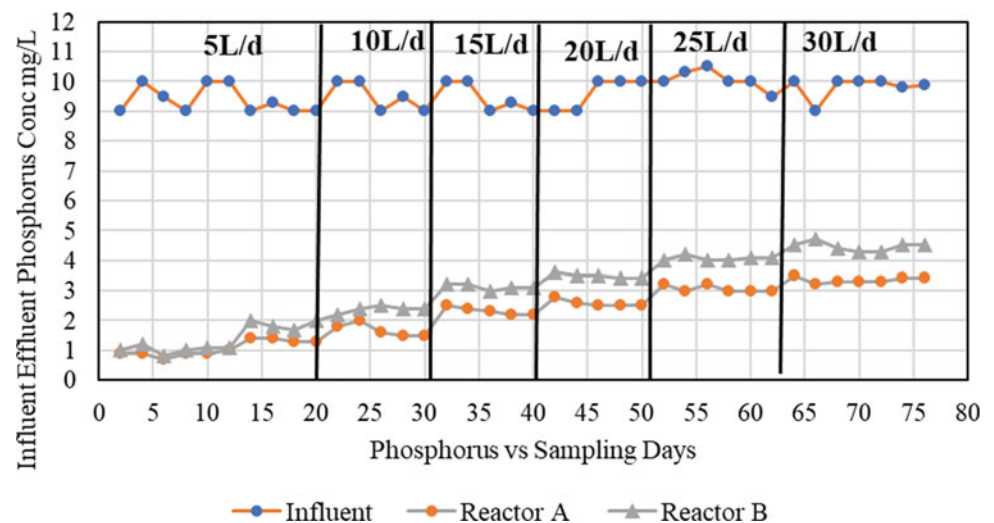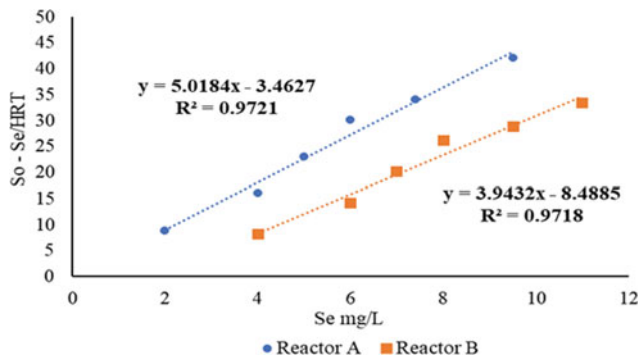
Fig. 3 First order substrate removal plot for phosphorus

4 Conclusions

The performance of palm oil clinker showed high efficiency in removing phosphorus more than control in all experimental conditions. The average removal of PO_4 reached 88% for reactor A while 77% for reactor B with flowrate 5 L/d. While for the correlation coefficient (R^2) of 0.9721 and 0.9718 for reactor A and B, respectively. The submerged media provided a large surface area for biomass. The submerged media served as a filtration medium for nutrient removal throughout the study.

The results at steady-state conditions show that PO_4 removal was high at longer HRT. The PO_4 removal was at 88, 81, 74.4, 73.3, 70, and 66% and 77.7, 72.2, 66.6, 65, 60 and 55% for reactor A and B, respectively, with decreasing HRT for reactor A and B, respectively, in the range of 5, 10, 15, 20, 25 and 30 L/d, the results indicated the acclimation of phosphorus was successful in the reactor. Phosphorus taking up by microbes and used up by microbes for their nutrient's wastewater (Yuan et al. 2012).

It was found out that the PO_4 removal efficiency slightly reduce with changing in flow rate. It is well known that short HRT alters the dynamic balance, composition, and spatial distribution of the ecological structure of microbial systems and could decrease substrate removal efficiency due to incomplete biodegradation (Ma et al. 2009). The increase of flowrate coincides with an increase in substrate concentration and metabolic activities. The consumption of substrate results in cell synthesis and growth. Thus, at higher HLR, more substrate is supplied to the microorganisms which increases their metabolic activities.

3.2 First-Order Kinetic Model for PO_4

The steady-state data were fitted into the plot of S_O-Se/HRT Versus Se in Fig. 3. The substrate removal rate (K_1) for reactors A and B was determined to be 5 and 3.9 per day, with correlation coefficients (R^2) of 0.9721 and 0.9718, respectively. The magnitude of the first-order removal rate obtained in this research was greater than the report of Isik and Sponza (Işik and Sponza 2005), who obtained a K_1 of 0.615 per day in a UASB reactor treating wastewater, and lower than the report of Amin et al. who obtained a K_1 of 49.81 per day in a non-adapted treating wastewater (Amin et al. 2014).

References

B.N. Al-dhawi, S.R. Kutty, N.M. Almahbashi, A. Noor, A.H. Jagaba, Organics removal from domestic wastewater utilizing palm oil clinker (POC) media in a submerged attached growth systems. Int. J. Civ. Eng. Technol. **11**(6), 1–7 (2020)

B.N.S. Al-dhawi, S.R.M. Kutty, A.A.S. Ghaleb, N.M.Y. Almahbashi, A.A.H. Saeed, A.B.A. Al-Mekhlafi, Y.A.A. Alsaeedi, A.H. Jagaba, Pretreated palm oil clinker as an attached growth media for organic matter removal from synthetic domestic wastewater in a sequencing batch reactor. Case Studies in Chemical and Environmental Engineering 7, 100294 (2023).

S.C. Ayaz, Ö. Aktaş, N. Findik, L. Akça, Phosphorus removal and effect of adsorbent type in a constructed wetland system. Desalin. Water Treat. **37**(1–3), 152–159 (2012)

A. Bawiec, Efficiency of nitrogen and phosphorus compounds removal in hydroponic wastewater treatment plant. Environ. Technol. **40**(16), 2062–2072 (2019)

L.E. De-Bashan, Y. Bashan, Recent advances in removing phosphorus from wastewater and its future use as fertilizer (1997–2003). Water Res. **38**(19), 4222–4246 (2004)

B.N.S. Al-dhawi, S.R.M. Kutty, G. Hayder, B.M.E. Elnaim, M. Mnzool, A. Noor, A.A.H. Saeed, N.M.Y. Almahbashi, A. Al-Nini, A.H. Jagaba, Adsorptive Removal of Boron by DIAION™ CRB05: Characterization, Kinetics, Isotherm, and Optimization by Response Surface Methodology. Processes 11(2), (2023).

A. Jagaba et al., Sequencing batch reactor technology for landfill leachate treatment: a state-of-the-art review. J. Environ. Manage. **282**, 111946 (2021)

Y. Ma, Y. Peng, X. Wang, Improving nutrient removal of the AAO process by an influent bypass flow by denitrifying phosphorus removal. Desalination **246**(1–3), 534–544 (2009)

A. Noor, S.R. Kutty, N.M. Almahbashi, V. Kumar, A.A. Ghaleb, B.N. Al-Dhawi, Integrated submerged media extended aeration activated sludge (ISmEAAS) reactor start-up and biomass acclimatization. J. Hunan Univ. Nat. Sci. **48**(9) (2021)

Á. Robles et al., New frontiers from removal to recycling of nitrogen and phosphorus from wastewater in the circular economy. Biores. Technol. **300**, 122673 (2020)

B.N.S. Al-dhawi, S.R.M. Kutty, L. Baloo, N.M.Y. Almahbashi, A.A.S. Ghaleb, A.H. Jagaba, V. Kumar, A.A.H. Saeed, Treatment of synthetic wastewater by using submerged attached growth media in continuous activated sludge reactor system International Journal of Sustainable Building Technology and Urban Development, 13(1), 2-10 (2022).

C. Weihrauch, C.J. Weber, Phosphorus enrichment in floodplain subsoils as a potential source of freshwater eutrophication. Sci. Total Environ. **747**, 141213 (2020)

Z. Yuan, S. Pratt, D.J. Batstone, Phosphorus recovery from wastewater through microbial processes. Curr. Opin. Biotechnol. **23**(6), 878–883 (2012)

Multi-Step Ahead Time-Series Forecasting of Sediment Load Using NARX Neural Networks

Mahmud Iwan Solihin, Gasim Hayder, Haris Al-Qodri Maarif, and Qaiser Khan

Abstract

River sedimentation is a universal issue in a river catchment. It can affect the reservoir ability, the river flow, and dam structure including the hydropower capacity. Therefore, having multi-step ahead forecasting for the sediment load is beneficial in terms of research and applications. This study discusses and presents a case study in multi-step ahead forecasting for the sediment load using non-linear autoregressive with exogenous inputs (NARX) neural networks. We use sediment data that was recorded from 8 locations in the Ringlet reservoir (upstream sections) in Malaysia. The results suggest that the NARX neural networks have good capability to do multi-step ahead forecasting for sediment load in a recursive way (closed-loop mode) based on its past values and the past values of suspended solid and discharge. The model is evaluated with performance metrics yielding NSE = 0.99 (Nash–Sutcliffe efficiency coefficient) for both the training and test dataset, and RMSE (root means square error) of 0.22 and 0.25, respectively, training and test dataset.

Keywords

Sediment load • River system • NARX • Neural networks • Multi-step ahead forecasting

M. I. Solihin (✉)
Department of Mechanical and Mechatronics Engineering, UCSI University, Cheras, Malaysia
e-mail: mahmudis@ucsiuniversity.edu.my

G. Hayder · Q. Khan
Department of Civil Engineering, College of Engineering, Universiti Tenaga Nasional (UNITEN), Selangor Darul Ehsan, 43000 Kajang, Malaysia

H. A.-Q. Maarif
Computer Science Department, Nusa Putra University Sukabumi, Kabupaten Sukabumi, Indonesia

1 Introduction

Estimation and prediction of suspended sediment load is important in water management and monitoring of environmental issues (Melesse et al. 2011). In a prior work, multiple machine learning (ML) techniques were used to estimate sediment load from available input predictor variables (Hayder et al. 2021). The two predictor variables are suspended solid and discharge. The sufficient review on the important of sediment load estimation has also been discussed. However, the study is more focused on revealing the correlation between sediment load in the catchment area with the input variables, namely suspended solid and discharge.

This paper extent this earlier study by introducing multi-step ahead forecasting where artificial neural networks (ANN) will be used to forecast the sediment load based on its past values, the input variables and their historical data. The proposed multi-step ahead forecasting takes the popular time-series forecasting architecture namely non-linear autoregressive with exogenous inputs (NARX) with the internal function based on neural networks. This hybrid approach makes up an architecture known as non-linear autoregressive with exogenous inputs (NARX) neural networks. This architecture has been applied in various task for multi-step ahead forecasting ranging across disciplines not only in hydrology (Guo and Xue 2014; Sarkar et al. 2019).

In the applications of hydrology especially suspended sediment load forecasting, some studies have used that particular NARX architecture with different input variables and different machine learning methods and yielding various interesting results (Mohammadi et al. 2019; Kumar et al. 2017). Some studies use particular neural networks as the prediction engine in the NARX architecture, i.e., NARX neural networks (Bouzeria et al. 2017; Alarcon 2021; Afan et al. 2014; Nivesh and Kumar 2017). These vibrant research interest of using machine learning in the area of hydrology

indicates the potential impact of application and contribution in solving problems in water management and environment systems.

This study aims to further explore and justify the important of this hybrid multidisciplinary approach of computer science and hydrology by presenting the case study of sediment load forecasting using NARX neural networks. The study employs the data was recorded in upstream catchment of Ringlet reservoir, Cameroon Highland, Malaysia.

2 Study Area and Data

There are 8 upstream area in Ringlet reservoir catchment located in Cameroon Highland, Pahang, Malaysia. This location is taken as the case study where there data was gathered (Hayder et al. 2021). The geographical map is shown in Fig. 1. Within the Cameron Highlands, there are six water catchments: Bertam, Lemoi, Mensun, Terla, Telom and Wi. In addition, the district contains various towns such as Kuala Terla, Kampung Raja, Kea Farm, Teringkap, Brinchang, Tanah Rata and Ringlet as the district's southernmost town (Gasim et al. 2009). The largest reservoirs in the Cameron Highlands district are Ulu Jelai and Sultan Abu Bakar (SAB) Dam. Ringlet Dam is another name for SAB Dam, which was erected in the 1960s with 19,000 m^3 of rockfill and 52,000 m^3 of concrete standing 39.6 m height and 135 m long.

Ringlet Reservoir contributes 20% of total power generation in West Malaysia as part of the National Electric Board's Cameron Highlands Hydroelectric Scheme. Ringlet Reservoir, in addition to generating hydropower for Jor Power Plant, it serves as a flood control reservoir for residents in the Bertam Valley. The system was under the care of Malaysian Metrological Department (MMD), Tenaga Nasional Berhad (TNB) and the Department of Irrigation and Drainage (DID). Generally, Ringlet reservoir catchment is equipped with a good hydrological monitoring system including stream flow, rainfall and weather stations (Abdul Razad et al. 2018). Nonetheless, the reservoir storage volume has been depleted because of sedimentation, affecting the power station's energy output. The worst-case situation occurs when the Ringlet Reservoir gradually loses its ability to hold large flood inflows, forcing flood discharge through the spillway to be controlled (Sidek 2013).

Three important variables, i.e., discharge (DC) in mg/L, suspended solid (SS) in m^3/s and sediment load (SL) in ton/day units were collected as the raw data. The available information on DC and SS in the 8 (eights) spots neighboring the Ringlet reservoir catchment area are compiled after substantial pre-processing and cleansing; the locations are listed in this reference (Hayder et al. 2021). Many daily data are missing so that only left some hundred instances can be used for this study. From December 12, 1997, to May 12, 2010, 405 data instances were compiled after extreme outliers were removed. Figure 2 shows the boxplot of the data where several outliers are still detected on each variable although the extreme outliers are already removed.

Despite the actual data is not in a uniform temporal time-series sequence, this research assumes that the compiled data is in a uniform temporal time-series sequence so that the NARX neural networks model development is more focused rather than the validity of the data and the model itself. Therefore, on order to have higher applicability impact, the data quality must be improved in the future since the main ingredient of machine learning-based model is the data.

3 Methodology

The architecture of NARX neural networks can be seen in Fig. 3 (Thapa et al. 2020). It is applied as multivariate estimator to perform prediction on a number of step ahead values of the sediment load using the lagged values of both SS and DC as well as the previously estimated values of SL.

The predictive model used in here is NARX neural networks. It is essentially an extension of non-linear autoregressive (NAR) model by combining additional relevant time-series features to the forecasting model. The non-linearity of the model is handled by the neural networks. Here, the standard multilayer neural networks where the architecture and the training algorithms is listed in Table 1.
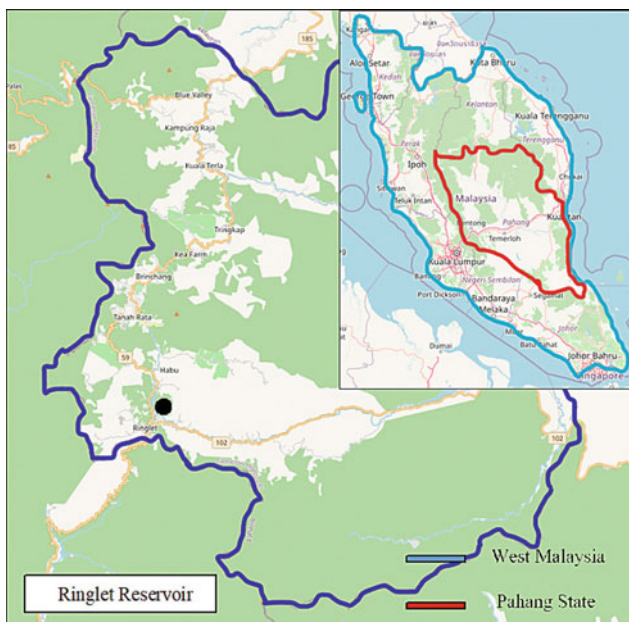
Fig. 1 The map of the study area at Cameron Highlands, Malaysia
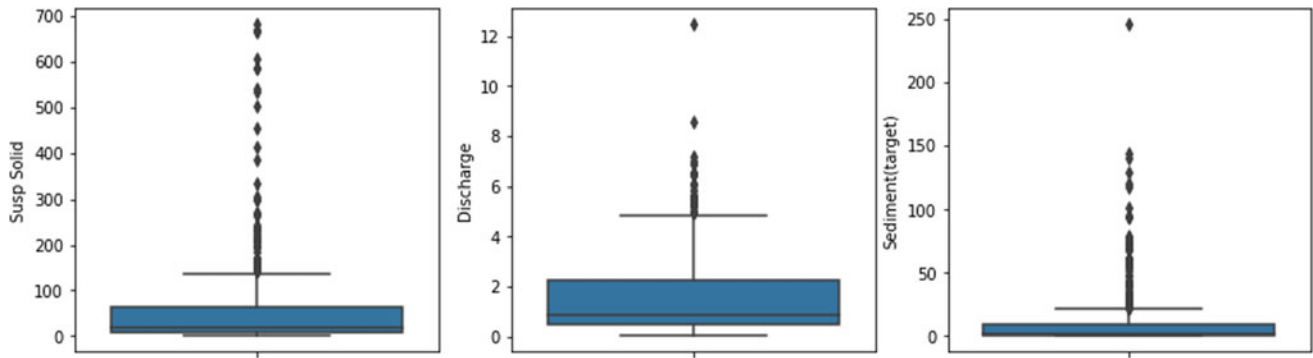
Fig. 2 Boxplot of the data
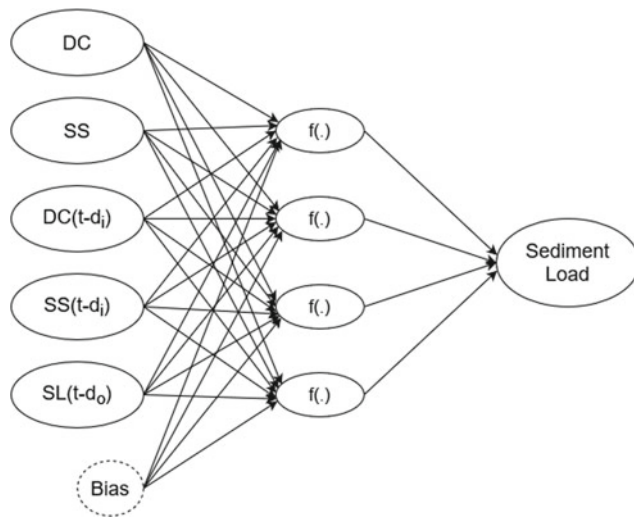
Fig. 3 The architecture of the proposed NARX neural networks

The implementation is performed in MATLAB 2019b software under the university license.

Firstly, the training/learning of NARX neural networks model is performed by feeding the data consisting of input and target variables. Then, the trained model will be evaluated using test dataset once the training performance is satisfactory. Here, we use the first 85% of the daily data for training. The rest 15% proportion is used as test dataset. This proportion is quite common in machine learning model development.

This study performs regressive model development. For regression, the model accuracy can be evaluated using some common metrics such as presented in Pena et al. (2020). Similarly in this study, the metric used to evaluate the model accuracy are Nash–Sutcliffe efficiency coefficient (NSE) and root mean squared error (RMSE). These two metrics can be expressed as follows:

$$\text{RMSE} = \sqrt{\sum_{i=1}^{n} \frac{(\hat{y}_i - y_i)^2}{n}} \tag{1}$$

$$\text{NSE} = 1 - \frac{\sum_{i=1}^{n} (y_i - \hat{y}_i)^2}{\sum_{i=1}^{n} (y_i - \overline{y}_i)^2} \tag{2}$$

The regression performance of hydrological model is often assessed using NSE. According to Pena et al. (2020), NSE outperforms other metric such as coefficient of determination, (regression coefficient). It is indicated that NSE > 0.75 is substantially very nice fit model while NSE < 0.5 implies poor performance of the model.

4 Results

The first experimentation is to get optimum delay (lag) number for the input (d_i) and the feedback (d_o) as closed-loop mode NARX neural networks architecture is implemented. Here, the auto-correlation and cross-correlation analysis are conducted. As shown in Fig. 4, the sample auto-correlation function for SL has quite significant correlation of its delayed value of 1–5, i.e., previous 1st to 5th months.

Table 1 Architecture of the multilayer neural networks used in the NARX neural networks

Total hidden layer	2 hidden layers
Total neurons in hidden layers	[5 5]; five neurons in each layer
Training algorithm	Bayesian regularization (*trainbr*)
Activation functions at hidden layers	Tangent sigmoid + sigmoid function
Activation functions at output layer	Linear function (*purelin*)
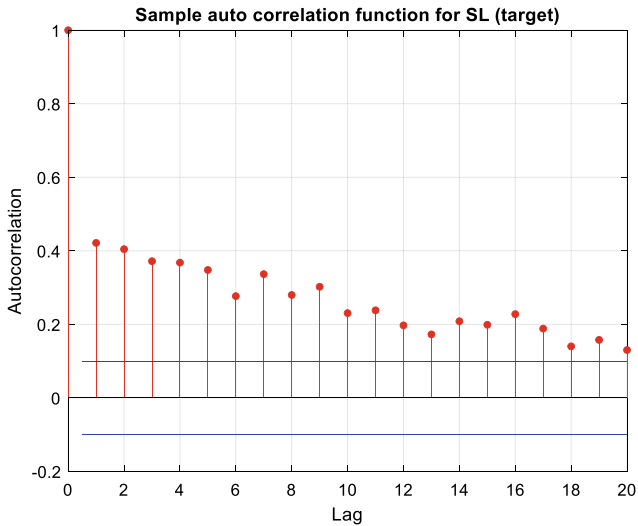
Fig. 4 Graph showing sample auto correlation function (SL)

Likewise, the cross-correlation analysis between SL and SS, and also between SL and DC are also conducted. As shown in Fig. 5, some observation can be drawn as initial assessment for the features/input variable selection for the NARX neural networks model. SL has correspondingly very significant correlation to the present (delay of 0) value of both SS and DC. It extents the correlation between SL and both SS and DC with weaker value up to about lag 2 (past two months). With this observation, the developed NARX neural networks forecasting model can be expressed as:

$$\widehat{SL}(t) = f\big(SS(t), SS(t-1), SS(t-2), DC(t), DC(t-1), DC(t-2),$$
$$\widehat{SL}(t-1), \widehat{SL}(t-2), \widehat{SL}(t-3), \widehat{SL}(t-4), \widehat{SL}(t-5)\big)$$

(3)
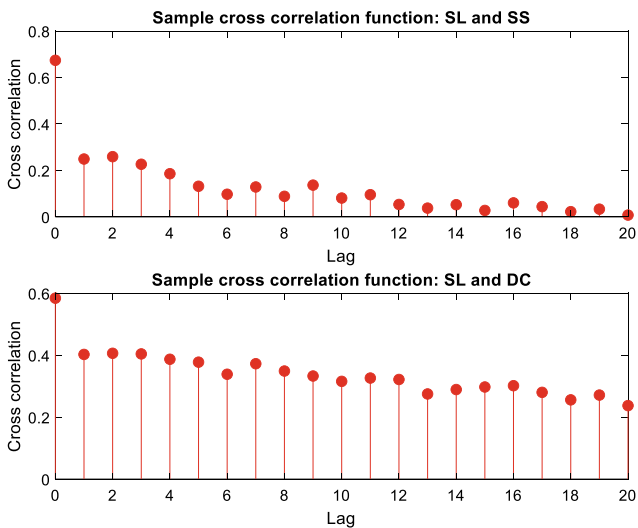
Fig. 5 Graph showing cross-correlation function (SL-SS and SL-DC)
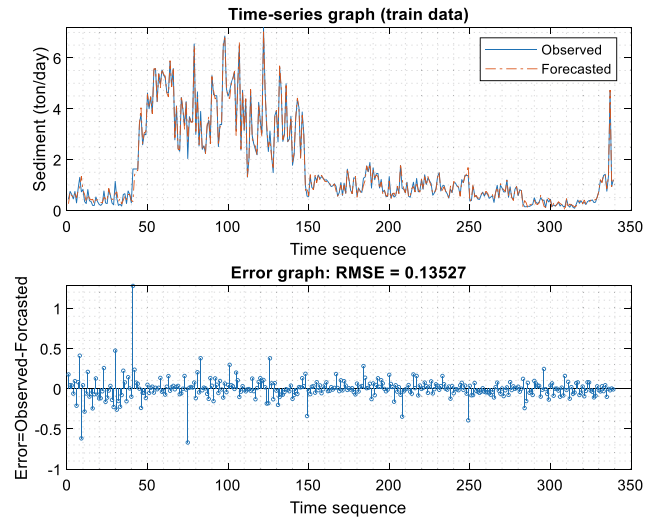
Fig. 6 Graph showing forecasting performance evaluated on training data set

The forecasting result evaluated on training data is presented in Figs. 6 and 7. With the outcome of NSE = 0.99 and RMSE = 0.14, the model fits well the training dataset. The NARX neural networks model produces very high NSE and low RMSE. The blue line (diagonal line) in Fig. 7 indicates the fitting line for regression between the observed and forecasted values.

Furthermore, the forecasting result evaluated on test dataset is presented in Figs. 8 and 9. The successfully trained model is used recursively to predict 61 step ahead, i.e., prediction in a closed-loop mode. The result indicates excellent capability of the model with NSE = 0.99 and RMSE = 0.25, i.e., only slightly lower RMSE as comparted
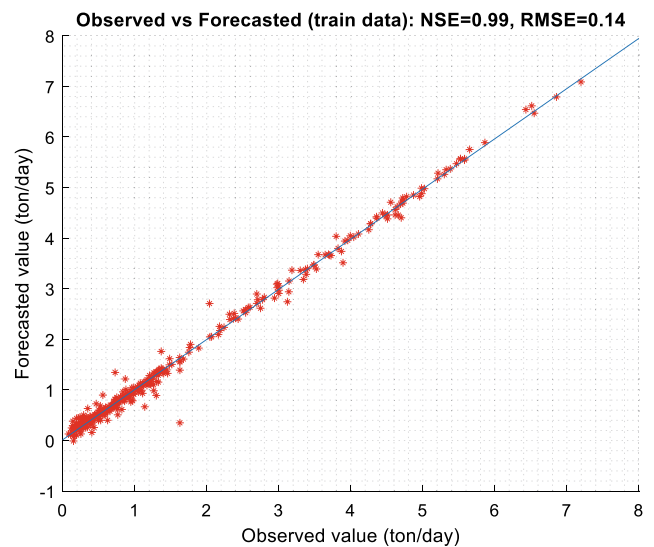
Fig. 7 Graph showing observed versus forecasted value (training dataset)
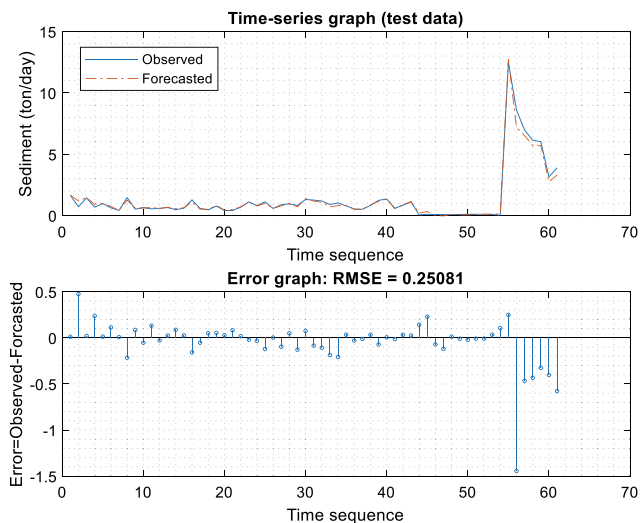
Fig. 8 Graph showing forecasting performance evaluated on test dataset
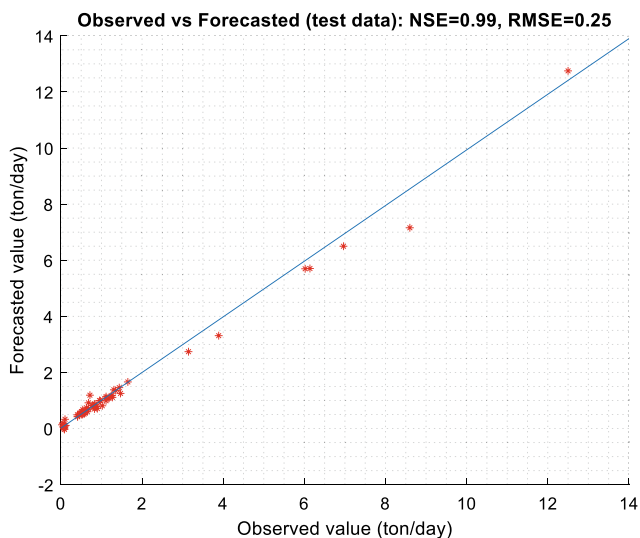
Fig. 9 Graph showing observed versus forecasted value (test dataset)

to that on training data. This means the model can generalize the data very well. This also indicates the good capability of the Bayesian regularization algorithm used in the model training.

5 Conclusion

In this study, sediment load forecasting using NARX neural networks have been proposed. The forecasting is performed in multi-step ahead manner. The study employed the data collected from 8 upstream stations of Ringlet reservoir catchment located in Cameroon Highland, Pahang, Malaysia. The results show the excellent capability of NARX

neural networks to perform multi-step ahead forecasting of sediment load in recursive way based on its past values, the past values of suspended solid and discharge. The model produces low RMSE values for both training and testing data with Nash–Sutcliffe efficiency coefficient (NSE = 0.99). In the future, the data quality will be improved as in this study the data is assumed to be in uniform temporal of daily time-series. This to avoid some missing data and non-uniformity of the temporal sequence.

References

A.Z. Abdul Razad, L.M. Sidek, K. Jung, H. Basri, Reservoir inflow simulation using Mike Nam rainfall-runoff model. J. Eng. Sci. Technol. **13**(12), 4206–4225 (2018)

H.A. Afan, A. El-Shafie, Z.M. Yaseen, M.M. Hameed, W.H.M. Wan Mohtar, A. Hussain, ANN based sediment prediction model utilizing different input scenarios. Water Resour. Manag. **29**(4), 1231–1245 (2014). https://doi.org/10.1007/s11269-014-0870-1

V.J. Alarcon, Hindcasting and forecasting total suspended sediment concentrations using a NARX neural network. Sustain. **13**(1), 1–18 (2021). https://doi.org/10.3390/su13010363

H. Bouzeria, A.N. Ghenim, K. Khanchoul, Using artificial neural network (ANN) for prediction of sediment loads, application to the Mellah catchment, northeast Algeria. J. Water l. Dev. **33**(1), 47–55 (2017). https://doi.org/10.1515/jwld-2017-0018

M.B. Gasim, S. Surif, M.E. Toriman, S.A. Rahim, R. Elfithri, P.I. Lun, Land-use change and climate-change patterns of the Cameron highlands, Pahang, Malaysia. Arab World Geogr. **12**(1–2), 51–61 (2009). https://doi.org/10.5555/ARWG.12.1-2.L2P14J2833G2Q4L7

W.W. Guo, H. Xue, Crop yield forecasting using artificial neural networks: a comparison between spatial and temporal models. Math. Probl. Eng. **2014**(January), 2014 (2014). https://doi.org/10.1155/2014/857865

G. Hayder, M.I. Solihin, K.F. Bin Kushiar, A performance comparison of various artificial intelligence approaches for estimation of sediment of river systems. J. Ecol. Eng. **22**(7), 20–27 (2021). https://doi.org/10.12911/22998993/137847

S. Kumar, A. Pandey, B. Yadav, Assessing the applicability of TMPA-3B42V7 precipitation dataset in wavelet-support vector machine approach for suspended sediment load prediction. J. Hydrol. **550**, 103–117 (2017). https://doi.org/10.1016/j.jhydrol.2017.04.051

A.M. Melesse, S. Ahmad, M.E. McClain, X. Wang, Y.H. Lim, Suspended sediment load prediction of river systems: an artificial neural network approach. Agric. Water Manag. **98**(5), 855–866 (2011). https://doi.org/10.1016/J.AGWAT.2010.12.012

B. Mohammadi, Y. Guan, R. Moazenzadeh, M. Jafar, S. Safari, Catena Implementation of hybrid particle swarm optimization-differential evolution algorithms coupled with multi-layer perceptron for suspended sediment load estimation. Catena, December 2019, 105024 (2020). https://doi.org/10.1016/j.catena.2020.105024

S. Nivesh, P. Kumar, Modelling river suspended sediment load using artificial neural network and multiple linear regression: Vamsadhara River Basin, India. Int J. Chem. Stud. **5**(5), 337–344 (2017)

M. Pena, A. Vazquez-Patino, D. Zhina, M. Montenegro, A. Aviles, Improved rainfall prediction through nonlinear autoregressive network with exogenous variables: a case study in Andes High Mountain region. Adv. Meteorol. **2020** (2020). https://doi.org/10.1155/2020/1828319

R. Sarkar, S. Julai, S. Hossain, W.T. Chong, M. Rahman, A comparative study of activation functions of NAR and NARX neural network for long-term wind speed forecasting in Malaysia. Math. Probl. Eng. **2019** (2019). https://doi.org/10.1155/2019/6403081

L. Sidek, Hydropower reservoir for flood control: A case study on ringlet. J. Flood Eng. **4**(June 2013), 87–102 (2013)

S. Thapa et al., Snowmelt-driven streamflow prediction using machine learning techniques (LSTM, NARX, GPR, and SVR). Water (Switzerland) **12**(6) (2020). https://doi.org/10.3390/w12061734

River Water Suspended Sediment Predictive Analytics Using Artificial Neural Network and Convolutional Neural Network Approach: A Review

Qaiser Khan, Gasim Hayder, and Faiq M. S. Al-Zwainy

Abstract

For water resource management and water quality challenges, estimating suspended sediment is crucial. It demands accurate data and information on suspended sediment concentrations (SSC). Because real sampling can be difficult during severe weather and certain old approaches will not yield enough data, engineers are developing new accurate forecasting technologies. The aim of this study is to see if machine learning techniques like convolutional neural network (CNN) and artificial neural network (ANN) could be utilized to estimate SSC in Malaysia's Langat stream. The CNN is a form of machine learning method that has not gotten much attention around SSC prediction. The prediction model created in this work is intended for use in the water quality monitoring of Langat stream in Malaysia. River discharge and suspended solids will be the input variables for the models. Both models will be analyzed using the three criteria for performance including root mean square error (RMSE), coefficient of determination (R^2), and mean absolute error (MAE) to find which is more accurate in predicting the SSC for this river. The model with the top performance will have the lowest MAE and RMSE values as well as the high value of R^2. This study will contribute to demonstrating how machine learning may be used to forecast future suspended sediment concentrations in rivers.

Q. Khan (✉)
College of Graduate Studies, Universiti Tenaga Nasional (UNITEN), Selangor Darul Ehsan, 43000 Kajang, Malaysia
e-mail: qaiser.khan@uniten.edu.my

G. Hayder
Department of Civil Engineering, College of Engineering, Universiti Tenaga Nasional (UNITEN), Selangor Darul Ehsan, 43000 Kajang, Malaysia

F. M. S. Al-Zwainy
Forensic DNA for Research and Training Center, Al-Nahrain University, Baghdad, Iraq

Keywords

Suspended sediment • CNN • ANN • R^2 • RMSE • MAE • Langat river

1 Introduction

Streams are important in the evolution of human society, and they have their own socioeconomic element (Adnan et al. 2019; Yadav et al. 2018; Duru 2015). Sediment transport is complicated and varies depending on the basin's topography, geological state, and flow parameters (Ehteram et al. 2019; Hayder et al. 2021; Cisty et al. 2021; Farzin and Valikhan Anaraki 2021; ÜNEŞ et al. 2020). Due to overland flow during storm events, erosion caused by mining and agricultural activities and other kinds of development of the land may bring enormous quantities of silt into rivers and streams (Martinez 2019; ÜNEŞ et al. 2020; Aziz et al. 2021; AlDahoul et al. 2021; Ehteram et al. 2019; ÜNEŞ et al. 2020; Rezaei and Vadiati 2020; Martinez 2019; Farzin and Valikhan Anaraki 2021; Yilmaz et al. 2020; Yadav et al. 2018; Aziz et al. 2021). Furthermore, lateral channel migration caused by downstream sediment aggradation increases severe flooding during heavy rains due to a large loss of channel capacity (Yadav et al. 2021). As a result, the habitat of aquatic species living in rivers is reduced (Sa'ad et al. 2021; Bajirao et al. 2021). The Langat River drains a densely inhabited and developed area (Juahir et al. 2011; Basheer et al. 2017; Fung et al. 2020). The accurate estimation of a river's sediment load is a critical issue in water engineering. As a result, multiple studies have been done to approximate the volume of transported sediment by linking this factor to hydraulic factors, river geometry, and sediment characteristics. However, due to significant inaccuracies, these equations have not been widely used (Emamgholizadeh and Demneh 2019). Artificial intelligence technologies have become increasingly essential in hydrological

prediction and estimating suspended sediment (SS) amounts. Convolutional neural network (CNN) and artificial neural network (ANN), for example, are two types of neural networks (Ehteram et al. 2019; ÜNEŞ et al. 2020; Rezaei and Vadiati 2020; Chen et al. 2020; Cisty et al. 2021; Fadaeea et al. 2020; Yadav et al. 2021; Nourani et al. 2021; Hayder et al. 2020). The objective of this research is to review about two artificial intelligence modeling methods namely CNN and ANN and effective input variable combinations.

2 Related Literature Review

2.1 Overview of ANN

The biological neural system, or brain, inspired the development of ANN. In comparison with today's high-speed computers, the neural system contains many neurons that can perform jobs faster. Signals are sent from one neuron to another by real neurons. These signals are sent across a weighted or biased connection (Abu Bakar 2013). The function of a real neuron and an artificial neuron is very similar. Three crucial components drive the evolution of ANN into other algorithms. Many other ANN derivations have emerged because of evolution. The most important are the multilayer perceptron and the radial basis function. As indicated in Fig. 1, the three layers (input, hidden, and output) are the primary components of ANN. The ANN's hidden layer is not limited to just one but can expand to incorporate multiple layers (Hafeez et al. 2019). ANNs, however, do not have precise formulations or equations to describe the prediction process, unlike traditional approaches that use formulas and equations with multiple parameters. As a result, ANNs are thought of as black-box models, with the input determining the output (Abu Bakar 2013). Neurons in the buried layer compute weight to produce the expected output from the supplied input.

2.2 Suspended Sediment Concentrations Prediction Using ANN

Based on research conducted by Hafeez et al. (2019), three optically active WQIs were estimated using four machine
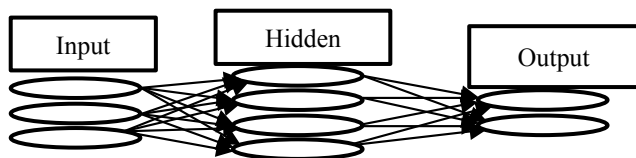
Fig. 1 Three-layer ANN structures (input, hidden, and output layers) were applied to predict suspended sediment

learning algorithms. All models have excellent correlations for Chl-a concentration, with ANN having the greatest performance. For SS prediction, the ANN produced the best results, with the RMSE and MAE lowest values. A second test was carried out to assess the techniques of machine learning for picking a reliable model. ANN outperformed the other models. Nivesh and Kumar (2017) conducted yet another investigation in which MLR and ANN were put to the test. In terms of all metrics, the ANN-2 model outperformed the other models. The ANN case-2 models have been created employing one hidden layer with distinct neurons to see the influence of antecedent rainfall with time step $t-1$ in addition to Qt, $Qt-1$, and $St1$. Suspended solid concentration (mg/L) modeling was reported for selected peaks from the testing stage using sediment rating curve (SRC), ANN, adaptive neuro-fuzzy inference system (ANFIS), and sediment linear regression (SLR), in situations S1, S2, S3, and S4 according to Mohamed (2018) work. ANFIS and ANN demonstrate that machine learning approaches outperform traditional methodologies. The ANFIS is inferior to the ANN. In the investigation conducted by Yadav et al. (2018), the GA approach is intended to create consecutive populations with a variety of people with various traits. The GA was used in this investigation because of to choose five key variables for the models of ANN, specifically, the combination coefficient, the hidden layers, the number of neurons, the transfer function, inputs, as well as bias weights. The GA-ANN outperformed the classic neural network and regression models in terms of reducing the MAE and RMSE. In the research done by Taşar et al. (2017), ANN estimations slightly outperformed the multiple linear regression (MLR) and M5 tree (M5T) model values for sediment real-time daily concentrations in the test phase. When a comprehensive assessment is carried out, the observed finding is that ANN has a strong correlation and small error rates. In this paper done by Fadaeea et al. (2020), the butterfly optimization algorithm (BOA) is a meta-heuristic algorithm inspired by butterflies' food-finding method. The butterflies serve as search variables in this system, detecting several smells from various flowers to discover the best food source, whereas the genetic algorithm (GA) considered as a population-based program. The SSL was predicted using three ANN models: ANN-GA, ANN-BOA, and ANN-ML. In the train and test phases, the ANN-GA and ANN-BOA models outperformed the traditional ANN model. Nonetheless, in the test stage, ANFIS-BOA demonstrated the highest accuracy of all the models and, as a result, was able to replicate the SSL clearer than the other types. Research conducted by Moeini et al. (2021), it mentioned that on the training dataset, the ANN performed well. However, it was unable to successfully replicate the pattern in the prediction stage, which could be owing to an overfitting problem in the training step caused

by the ANN model's complexity. Alizadeh et al. (2018) said that when comparing the characteristics of various techniques of machine learning which are the extreme learning machine (ELM), support vector regression (SVR), and ANN function in the same way and have the same error metrics. According to this research, aside from the backpropagation algorithm, ANNs have been trained using the metaheuristic algorithms TLBO and ABC, which have been used in several pieces of research in recent years. The TLBO and ABC algorithms were utilized to overcome the limitations of the backpropagation technique and attain lower values of error by acquiring more acceptable values in the training process of ANN, such as threshold and weight values. The ANN model has the best accuracy for time t. The attained RMSE value from the ANN-ABC was greater than that from ANN-BP, while the MAE value was lower. While the models gave similar results to each other, it is clear that the ANN-ABC and ANN-BP produce better outcomes when examining the error values. ANN-based models gave better results in terms of capturing peak values in forecasting of SSL in general according to Bajirao et al. (2021), Hayder et al. (2021), Mamun et al. (2020), Yilmaz et al. (2020). Table 1 shows the water quality estimation using ANN summary.

2.3 Overview of CNN

CNN is one of the methods of artificial intelligence technique that has not caught considerable attention for the purpose of the SSL prediction. Based on past literature evaluations, this model, which is a kind of deep learning process, has shown a lot of potential in other disciplines. The architecture of a CNN is shown in Fig. 2. There are numerous benefits of using this model to address issues in both technical and non-technical sectors. The fact that CNNs are end-to-end artificial intelligence is one of the key advantages of using them. Because of this direct mapping capacity, developing inferior handmade features, correspondingly recognized as quality engineering, is a moment procedure that can result in noisy image representation with low discriminative strength, which is no longer necessary. CNNs are also resistant to a variety of demanding scenarios. Furthermore, because the same coefficients are used throughout the convolutional layer's space, the memory required for CNNs is greatly decreased. CNN training time is further lowered because the number of parameters is much lowered, creating training extra reasonable (Huang et al. 2020; Baek et al. 2020; Pu et al. 2019; Xue et al. 2021; Van et al. 2020; Chen et al. 2020; Song 2021; Kabir et al. 2020; Kamilaris and Prenafeta-Boldú 2018; Hijazi et al. 2015).

2.4 Suspended Sediment Concentrations Prediction Using CNN

The model performance using CNN was compared to a support vector regression. Several accepted performance indicators demonstrated that the suggested CNN was greater compared to the SVR in forecasting flood concentrations in this investigation as mentioned by AlDahoul et al. (2021). The viability of utilizing a CNN-based model to estimate the power production from a power converter system of a maritime wave using a twin buoy oscillating device was examined by Ni and Ma (2018). Multi-input CNN techniques were utilized for training and evaluation. According to the research, the CNN model outperforms the ANN in predicting maritime wave power production. In a research done by Pu et al. (2019), they evaluate a CNN performance to SVM and RF to assess its performance. The best classification result was attained by CNN, which outperformed the SVM-based and RF-based approaches. The CNN was exact

Table 1 Summary of estimation of water quality using ANN

Authors	Type of model	Parameters	Locations
Hafeez et al. (2019), Nivesh and Kumar (2017), Mohamed (2018), Yadav et al. (2018), Taşar et al. (2017), Fadaeea et al. (2020), Moeini et al. (2021), Alizadeh et al. (2018), Yilmaz et al. (2020), Hayder et al. (2021), Bajirao et al. (2021), Mamun et al. (2020)	Artificial neural network (ANN)	Chlorophyll-a concentration, suspended solids (SS) concentration, turbidity, water salinity, surface water temperature, time, and space complexity	Waters of Hong Kong; Vamsadhara River Basin, India; Thames River, Canada; Mahanadi River, India; Iowa Station, USA; Eagle Creek Watershed, Indiana; USA; Wailuku River entering Hilo Bay, Pacific Ocean; Çoruh River Basin; Cameron Highlands; Koyna River basin, India; Nakdong River, South Korea

Fig. 2 Architecture of a CNN
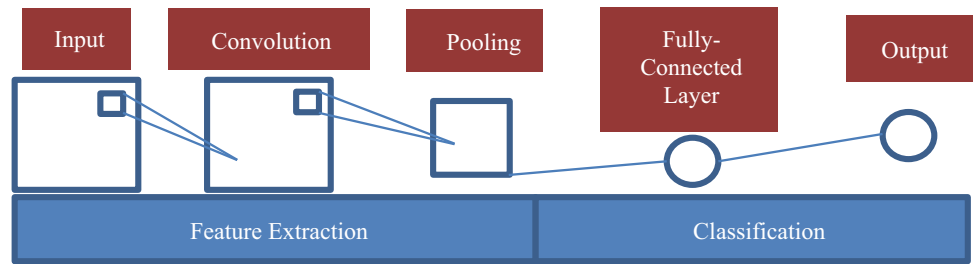
of all Erhai Lake water value categorization techniques. Because of its tremendous learning capabilities, the CNN can learn discriminative and sophisticated characteristics from multispectral images in addition to shallow features like color and texture. As a result, the CNN had the best classification results. As shown in research conducted by Xue et al. (2021), the CNN performance was superior to the traditional methods. This indicates the dominance of CNN applied to predict the chlorophyll-a concentration. The CNN model may greatly enhance prediction efficiency in the testing period at Chau Doc and Can Tho stations, according to Van et al. (2020) study. The best CNN model improves the RMSE, MAE, and R values for Chau Doc and Can Tho, respectively, from 89.571, 66.348, and 0.9994 and 834.01, 652.742, and 0.978. In terms of discharge prediction, the CNN model performs better than the LSTM model. The discharge peaks are underestimated by both models. The CNN model, on the other hand, outperforms the LSTM model in this case. Song (2021) stated that, because of the results of this investigation and the comparison between this study and prior studies, this study believes that the CNN model employing hydrological images might be used as a pollution load prediction model. Unlike the previous work, which used a regular ANN model, the CNN technique in this research improved the ability to simulate pollution loads by reflecting two-dimensional spatial information. Table 2 states the summary of water quality estimation using CNN.

2.5 Performance Criteria

In a research carried out by Zounemat-Kermani et al. (2020), it uses Nash–Sutcliffe efficiency, the coefficient of

determination, the mean absolute error, and the root mean square error to evaluate the predictive capability of the applied types. The overall deviation statistical measurements of model evaluation, such as RMSE and MAE, are among the finest. The correlation between observed and modeled values is represented by R^2 (Mohamed 2018; Mamun et al. 2020; Sami et al. 2021). The following are the mathematical formulations:

$$\text{MAE} = \frac{1}{n} + \sum_{i=1}^{n} |Xi - X|, \tag{1}$$

$$\text{RMSE} = \sqrt{\frac{1}{n} \sum_{i=1}^{n} (Xi - Yi)^2}, \tag{2}$$

$$R^2 = 1 - \frac{\text{SSR}}{\text{SST}'}; \quad \text{SSR} = \sum_{i=0}^{n} (Yi - f(Xi))^2;$$

$$\text{SSR} = \sum_{i=0}^{n} (Yi - f(Xi))^2 \tag{3}$$

3 Conclusion

In the past decade, research has shown that artificial intelligence models are efficient in predicting suspended solid concentration (SSC). The past results showed that artificial neural network (ANN) provided acceptable results in predicting suspended solid concentration (SSC). In the other hand, convolutional neural network (CNN) has not been used much in predicting suspended solid concentration (SSC) in Langat River, Malaysia. ANN and CNN have

Table 2 Summary of estimation of water quality using CNN

Authors	Type of model	Parameters	Locations
AlDahoul et al. (2021), Ni and Ma (2018), Pu et al. (2019), Xue et al. (2021), Van et al. (2020), Song (2021)	Convolutional neural network (CNN)	Water level, suspended sediment load, wave power generation, chlorophyll-a concentration, rainfall–runoff, and pollutant loads	Johor River, Malaysia; Erhai Lake and Chaohu Lake, China; Dongting Lake, China; Chau Doc and Can Tho Stations, Vietnam; Paldang watershed, South Korea

performed fine compared to the other AI techniques in the prediction performance. It is important that future researchers should utilize these models as it has shown a lot of potential in the past studies. The results in the future research would be established on the performance criteria that are important such as the mean absolute error, the root mean square error, and the coefficient of determination. The model that would perform better under these performance criteria should be selected as being the best model for suspended solid concentration (SSC).

References

A.S. Abu Bakar, Prediction of suspended sediment concentration in Kinta River using soft computing techniques (2013)

R.M. Adnan, Z. Liang, A. El-Shafie, M. Zounemat-Kermani, O. Kisi, Prediction of suspended sediment load using data-driven models. Water **11**(10), 2060 (2019)

N. AlDahoul, Y. Essam, P. Kumar, A.N. Ahmed, M. Sherif, A. Sefelnasr, A. Elshafie, Suspended sediment load prediction using long short-term memory neural network. Sci. Rep. **11**(1), 1–22 (2021)

M.J. Alizadeh, M.R. Kavianpour, M. Danesh, J. Adolf, S. Shamshirband, K.W. Chau, Effect of river flow on the quality of estuarine and coastal waters using machine learning models. Engineering Applications of Computational Fluid Mechanics **12**(1), 810–823 (2018)

A. Aziz, Y. Essam, A.N. Ahmed, Y.F. Huang, A. El-Shafie, An assessment of sedimentation in Terengganu River, Malaysia using satellite imagery. Ain Shams Engineering Journal (2021)

S.S. Baek, J. Pyo, J.A. Chun, Prediction of water level and water quality using a CNN-LSTM combined deep learning approach. Water **12**(12), 3399 (2020)

T.S. Bajirao, P. Kumar, M. Kumar, A. Elbeltagi, A. Kuriqi, Superiority of hybrid soft computing models in daily suspended sediment estimation in highly dynamic rivers. Sustainability **13**(2), 542 (2021)

A.O. Basheer, M.M. Hanafiah, M.J. Abdulhasan, A study on water quality from Langat River Selangor. Acta Scientifica Malaysia (ASM) **1**(2), 1–4 (2017)

Y. Chen, L. Song, Y. Liu, L. Yang, D. Li, A review of the artificial neural network models for water quality prediction. Appl. Sci. **10**(17), 5776 (2020)

M. Cisty, V. Soldanova, F. Cyprich, K. Holubova, V. Simor, Suspended sediment modelling with hydrological and climate input data. J. Hydroinf. **23**(1), 192–210 (2021)

U. Duru, Modeling sediment yield and deposition using the swat model: a case study of Cubuk I and Cubuk II reservoirs, Turkey (Doctoral dissertation, Colorado State University) (2015)

M. Ehteram, S. Ghotbi, O. Kisi, A. Najah Ahmed, G. Hayder, C. Ming Fai et al., Investigation on the potential to integrate different artificial intelligence models with metaheuristic algorithms for improving river suspended sediment predictions. Applied Sciences **9**(19), 4149 (2019)

S. Emamgholizadeh, R.K. Demneh, A comparison of artificial intelligence models for the estimation of daily suspended sediment load: a case study on the Telar and Kasilian rivers in Iran. Water Supply **19**(1), 165–178 (2019)

M. Fadaeea, A. Mahdavi-Meymandb, M. Zounemat-Kermanic, Suspended sediment prediction: on the analogy between BOA and GA algorithms (2020)

S. Farzin, M. Valikhan Anaraki, Modeling and predicting suspended sediment load under climate change conditions: a new hybridization strategy. Journal of Water and Climate Change (2021)

K.F. Fung, Y.F. Huang, C.H. Koo, M. Mirzaei, Improved SVR machine learning models for agricultural drought prediction at downstream of Langat River Basin, Malaysia. Journal of Water and Climate Change **11**(4), 1383–1398 (2020)

S. Hafeez, M.S. Wong, H.C. Ho, M. Nazeer, J. Nichol, S. Abbas et al., Comparison of machine learning algorithms for retrieval of water quality indicators in case-II waters: a case study of Hong Kong. Remote sensing **11**(6), 617 (2019)

G. Hayder, I. Kurniawan, H.M. Mustafa, Implementation of machine learning methods for monitoring and predicting water quality parameters. Biointerface Res. Appl. Chem **11**, 9285–9295 (2020)

G. Hayder, M.I. Solihin, K.F.B. Kushiar, A performance comparison of various artificial intelligence approaches for estimation of sediment of river systems. Journal of Ecological Engineering **22**(7), 20–27 (2021)

S. Hijazi, R. Kumar, C. Rowen, *Using convolutional neural networks for image recognition* (Cadence Design Systems Inc., San Jose, CA, USA, 2015), pp.1–12

C. Huang, J. Zhang, L. Cao, L. Wang, X. Luo, J.H. Wang, A. Bensoussan, Robust forecasting of river-flow based on convolutional neural network. IEEE Transactions on Sustainable Computing **5**(4), 594–600 (2020)

H. Juahir, S.M. Zain, M.K. Yusoff, T.T. Hanidza, A.M. Armi, M.E. Toriman, M. Mokhtar, Spatial water quality assessment of Langat River Basin (Malaysia) using environmetric techniques. Environ. Monit. Assess. **173**(1), 625–641 (2011)

S. Kabir, S. Patidar, X. Xia, Q. Liang, J. Neal, G. Pender, A deep convolutional neural network model for rapid prediction of fluvial flood inundation. J. Hydrol. **590**, 125481 (2020)

A. Kamilaris, F.X. Prenafeta-Boldú, A review of the use of convolutional neural networks in agriculture. J. Agric. Sci. **156**(3), 312–322 (2018)

M. Mamun, J.J. Kim, M.A. Alam, K.G. An, Prediction of algal chlorophyll-a and water clarity in monsoon-region reservoir using machine learning approaches. Water **12**(1), 30 (2020)

M.J. Martinez, Investigation of suspended-sediment concentration in the mississippi river using laser diffraction and remote sensing surrogate methods (Doctoral dissertation, Saint Louis University) (2019)

M. Moeini, A. Shojaeizadeh, M. Geza, Supervised machine learning for estimation of total suspended solids in urban watersheds. Water **13**(2), 147 (2021)

I. Mohamed, Modeling of suspended sediment concentration using conventional and machine learning approaches, in Thames River, Canada (2018)

S. Nivesh, P. Kumar, Modelling river suspended sediment load using artificial neural network and multiple linear regression: Vamsadhara River Basin. India. Ijcs **5**(5), 337–344 (2017)

C. Ni, X. Ma, Prediction of wave power generation using a convolutional neural network with multiple inputs. Energies **11**(8), 2097 (2018)

V. Nourani, H. Gokcekus, G. Gelete, Estimation of suspended sediment load using artificial intelligence-based ensemble model. Complexity 2021 (2021).

F. Pu, C. Ding, Z. Chao, Y. Yu, X. Xu, Water-quality classification of inland lakes using Landsat8 images by convolutional neural networks. Remote Sensing **11**(14), 1674 (2019)

K. Rezaei, M. Vadiati, A comparative study of artificial intelligence models for predicting monthly river suspended sediment load. Journal of Water and Land Development (2020)

F.N.A. Sa'ad, M.S. Tahir, N.H.B. Jemily, A. Ahmad, A.R.M. Amin, Monitoring total suspended sediment concentration in spatiotemporal domain over Teluk Lipat utilizing Landsat 8 (OLI). Applied Sciences **11**(15), 7082 (2021)

B.H.Z. Sami, B.F.Z. Sami, C.M. Fai, Y. Essam, A.N. Ahmed, A. El-Shafie, Investigating the reliability of machine learning algorithms as a sustainable tool for total suspended solid prediction. Ain Shams Engineering Journal (2021)

C.M. Song, Application of convolution neural networks and hydrological images for the estimation of pollutant loads in ungauged watersheds. Water **13**(2), 239 (2021)

B. Taşar, Y.Z. Kaya, H. Varçin, F. Üneş, M. Demirci, Forecasting of suspended sediment in rivers using artificial neural networks approach. International Journal of Advanced Engineering Research and Science **4**(12), 237333 (2017)

F. Üneş, A.B. Karaeminoğullari, B. Taşar, Forecasting of river sediment amount using machine model. International Journal of Environment, Agriculture and Biotechnology **5**(1), 9–15 (2020)

S.P. Van, H.M. Le, D.V. Thanh, T.D. Dang, H.H. Loc, D.T. Anh, Deep learning convolutional neural network in rainfall–runoff modelling. J. Hydroinf. **22**(3), 541–561 (2020)

Y. Xue, L. Zhu, B. Zou, Y.M. Wen, Y.H. Long, S.L. Zhou, Research on inversion mechanism of chlorophyll—a concentration in water bodies using a convolutional neural network model. Water **13**(5), 664 (2021)

A. Yadav, S. Chatterjee, S.M. Equeenuddin, Suspended sediment yield estimation using genetic algorithm-based artificial intelligence models: case study of Mahanadi River India. Hydrological Sciences Journal **63**(8), 1162–1182 (2018)

A. Yadav, S. Chatterjee, S.M. Equeenuddin, Suspended sediment yield modeling in Mahanadi River, India by multi-objective optimization hybridizing artificial intelligence algorithms. Int. J. Sedim. Res. **36**(1), 76–91 (2021)

B. Yilmaz, E. Aras, M. Kankal, S. Nacar, Suspended sediment load prediction in rivers by using heuristic regression and hybrid artificial intelligence models. Sigma: Journal of Engineering & Natural Sciences/Mühendislik ve Fen Bilimleri Dergisi **38**(2) (2020)

M. Zounemat-Kermani, A. Mahdavi-Meymand, M. Alizamir, S. Adarsh, Z.M. Yaseen, On the complexities of sediment load modeling using integrative machine learning: application of the great river of Loíza in Puerto Rico. J. Hydrol. **585**, 124759 (2020)

Self-organizing Algorithm for Fairness in Joint Admission and Power Control for Cognitive Radio Cellular Network

Khalid Kuna, Rashid A. Saeed, Elmustafa Sayed Ali, and Amin Babiker

Abstract

The ever-increasing growth in wireless applications and services indicates the importance of effective use of the limited radio spectrum. Cognitive Radio enables unauthorized secondary users opportunistic access to channels not used by primary users if interference with primary users (PUs) does not exceed pre-defined limits. System modules may be removed according to different Quality of Service (QoS) and SINR required for the base station (BS). This paper is proposing a joint admission and power control scheme (JAPC) as a self-organizing algorithm (SOA) to solve the problem of the fairness related to secondary users (SUs) in cognitive cell. Results show that the proposed scheme obtains more fairness and bitrate compared to previous work.

Keywords

Power control • Cognitive radio (CR) • Fairness • Admission control • Quality of service (QoS) • Self-organizing algorithm (SOA) • Joint admission and power control scheme (JAPC)

K. Kuna (✉) · A. Babiker
Faculty of Engineering, Alneelain University, Khartoum, Sudan
e-mail: khalidkonna@hotmail.com

R. A. Saeed
Department of Computer Engineering, College of Computers and Information Technology, Taif University, P.O. Box 11099 Taif, 21944, Saudi Arabia

E. S. Ali
Department of Electrical and Electronics Engineering, Red Sea University, Port Sudan, Sudan

R. A. Saeed · E. S. Ali
Department of Electronics Engineering, Sudan University of Science and Technology, Khartoum, Sudan

1 Introduction

In cellular communications, licensed wireless primary users (PUs) cannot assign to all frequency channels anytime and anywhere, this because it may leads to create many holes in the spectrum. Cognitive radio (CR) technology enables improved spectrum use efficiency. In cellular CR networks, unlicensed secondary users (SUs) can transmit using free spectrum, and ensures not interrupts to the PUs operations (Shaat 2012). The secondary users (SUs) can be work with the base station (BS) by ensuring that, there are no interferences with the primary users (PUs) above pre-defined threshold (Saeed et al. 2010). In cognitive radio networks (CRN), different SUs define the type of Quality of Service (QoS) and may vary depending on the type of unit. However, these networks may facing interference limitations on the PUs and SUs QoS requirements. Therefore, solutions must be found to provide an effective energy intake and control scheme (Saeed et al. 2006).

Traditional algorithms cannot be applied directly because they treat all users with the same criterion. Therefore, these algorithms are not able to solve CR networks issues if the users have different criterions. Accordingly, the use of CR approach in cellular networks is a practical challenge. The challenge is that it requires accurate and rapid sensing of the spectrum (Xiang 2011). CR concept enables secondary users to access the primary users channels with simultaneous transmission when the core network sufficiently protected. Generally, simultaneous transmission control with defining the Pus, SUs powers and selecting desirable SUs for the network is one of the most important challenges (Al-Hmoudi et al. 2011; Baykas 2012). The complexity lies in the mechanism of finding the best channel assignment for the units. Therefore, one of the most important requirements that the possible solutions to these problems must meet is to maintain the overall system productivity and reduce energy consumption.

In CR networks, different SUs need QoS at different levels and therefore make different payments based on the level of QoS provided (Dimitrakopoulos 2011; Suliman et al. 2015). The problems of joint admission and power control in the cognitive cell on the part of the network operator are the increase in revenue from SUs that are subject to interference constraints on the QoS requirements for both PUs and SUs (Naghian and Baghaie 2002). In addition, there different schemes that proposed to solve the previous problem. One of these solutions is Joint Admission and Power Control scheme (JAPC) (Nahla et al. 2021; Xin and Wang 2008). The shared ability and acceptance control of Joint Admission and Power Control scheme is inviting approach, which helps to realize the concept of coexistence between both PUs and SUs. It also allows both of them to work on the same spectrum without harmful interference. (Saeed et al. 2009b; Saeed and Mokhtar 2012).

This paper presents a new contribution that differs markedly from previous studies. In this paper, we formulate the problem of the fairness to SUs. Secondly, we propose a self-organizing algorithm (SOA) scheme with dynamic system of power control to solve the formulated fairness problem. The results of using SOA were expected to enables much fairness than other schemes.

2 Literature Review

In the past, few studies have been done regarding co-acceptance allocation problems related to control and power in CRN. Researchers in Zhang et al. (2007), investigate on the power allocation control problem in cellular CRN. Authors explained how to ensure QoS for Pus and SUs, which can be translated into degree and signal-to-interference ratio as well as noise (SINR). The authors also pointed that the density and mobility of secondary users influences the possibility of their support due to the limitations mentioned. In addition, they review the possibilities to increase the total revenue of cellular cognitive networks output by finding a subset of secondary users. The authors introduced the power distribution and joint control algorithm, and then evaluate their performance. The results give an advantage over the traditional algorithms.

For device-to-device (D2D) communications, a higher data rate must be achieved in wireless networks. Authors in Azam et al. (2015) examine the challenges faced by cellular users with D2D associated with the energy allocation process for the purpose of improving overall productivity. The authors used the OAA method based on linear approximation to fix the joint access control, power allocation, and the mode selection problems. The results show that the method gives an optimum content and high efficiency in achieving service quality.

A study presented in Gallardo and Jakllari (2018) reviews mechanism to solving the problem of internet acceptance control in multi-hop CRNs. In the proposed scheme, the channel access is organized through a simple TDMA and PU activity designed as an on/off operation. The authors used a random scheduling algorithm to mitigate the problem of online acceptance control and analyzed it. They calculate the average available bandwidth with scheduling between sources in cognitive radio networks.

Authors in Kim et al. (2008) investigate on the dynamic spectrum-sharing between PUs and SUs in a CRN. They provide a solution to the fair spectrum sharing among SUs subjected to QoS constraints related to minimum SINR and transmission ratio, in addition to PUs interference constraints. Moreover, authors develop a framework for joint admission control and power allocation for secondary user. Through the analysis, the researchers concluded that the developed framework has efficacy in terms of primary and secondary user throughput in network.

In Xing et al. (2006), the authors put forward the study of the similar problem in prosthetic receivers with one PU and several SUs. The authors introduced a Distributed Constrained Power Control (DCPC) algorithm to achieve maximum yield with the aid of a potential game. However, this study assumed only a single PU in the system. In Xiang et al. (2008) the study proposes a JAPC-MRER. Researchers ignored the SUs, which removed and only focused in the secondary revenue of submitted SUs. In Roy and Kundu (2011), authors explored the performance of the all joint admission and power control algorithms used in CR networks based CDMA in shaded medium. However, this study also ignored the SUs, which removed and only focused in the secondary revenue of submitted SUs.

In Piran et al. (2020), authors review the quality of service and experience provisioning systems in multimedia communications over CR networks. They highlight the concepts related to QoS and QoE in CR multimedia communication. The authors also presented a number of characteristics of using multimedia services for customer records as well as critical challenges related to QoS requirements and QoE. In addition, they discussed the spectrum sensing features, resource allocation management, a network, and energy consumption management, with discussion of many solutions for each of them.

The authors in Gulzar et al. (2021) proposed an algorithm to address the power control problem of CR networks, where the spectrum utilization problem in the wireless system can be solved by using a non-cooperative game. The non-cooperative game works according to the theory that each player increases his advantage in a competitive environment. The results show that the proposed algorithm improves network performance in terms of high SINR rate and low power consumption.

In Rahim et al. (2020) researchers introduced the concept of Gale Shapley match algorithm to get a better match with suitable channels from the free spectrum, so that it can improve the level of QoS intended for SUs. The study determines the SUs tasks from a channel perspective and allocating the spectrum to them with the adoption of calculating the PUs appearing probability on channel again. The proposed algorithm examine the possibility of using objective functions in the development of favorite lists of secondary users and passive channels by means of Gale Shapely matching theory to choose a suitable SU channel pairs. Through evaluation, results showed a considerable enhancement in terms of overall satisfaction of SUs compared to other technologies.

Authors in El-Saleh et al. (2021) proposed a multipurpose Joint Admission and Power Control scheme (JAPC) optimization to increases the CR network throughput and decreases power consumption. They used an improved swarm intelligence algorithm to optimize the multipurpose JAPC. The study improves the convergence speed and stability of swarm intelligence used in multipurpose JAPC. Results prove that the optimized swarm intelligence algorithm enhanced both overall throughput and power consumption for CR network consists random PUs and SUs.

3 Power Control Algorithms for Cognitive Radio Cellular Network

Cognitive radio (CR) concept dictates unlicensed unused spectrum (Alsolami et al. 2021). In CRN, secondary users (SUs) support CR by sensing available spectrum and then effectively sharing that spectrum with primary users (PUs) (Saeed et al. 2009a; Zhang 2008). However, the process of spectrum sharing between PUs and SUs is considered an important issue, especially since it is exposed to large interference between the Pus (Hasan et al. 2013). Several previous studies addressed the interference problem using control power algorithms to reduce the impact of the above problem (Saeed et al. 2009a; Saeed 2011). We investigated on using the self-organizing algorithm (SOA) based on JAPC algorithm and minimal SINR removal algorithm (MSRA) approaches to improve CR spectrum and minimizing the SINR.

The self-organizing algorithm is working after removed SUs with the less value of SINR. Usually, these SUs located at the edge of cell, and the received power from SUs to the BS is not satisfied (Mokhtar et al. 2021). The SOA checks the safety zone and going to inform the SU to increase the SINR by sending command to removed SUs. Then SOA searching for the SUs with maximum SINR and sending a

Fig. 1 Self-organization algorithm
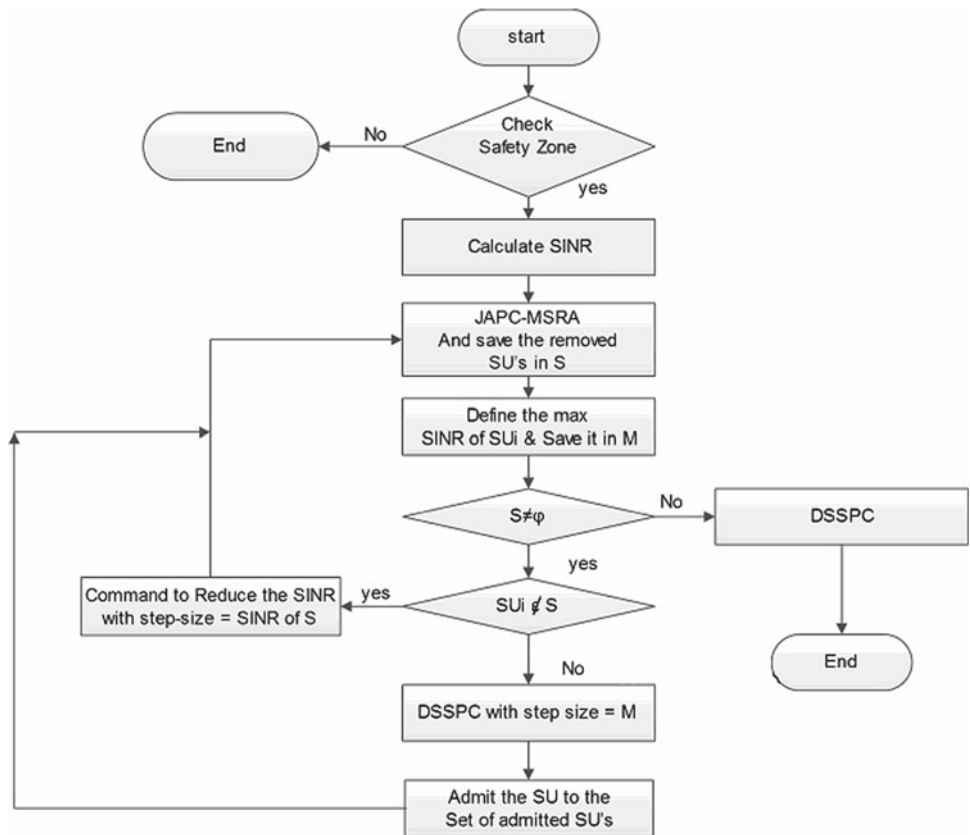
command to inform these SUs to reduce their SINR. The removed SUs will be admitted, and the SUs with maximum SINR will be removed. It is look like replacing them as shown in Fig. 1.

The method used in this study will utilize the use of dynamic step-size power control commands (DSSPC), the SIR/power, and mobile site help data. Accordingly, the concept presented an update to the dynamic interface process of controlling the energy, admission and delivery, which helps to improve the convergence between the proposed energy control mechanisms.

4 Simulation Model and Parameters

The system model consists of a general scenario consisting of a number of SUs and PUs. The base station can accept SUs is used if the PUs interference is less than the previous ones, according to certain thresholds (see Fig. 2). The base station (BS) is assumed to be located at the cell center. It's operated to provide services to SUs with the existence of PUs distributed around the cell. The model shows that SUs enable to access the same spectrum and try to send data to the BS at the same time while the PUs were in receiving mode. This scenario can leading to that PUs to be interfered to SUs.

The calculations related to the evaluated model are focusing to study the performance of the three JAPC schemes with the performance of SOA. The simulation parameters illustrated in Table 1, which provides estimation for interference

Table 1 Parameters for simulation

Parameter	Values
Number of admitted SU in SOA	120
Number of max. replaced SU	30
Number of available channels	120
Interference threshold	1.5
Optimized SINR	1.4–1.9

related to the SUs interference, in addition to values of calculated SINR corresponding to the number of SUs. The simulation calculations are depends to evaluate the self-organization algorithm (SOA) in terms of SUs interference.

5 Simulation Result and Discussion

The result in Fig. 3 shows the calculated interferences corresponding to the amount of SUs with and without using the self-organization algorithm (SOA). The calculation of SUs interferences observing that, the interference constraints in to the PU and SU set before using the SOA, obviously shows the increases in SUs numbers will increase the interference. However, after use of the SOA, the system making fairness to the system by re-adding and removing "replacement" of SU by making maximum number of SU in system and replace the other SU which reduces the interference constraints in the system.

Fig. 2 Simulation system model
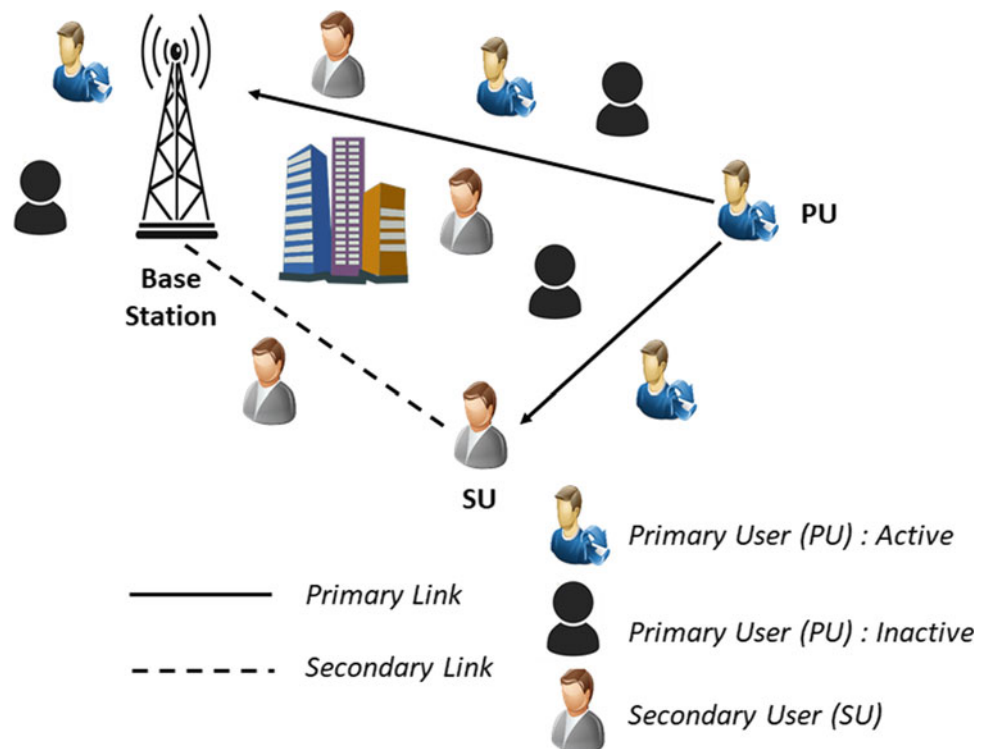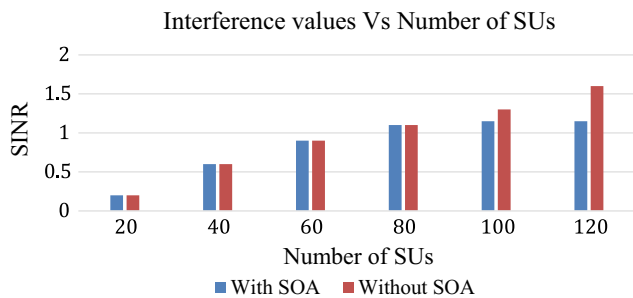
Fig. 3 Performance evaluation of using SOA in term of interference values versus number of SUs

6 Conclusions

The hasty wireless applications growing over the last few decades have initiated a massive demand for wireless network services. Due to the scarcity of the wireless spectrum especially below 10 GHz, wireless industry is unable to catch the fast growing and it becomes quite challenging to grow their revenue. There are many ideas have been proposed by researchers to overcome this problematic issue. One of the potential solutions was to increase the utilization rate of the existing spectrum by using cognitive radio. In this paper, the problem of interference that directs the use of the common spectrum and the increase of the secondary spectrum studied to improve the quality of service. Where the algorithm SOA performance is analyzed to ensure that interference between PUs minimized. The proposed self-organizing algorithm for fairness in joint admission and power control gives more efficient and fairly improvement when compared to other schemes. The self-organizing algorithm enables to improve the system performance in term of power interference on Pus. Moreover, it ensures that system making fairness by limits the maximum number of SU and replace them in order to reduce the interference constraints, in addition to minimize the SINR by 45% in network consists more than 120 SUs.

References

M.I. Al-Hmoudi, R.A. Saeed, A.A. Hasan, O.O. Khalifa, O. Mahmoud, A. Sellami, Power control for interference avoidance in femtocell network. Austr. J. Basic Appl. Sci. (AJBAS), 416–422 (2011)

F. Alsolami, F.A. Alqurashi, M.K. Hasan, R.A. Saeed, S. Abdel-Khalek, A.B. Ishak, Development of self- synchronized drones' network using cluster-based swarm intelligence approach. IEEE Access **9** (2021)

M. Azam et al., Joint admission control, mode selection and power allocation in D2D communication systems. IEEE Trans Veh Technol (2015)

T. Baykas, M. Kasslin, M. Cummings, H. Kang, J. Kwak, R. Paine, A. Reznik, R. Saeed, S.J Shellhammer, Developing a standard for TV white space coexistence: Technical challenges and solution approaches. IEEE Wirel. Commun. Mag. **19**(2), 10–22 (2012)

G. Dimitrakopoulos, P. Demestichas, D. Grandblaise, K. Mößner, CCSR The University of Surrey, J. Hoffmeyer, J. Luo, Cognitive radio, spectrum and radio resource management. Wireless World Res. Forum (2004)

A.A. El-Saleh, T.M. Shami, R. Nordin, M.Y. Alias, I. Shayea, Multi-objective optimization of joint power and admission control in cognitive radio networks using enhanced swarm intelligence. Electronics **10**, 189 (2021). https://doi.org/10.3390/electronics10020189

G.A. Gallardo, G. Jakllari, L. Canourgues, A.-L. Beylot, Statistical admission control in multi-hop cognitive radio networks. IEEE/ACM Trans. Netw. **26**(3), 1390–1403 (2018)

W. Gulzar, A. Waqas, H. Dilpazir et al., Power control for cognitive radio networks: A game theoretic approach. Wirel. Pers. Commun. **123**, 745–759 (2022). https://doi.org/10.1007/s11277-021-09156-x

M.K. Hasan, A.F. Ismail, A.H. Abdalla, K. Abdullah, H. Ramli, S. Islam, R.A. Saeed, in *Inter-Cell Interference Coordination in LTE-A HetNets: A Survey on Self-Organizing Approaches*. 2013 International Conference on Computing, Electrical and Electronics Engineering (ICCEEE), Aug 2013, pp. 196–201

D. Kim, L. Le, E. Hussein, Joint rate and power allocation for cognitive radios in dynamic spectrum access environment. IEEE Trans. Wirel. Commun. **7**(12) (2008)

R.A. Mokhtar, R.A. Saeed, H. Alhumyani et al., Cluster mechanism for sensing data report using robust collaborative distributed spectrum sensing. Clust. Comput. (2021)

S. Naghian, M. Rintamäki, R. Baghaie, in *Dynamic Step-Size Power Control in UMTS*. IEEE International Conference, 15–18 Sept 2002

N. Nurelmadina, M.K. Hasan, I. Mamon, R.A. Saeed, K. Akram, Z. Ariffin, E. Sayed Ali, R.A. Mokhtar, S. Islam, E. Hossain, M.A. Hassan, A systematic review on cognitive radio in low power wide area network for industrial IoT applications. Sustainability **13**(1), 338 (2021)

M.J. Piran, Q.-V. Pham, S.M. Riazul Islam, S. Cho, B. Bae, D.Y. Suh, Z. Han, Multimedia communication over cognitive radio networks from QoS/QoE perspective: A comprehensive survey. J. Netw. Comput. Appl. **172** (2020)

M. Rahim, A.S. Alfakeeh, R. Hussain, M.A. Javed, A. Shakeel, Q. ul Hasan, A. Israr, AO. Alsayed, S.A. Malik, Efficient channel allocation using matching theory for QoS provisioning in cognitive radio networks. Sensors **20**, 1872 (2020). https://doi.org/10.3390/s20071872

S.D. Roy, S. Kundu, Performance of joint admission and power control algorithms for cognitive radio CDMA networks in shadowed environment. Int. J. Commun. Netw. Secur. **1**(1), Article 2

R.A. Saeed, *TV White Space Spectrum Technologies: Regulations, Standards, and Applications* (CRC Press, USA, 2011). ISBN: 9781439848791

R.A. Saeed, S. Khatun, B.M. Ali, M. Khazani, in *Modeling of In-Band Interference Power of Ultra-Wideband*. International Conference on Computer and Communication Engineering (ICCCE '06), vol. (2), Kuala Lumpur, Malaysia, 9–11 May 2006, pp. 910–916

R.A. Saeed, S. Khatun, B.M. Ali, in *Adaptive Power Control (APC) for CDMA-Based UWB Home Network*. IEEE International Conference on Antennas, Propagation and Systems (INAS2009a), 3–5 Dec 2009, Johor Bahru, Malaysia

R.A. Saeed, S. Khatun, B.M. Ali, M. Khazani, Performance enhancement of UWB power control using ranging and narrowband interference mitigation technique. Int. Arab J. Inf. Technol. (IAJIT) **6**(2), 13–22 (2009b)

R.A. Saeed, S. Khatun, B.M. Ali, M. Khazani, A joint PHY/MAC cross-layer design for UWB under power control. Comput. Electr. Eng. (CAEE) **36**(3), 455–468 (2010)

R.A. Saeed, R.A. Mokhtar, in *TV White Spaces Spectrum Sensing: Recent Developments, Opportunities and Challenges*. The 6th International Conference SETIT 2012: Sciences of Electronic, Technologies of Information and Telecommunications (SETIT2012), Tunisia, Apr 2012, pp. 634–638

M.M.R. Shaat, *Resource Management in Multicarrier Based Cognitive Radio Systems* (Universitat Politècnica de Catalunya (UPC), Barcelona, 2012)

K.B. Suliman, R.A. Saeed, R.A. Alsaqour, On chip communication architecture power estimation in high frequency high power model. ARPN J. Eng. Appl. Sci. **10**(12), 5126–5131 (2015)

J. Xiang, *Resource Management and Optimization for Cognitive Radio Networks* (University of Oslo, 2011)

J. Xiang, Y. Zhang, T. Skeie, in *Joint Admission and Power Control for Cognitive Radio Cellular Networks*. 11th IEEE Singapore International Conference on Communication Systems, 2008, pp. 1519–1523. https://doi.org/10.1109/ICCS.2008.4737437

Q. Xin, X. Wang, J. Cao, W. Feng, in *Joint Admission Control, Channel Assignment and QoS Routing for Coverage Optimization in Multi-hop Cognitive Radio Cellular Networks*. IEEE International Conference on Communications (ICC 2008), 19–21 Nov 2008

Y. Xing, C.N. Mathur, M.A. Haleem, R. Chandramouli, K.P. Subbalakshmi, in *Priority Based Dynamic Spectrum Access with QoS and Interference Temperature Constraints*. IEEE International Conference on Communications, 2006, pp. 4420–4425. https://doi.org/10.1109/ICC.2006.255334

L. Zhang, Joint beam forming and power allocation for multiple access channels in cognitive radio networks. IEEE J. Sel. Areas Commun. **26**(1), 38–51 (2008)

L. Zhang, Y. Liang, Y. Xin, in *Joint Admission Control and Power Allocation for Cognitive Radio Networks*. 2007 IEEE International Conference on Acoustics, Speech and Signal Processing—ICASSP '07, 2007, pp. III-673–III-676. https://doi.org/10.1109/ICASSP.2007.366769

The Role of SWOT Analysis in Improving Operational Performance (Analytical Study in a Prefabricated Building Factory)

Mueyyed Akram Omar Arslan, Sivadass Thiruchelvam, Gasim Hayder, and Sawsan Ibrahim Rajab

Abstract

The SWOT analysis has received its share of attention from administrative researchers, as it represents the diagnostic tool that the organization adopts in determining the factors and variables that can affect its operational performance and thus be reflected in its operational performance, which represents the identity adopted by the organization to define itself and its products to the customer. Hence, this study came to define the SWOT analysis and its role in the operational performance of the prefab factory. By determining the correlation and impact of this analysis on operational performance and collecting data related to the study variables, an intentional sample was selected, representing the factory director, members of the board of directors, and supervisors. Production lines surveyed their views by adopting a questionnaire designed for this purpose, distributed 25 questionnaires, and recovered from them 19 valid questionnaires for analysis with a 75% confidence degree. Among the proposals that we hope will be useful to the organization in question in its factory.

Keywords

SWOT analysis • Operational performance • Prefabricated building

M. A. O. Arslan (✉)
College of Graduate Studies, Universiti Tenaga Nasional (UNITEN), 43000 Kajang, Malaysia
e-mail: Alparslan1961.ma@gmail.com

S. Thiruchelvam · G. Hayder
Department of Civil Engineering, College of Engineering, Universiti Tenaga Nasional (UNITEN), 43000 Kajang, Malaysia

Institute of Energy Infrastructure, Universiti Tenaga Nasional (UNITEN), 43000 Kajang, Selangor Darul Ehsan, Malaysia

S. I. Rajab
Kirkuk Technical Institute, Northern Technical University, Mosul, Iraq

1 Introduction

The emergence of environmental analysis is due to many challenges facing business organizations, which are rapid environmental changes (Huo et al. 2016), the difficulty of predicting threats, the severity of their danger, and the extent of the organization's ability to adapt and survive (Staik0uras and Mamatzakis 2007), which makes the continuation of these organizations very difficult if they are unable to study and analyze their internal environment and External to achieve its objectives (Durdyev et al. 2018; Huo et al. 2016).

SWOT analysis is one of the environmental analysis tools that enable the organization to identify strengths and weaknesses in its internal environment and identify opportunities and threats in its external environment (Al-Jaber and Hamid 2007), which helps it achieve its goals by seizing opportunities and reducing environmental threats (Xie et al. 2020), enhancing strengths, and addressing weaknesses and the extent of the impact this is in operational performance. Based on the foregoing and to achieve the study's goals and objectives, it was divided into four sections: the first body its methodology, the second presented the theoretical framework, the third presented a presentation of its analytical side, and it was concluded with the fourth topic, which was devoted to the conclusions and suggestions reached by the study.

The prefab factory faces a set of challenges that directly affected the achievement of its goals as a result of the environmental changes that made its survival and continuity in the labor market very difficult, as was noticed through field visits to the site of the researched company (the prefab factory) that its management did not adopt appropriate tools that enable it to Study and analysis of the work environment at the internal and external levels, which is reflected in its operational performance, which is a function that indicates the good analysis of the impositions, threats, and use of internal resources that characterize the organization in the world of competition with its counterparts from other organizations. Based on the foregoing, we can present the

problem of the study through the following question: Does SWOT analysis affect the operational performance of the company understudy?

The study derives its importance from the necessity of accrediting business organizations in general and the company investigated in particular (SWOT) analysis in identifying environmental variables and taking appropriate decisions that may affect their operational performance.

The objectives of the study can be defined based on a theoretical and applied attempt to study the SWOT analysis and operational performance and to determine the nature of the relationship between the two dimensions of the study. The study seeks to prove the two hypotheses: firstly, there is a significant correlation between a SWOT analysis and operational performance; and secondly, there is a significant effect of SWOT analysis on operational performance.

2 Settings or Methods or Materials

This factory was chosen for its excellence in the integration of the manufacturing process, which helped in evaluating the production process in its various stages, as well as the problems that this organization suffers from, including damage to the final or semi-finished products.

A questionnaire designed for this purpose was used, a total of 25 questionnaires were distributed, and 19 were retrieved from them that were valid for analysis and with a confidence degree of (75%). To be useful to the organization in question in its plans.

To obtain the data and information necessary to test and prove the hypothesis, the theoretical side has been covered in many sources that were represented by scientific references such as books, magazines, studies, and theses related to the study. To the factory records, as well as using the checklist called the gap analysis examination (Xie et al. 2020; Durdyev et al. 2018), which aims to diagnose the gap between the reality of the quality management system in an organization and the standard requirements in the international standard (ISO 9001:2015) (Durdyev et al. 2018). For this purpose, the heptagonal scale was used (Durdyev et al. 2018), as a specific weight was assigned to each of the paragraphs of that scale (Kumar and Phrommathed 2006), and accordingly, the analysis was done and the results were reached (Kumar and Phrommathed 2006).

3 Results

This part of the study deals with testing the hypothesis of the study using some statistical methods, through which we seek to prove the reality of the relationship between each of the (SWOT) analyses and operational performance in the prefab factory through the following.

3.1 Analyzing the Correlation Between a SWOT Analysis and Operational Performance

The results shown in Table 1 indicate that there is a significant correlation between (SWOT) analysis as an explanatory variable and operational performance as a response variable. There are two variables, and it is clear through the correlation matrix (Kumar and Phrommathed 2006) that there is a significant correlation between the combined SWOT analysis indicators and operational performance which states that "there is a significant correlation between a SWOT analysis and operational performance.

3.2 Analyzing the Impact Relationships Between a SWOT Analysis and Operational Performance

According to the data of Table 2, it is clear that there is a significant impact relationship of (SWOT) analysis on operational performance, as the value of the coefficient of determination ($R2$) is (0.665), meaning that (SWOT) analysis explains its value (0.665) of the factors and determinants that affect performance. In addition to the presence of other random variables that can affect operational performance as well, the value of (beta coefficient) is (0.915), which means that the change of one unit concerning (SWOT) analysis affects the same amount of operational performance, and this effect is supported by the value of (F) calculated and amounting to (98,097), which is greater than its tabular value of (11.259), at the level of significance (0.00), which we see as a logical result, as this analysis contributes to building strategic plans that enable the organization to take the correct and appropriate decisions to achieve what has been set in the plans from objectives, as well as ensuring survival and continuity in a highly competitive market. Based on the foregoing, the second main hypothesis can be accepted, which states that "there is a significant impact relationship for SWOT analysis on operational performance.

Table 1 The correlation between the SWOT analysis dimension and operational performance

Explanatory dimension	SWOT analysis
Responsive dimension	
Operational performance	0.822*

$^*P \leq 0.01$, $N = 19$

Source Prepared by researchers based on electronic calculator output

Table 2 Results of the total simple linear regression of the SWOT matrix analysis in operational performance

Explanatory dimension	SWOT analysis			
Responsive dimension	P.V	The calculated F value	$R2$. coefficient of determination	beta coefficient value
Operational performance	0.00	98.96	0.665	0.915

$^*P \leq 0.01$, $N = 19$

Source Prepared by researchers based on electronic calculator output

4 Conclusion

The study reached some conclusions, the most important of which are the following:

1. The company has a positive history in the field of prefabricated construction, as the company possesses evidence of successful projects that contributed to their completion in various Iraqi governorates under complex environmental conditions as a result of the economic blockade that was imposed on Iraq during the past decades.
2. The company possesses high skills, experiences, and competencies, specifically in the engineering fields, that will enable it to progress and develop if these competencies are widely employed and supported by the requirements and requirements necessary for the advancement of work.
3. The company achieves growth and profits, but it does not rise to the required level as a result of the many influences that imposed themselves on the company and its activities.
4. To analyze whether a significant role in the company's operational performance, as the results proved a correlation of (SWOT) analysis by (0.822), with operational performance, and the impact of (SWOT) analysis by (0.665) on operational performance, which imposes on the studied factory to give an analysis (SWOT) importance, concern and its adoption as a work method for developing its operational performance.

5 Recommendations

Based on the conclusions of the study, a set of proposals were presented, which we hope will be useful to the broadcast organization, and other similar organizations. The proposals are as follows:

1. Investing in the company's reputation, history, and expertise in the field of prefabricated construction, specifically within the reconstruction and construction projects undertaken by the state in various sectors.
2. Updating production lines and providing them with modern machines and equipment that enable them to keep pace with the changes taking place in modern production technologies.
3. Activating research and development activities, and providing sufficient supplies for employees to enable them to provide the best that advances the company's activities and operations.
4. Studying market developments through market research that diagnoses the customer's renewable and changing needs and requirements.
5. Activating marketing research activities to develop the company's market share in the future.

References

A. Al-Jaber, S.A. Hamid, The relationship between strategic analysis and alliance strategy and their impact on organizational performance, (a prospective study of the opinions of samples of the Ministry of Housing and Construction). Ph.D. thesis, College of Administration and Economics, University of Baghdad, Baghdad, Iraq, 2007

G.P. Cachon, M.A. Lariviere, Supply chain coordination with revenue-sharing contracts: strengths and limitations. Manage. Sci. J. **51**(1) (2005)

S. Durdyev, E.K. Zavadskas, D. Thurnell, A. Banaitis, A. Ihtiyar, The sustainable construction industry in Cambodia: awareness, drivers, and barriers. Sustainability **10**(2), 392 (2018)

B. Huo, M. Gu, D. Prajogo, Flow management and its impacts on operational performance. J. Prod. Plann. Control **27**(15), 1233–1248 (2016)

S. Kumar, P. Phrommathed, *New Product Development: An Empirical Approach to the Study of the Effects of Innovation Strategy, Organization Learning, and Market Conditions*, vol. 191 (Springer Science & Business Media, 2006)

C. Staik0uras, E. Mamatzakis, Operating performance of the banking industry: an empirical investigation of the South Eastern European region. South-Eastern Europe J. Econ. **2**, 245–266 (2007)

M. van Woerkom, Strengths use and work engagement: a weekly diary study. Eur. J. Work Organ. Psy. **25**(3), 384–397 (2016)

L. Xie, Y. Chen, B. Xia, C. Hua, An importance-performance analysis of prefabricated building sustainability: a case study of Guangzhou. Adv. Civ. Eng. (2020)

Developing Performance Dashboard for Operational KPIs of Water Distribution Network

Yousuf Said Mohammed, Sivadass Thiruchelvam, Gasim Hayder, and Siti Indati Mustapa

Abstract

Developing and implementing dashboards are prevalent in the vast advanced companies. This paper proposes to develop dashboards for the performance management of water distribution networks aimed at improving the efficiency and productivity by implementing operational excellence approach. Efficient operation of the water distribution networks is essential. Losses and failures along the water distribution network are major challenges for the water organizations around the world. Operational information from systems and field teams provide massive amount of data and many opportunities to monitor and evolve the effectiveness of water distribution networks. The collected information from the required measurements can be shown digitally on professional dashboard with graphs and trends that characterize the indicators in a clear to understand by visual demonstration. A practical performance dashboard was successfully developed and implemented in the chosen zone for the main factors of water networks such as leaks, shortages, new connections, preventive maintenance, corrective maintenance, and pressure readings. The results are automatically updated daily and monthly. Data gathering was conducted through the used operational technical systems and records from field teams. Customized dashboards allow the users to explore the performance metrics as per the requirements and review their accomplishments and patterns. This facilitates motivation to improve performance and reach to professional benchmarks. There is great potential of digital technology for managing works in the proposed procedures assisting water authorities in improving the service quality, communications and promoting a culture of continuous improvement.

1 Introduction

The use of dashboards for professional management in many businesses and fields is increasing in the sophisticated organizations for improving the performance and productivity. Using of the graphic analytic methods is highly affective for improving the operations management, efficiency, quality, and staff performance. This tool has grown dramatically in the last 10 years, because of the development of Technologies and Information (Hensley et al. 2021).

Performance dashboards are using dynamic graphic screens to show improvement of the performance, productivity, and trends behavior of related business. These visual presentations on computer screens are interacting with the users to choose, categories, filter, zoom in, and overview data. It is updated continuously which resulting variation on the results and trends over the time. Sometimes the information can be displayed as real time and the update is every few seconds. Applying the visional influence is great to summarize and link a large amount of information, operational dashboards empower the users to effectively identify the characteristics to classify patterns. This methodology is

Y. S. Mohammed (✉)
College of Graduate Studies, Universiti Tenaga Nasional (UNITEN), 43000 Kajang, Selangor, Malaysia
e-mail: yousuf.alsiyabi@owwsc.nama.om

Oman Water and Wastewater Services Co, Muscat, Sultanate of Oman

S. Thiruchelvam · G. Hayder
Department of Civil Engineering, College of Engineering, Universiti Tenaga Nasional (UNITEN), 43000 Kajang, Selangor, Malaysia

S. I. Mustapa
Institute of Energy Policy and Research (IEPRe), Universiti Tenaga Nasional (UNITEN), 43000 Kajang, Selangor, Malaysia

cognitive tools that progress control over huge, mixed, and transitioning of data (Young and Kitchin 2020).

Water supply networks are very basic for the people life. It is critical component in the country's infrastructure, providing healthy and comfortable life required safe and continuous drinking water. Measuring the efficiency of water distribution networks can create benchmarking references and baselines to improve the quality of services and provide valuable information about the level of effectiveness in the sector (Storto 2020). Therefore, the closed monitoring of the related parameters progress is required for achieving better level.

2 Methods

The various requirements for the dashboard are mainly to have appropriate it functional and practical use. The entire chosen of KPIs should be implemented in the dashboard. Then, it is considered to have clear colors and meaningful for each parameter. Overstated using of colors can confuse the users, so it is preferred to have limited colors and ranges on the dashboards. Additionally, the users should have basic skills for graphs readings and meanings of shown numeracy. Finally, there are professional computer programs for creating the required customized dashboard, for example, Power BI, Qlik Sense, or QlikView. Each of these programs has its features and strengths for graph options, data connectivity, etc. (Baalbergen 2019).

Oman Water and Wastewater services Company OWWSC is providing potable water in Sultanate of Oman. The system is complicated due to the geographical nature there. In some fields, there are challenges to have excellent implementations of the company strategies. There are areas that need to be improved in management of performance, because it is affecting the productivity, service quality, and creation of effective decisions. Therefore, improving the performance of the staff and departments inside the water authority organization is essential. However, the management of water distribution networks from the production sites to the customers is very complex mission with many steps and processes (Taha et al. 2020). Dashboard was constructed in Muscat water networks—zone 3 with daily and monthly operational data from the last 3 months from customer relationship management system (CRM) for complaints and field teams' technical reports, using the excel formats which planned to be moved later in power BI system. The dashboard was designed to display 12 technical parameters. (leaks, shortages, preventive maintenance, planned maintenance, pressure, flow, power consumption, rehabilitation, assets status, DMAs isolation, shutdowns, leak detection).

Reduction of leaks and complaints water distribution networks is essential priority. This paper presented performance parameters, such as the Leakage Performance Index (LPI), to reduce leakages starting from clear and continuous measurements of pressure and flow rate. This strategy was efficient to minimize the leakages (Cavazzini et al. 2020).

3 Results

Figures 1 and 2 show the main used parameters of performance dashboard in water distribution networks for the leaks and shortages complains. The results demonstrate an increase of the efficiency from July 21 to September 21 due to applying of required field actions and using the dashboards concept and to monitor the daily progress.
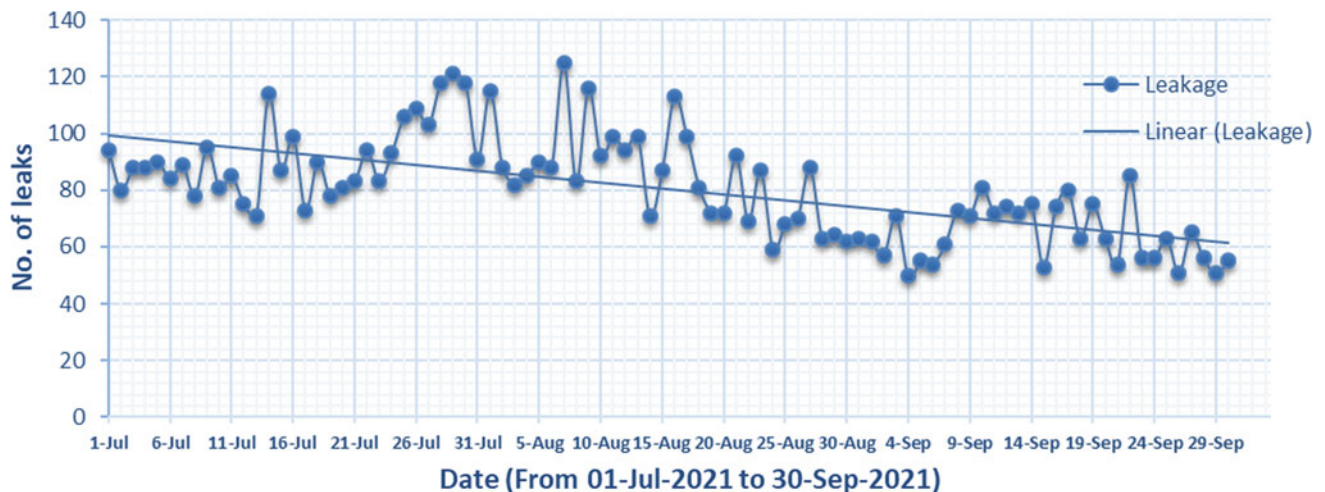
Fig. 1 Reduction of number of leaks from month of July 21 up to end of September 21
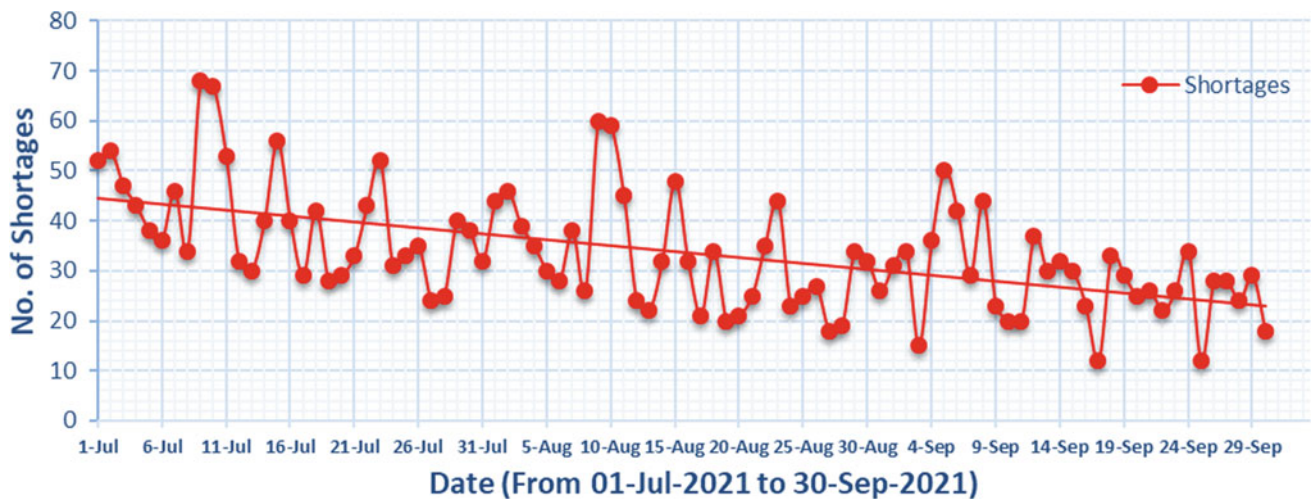
Fig. 2 Reduction of number of shortages from month of July 21 up to end of September 21

- The implementation of performance dashboards started in water distribution networks in Muscat Zone-3 in the month of July 21, as shown the impact on the performance is demonstrated in next months. The reduction in leaks and shortages is interesting for August-21 and September-21 compared with July 2021.
- By continuously monitoring of the progress in the shown parameters on the operational dashboard, the teams and technical staff is looking always for better results by implementing solutions and following the impact on the dashboards.
- The reduction of leaks and shortages came after applying few action plans related to pressure management, rehabilitations of small routes, and controlling the supply to some parts.

different level of technical skills to understand the meaning of graphs and numbers (Baalbergen 2019).

The management-level dashboard is not same for the technical teams, so it is important to have flexible dashboards which can summarize or expand the information.

The presented results in Table 1 show that the use of performance indicators and dashboards has a direct impact on raising efficiency, as the number of leaks decreased with the passage of time, and the same thing happened with regard to water service interruptions as shown in Table 1.

The gradual successful improvement of the performance can be partially due to continuously available information about the work progress and current efficiency of the water networks, because in case of any failures, the results will be displayed directly. The teams are trying to increase the quality of service by reducing the failures. Keeping the eyes on dynamic visual screens enhance everyone to give more productivity.

4 Discussion

The concept of performance improvement by using key performance indicators is substantial for the growth of the organizations and businesses. This paper presents monitoring, selecting, evaluating, and visualizing operational KPIs in professional technical dashboard. The dashboard is required to be appropriate for different skills capabilities of the users. During developing the required dashboard, it is significant to know the users, because each employee has a

5 Conclusions

The objective of this study was to develop a customized operational dashboard for the technical teams and staff to increase the performance and efficiency. The results were impressive with direct increase of the motivation and productivity within 3 months. It is expected that the used performance dashboard will be very beneficial for technical

Table 1 Change in number of leaks and shortages from July 21 to September 21

Month	Leakage	% Change	Shortages	% Change
July 21	2839	–	1,250	–
August 21	2636	− 7.2%	1,012	− 19.0%
September 21	1928	− 26.9%	842	− 16.8%

teams and managers to support them fulfill the tasks more quickly with better quality. Also, the mentioned methodology of clear dashboards is improving the communication and discussion between the groups in the organization due to more clarity of the related parameters and linked factors between different departments. The managers and field teams think that the use of the dashboard is an affective concept and with more motivation in the work environment. The implementation of the performance dashboards can be deeper to complicated parameters and levels to cover and link all affective factors which can be considered as future plans in the company.

References

T. Baalbergen, *Monitor KPI'S with a performance dashboard* (University Twente, Enschede, Netherlands, 2019)

G. Cavazzini, G. Pavesi, G. Ardizzon, Optimal assets management of a water distribution network for leakage minimization. Sustainable Cities and Society **54**, 11 (2020)

N.B. Hensley, M.C. Grant, B.C. Cho, G. Suffredini, J.A. Abernathy, How do we use dashboards to enhance quality in cardiac anesthesia? Journal of Cardiothoracic and Vascular Anesthesia 8 (2021)

C.L. Storto, Measuring the efficiency of the urban integrated water service by parallel network DEA: The case of Italy. Journal of Cleaner Production **276**(2020), 123170 (2020)

A.L.W. Taha, S. Sharma, R. Lupojad, A.L.N. Fadhl, M. Haiderac, Assessment of water losses in distribution networks: methods, applications, uncertainties, and implications in intermittent supply. Resources, Conservation & Recycling **152**(2020),104515 (2020)

G.W. Young, R. Kitchin, Creating design guidelines for building city dashboards. International Journal of Human-Computer Studies **140** (2020) 102429 (2020)

Biological Nitrogen Removal of Monoethanolamine (MEA) from Petrochemical Wastewater Using an Activated Sludge Process

N. N. H. Ismail, S. R. M. Kutty, L. Baloo, A. N. F. Akma, M. A. H. M. Fauzi, M. A. Razali, N. Azmatullah, and M. R. Marzuki

Abstract

Monoethanolamine (MEA) has been widely used for the removal of carbon dioxide and hydrogen sulfide in natural gas processing plant. However, during the treatment process of wastewater at Petronas Chemical Olefins Glycol Derivates (PCOGD), a small amount of amine (MEA) gets carried over from the process plant causing spikes in ammonia. Therefore, treatment of MEA-contaminated wastewater is a major concern in most amine sweetening plants. The objective of this study is to determine the impact of MEA on removal of nitrogen compounds using two trains of activated sludge treatment system. In this study, MEA wastewater was treated via a bench-scale of two trains that consist of three reactors known as reactor A1T1, A2T1, and A1T2. Train 1 will have two bench-scale activated sludge systems connected in series which is reactor A1T1 and reactor A2T1, while Train 2 is consisted of a single bench-scale activated sludge system which are reactor A1T2. The raw influent wastewater from PCOGD will be fed with varying concentrations of MEA (50, 100, 500, and 1000 mg/L). Influent and effluent samples were monitored for pH value, alkalinity, ammonia, and Total Kjeldahl Nitrogen. Based on the result, it can be observed that the addition of MEA decreases the percentage removal of nitrogen and slows down the nitrification process in all reactors. Throughout the study, Train 1 performed slightly better than train 2 since the impact of MEA was absorbed by the first reactor in train 1. However, alkalinity must be added and maintained to provide for nitrification in the second reactor. This study indicates that using activated sludge system to remove MEA contaminants from wastewater is both feasible and desirable.

1 Introduction

In Malaysia, PETRONAS Chemical Groups Berhad is a leading integrated chemicals producer as well as one of the largest in Southeast Asia. PETRONAS Chemicals Group Berhad composed of group of companies known as Petronas Chemical Olefins Glycol Derivates (PCOGD) which manufacture a wide range of petrochemical products, ranging from ethylene and propylene feedstock to intermediate products such as ethylene oxide, ethylene glycol, butanol, and various ethylene oxide derivatives, as well as basic and high-performance chemicals. The manufacturing of petrochemical products had resulted in increased CO_2 emissions. Because of MEA's strong absorptive toward CO_2 across a wide range of partial pressures and quick response rate, it is widely utilized in CO_2 post-combustion capture in PETRONAS chemical plant. Additionally, MEA's hydroxyl group (OH) lowers its vapor pressure that subsequently increasing CO_2 solubility, while its amino group generates an alkaline condition for acid gas (CO_2) absorption (Nurrokhmah et al. 2013). This advantage makes MEA the most suitable solvent for industrial applications such as gas sweetening and power plants because of these benefits. However, the loading capacity is limited to 0.5 mol CO_2 per mole of amine due to stoichiometry. The production of petrochemical product had producing wastewater from derivates plants. In the Effluent Treatment System (ETS), wastewater generated by the process plants is being treated

N. N. H. Ismail (✉) · S. R. M. Kutty · L. Baloo · A. N. F. Akma · M. A. H. M.Fauzi · M. A. Razali · N. Azmatullah
Universiti Teknologi Petronas, Persiaran UTP, 32610 Seri Iskandar, Perak, Malaysia
e-mail: nur_16002421@utp.edu.my

M. R. Marzuki
Petronas Chemical Olefins Glycol and Derivatives (PCOGD), 24300 Kerteh, Terengganu, Malaysia

Fig. 1 Effluent treatment system in PCOGD
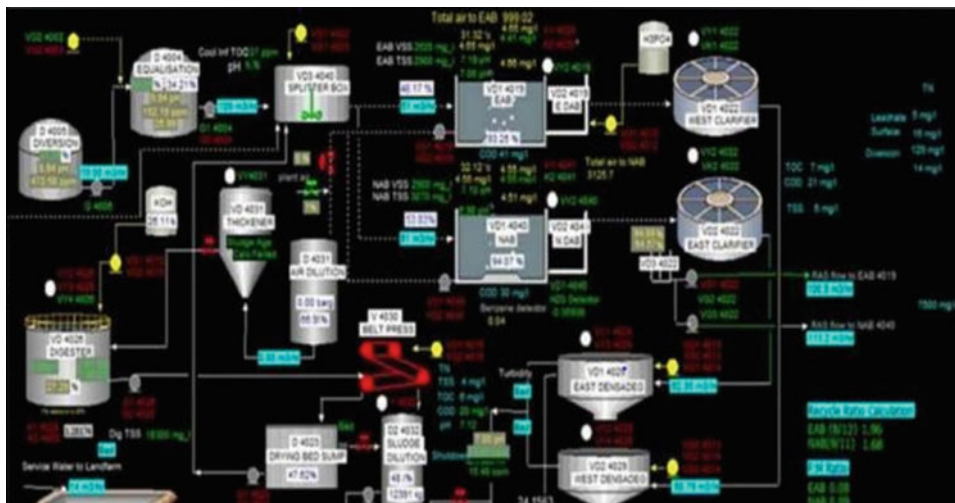
with an activated sludge plant. Figure 1 shows the effluent treatment system used by PCOGD.

Currently, wastewater generated from the wide range of petrochemical products from a feedstock of Ethylene and Propylene in PCOGD is being treated using an extended aeration-activated sludge plant in the Effluent Treatment System (ETS). However, ETS in PCOGD has been experiencing spikes in ammonia from the activated sludge effluent when there was an amine (MEA) carryover from the process plant. Hence, this study seeks to investigate the impact of the MEA on nitrogen removal in the activated sludge system. This study will be observed and determine the maximum concentration of MEA will affect the treatment process of the petrochemical wastewater to meet the effluent discharge limit set by Malaysian Environmental Quality (Industrial Effluents) Regulations, 2009, and to proposed a better train configuration of activated sludge treatment system in treating MEA wastes.

2 Methods and Materials

2.1 Flow of Work

The experimental research was performed as follows:

  i. The industrial wastewater collected from the industry will be biologically treated in a two-train system. Train 1 is composed of both conventional and extended aeration activated sludge systems, whereas Train 2 is composed of only extended aeration activated sludge systems. This is to determine which train will function well to reduce the impact of monoethanolamine (MEA) on the nutrient removal in an activated sludge process.

 ii. The test will be conducted for acclimatization phase 1 and acclimatization phase 2. Acclimatization phase 1 will be conducted by diluting the wastewater collected from PCOGD with a dilution factor of 1:6 while for acclimatization phase 2, testing was conducted with concentrated wastewater.

iii. The test will be conducted with the addition of monoethanolamine (MEA). The raw influent concentration of MEA will be varied to 50, 100, 500, and 1000 mg/L. This is to determine the maximum hydraulic and organic loading to the system.

iv. The samples were monitored for pH value, alkalinity balance, ammonia–nitrogen, and Total Kjeldahl Nitrogen with a frequency of three times per week. Finally, the data were collected and analyzed.

2.2 Setting up of Treatment System

For the investigation of the nitrogen removal of the activated sludge system, it is proposed to conduct a bench-scale study in two trains as shown in Fig. 2 by using 3 reactors known as reactor A1T1, A2T1, and A1T2. Both trains will be set up for the experiment to treat the wastewater from PCOGD.

2.3 Experimental Methodology

During the acclimatization phase, biomass from PCOGD will be used for reactor start-up in both trains. PCOGD wastewater will be fed into the systems at a continuous flow rate of 10 L/day until steady-state conditions are achieved (detention time = 24 h). Once acclimatization is complete, MEA will be fed into the influent tank in four stages at

Fig. 2 Setting up treatment system in two train
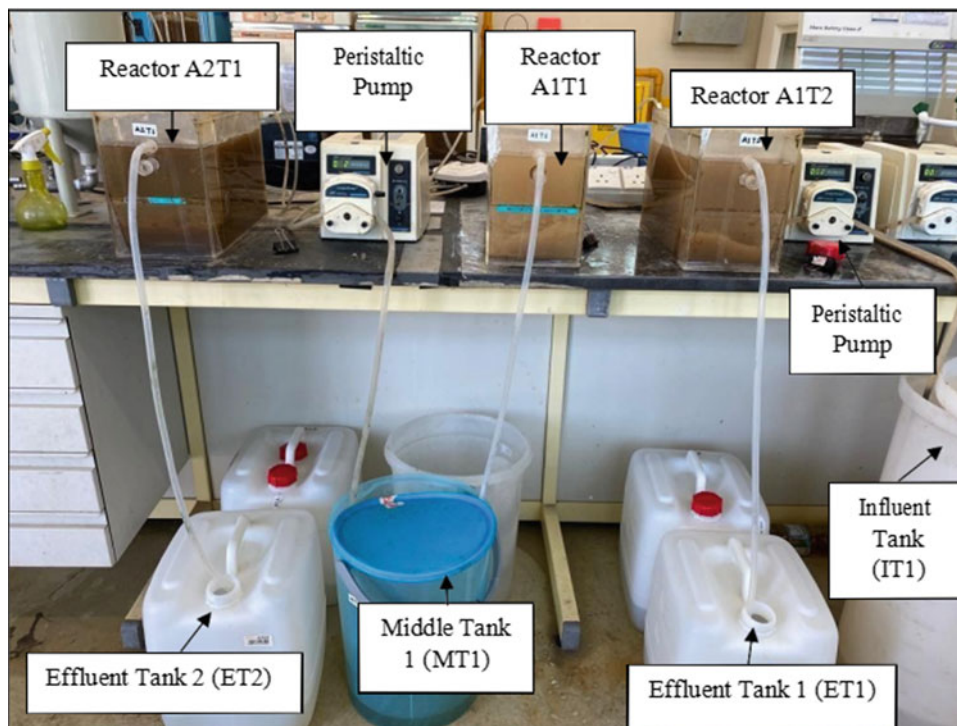
concentrations of 50, 100, 500, and 1000 mg/L, or until the activated sludge system's inhibitory effect on the parameters examined is observed. The effect of MEA concentration on the wastewater parameters will be monitored until a state is achieved. Another reactor will be used as a control for both trains. In this control reactor, the wastewater will be fed with the PCOGD wastewater only (without any addition of MEA). The alkalinity of the raw wastewater will be measured to determine the amount of sodium bicarbonate to be added to the system to maintain the nitrification process. The solution proposed is to conduct the bench-scale study in two trains as the following:

2.3.1 Train 1

In this Train 1, two bench-scale activated sludge systems will be set up as in series. The first aeration tank will be for the degradation of organic matter while the second aeration tank is for nitrification. Both tanks will be fabricated with a volume of 10 L. Wastewater from PCOGD will be fed into the system at constant flowrate of 10 L/day in each reactor. The biomass in the reactors will be acclimatized using the biomass from PCOGD and wastewater from PCOGD. Train 1 consists of two reactors which are reactor A1T1 and reactor A2T1. Each reactor consists of an aeration chamber and the final settler. The metabolic process for the degradation of the wastewater occurs through the action of micro-organisms utilizing the wastewater as food and producing the sludge as a by-product. The first aeration tank will be operated in the conventional aeration activated

sludge process mode (with sludge age of 5 days; MLSS of 1500 mg/L), where ammonia nitrogen is produced in the aeration chamber by microorganisms through oxidation, synthesis, and endogenous respiration. The ammonia is reduced to nitrate in the second aeration tank (sludge age of 30 days: MLSS of 4000 mg/L). Wasting of activated sludge from the aeration tank will be conducted at periodic intervals to maintain the concentration of biomass into the bioreactor and the required sludge age. After the treatment from the two aeration tanks, the wastewater will then be settled in a clarifier tank.

2.3.2 Train 2

In train 2, one bench-scale activated sludge system as in Fig. 5, operated at extended aeration will be used for the degradation of organic matter from PCOGD. The aeration tank will be fabricated with a volume of 10 L. Wastewater from PCOGD will be fed into the system at constant flow rate to achieve a detention time of 24 h. The biomass in the reactors will be acclimatized using the biomass from PCOGD and wastewater from PCOGD. The biomass in the aeration tank will be maintained at 4000 mg/L and will be acclimatized using PCOGD prior varying the flow rate. Wasting of activated sludge will be conducted at periodic intervals from the aeration tank to maintain the sludge age at 40 days. It is expected that nitrification of the organics will occur in the aeration tank. After the treatment from the aeration, the wastewater will be settled in the clarifier. Table 1 shows the summary of Train 1 and Train 2.

Table 1 Summary of Train 1 and Train 2

Train	1				2	
Reactor	A1T1		A2T1		A1T2	
Type of activated sludge	Conventional aeration activated sludge mode		Extended aeration activated sludge mode		Extended aeration activated sludge mode	
Tank	IT1	MT1	MT1	ET1	IT1	ET2

2.4 Sampling Monitoring and Testing Method

The wastewater collected from PCOGD will be treated biologically using the two trains of activated sludge systems proposed above. Influent and effluent from the system will be analyzed for parameters such pH value, alkalinity balance, ammonia–nitrogen, and Total Kjeldahl Nitrogen. Throughout the study, wastewater samples will be collected every two days (sampling three times a week) and will be measured in triplicates for both trains to ensure results consistency. Table 2 showed the materials and methods used during the testing.

3 Results

3.1 Results of pH Throughout the Study Period

pH value was measured at IT, MT1, ET1, and ET2 throughout the study period and plotted as in Fig. 3.

3.2 Results of Alkalinity Balance for all Reactors Throughout the Study Based on Influent Ammonia

The alkalinity requirements for all reactors were evaluated in this section for reactors A1T1 and A2T1 for Train 1, and reactor A1T2 for Train 2. The alkalinity parameters that were observed include influent alkalinity, alkalinity required for nitrification, alkalinity removed, and alkalinity to be added to maintain the effluent alkalinity of 100 mg/L as $CaCO_3$.

3.2.1 Alkalinity Balance for Reactor A1T1
Alkalinity balance for Reactor A1T1 were evaluated throughout the study and were plotted as shown in Fig. 4.

3.2.2 Alkalinity Balance for Reactor A2T1
Alkalinity balances for Reactor A2T1 were observed throughout the study and were plotted as in Fig. 5.

3.2.3 Alkalinity Balance for Reactor A1T2
Alkalinity balance for Reactor A1T2 was evaluated throughout the study and was plotted as in Fig. 6.

3.3 Results of Nitrification Rate Throughout the Study Period

The nitrification rate was evaluated for the reactors using the following equation:

$$\frac{(S_0 - S_e)Q}{XV}$$

S_0 influent ammonia concentration (mg/L),
S_e effluent ammonia concentration (mg/L),
Q flow rate of the aeration tank 10 L/d,
X MLVSS concentration in the aeration tank (mg/L).
V volume of the aeration tank, 10.6 L.

The rate removal of ammonia per milligram of MLVSS per day were measured and monitored throughout the study for reactors A1T1, A2T1 for Train 1, and A1T2 for Train 2 as shown on Fig. 7. According to Hauser et al. (2013), MEA is highly degradable via nitrate respiration, using nitrate as

Table 2 Materials and methods

Parameters	Materials	Method
Ammonia	Nessler reagent, polyvinyl alcohol, mineral stabilizer, 100 mL flask, 1 pipette, sample cells cuvette, DR3900 spectrometer and distilled water	APHA 4500N
Total Kjeldahl Nitrogen	Wastewater samples (influent and effluent), distilled water, selenium tablet, concentrated sulfuric acid (H_2SO_4), sodium hydroxide (NaOH), pipette, measuring cylinder, 250 mL digestion tube, stainless steel digestion tube rack, block digester, TKN distillation machine (KjelMaster K-375), stainless steel crucible tongs	APHA 4500N
Alkalinity	Burette, measuring cylinder, conical flask, ph meter, distilled water, penolphthalein indicator, methyl orange indicator, 0.02 N sulfuric acid solution	APHA 2320
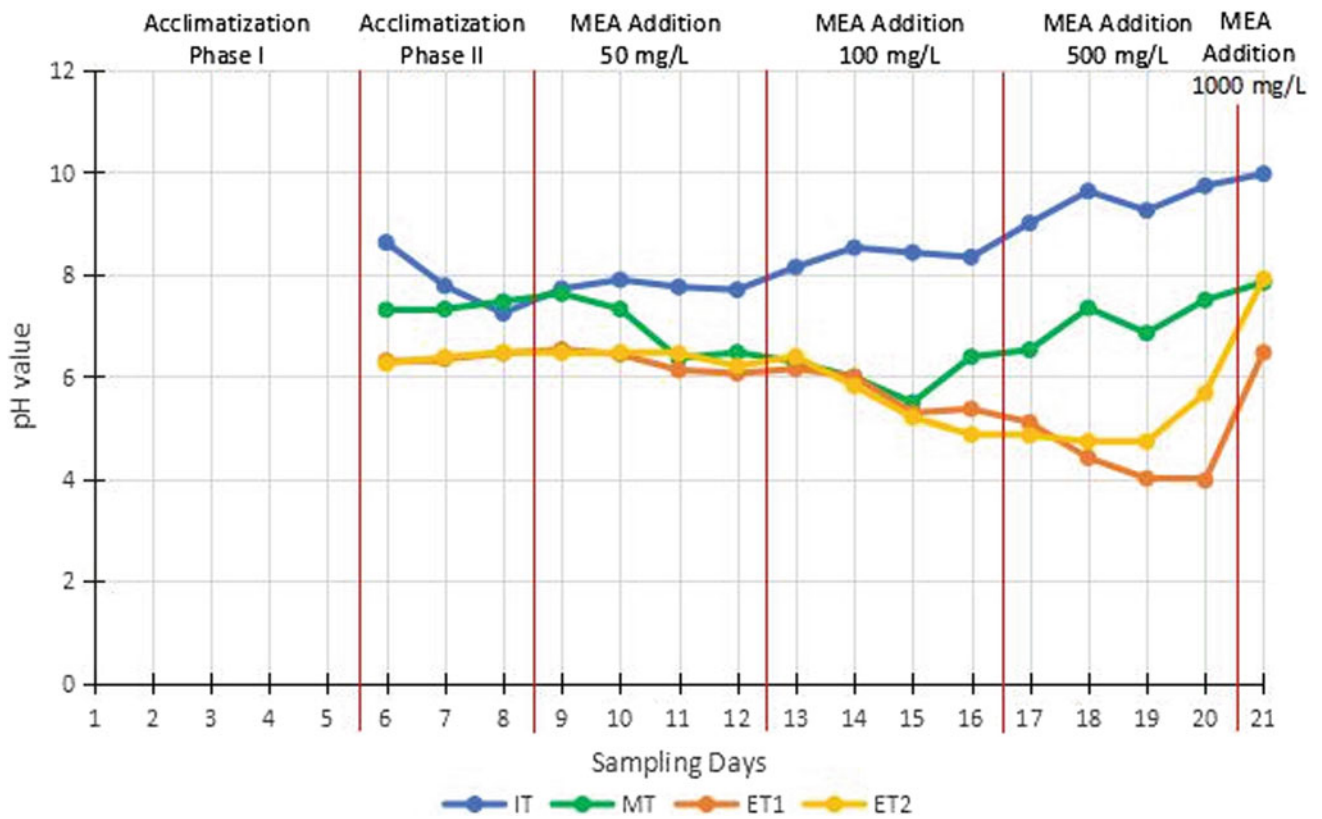
Fig. 3 Graph of pH value versus sampling days
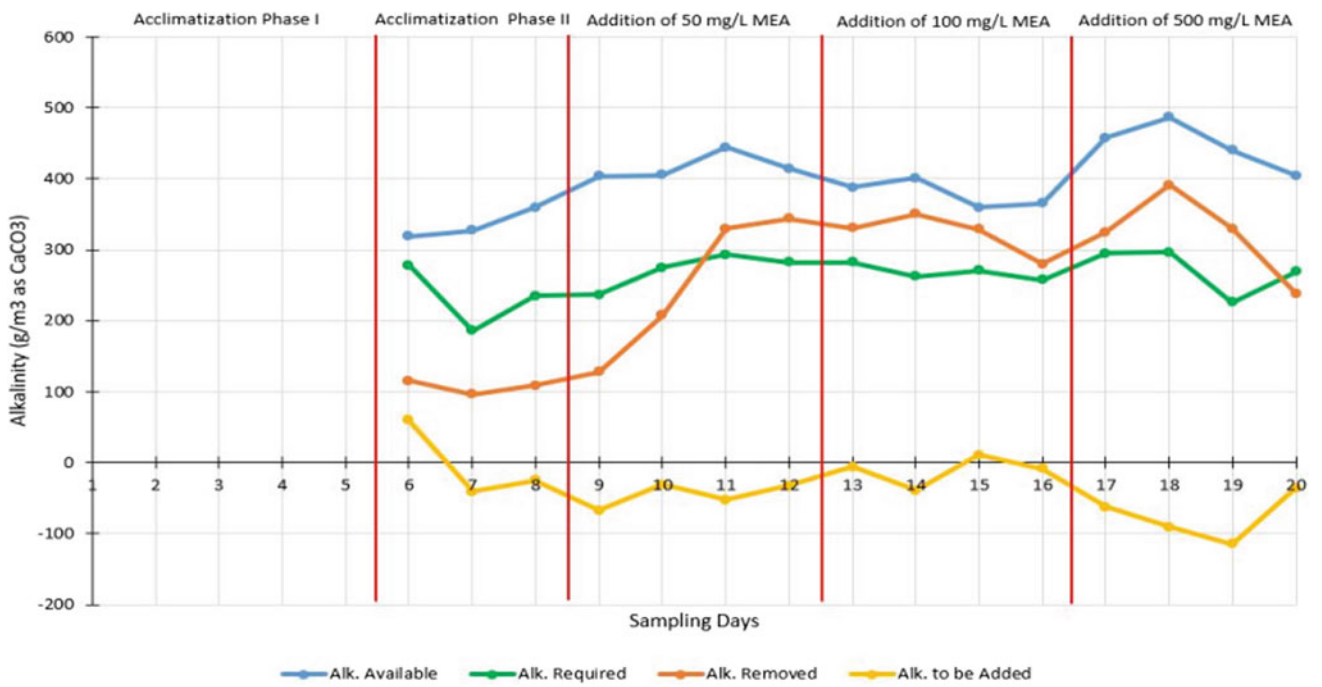
Fig. 4 Alkalinity versus sampling days for Reactor A1T1
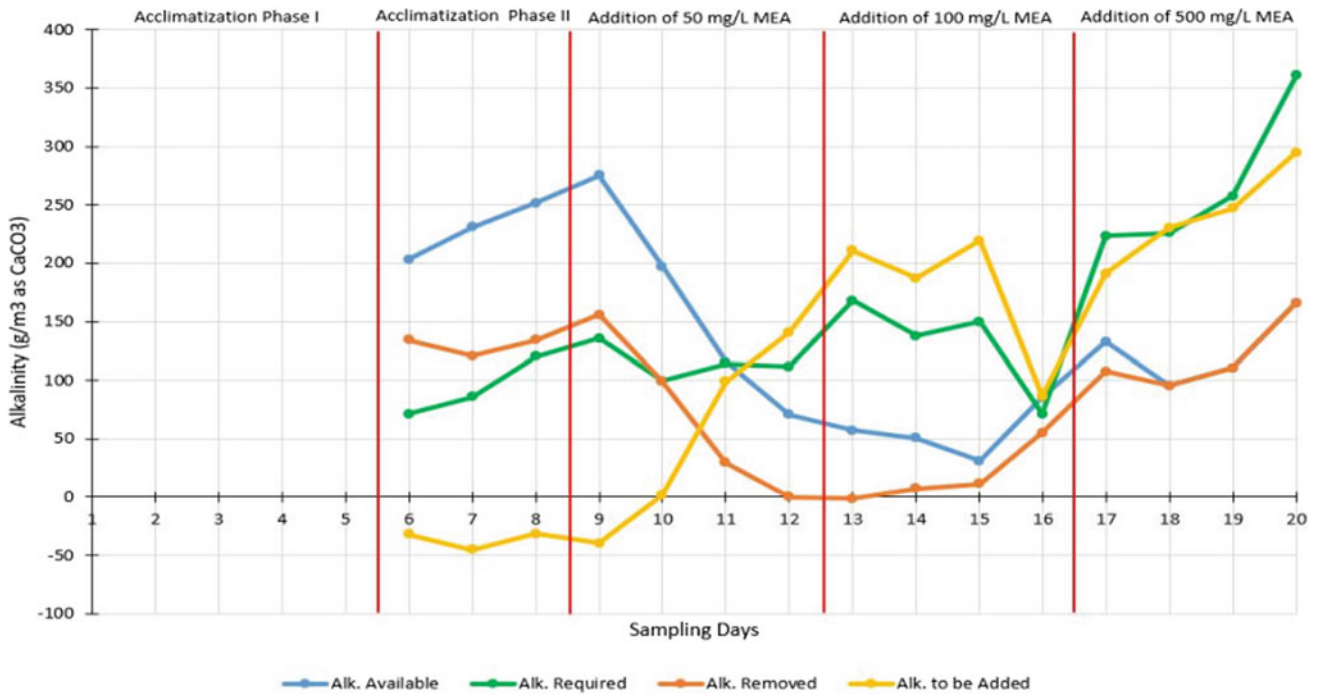
Fig. 5 Alkalinity versus sampling days for Reactor A2T1
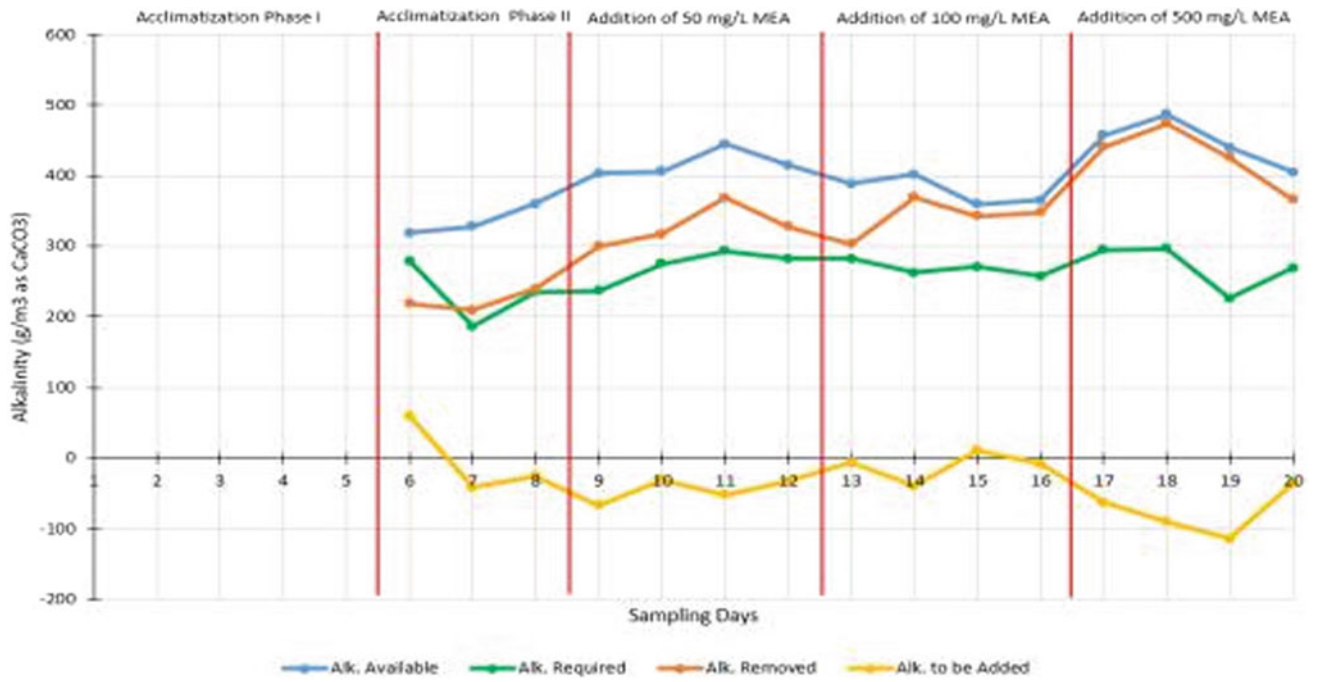
Fig. 6 Alkalinity versus sampling days for reactor A1T2
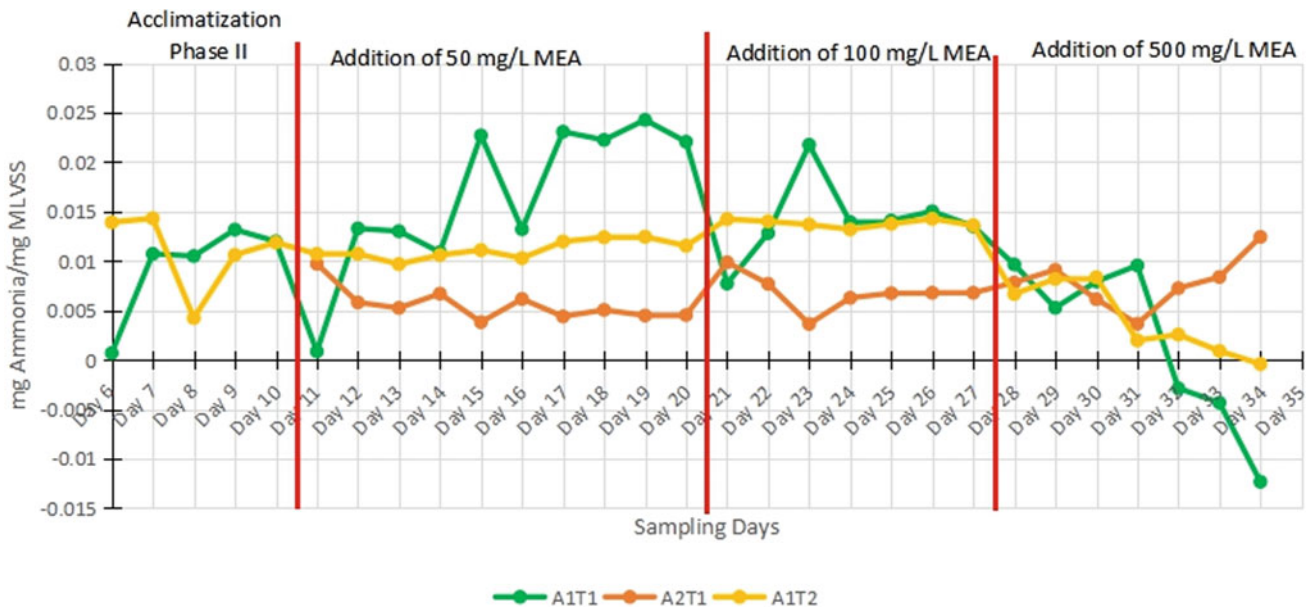
Fig. 7 Graph of removal of ammonia per milligram of MLVSS per day

Table 3 Average ammonia removal

Addition of MEA concentration (mg/L)	Average ammonia removal (mg Ammonia/mg MLVSS)		
	A1T1	A2T1	A1T2
50	0.02297	0.000461	0.013054
100	0.01421	0.006764	0.013880
500	0.001827	0.007823	0.003476

an electron acceptor and ammonia as an end product. MEA also reacts with ammonia in wastewater to form ethylene-diamine, another organic nitrogen (Weissermel et al. 2003).

Table 3 shows the averaged ammonia removal (mg Ammonia/mg MLVSS) throughout the study period.

3.4 Results of Total Kjeldahl Nitrogen (TKN) Removals in mg TKN removed/mg MLVSS.day for all Reactors Throughout the Study

The rate of removals of TKN were measured and monitored throughout the study for reactors A1T1, A2T1 for Train 1 and A1T2 for Train 2.

Table 4 shows the averaged TKN removal (mg TKN/mg MLVSS) throughout the study period.

4 Discussion

4.1 Discussion of pH Value Throughout the Study Period

Based on Fig. 3, during the acclimatization phase 2, the pH value of IT1, MT1, ET1, and ET2 were approximately 7.9, 7.4, 6.4, and 6.4, respectively. After the addition of 50 mg/L of MEA on Day 9, influent pH does not have much impact and stabilized at 7.8 pH. The pH of MT1 decreased and stabilized to 6.4 on Day 11. While pH of ET1 and ET2

Table 4 Average TKN removal

Addition of MEA concentration (mg/L)	Average TKN removal (mg TKN/mg MLVSS)		
	A1T1	A2T1	A1T2
50	0.111577	0.0070395	0.042113
100	0.174923	0.0134162	0.094860
500	0.135418	0.0357197	0.055964

stabilized to pH 6.1 and pH 6.5 on sampling Day 11 and Day 12, respectively. With increased addition of MEA to 100 mg/L, influent pH increased to pH 8.5 on sampling day 14. However, pH of MT1 decreased to pH 5.5 on Day 15 before slightly increasing to pH 6.4 on sampling day 16. Effluent pH at ET1 experiences a slight drop to pH 5.3 before stabilizing and effluent pH at ET2 drops to pH 4.9 on Day 16.

When the concentration of MEA was further increased to 500 mg/L from Day 17, influent pH continued to increase to pH 9.6 on Day. At MT1, there was also a slight increase of pH to pH 7.3 on Day 18. pH of ET1 continued to decrease to pH 4.0 on Day 20 while pH of ET2 was not impacted until Day 20 where the pH increased slightly to pH 5.7. On day 21, the MEA concentration was further increased to 1000 mg/L and did not impact the pH of IT and MT1 to pH value of pH 10.0 and pH 7.8, respectively. However, at ET1 and ET2, there was an increase in pH to pH 6.5 and pH 7.9, respectively. pH at MT1 throughout the study was steady in the beginning. However, when MEA was increased from 50 mg/L to 100 mg/L, it was observed that the pH dropped slightly. This may be due to some nitrification in reactor A1T1 and caused the pH to drop. When the MEA concentration was increased to 500 mg/L, the pH at MT1 continued to increase correspondingly to the influent pH. pH at ET1 and ET2 continued to decrease due to increased nitrification in reactors A1T1 and A1T2, which produced hydrogen ions that resulted in the drop in pH as shown in Eq. 1.

Equation 1: Oxidation of Ammonia to Nitrate (Metcalf and Eddy 2014).

$$2NH_4 + 2O_2 \rightarrow NO_3^- + 2H^+ + H_2O$$
$$NH_4 + 2HCO_3^- + 2O_2 \rightarrow NO_3^- + 2CO_2 + 3H_2O \qquad (1)$$
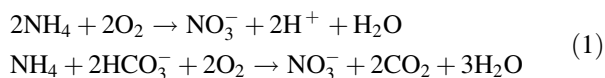
However, in the above equation, 2 mol of alkalinity are consumed per mole of NH_4-N oxidized, which is equal to 7.14 g of alkalinity as $CaCO_3$ consumed per mg of NH_4-N oxidized [$2 \times (50$ g $CaCO_3$/eq$)/14$]. The actual amount of oxygen and alkalinity consumed per unit of ammonia removed in nitrification systems is less than predicted by the above stoichiometric equations because some of the ammonia removed will be incorporated into the biomass produced during nitrification (Metcalf and Eddy 2014). Effluent alkalinity for A1T1 and A1T2 was not maintained at any concentration to maintain the pH. Effluent alkalinity should be controlled at 70–80 mg/L as $CaCO_3$ to maintain a pH of 7. This is because, nitrous acid (HNO_2) is also produced during the oxidation of ammonium ions as shown in Eq. 2 below. This destroys alkalinity:

Equation 2: Oxidation of Ammonium ions to Nitrous Acid (Environmental Consultant 2013)

$$H^+ + NO_2^- \rightarrow HNO_2 \qquad (2)$$
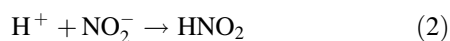
If the pH drops below 6.7, there is a significant decrease in nitrification. Therefore, it is important to maintain an adequate alkalinity in the aeration tank to provide pH stability and to provide inorganic carbon for nitrifiers. The optimal pH range for nitrification is 7.2–8.0. A substantial reduction in nitrification activity occurs at pH levels below 6.7 (ECOS 2013).

4.2 Discussion of Alkalinity Balance for all Reactors Throughout the Study Period

The alkalinity required for Nitrification was obtained by the Eq. 3, and the alkalinity removed was calculated by the Eq. 4 from the removal of alkalinity after going through the reactor. Residual alkalinity was calculated using the Eq. 5. The residual alkalinity concentration needed to maintain pH 7 was determined to be 100 g/m³ as $CaCO_3$. For the alkalinity balance for the reactors, influent alkalinity, alkalinity used, alkalinity required for nitrification, and the alkalinity to be added were plotted for each reactor throughout the study period.

Equation 3:

$$\text{Alkalinity Required for Nitrification} = 7.14 \times \text{Influent Ammonia} \qquad (3)$$

Equation 4:

$$\text{Alkalinity Removed} = \text{Influent Alkalinity} - \text{Effluent Alkalinity} \qquad (4)$$

Equation 5:

$$\text{Residual Alkalinity} = \text{Alkalinity available} - \text{Alkalinity used} + \text{Alkalinity to be added} \qquad (5)$$

4.2.1 Discussion of Alkalinity Balance for Reactor A1T1

From Fig. 4, during the acclimatization phase, the alkalinity required for nitrification ($7.14 \times$ Influent Ammonia) is higher than the alkalinity removed. This shows that there is not much nitrifiers in the reactor during this phase as it was operated at conventional aeration mode. Alkalinity available (influent alkalinity) is also high from the raw influent wastewater. When MEA was added at 50 mg/L, the alkalinity in the influent increased to an average of approximately 400 mg/L as $CaCO_3$. During this phase (addition of 50 mg/L of MEA), it can be observed that the alkalinity removed increased steadily and after Day 11, alkalinity removed exceeded the alkalinity required for nitrification. The

conditions seem to be favorable to growth of nitrifiers. There is sufficient alkalinity available for the nitrifiers to utilize. This shows that the nitrifiers starts to increase with addition of 50 mg/L of MEA. This growth trend continued with increased addition of MEA throughout the study period.

4.2.2 Discussion of Alkalinity Balance for Reactor A2T1

From Fig. 5, it can be observed that during acclimatization phase 2, alkalinity available (alkalinity at MT1) is high and sufficient to provide for the alkalinity required by the nitrifiers for nitrification (7.14 × ammonia–nitrogen at MT1). Alkalinity removed through reactor A2T1 was slightly higher than the alkalinity used for nitrification. This shows that the nitrifiers were sufficiently provided for nitrification in acclimatization phase 2. Hence, the amount of alkalinity to be added to maintain effluent alkalinity of 100 mg/L as $CaCO_3$ is negative. When 50 mg/L of MEA was added, there was a gradual increase in the alkalinity required for nitrification. This was because ammonia–nitrogen at MT1 decreased throughout this phase. Alkalinity available (alkalinity at MT1) was also seen to drop as it was removed in reactor A1T1. After Day 11, there was insufficient available alkalinity for nitrification to occur. The nitrifiers are now lacking in alkalinity required for nitrification in reactor A2T1 from Day 11. It can be observed that due to insufficient alkalinity in the effluent, pH at ET1 continued to decrease below pH6. The nitrifiers are impacted with lack of alkalinity addition and caused the rate of nitrification to drop. This state of insufficient alkalinity (alkalinity at MT1) can be observed till the end of the study during the addition of 100 mg/L MEA. Nitrification could be enhanced by addition of external source of alkalinity. However, when 500 mg/L of MEA was added, it can be observed that alkalinity available (alkalinity at MT1) are all removed by the nitrifiers. However, there was insufficient alkalinity available for nitrification.

4.2.3 Discussion of Alkalinity Balance for Reactor A1T2

From Fig. 6, generally, if alkalinity is to be maintained at 100 mg/L in the effluent, no alkali is required to be added throughout the study period. This is because from the graph, it can be observed that alkalinity removed is lower than alkalinity required for nitrification throughout the study. The alkalinity available (influent alkalinity) is higher than the alkalinity removed throughout the study period. However, there was steady increase of alkalinity removed from the beginning until the end of the study approaching the alkalinity available in the influent. This shows that there is gradual growth of nitrifiers for nitrification. Also, there was a gradual increase in alkalinity required for nitrification with increased addition of MEA throughout the study.

4.3 Discussion of Nitrification Rate Throughout the Study Period

The nitrification rate was evaluated for the reactors using the following equation:

$$\frac{(S_0 - S_e)Q}{XV}$$

where:

S_0 influent ammonia concentration (mg/L),
S_e effluent ammonia concentration (mg/L),
Q flow rate of the aeration tank 10 L/d,
X MLVSS concentration in the aeration tank (mg/L).
V volume of the aeration tank, 10.6 L.

Based on Fig. 7, during acclimatization phase 2, from Day 6 to Day 10, the influent was fed at full concentration. From Fig. 7, it is observed that the removal of ammonia per mg of MLVSS per day was calculated to be at an average of 0.01610 and 0.01098 mg of ammonia per mg MLVSS per day for reactor from A1T1 and A1T2. However, for reactor A2T1, there was not enough of raw wastewater. From Day 11 to Day 21, the reactor was fed with 50 mg/L of MEA. From the Fig. 7, it can be observed that the removal of Ammonia per mg of MLVSS per day showed an increasing trend in reactor A1T1 with removal average of 0.02297 mg of Ammonia per mg MLVSS per day. For reactor A2T1 and A1T1, the removal of Ammonia per mg of MLVSS per day was calculated to be at an average of 0.000461 and 0.013054 mg of Ammonia per mg MLVSS per day.

From Day 21 to Day 27, the reactor was fed with 100 mg/L of MEA. The average reading of Ammonia removals was at, 0.01421, 0.006764 and 0.013880 mg of Ammonia per mg of MLVSS per day for reactor A1T1, A2T1, and A1T2, respectively. From Day 28 to Day 35, the reactor was fed with 500 mg/L of MEA. The average reading of Ammonia removals was at, 0.001827, 0.007823 and 0.003476 mg of Ammonia per mg of MLVSS per day for reactor A1T1, A2T1 and A1T2, respectively.

Table 3 shows the summary of averaged ammonia removal. It can be seen that the nitrification rate increased slightly for A2T1 with addition of 500 mg/L of MEA, indicating that nitrifiers was thriving in reactor A2T1 but for reactor A1T2, the nitrification rate seemed to drop. However, it should be noted that degradation of organic-nitrogen also produced ammonia- nitrogen which was also available for the nitrifiers to nitrify. Hence to determine the exact nitrification rate, the amount of ammonia–nitrogen produced from the oxidation of the organic nitrogen need to be included.

The nitrification process is pH dependent, where the optimum pH for metabolism and growth of the autotrophic nitrifiers within pH 7–8 (Colaco 2009). According to

Benninger and Sherrard (1978), nitrifiers which consists of Nitrosomonas and Nitrobacter are responsible for the oxidation of NH_4^+-N to NO_3^--N in a two-step sequential reaction. Besides that, MEA tends also to react with ammonia in the wastewater to form ethylenediamine, another organic nitrogen (Klaus et al. 2003). The MEA also ionizes dissolved acidic compounds, making them polar and considerably more soluble.

4.4 Discussion of Total Kjeldahl Nitrogen (TKN) Removals in mg TKN removed/mg MLVSS.day for all Reactors Throughout the Study

The TKN removal rate was evaluated for the reactors using the following equation:

$$\frac{(S_0 - S_e)Q}{XV}$$

where:

S_0 influent TKN concentration (mg/L),
S_e effluent TKN concentration (mg/L),
Q flow rate of the aeration tank 10 L/d,
X MLVSS concentration in the aeration tank (mg/L).
V volume of the aeration tank, 10.6 L.

Based on Fig. 8, during acclimatization phase 2, from Day 6 to Day 8, the influent was fed at full concentration. From Fig. 8, it was observed that the removal of TKN per mg of MLVSS per day was calculated to be at an average of 0.05187 and 0.04751, mg of TKN per mg MLVSS per day

for reactor from A1T1 and A1T2. However, for reactor A2T1, there was not enough of raw wastewater. The removal was steady for both reactors during this period. From Day 9 to Day 12, the reactor was fed with 50 mg/L of MEA. From the Fig. 8, it can be observed that the removal of TKN per mg of MLVSS per day showed an increasing trend in reactor A1T1 with removal average of 0.111577 mg of TKN per mg MLVSS per day. This indicates that organic removal is increased in reactor A1T1 with addition of MEA. For reactors A2T1 and A1T2, the removal of TKN per mg of MLVSS per day was calculated to be at an average of 0.0070395 and 0.042113 mg of TKN per mg MLVSS per day.

From Day 13 to Day 16, the reactor was fed with 100 mg/L of MEA. From the Fig. 8, it can be observed that the removal of TKN per mg of MLVSS per day showed an increasing trend in reactor A1T1 and A1T2 with removal average of 0.174923 mg and 0.0134162 of TKN per mg MLVSS per day. This showed an increased organic degradation and nitrification in both reactors. The growth of nitrifiers is now prominent in reactor A2T1. For reactor A2T1, the removal of TKN per mg of MLVSS per day was calculated to be at an average of 0.094860. From Day 17 to Day 20, the reactor was fed with 500 mg/L of MEA. The average reading of TKN removals was at, 0.135418, 0.0357197, and 0.055964 mg of TKN per mg of MLVSS per day for reactor A1T1, A2T1, and A1T2, respectively. It can be observed that there was increased nitrification and organic degradation in reactor A1T2, but there was decreased organic degradation and nitrification in reactors A1T1 and A2T1. This drop is contributed due to insufficient alkalinity for nitrification and also insufficient organic
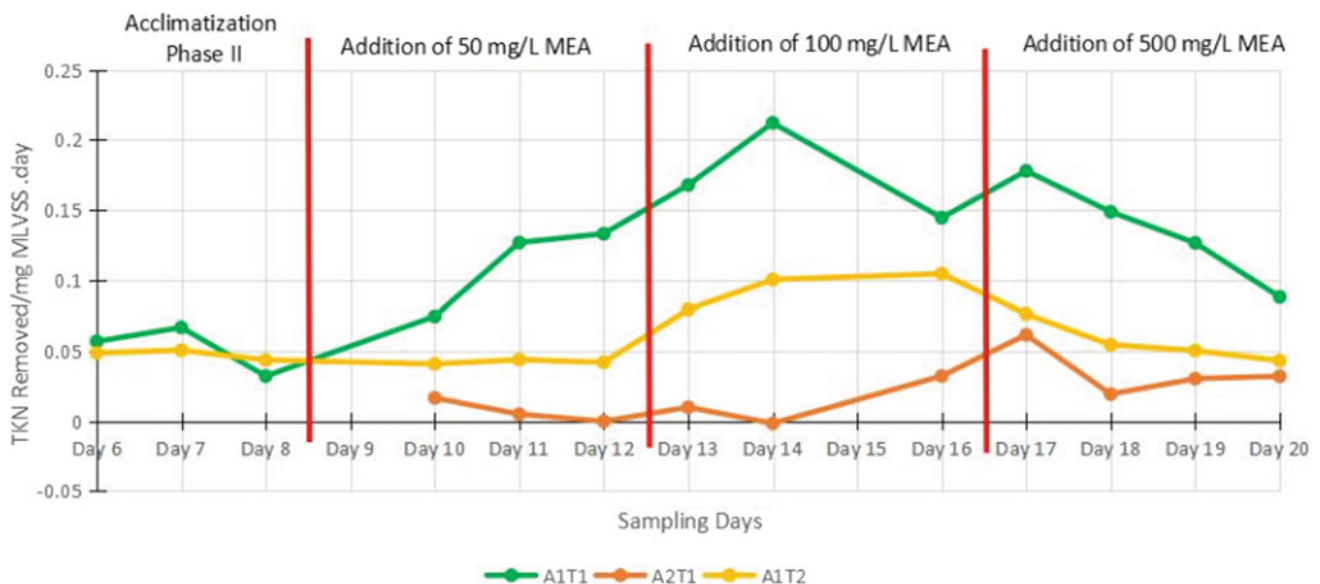
Fig. 8 Removal of TKN per milligram of MLVSS per day

degradation which results higher organic-N in the effluent. Table 4 shows the summary of averaged TKN removal.

Total Kjeldahl Nitrogen (TKN) is composed of organic nitrogen and ammonia–nitrogen in the wastewater. The organic nitrogen will also be oxidized to ammonia–nitrogen and nitrified together with the feed ammonia–nitrogen. Alkalinity plays an important role in this study as addition of MEA also increased the alkalinity in the feed from the OH^- released from MEA and contributes towards nitrification at the beginning of the study. This increased in alkalinity supplements the alkalinity needed by the nitrifiers for nitrification. Even with slight increase in alkalinity, most of the alkalinity is removed in the effluent for both trains. With increased MEA concentration, more ammonia is released in the biological reactors through biological degradation and hence, higher alkalinity was used up in the reactors resulting with lower alkalinity in effluents from both trains. Without any alkalinity addition, the buffering capacity was reduced causing the pH of effluents from reactor to drop. According to Curtin et al. (2011), alkalinity will be used at a rate of 7.14 mg $CaCO_3$ per 1 mg nitrogen during the nitrification process. To keep the pH in the system stable, effluent alkalinity of at least 50 mg/L, preferably 100 mg/L, is recommended.

5 Conclusions

It can be concluded that the addition of MEA decreases the percentage removal of nitrogen and slows down the nitrification process in all reactors. The addition of 50 and 100 mg/L of MEA did not affect the nitrification in all reactors. However, with the addition of 500 mg/L of MEA, the percentage removal of nitrogen compound drop drastically but did not inhibit the growth of nitrifiers as nitrification is still occurring, even at a slower rate. The addition of 1000 mg/L of MEA increased the nitrogen effluent in both trains which exceeded the influent concentration. It is important to maintain the nitrification process in the reactor as it can effectively remove nitrogen from wastewater. Besides that, alkalinity was important in the nitrification process since the addition of MEA provided additional alkalinity as well as increased ammonia in the reactors for nitrification. Since the impact of MEA was absorbed by the first reactor in train 1, it can be concluded that train 1 performed slightly better than train 2. It is advised that two reactor configurations be adapted to reduce the impact of MEA addition to activated sludge systems. The operating conditions of the first reactor should also be monitored to avoid nitrification. Therefore, alkalinity must be added and maintained to allow for nitrification in the second reactor. If train 2 is to be used, the MEA concentration in the feed should be limited to 100 mg/L to prevent interference with the nitrification process. However, alkalinity in the influent feed must be monitored and provided to ensure adequate nitrification while also buffering the reduction in pH in the final effluent due to nitrification in the reactor.

References

R. Benninger, J. Sherrard, Nitrification and alkalinity relationships in activated sludge. J. (Water Pollut. Control Fed.) **50**(9), 2132–2142 (1978)

A.B. Colaco, Biological water treatment for removal of ammonia from industrial process water. Universidade Técnica de Lisboa, 1–61 (2009)

K. Curtin, S. Duerre, B. Fitzpatrick, P. Mayer, Biological nutrient removal. Minnesota Pollut Control Agency 1–62 (2011)

ECOS: Wastewater nitrification: how it works. Environmental Consultants. https://www.ecos.ie/wastewater-nitrification-how-it-works/. 22 July 2013

I. Hauser, A.B. Colaço, J.A. Skjaeran, A. Einbu, K. Ostgaard, H.F. Svendsen, F.J. Cervantes, Biological N removal from wastes generated from amine-based CO_2 capture: case monoethanolamine. Appl. Biochem. Biotechnol. 1449–1458 (2013)

Metcalf & Eddy Inc., G. Tchobanoglous, F.L. Burton, R. Tsuchihashi, H.D. Stensel, *Wastewater Engineering: Treatment and Resource Recovery*, 5th edn. (McGraw-Hill Professional, 2014), pp. 1–2018

L. Nurrokhmah, T. Mezher, M.R.M. Abu-Zahra, The evaluation of monoethanolamine-based CO_2 post-combustion capture process waste handling approaches considering the regulations in UAE. Energy Proc. **37**, 751–758 (2013)

K. Weissermel, H.-J. Arpe, C.R. Lindley, S. Hawkins, in *Chap. 7. Oxidation Products of Ethylene*. Industrial Organic Chemistry (Wiley-VCH, 2003), pp. 159–161

Application of Fuzzy Analytical Hierarchy Process for Revising OIU Main-Campus Masterplan to Ensure Sustainable Environment

Eltayeb H. Onsa Elsadig, Ghassan M. T. Abdalla, Muna Mustafa Eltahir, Gasim Hayder, Abderrahim Lakhouit, Isam M. Abdel-Magid, Hisham I. Abdel-Magid, Anis Ben Messaoud, Ahmed H. A. Yasin, Omer A. Sayed, and Mohamed B. Elsawi

Abstract

Omdurman Islamic University is one of the oldest universities in Sudan. OIU campus masterplan (CMP) was first developed in 1978 and revised in 2002. Yet too many important parts of the revised CMP need to be redesigned and constructed. Revising the existing university masterplan is complicated and needs to be tackled carefully in the light of new conceptual criteria without affecting the ongoing educational, research, and administrative activities. Furthermore, for the sustainability of the facilities to be increased, there are key approaches, namely, environmental-friendly materials, environmental-friendly landscape, safety, conservation of energy, and extended operation life. The Fuzzy Analytical Hierarchy Process (FAHP) is to solve multi-level and complex decision-making problems in a systematic approach. Based on experts' judgment on several design alternatives and criteria in addition to sub-criteria. The opinions are compared in a pairwise fashion based on three expertise and three decision-makers as the criteria and sub-criteria to assess how their contribution to the target. This paper aims at building a new assessment framework for sustainable CMP to be later applied to the case study of OIU main campus in Sudan. To assess the proposed CMP in terms of sustainability, three sustainable alternatives (A1, A2, and A3) are proposed, along with four criteria and 13 sub criteria (factors). The alternatives are studied for the best alternative selection. Each of the criterion and factor weight is calculated using the FAHP. The analysis result shown a rational procedure which utilizes successfully the use of FAHP to help the decision processes for the OIU revised CMP.

Keywords

University campus • Masterplan • Fuzzy analytical hierarchy process • Sustainable environment • NEOM

Highlights

1. A method for developing a new assessment framework for a sustainable campus master plan was devised and used to a case study.
2. An environmental, economic, ecological, and management criterion framework was proposed.
3. As a case study, the Omdurman Islamic University choices were adopted.
4. The relevance of weighting on alternative selection is reflected in sensitivity analysis.

1 Introduction

1.1 About Omdurman Islamic University

Omdurman Islamic University (OIU) is the name of the former Omdurman Scientific Institute (OSI). The OSI is one of the foremost private scientific institute established in Sudan, which have been graduated many personalities and prominent scholars from it. The colonial government at that

E. H. O. Elsadig (✉) · A. Lakhouit · A. B. Messaoud · M. B. Elsawi
Department of Civil Engineering, Faculty of Engineering, University of Tabuk, Tabuk, Kingdom of Saudi Arabia
e-mail: e.onsa@ut.edu.sa

G. M. T. Abdalla · A. H. A. Yasin · O. A. Sayed
University of Tabuk, Tabuk, Kingdom of Saudi Arabia

M. M. Eltahir
Omdurman Islamic University, Omdurman, Sudan

G. Hayder
Department of Civil Engineering, College of Engineering, Universiti Tenaga Nasional (UNITEN), 43000 Kajang, Malaysia

I. M. Abdel-Magid
Elrazi University, Khartoum, Sudan

H. I. Abdel-Magid
Lirio Academy, London, UK

time has been asked by Sudanese scholars to establish the OSI which has been agreed and established in the year 1912. The OSI in Sudan resembles the Egyptian Al-Azhar religious education system. The OSI was upgraded until later became Omdurman Islamic University in 1965.

The built area of the OIU campus is approximately 800 acres (3360 km^2) in Omdurman city near the left bank of the White Nile. Besides oriented as a primarily Islamic studies, it is also serves other fields of studies as well, such as agriculture, engineering, medicine, and many more. It is worthwhile mentioning that OIU is a federation member of the universities of the Islamic World.

The first masterplan for OIU campus was approved around 1978. This MP adopted the ring-orientation of all buildings: OIU administration, main library, main mosque, and auxiliary premises were located at the center; the faculties and institutes spread around the ring having common radial orientation towards the center.

Until 2000, only small parts of the approved OIU first MP were executed, so it became inevitable to revise the campus MP. In 2002, the Faculty of Engineering Sciences at OIU proposed a revised MP for the campus in which a wide ring road was proposed with all the educational and administrational premises lies on the left and right sides of the ring road. Recently, in 2015, some updates were introduced to the 2002 MP. Figures 1, 2, 3 and 4 and Table 1 show the progress in executing OIU MP for the years 2004, 2011, and 2021.

It seems none of the above OIU MPs ensures sustainable environment, an issue that became vital for any educational campus planning nowadays. Waste minimization transportation demand management, energy production and

Fig. 2 OIU campus—2011

Fig. 3 OIU campus—2021

consumption, building construction, academic integration of sustainability, purchasing, water systems, and more are the examples of the Sustainability issues.

The Fuzzy Analytical Hierarchy Process (FAHP) is broadly used as the multi-criteria decision-making methods (MCDM). In any decision-making and planning process, a systematic and logical approach is to be used to reach at solutions. In MCDM analysis, the most common method is the fuzzy set theory to deal with uncertainties Pedro Moura et al (2021), Michigan State University (2021), University of Colorado Boulder (2021).

Fig. 1 OIU campus—2004 (*Google earth* ©)
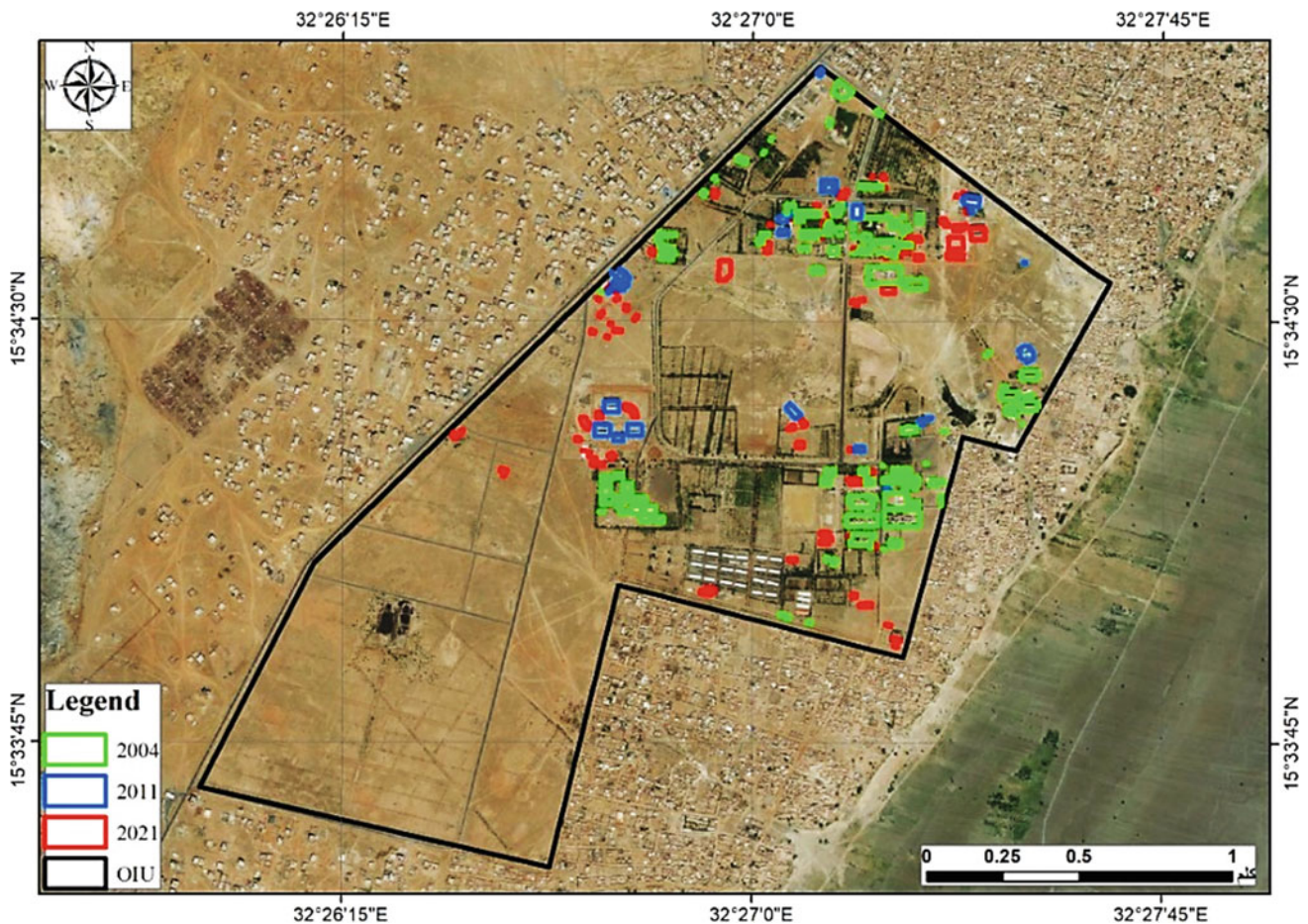
Fig. 4 Summary of the progress in executing OIU campus MP for years 2004–2021

Table 1 Progress in built area at OIU main campus

Year	Built area (m²) *not including open space and roads*
2004	134,500
2011	166,000
2021	206,700
Expected in new MP	450,000

The decision-making for selection between different designs options of re-plan of existing university masterplan is not easy in the existence of several affecting criteria. The research objective is to develop FAHP for selection between design alternatives of OIU MP. The developed process will depend on intuitionistic fuzzy sets, on way to assist OIU decision-makers to decide and select the most appropriate design considering the environmental sustainability.

The opinion of experts and decision-makers is pairwise analyzed for the selection between the design alternatives. A questionnaire is designed and analyzed using most recent FAHP approaches. The group of evaluations weights is studied using spreadsheets established by the researchers.

1.2 Justification

Why re-planning of OIU main campus masterplan (MP)? the reasons are:

- Existing OIU main campus masterplan was more than 20 years old.
- More than half of the components of OIU main campus (MP) yet need to be implemented.
- OIU need to compare the present alternatives and see how to reduce the environmental impact of material, operation, and design.

2 Methods

2.1 Analytic Hierarchy Process (AHP)

The AHP system is first introduced by Satty (1980). In AHP, categories to compare between different alternatives are identified and given relative weights by evaluators. The

Fig. 5 Triangular member function
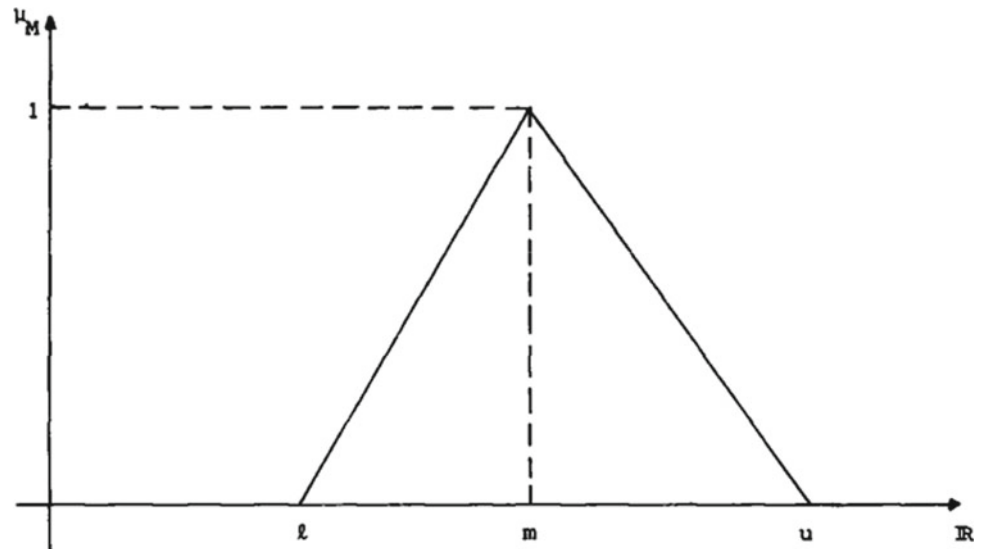
alternatives are then given a score for each of these categories. The best alternative is then identified by calculating a weighted sum for each alternative and selecting the alternative with the highest score. The main problem with AHP is the integer ranking process (1–9) since the evaluator must select a definite value for each category/alternative whereas his opinion might be anything within a range. These definite values might even accumulate and lead to sub-optimal selection. To overcome this limitation, Laarhoven proposed the use of fuzzy numbers for the ranking process (van Laarhoven and Pedrycs 1983). Fuzzy numbers are not definite (crisp) values. They define an interval or range that belong to a certain category (rank). A member function identifies how strongly related each value belongs to an interval. Laarhoven used fuzzy numbers with triangular member functions as defined in Eq. (1) and shown in Fig. 5 for the ranks. Each rank is defined by three parameters: the lower limit l_i, the modal m_i, and the upper limit u_i (Table 2). In the member functions, only the modal is related to the

rank with value (relation) 1. The intervals $[l, m]$ and $[m, u]$ are shared by previous and subsequent ranks.

$$\mu_M(x) = \begin{cases} \frac{1}{m-l}x - \frac{l}{m-l}, & x \in [l, m] \\ \frac{1}{m-u}x - \frac{u}{m-u}, & x \in [m, u] \\ 0, & \text{otherwise} \end{cases} \quad (1)$$

Using these ranks, van Laarhoven and Pedrycs (1983) developed linear equations to calculate the lower, modal, and upper limits from the experts' response. However, a unique solution was not always possible using his method.

Buckely proposed the use of geometric mean to implement FHAP (Buckely 1985). If evaluations from several experts are available, the geometric mean of their evaluations is used for comparison. Assuming trapezoidal member functions, Buckley derived the member function for the alternative and then used α cuts to compare two alternatives each time. The alternatives are then classified in descending

Table 2 AHP and FAHP weights

Intensity of Importance/Evaluator decision	AHP Weight (i)	FAHP Weight (l, m, u)
Equal Importance (EI)	1	(1,1,1)
Equal to Moderate Importance (EMI)	2	(1,2,3)
Moderate Importance (MI)	3	(2,3,4)
Moderate to Strong Importance (MSI)	4	(3,4,5)
Strong Importance (SI)	5	(4,5,6)
Strong to Very Strong Importance (SSI)	6	(5,6,7)
Very Strong Importance (VSI)	7	(6,7,8)
Very Strong to Extreme Importance (SEI)	8	(7,8,9)
Extreme Importance (ExI)	9	(9,9,9)
Reciprocity property	$1/i$	($1/u, 1/m, 1/l$)

order. Nang extended this method by using center of gravity to calculate decision weights (Nang-Fie 2008). His algorithm produces three decision matrices (lower bound, most likely, and upper bound) to reflect three levels of uncertainty.

The most widely used algorithm is the one developed by Chang (1996). Chang used extent analysis to develop an algorithm to compare fuzzy numbers and calculate the weights for criteria and alternatives assuming triangular fuzzy member functions. If there is more than one evaluator, the average of their evaluations is calculated first, then the sum (S_i) of each row in the evaluation matrix is calculated and divided by the sum of the matrix. Based on the modal value (m_i) of the sum, the degree of possibility that $S1 \geq S2$ is calculated by:

$$V(M_1 \geq M_2) = 1 \quad \text{iff } m_1 \geq m_2$$
$$V(M_2 \geq M_1) = \text{hgt}(M_1 \cap M_2) = \frac{l_1 - u_2}{(m_2 - u_2) - (m_1 - u_1)}$$

$$(2)$$

The weight vector is then calculated by:

$$W' = (\min(V(S_1 \geq S_2, S_3, S_4, \ldots)), \min(V(S_2 \geq S_1, S_3, S_4, \ldots)),$$
$$\min(V(S_3 \geq S_1, S_2, S_4)), \ldots)$$

$$(3)$$

$$W = \frac{(w_1, w_2, w_3)}{\sum(w'_i)} \tag{4}$$

Modifications to Chang's algorithm have been proposed in Enea and Piazza (2004) and Klir (1997) to include constraints on the numbers of fuzzy and improve the criteria weights; however, in several cases, they produce identical results to Chang's algorithm.

2.2 The Design Alternatives

Three design alternatives will be studied to choose the most appropriate alternative for re-planning OIU MP. Each alternative shall ensure sustainable environment. The alternatives are:

A1: Consider Omdurman city planning characteristics.
A2: Consider Islamic planning approach.
A3: Follow modern trends in university campus planning.

The impact of each alternative is expected to be reflected on the performance in OIU main campus and the life pattern of the surrounding areas, the local economy and environment, and other issues might render the officials to think in depth to decide and answer the question: *which of the above mentioned three design alternatives is most appropriate?*

The measuring criteria are complex and are not so clear or predetermined for such kind of decision-making procedure. Expert engineers/architects shall help the decision makers to follow a philosophy and analyze the situation and, thereby, create suitable criteria giving him evidence that the selected criteria shall strictly lead to the appropriate decision (Alyamani and Long 2020; Heo et al. 2021; Balioti et al. 2018).

2.3 Establishing Criteria and Factors (Sub-criteria)

In establishing the main criteria, the following general principles shall always be acknowledged: arrange campus buildings, circulation, open space, and utility systems to: establish positive interactions among academic, cultural, outreach, research, and operational activities. Also, the campus shall create a life-learning resource integral to the OIU vision.

Criteria involved in universities CMP and re-planning generally include the following four principles which were chosen to be the main criteria for re-planning OIU CMP: Circulation; Environmental sustainability; Land use and facilities; and Cost. Furthermore, each criterion has influencing factors (sub criteria) as shown in Table 3.

Description of sub-criteria

C_{11} Implementation of compact campus development:

Benefits to be achieved are: protect and preserve existing facilities, natural areas, and systems to support research and teaching; conserve land, optimize land productivity; strengthen ties between undergraduate teaching and research; and link campus with neighboring areas.

C_{12} Recognition of historically significant aspects:

Recognize historically important aspects of OIU campus and its heritage as learning laboratory and a living and a park.

C_{13} Acknowledgment of existing facilities:

Renovations and new buildings design to be architecturally harmonious with their contextual surroundings and compatible with the existing adjacent buildings best features.

C_{21} Optimize environmental impacts:

By minimizing the impacts on the environmental and maximizing conservation of the resource through compact land use and wise use of building materials, integrate

Table 3 Criteria and sub criteria

Criteria	Sub criteria (Factors)
C_1: Land use	C_{11} Implementation of compact campus development
	C_{12} Recognition of historically significant aspects
	C_{13} Acknowledgment of existing facilities
C_2: Environmental sustainability	C_{21} Minimizing the environmental impacts
	C_{22} Encourage renewable resource
	C_{23} Recognizing climate vulnerability
	C_{24} Construction materials to be (eco-friendly)
C_3: Circulation	C_{31} Setting circulation priorities
	C_{32} Emphasize personal safety
	C_{33} Providing effective transportation network
C_4: Cost and financial aspects	C_{41} Availability of fund
	C_{44} Cost of construction and furnishing
	C_{43} Cost of operation

development guidelines with low-impact, and protecting environmental systems.

C_{22} Encourage renewable resource:

Continuously attempting building and utility systems that decrease hazardous materials and waste and encourage the use of renewable resource.

C_{23} Recognizing climate vulnerability:

By attempting land use issues associated with climate vulnerability e.g., temperature extremes management and storm water.

C_{24} Construction materials (eco-friendly):

Using the green materials. It means new materials of construction with few emissions and environmental impacts.

C_{31} Setting circulation priorities:

Design and plan for the following circulation priorities: Incorporate traffic-calming measures where appropriate.

C_{32} Emphasize personal safety:

Assuring safety of the personal in the circulation system's design and planning.

C_{33} Providing effective transportation network:

Design and plan for the following circulation priorities: firstly pedestrians; secondly non-motorized transportation; thirdly mass transit and service vehicles; and lastly private vehicles.

C_{41} Availability of fund:

Assuring to what extent the MP implementation fund will be available according to a desirable disbursement plan.

C_{42} Cost of construction and furnishing:

Optimizing the total cost of: new constructions, rehabilitation of old facilities including all furniture, equipment, services, etc.

C_{43} Cost of operation:

Setting proper implementation management system.

3 Results

3.1 Weights of the Criteria

Table 4 presents the weights of the criteria obtained from the opinion of the experts. Table 5 gives the weights of the same criteria as depicted from the opinion of the decision-makers.

Table 4 Weights of the criteria —Experts' opinion

Criteria	C_1	C_2	C_3	C_4
Weight	0.2319	0.2401	0.2225	0.3055

Table 5 Weights of the criteria—Decision-makers (DMs) opinion

Criteria	C_1	C_2	C_3	C_4
Weight	0.2188	0.2040	0.2040	0.3728

Table 6 Weights of the sub criteria (factors)—Experts' opinion

Criteria	C_1			C_2			
Sub criteria	C_{11}	C_{12}	C_{13}	C_{21}	C_{22}	C_{23}	C_{24}
Weight	0.3401	0.3284	0.3315	0.2431	0.2452	0.2374	0.2743
Criteria	C_3			C_4			
Sub criteria	C_{31}	C_{32}	C_{33}	C_{41}	C_{42}	C_{43}	
Weight	0.3401	0.3284	0.3315	0.3322	0.3345	0.3333	

Table 7 Weights of the sub criteria (factors)—Decision-makers (DMs) opinion

Criteria	C_1			C_2			
Sub criteria	C_{11}	C_{12}	C_{13}	C_{21}	C_{22}	C_{23}	C_{24}
Weight	0.3382	0.3378	0.3240	0.2514	0.251	0.2493	0.2483
Criteria	C_3			C_4			
Sub criteria	C_{31}	C_{32}	C_{33}	C_{41}	C_{42}	C_{43}	
Weight	0.3339	0.3339	0.3322	0.3341	0.3329	0.3329	

3.2 Weights of the Sub Criteria

Tables 6 and 7 present the weights of the sub-criteria obtained from the opinion of the experts and the decision-makers, respectively.

3.3 Alternatives Scores

Tables 8 and 9 present the alternatives scores obtained from the opinion of the experts and the decision-makers, respectively, see also Figs. 6 and 7.

4 Discussion

The cost criterion (C_3) received the highest weight from opinion of the experts and DMs, while the environmental sustainability criterion (C_2) came in second rank.

The weights of the factors (sub criteria, C_{ij}) for each criterion are found more-or-less not differing much from each other. This result is probably due to the limitation of linguistic diversity of selection.

Assessing the three design alternatives, both the experts and DMs gave the highest scores to the re-planning of OIU

Table 8 Alternatives scores—Experts' opinion

Alternatives	Criteria				Overall scores
	C_1	C_2	C_3	C_4	
A1	0.2744	0.3364	0	0.3644	0.350775
A2	0.2711	0.3364	0.4762	0.2713	0.248497
A3	*0.4545*	*0.3273*	*0.5238*	*0.3644*	*0.400327*

Table 9 Alternatives scores Decision-makers (DMs) opinion

Alternatives	Criteria				Overall scores
	C_1	C_2	C_3	C_4	
A1	0.2967	0.4032	0.3844	0.3358	0.255727
A2	0.2880	0.2932	0.1588	0.2502	0.332474
A3	*0.4152*	*0.3036*	*0.4569*	*0.4140*	*0.411853*

Fig. 6 Alternatives scores—Experts' opinion

Fig. 7 Alternatives scores—MDs' opinion

main campus MP following the modern trends in university campus planning (A3).

5 Conclusions

The current research implements the FAHP method as a MCDM approach to establish a sustainable selection tool that quantifies four key sustainable criteria based on priorities. The tool can be used by decision maker or expert architect during the evaluation of several alternatives for re-planning university campus masterplan considering sustainable environment. The chosen criteria in this study are project cost, land use, environmental sustainability, and circulation. The criteria ranking is based on relative importance would help decision-makers and designers to identify university MP project features that require more consideration, better resources allocation, and to improve the evaluation of the sustainable options.

This research limitations include the literature sample size that considered to assist the experts and DMs the chosen

criteria in the pairwise comparison. Also, the study results are influenced by the experiences and knowledge of the participated experts and decision-makers.

It is worthwhile mentioning that main campuses of OIU and University of Tabuk, KSA, look very similar regarding the size, current situation, execution progress, and general principles and requirements. Hence, the procedures stated in this research can possibly be applied to UT considering also the uniqueness of UT being part of NEOM, the most challenging project in KSA.

References

R. Alyamani, S. Long, The application of fuzzy analytic hierarchy process in sustainable project selection. MDPI. Sustainability **12**, 8314. https://doi.org/10.3390/su12208314

V. Balioti, C. Tzimopoulos, C. Evangelides, Multi-criteria decision making using TOPSIS method under fuzzy environment. Application in Spillway selection, in *Proceedings MDPI* (2018)

J. Buckely, Fuzzy hierarchical analysis. Fuzzy Sets Syst. **17**, 233–247 (1985)

D.-Y. Chang, Applications of the extent analysis method on fuzzy AHP. Eur. J. Oper. Res. **95**, 649–655 (1996)

M. Enea, T. Piazza, Project selection by constrained fuzzy AHP. Fuzzy Optim. Decis. Making **3**, 39–62 (2004)

E. Heo, J. Kim, K.J. Boo, Analysis of the assessment factors for renewable energy dissemination program evaluation using fuzzy AHP. Renew. Sustain. Energy Rev. **14**(8), 2214–2220 (2021)

G.J. Klir, Fuzzy arithmetic with requisite constraints. Fuzzy Sets Syst. **91**, 165–175 (1997)

Michigan State University, "Campus Planning Principles", https://ipf.msu.edu/construction/campus-master-plan/campus-planning-principles. Accessed 9 Dec 2021

P. Moura et al., IoT platform for energy sustainability in university campuses. MDPI. Sensors **21**, 357 (2021). https://doi.org/10.3390/s21020357

P. Nang-Fie, Application of AFP for selecting the suitable bridge construction method. Autom. Constr. **17**, 958–965 (2008)

T. Satty, *The Analytic Hierarchy Process* (McGraw-Hill, New York, 1980)

University of Colorado Boulder, "A Framework for the Future", https://www.colorado.edu/campusplanning/master-planning. Accessed 9 Dec 2021

P. van Laarhoven, W. Pedrycs, A fuzzy extension of Saaty's priority theory. Fuzzy Sets Syst. **11**, 229–241 (1983)

Literature Review on the Removal Methods of Monoethanolamine (MEA) in the Removal of Contaminants in Wastewater

A. N. F. Akhma, S. R. M. Kutty, L. Baloo, N. N. H. Ismail, M. A. Razali,
M. A. H. M. Fauzi, N. Azmatullah, and M. R. Marzuki

Abstract

This paper provides the literature on the investigation of biological organic removals of monoethanolamine (MEA) in an activated sludge system. A total of 31 papers cited and discussed with the purpose of providing information and understanding on the main topic of the research. The content of the paper includes several removal methods of MEA in wastewater, in the removal of contaminants, such as Advanced Oxidation Process, Adsorption Process, Membrane Technologies, and Biological Treatment Process. The Toxicity and Corrosivity of MEA on microorganisms were too discussed. At the end of each discussion made, the essence of research is presented for future researches, which will be useful for academics and practitioners.

Keywords

MEA • Monoethanolamine • Literature review • Methods of removal • Toxicity and Corrosivity

1 Introduction

Monoethanolamine (MEA) is commonly used in both domestic and industrial applications. Aqueous MEA is viscous, colourless, with an odour of ammonia. MEA is a dispersing agent for agricultural chemicals, aids in gas scrubbing in petroleum refineries, and is used to remove sulphur dioxide, carbon dioxide, hydrogen sulphide, and nitrogen dioxide from natural gases and other gases in the synthesis of surface active agents and polishes, amongst other things (Lam et al. 1999). MEA is the most common used amine for carbon dioxide absorption among industrially utilized alkanolamines, due to its high solubility, greater absorption capacity, and rapid reaction kinetics (Davidson 2007; Lee et al. 2012). This paper discussed on the various experimental works done by different authors in the removal of contaminants, with the presence of MEA. The role of MEA in this research is to remove carbon dioxide in petroleum refineries via various removal treatments.

There were a total of 11 papers discussing on the removal of MEA via Advance Oxidation Process, 8 papers discussing on the removal of MEA via Adsorption, 11 papers discussing on the removal of MEA via Biological Treatment, and 2 papers discussing on the removal of MEA via Membrane Technologies. A total of 2 papers discussing on the toxicity of MEA on microorganism and bacteria, and 1 paper discussing on the corrosivity of MEA with and without inhibitors.

Method of MEA removal include Advanced Oxidation Process, which helps on the degradation of organics at high concentrations, which involves a very reactive species known as hydroxyl radical ·OH. Next, Adsorption method is also discussed. It is a physical separation method used to reduce the concentration of dissolved pollutants in effluents. It is a natural process in which molecules of dissolved compounds are collected and adhered to the surface of an adsorbent solid. Absorbents such as MEA is commonly use in determining the suitability of MEA to remove or absorbed contaminants. Reverse osmosis, nanofiltration and ultrafiltration membrane technologies were discussed to determine the percentage performance of the separation process towards MEA rejection. Biological Treatment Process is a common method of pollutants removals, via organisms or extracellular enzyme. The treatment comprises of 3 categories including aerobic, anaerobic, and anoxic. Organisms including bacteria, fungi, yeast, algae or plant, is utilized in the removals of pollutants in bio treatment technologies. The

A. N. F. Akhma (✉) · S. R. M. Kutty · L. Baloo · N. N. H. Ismail ·
M. A. Razali · M. A. H. M. Fauzi · N. Azmatullah
Universiti Teknologi PETRONAS, Bandar Seri Iskandar,
32610 Tronoh, Perak, Malaysia
e-mail: amera_18003186@utp.edu.my

M. R. Marzuki
PCOGD, Kerteh, Malaysia

study on the toxicity of MEA were conducted to assess MEA waste toxicity towards microorganisms, in identifying the efficacy of microbiological methods for waste degradation acceleration. The corrosivity of MEA without and with the presence of oxidation inhibitors such as EDTA, formaldehyde, and Na_2SO_3 were discussed. Due to oxidative nature of MEA solvents, inhibitors were added to prevent the oxidation of MEA.

1.1 Objectives

This research aims to determine the extend research developments relating to the main research paper, with the topic: Biological Organic Removals of Monoethnolamine (MEA) in an Activated Sludge System, by providing various information and understanding of the results obtained from the research published to fellow researchers, which may be useful to other researchers for future studies.

2 Literature Review

2.1 Removal of MEA via Advanced Oxidation Process (AOP's)

AOP's are useful to degrade organics at high concentrations that are challenging to handle in a conventional biological oxidation unit. During the operation, a reactive hydroxyl radical ·OH is utilized. The most common methods for the generation of hydroxyl radical include, Fenton's treatment, UV/O_3, and UV/H_2O_2. UV/H_2O_2 process has few advantages including high capability on hydroxyl radical production, applicable in wide variation of pH and causes almost to none sludge formation during the treatment (Harimurti et al., 2012). AOP's are efficient in the degradation of MEA, as well as minimizing the toxicity of organic contaminant. Anotai et al. (2012) stipulated that the studies conducted by Sirtori et al. (2009) and Lucas et al. (2007) concluded that using a biological process in conjunction with Fenton's reagent may enhanced the decontamination and degradation process. In UV/H_2O_2 process oxidation, Eq. (1) is applicable in generating hydroxyl radical ·OH (Jones 2007).

$$H_2O_2 + hv \rightarrow 2 \cdot OH \tag{1}$$

According to Harimurti et al. (2012), the formation rate of ·OH radicals, which influenced by H_2O_2 concentrations and UV exposure, controls the rate of organic pollutant degradation. The usage of Fenton's reagent in AOPs aids in the decomposition of MEA waste (Harimurti et al. 2008, 2010). The Response Surface Method (RSM) used to perform the experiment on optimizing the oxidation process conditions of MDEA. From the investigation on the biodegradability of MEA via AOPs, it was observed that the removal of Total Organic Carbon (TOC) from the wastewater containing MDEA, via UV/H_2O_2 process reached up to 85%. The result proved that UV/H_2O_2 process improved the biodegradability of partially degraded MDEA. The optimal condition for the degradation of waste containing MDEA at initial concentration of contaminant are tabulated as in Table 1.

Putri et al. (2008); Harimurti et al. (2012) conducted a study on the degradation of salfolen via Fenton's reagent. Apart from that, Omar et al. (2010) conducted another analysis on the impact of Fenton's reagent's continuous addition mode on di-isopropanolamine mineralization (DIPA). In comparison to the one-time addition method, continual addition of Fenton's reagent performed the best. In the meantime, the usage of UV/H_2O_2 in AOPs was investigated. Fürhacker et al. (2003) stipulated that during the 28-day test period, MEA was not biodegradable in the batch bioreactor. This explains the effectiveness of advance oxidation processes (AOP's) in the degradation of MEA and reduction of the toxicity of organic contaminants. Amongst other methods of MEA removals, UV/H_2O_2 treatment is preferable as no formation of sludge was observed during the removal treatment, besides having a significant removal rate of organic contaminant.

Anotai et al. (2012) conducted a study on the treatment of TFT-LCD wastewater containing ethanolamine using fluidized-bed Fenton and Fenton processes. Fluidized-bed Fenton and Fenton processes experiments were conducted via a Box-Behnken design experiment. From the Fenton process experiment, it was concluded that the best settings of MEA removal at 5 mM is at pH 3, $[Fe^{2+}]$ = 5 mM and $[H_2O_2]$ = 60 mM. 96.4% of MEA concentration and 47% of TOC was removed. In comparison to fluidized-bed Fenton process, MEA removal efficiency was 98.9%, with 62% of TOC removed. The COD removal efficiency was 57.3% for Fenton process and 64.7% for fluidized-bed Fenton method. It was concluded that fluidized-bed Fenton method outperforms the Fenton process.

Table 1 The ideal conditions for the breakdown of MDEA-containing waste

Total organic Carbon (ppm)	Volume (mL)	UV Intensity (mW cm^{-2})	Temperature (°C)	pH	H_2O_2 initial concentration (M)	TOC removal after 180 min oxidation (%)
1000	400	12.06	30	9.52	0.23	85.99

The degradation of aqueous MEA using Fenton's reagent in conjunction with biological post-treatment was investigated by Harimurti et al. (2010). Wastewater containing amines, obtained from gas treatment facilities do not degraded easily, hence, the efficiency of Fenton's reagent in treating MEA wastewater was investigated and analysed. In a jacketed glass reactor, degradation tests were carried out. The effects of hydrogen peroxide, ferrous sulphate, and the pH of a solution on the pace of reaction were investigated, with pH 3 being the optimum. The degradation reaction is rather rapid initially, but gradually slows down with time. The author articulated that a larger fractional degradation of the organics in solution occurred when the initial COD of the feed solution is high. In comparison to a single injection of the reagent at the start of the process, a steady addition of H_2O_2 to the reaction mixture boosted COD elimination by 60%. Based on a simplified mechanistic model, a rate equation for amine mineralization was established, and the rate constant for COD elimination was obtained in lumped value. Activated sludge was used to biologically oxidize both partially degraded and "pure" MEA. The former substrate degraded much faster.

Harimurti et al. (2012) observed that aqueous alkanolamines including MEA, DEA, MDEA, and DIPA are commonly utilized for carbon dioxide scrubbing from natural gaseous. A substantial amount of alkanolamine is released into the wastewater during the shutdown of the desorption and absorption columns, as well as during cleaning and maintenance. It was found that conventional wastewater treatments are inadequate to treat the contaminated wastewater containing alkanolamines, therefore, advanced oxidation processes such as UV/H_2O_2 were introduced. The degradation of MEA waste was investigated in a laboratory setting by using UV/H_2O_2. It was hypothesized that biomass acclimatization in partially degraded amine was significantly quicker than that in untreated MEA. Glycine as well as other breakdown intermediates are predicted to stimulate quicker biomass growth (Harimurti et al. 2010).

Aqueous monoethanolamine (MEA) are commonly utilized for acid gases scrubbing (Harimurti et al. 2008). Natural gas processing plants may produce significant amounts of alkanolamine waste, which is a challenge to process with conventional biological treatment systems. Therefore, the chemical pre-treatment of MEA via Fenton's reagent prior to biological treatment was studied. COD removal rate by Fenton's oxidation was shown to be substantially dependent on the initial MEA concentration, with 54.5% COD eliminated at the maximum initial MEA concentration employed in the research. Glycine was found to be a degradation by-product in partially degraded MEA via FTIR and HPLC simulations. The aerobic biodegradability of partly degraded MEA in contrast to untreated MEA was explored utilizing

batch mixed culture experimentations to obtain the kinetic constants for aerobic biological treatment after 40% COD degradation via Fenton's reagent technique. The analysis indicated that the biodegradability of partially degraded MEA was greater than that of "pure" MEA, in accordance to the kinetic constants and shortened acclimatization phase. Significant amounts of dissolve ammonia were formed during both biological oxidation and Fenton's oxidation.

Maszelan and Buang (2014) led an investigation on the treatment of MEA via Photo-Fenton oxidation, with the presence of UV light. Various ferrous ion and hydrogen peroxide concentrations were evaluated during the study. According to the findings, the percentage removal of TOC is greater with the presence of UV light in comparison to that in the absence of UV light. The ideal concentration of ferrous ion is concluded to be 0.014 M, whereas the optimal concentration of hydrogen peroxide is 1.6 M, with both providing 99% removal of TOC. The reduction in TOC levels suggested that the Photo-Fenton oxidation process efficiently treated MEA waste. When hydroxyl radicals from the oxidation process reacted with organic substrate in MEA, the organic compounds in the wastewater substantially decreased.

2.2 Removal of MEA via Adsorption

Mohammad-Khah and Ansari (2009) and Kanawade et al. (2010) stipulated that adsorption is a physical method of separation utilized in reducing the concentration of dissolved pollutants in effluents. Adsorption is a natural phenomenon that occurs when molecules of a dissolved compound are attached to the surface of an adsorbent. Absorption method has an advantage over other approaches due to its sludge free nature (Kanawade et al. 2010). Razali (2013), Razali et al. (2010), Tong (2013), Isa (2014) and Muhammad (2013) have conducted the adsorption of COD, oil and MEA by using different absorbents, including alum, chitosan, rice husk, banana peel, sugarcane bagasse, etc., in determining the effectiveness of pollutants removal in wastewater.

Razali et al. (n.d.) studied three adsorbents activated carbon, rice husk and sugarcane bagasse and its adsorption performances were compared. Rice husk achieved has better oil and grease removal efficiency compared to activated carbon and sugarcane bagasse without considerable increase of the dosage. Rice husk to be fully utilized for MEA waste treatment as it is environmentally friendly, low cost and easily available for prompt usage rather than activated carbon. Investigated adsorbent did not affect the concentration by the adsorption treatment.

Razali et al. (2010) conducted another MEA investigation to compare the adsorption efficacy of chitosan to activated carbon, alum, and zeolite. From the investigation, it was

discovered that chitosan adsorbed COD, suspended solid and residue oil up to 83%, 57%, and 95%, respectively. Whereas COD was reduced by up to 80%, 73%, and 70% with activated carbon, alum, and zeolite, respectively, while suspended solid was reduced by up to 49%, 43%, and 38% with activated carbon, alum, and zeolite. Activated carbon removed 87% of residual oil, alum 64%, and zeolite 46%. The best adsorption performance was achieved by chitosan, followed by activated carbon, alum, and zeolite. However, MEA concentration was not affected by adsorption treatment.

Tong (2013) synthesized activated carbon from sawdust, which has a larger pore volume and specific surface area, hence it has a higher adsorption rate. According to the results, MEA concentration was lowered by 93%. In this study, banana peels and rice husk were used to treat MEA. Banana peels and rice husk managed to reduce COD and oil by 78.9%, 76.65% and 53.32%, 49.86%, respectively. Both adsorbent were capable to reduce amine concentration below 6% (Razali 2013). Another study was conducted using chitosan, rice husk, and activated carbon. Oil adsorption was 32.14%, 28.14% & 21.43%, respectively. The adsorption treatment had no impact on the MEA concentration in any of the adsorbents utilized in this study (Isa 2014). For the removals of oil, COD and amine concentration, activated carbon, and rice husk were used. The percentage removal efficiency of oil and COD reduction by activated carbon was 43.57% and 66.81%, respectively. While treated rice husk had a lower effectiveness of 37.83% and 53.32% in oil and COD removal, respectively. MEA concentration, on the other hand, remains constant for both adsorbents. Muhammad (2013) stipulated that the most effective adsorbent for oil residue is activated carbon, whereas MEA concentration

remained unchanged. Table 2 display that tabulated results of percentage of contaminants removed with respective absorbents used.

2.3 Removal of MEA via Membrane Technologies

Membrane technology is also another treatment for MEA removal. There are three different commercial membranes studied, which include reverse osmosis (RO), nanofiltration (NF), and ultrafiltration (UF). The effect of feed concentration, operating pressure, cross-flow velocity as well as pH towards the membranes were investigated (Binyam et al. 2009). According to Binyam et al. (2009), RO membrane has the greatest rejection, at around 99%, in comparison to the percentage rejection reached by NF and UF membranes, which are at 75% and 35%, respectively. The result obtained explains that RO membrane is applicable and most effective in the removals of MEA from the wastewater (Binyam et al. 2009). Table 3 show the tabulated the rejection separation percentage via different membrane technologies applied.

A study on the removal of MEA from wastewater via reverse osmosis membrane was also conducted by Borhan and Mat Johari (2014). According to the findings of the experiments, the tubular thin film composite polyamide (AFC99) membrane reject up to 98% of MEA when operated at a pressure of 2000 kPa with a feed concentration of 300 ppm at a pH level 4. Due to the efficiency of RO membrane in removing pollutants, it is the most preferred approach for the removal of MEA contaminants from wastewater.

Table 2 Adsorption of COD, Oil, and MEA using different adsorbents

No	Adsorbent	Pollutant	Removal efficiency	Reference
1	Activated carbon	COD & oil	80% & 87%	Razali et al. (n.d.)
			53% & 56%	Razali et al. (2010)
2	Chitosan	COD & oil	83% & 95%	Razali et al. (2010)
3	Alum	COD & oil	73% & 64%	Razali et al. (2010)
4	Sugarcane bagasse	COD & oil	70% & 42%	Razali et al. (n.d.)
5	Zeolite	COD & oil	70% & 46%	Razali et al. (2010)
6	Rice husk	COD & oil	53.32% &78.9%	Razali (2013)
7	Banana peel	COD & oil	49.86% &76.65%	Razali (2013)
8	Activated carbon by saw dust	MEA	93%	Tong (2013)
9	Rice husk	Oil	21.43%	Isa (2014)
	Chitosan		28.14%	
	Activated carbon		32.14%	
10	Activated Carbon	Oil & COD	43.57% & 66.81%	Muhammad (2013)
	Treated Rice husk		37.83% & 53.32%	

Table 3 Commercial Membranes with respective Rejection Percentage (Binyam et al. 2009)

Type of Commercial Membranes	Rejection of Separation process (%)
Reverse Osmosis	99
Nanofiltration	75
Ultrafiltration	35

2.4 Removal of MEA via Biological Treatment Systems

Biological treatment is a common method of pollutants removals, via organisms or extracellular enzyme. The treatment comprises of 3 categories including aerobic, anaerobic, and anoxic. Organisms including bacteria, fungi, yeast, algae or plant, is utilized in the removals of pollutants in bio treatment technologies. Composting, bioreactors, bio filters, and other biological treatments have the benefits of low cost, high removal rate, etc. (Boopathy 2000). MEA degradation products are classified into two types: primary and secondary degradation products. In accordance to Fredriksen and Jens (2013), organic acids, aldehydes, and ammonia are the reported compound classes for oxidative degradation of MEA. It was assumed that the products were formed due to autoxidation, which explains the oxidization of MEA in the influent sample. Lee et al., (2010) articulated that the oxidative degradation products of MEA with inhibitors such as EDTA were much lesser in comparison to MEA without the presence of inhibitors. Acetic acid, ammonium, and ethanol are the major breakdown products of MEA biodegradation (Bradbeer 1965; BUA 1994; Jones and Turner 1973; McVicker et al. 1997). Gottschalk (1985) stated that acetic acid and ethanol can be completely degraded via either methanogenesis (anaerobic) or tri carboxylic acid cycle (aerobic).

Urasaki et al. (2019) conducted a study on the electronic industry waste water contains TMAH, MEA, and sulphate. The batch feeding experiment with a single organic source and sulphate, as well as specific activity measurement of retained sludge, were conducted to study the behaviour of methanogenic degradation of MEA in an up flow anaerobic sludge blanket (UASB) reactor operated continuously at mesophilic conditions. The findings revealed that MEA was degraded by a methanogenic pathway with sulphate reduction, implying that MEA waste might be treated with methanogenic treatment with proper reactor handling.

Wang et al. (2013) implemented sequencing batch reactor (SBR) to investigate the influence of MEA inhibition and adaptation on biological degradation, as well as the removal of amine (MEA) at lab scale. It was concluded that 92% of 9000 mg/L of MEA was removed after 10.5 days of hydraulic retention time (HRT).

Mrklas et al. (2004) studied MEA biodegradation by conducting bench scale studies, where significant levels of MEA (31,000 mg/kg) was successfully biodegraded aerobically in the bioreactors. MEA degradation products including ethanol, ammonium, and acetate at approximately 8100 mg/kg, 8800 mg/kg, and 75,000 mg/kg, respectively, has entirely degraded without interfering with aerobic biodegradation.

Waste products are produced after the degradation of MEA. Li (2008) studied the biodegradation of waste amines by conducting a series of BOD tests and nine (9) syringe batch experiments cases under aerobic, micro aerobic, and anaerobic settings. It was observed that waste amines were effectively degraded at high reaction rates under aerobic, anaerobic, and micro aerobic settings, with 90% and more of amine COD removed. The BOD studies demonstrated that amine degradation occurs in first order, with the greatest reaction rate of 1.08/d obtained in reactors containing initial amine concentration of 125 mg/L. If pH was kept at neutral, concentration of amines as high as 2000 mg/L can be degraded. As a result, low-cost biological treatment plants may be proposed to manage waste amines while retrieving energy as CH_4.

Lam et al. (1999) conducted another sequencing batch reactor experimental studies on the investigation on the shock loads of MEA on activated sludge treatment system. From the investigation, it was concluded that monoethanolamine (MEA) is readily biodegraded by a mixed culture and is not inhibitory to this community at concentrations below about 1600 mg/L COD. Beyond this threshold, MEA was inhibitory to its own degradation. MEA degradation occurred over the tested temperature range of 15–35 °C with 25 °C being optimum for the culture studied. MEA degradation was little affected by pH from 4.5 to 8.0, but extremes of pH outside this range led to lower rates of degradation.

The investigation confirmed the biodegradation pathways of MEA and its breakdown products using indigenous microbes. The effectiveness of biological treatment in the removals of pollutants were supported by other studies conducted by Huang et al. (2017) and Haritash and Kaushik (2009).

2.5 Toxicity of MEA on Bacteria and Microorganisms

Liuzinas et al. (2007) conducted a laboratory scale study on the investigation on the toxicity of MEA on microorganisms via paper disc and wells methods for the determination of toxicity of MEA waste on bacteria and microorganisms. From the investigation it was observed that the toxicity test using method of wells is more sensitive in comparison to the

Table 4 Sensibility of bacteria to various concentrations of MEA (method of paper discs) (Liuzinas et al. 2007)

MEA concentration (%)	Diameter of sterile zone (mm)		
	Bacillus megaterium	Escherichia coli	Proteus mirabilis
100	8	10	8
75	6	6	5
50	3	4	4
25	3	2	3
10	2	0	3
5	1	0	1
1	0	0	0
0.1	0	0	0

Table 5 Sensibility of microorganism to various concentrations of MEA (method of wells) (Liuzinas et al. 2007)

MEA concentration (%)	Diameter of sterile zone (mm)				
	Acremonium roseum	Cladosporium herbarum	Fusarium culmorum	Penicillium expansum	Trichoderma harzianum
100	20	15	7	15	20
75	17	10	5	12	18
50	15	8	4	10	10
25	10	5	2	4	5
10	2*	3*	0	4*	5*
5	1*	2*	0	2*	4*
1	0	0	0	0	0
0.1	0	0	0	0	0

* Fungistatic effect

method of disc. Escherichia coli was the most sensitive for higher concentrations of MEA among the investigated bacteria. It was observed that the toxicity of MEA is higher in bacteria. MEA at concentrations of 5–25% have influence on some bacteria: fungistatical influence at 5% and fungicidal influence at 25%. Addition of MEA waste at various concentrations were made onto the bacteria and microorganisms and the results were tabulated as in Tables 4 and 5, respectively.

Repečkienė et al. (2010) conducted a toxicity test on microbial development by adding various concentrations of MEA waste onto it. The test was conducted by using paper disc technique, according to the diffusion of the tested substance to the medium. Sterile filter paper discs were soaked in MEA concentrations, which was appropriate for the experiment. Table 6 displays the responsiveness of microorganisms to numerous MEA loading waste. The author mentioned that MEA waste mixture is ecotoxic and environmentally harmful. Toxicity of MEA waste was assessed based on the resistance of various microorganism strains. The impact of MEA waste on bacterial growth was rather significant, as bacteria growth was inhibited when MEA level was at 1% and greater. At MEA concentrations up to 25%, Escherichia coli was the least impacted, while MEA concentrations 25% onwards inhibited all bacteria

alike. MEA waste inhibits the more sensitive bacterial strains at lowest concentrations of 5%. Amongst the treated yeast-like and yeasts fungi, Repečkienė et al. (2010) discovered that Aureobasidium pullulans was susceptible to MEA the most. MEA concentration ranging from 75 to 25% inhibited Candida lipolytica and Geotrichum fermentans. From concentration of 25% MEA, Rhodosporidium diobovatum, and Rhodotorula rubra growth was observed to be inhibited. To summarize, bacteria were more susceptible to MEA harmful effects than fungi.

2.6 Corrosivity of MEA with Various Presence of Inhibitor

Lee et al. (2012) studied the corrosivity of MEA with and without the presence of oxidation inhibitors by conducting corrosion tests, in accordance to ASTM G31. Due to oxidative nature of the alkanolamine solvents, inhibitors such as EDTA, formaldehyde, and Na_2SO_3 was added to the solution to avoid the solvents from oxidizing. The test was performed on stainless steel 304 specimens with the dimensions; 20 mm × 13 mm × 3 mm that had been polished with Al_2O_3 sand paper, rinsed with acetone, and let dried. An analytic balance with an initial weight precision of

Table 6 Sensibility of microorganisms to MEA waste concentrations (Repečkienė et al. 2010)

Microorganisms	MEA Concentrations (%)							
	100	75	50	25	10	5	1	0.1
Acremonium roseum	17	5	3	2	0	0	0	0
Aureobasidium pullulans	10	9	8*	6*	6*	8*	8*	6*
Bacillus megaterium	8	6	3	3	2	1	0	0
Cladosporium herbarum	12	8	4	2	0	0	0	0
Candida lipolytica	10	8	6	4	0	0	0	0
Escherichia coli	10	6	4	2	0	0	0	0
Fusarium culmorum	5	2	0	0	0	0	0	0
Geotrichum fermentans	15	10	10	8	0	0	0	0
Proteus mirabilis	8	5	4	3	3	1	0	0
Penicillium expansum	5 + 10*	10*	8*	6*	4*	2*	0	0
Rhodosporidium diobovatum	10	13*	8*	0	0	0	0	0
Rhodotorula rubra	8	6	0	0	0	0	0	0
Trichoderma harzianum	2 + 20*	10*	10*	10*	4*	3*	0	0

* Fungistatic effect

0.0001 g (W_o) was used to weighed the dried specimens. After being submerged in the test CO_2 saturated solutions at 120 °C for 48 h, the corroded specimens were withdrawn from the solutions, cleaned, and dried. The removal of CO_2 gas into fresh solution for 8 h was done to prepare the CO_2 saturated solution. The samples were reweighed and the final weight (W) were recorded. Equation (2) was applied to identify the corrosion rate (CR) [mm/y].

$$CR = \frac{(W_o - W)}{(A \times t \times D)} \tag{2}$$

where:

W_o [kg]	= Initial weight
W_I [kg]	= Final weight
A [m^2]	= Surface are of specimens (exposed).
t [y]	= Submerged time.
D [kg/m^3]	= Density of the specimens.

According to the test results, the rate of corrosion for MEA solution without inhibitor was 1.52 mm/y, whereas the corrosion rate of MEA solution with EDTA as the inhibitor was 1.46 mm/y. The results explain that oxidation inhibitors such as EDTA and Na_2SO_3 decreases the rate of corrosion. However, formaldehyde inhibitor increased the rate of corrosion slightly. Hence, the rate of corrosion of MEA with the presence of inhibitors was in the sequence of formaldehyde > EDTA > Na_2SO_3. Several studies agreed that there is a connection between oxidation inhibitors and the degradation, as well as the corrosivity of MEA (Goff et al. 2006; Lee et al. 2012).

3 Summary of the Papers

From the literature review on the removal of MEA via AOP's, the significant information was listed:

(a) AOP's are efficient to the degradation of MEA, as well as to the reduction of the toxicity of organic contaminant. This is because of the absence of sludge formation during the treatment, apart from having high capability of producing hydroxyl radical. Also, AOP's are applicable in wide variation pH.

(b) Combination of Fenton's reagent and biological process may enhance the decontamination and degradation process.

(c) AOP's are effective in MEA degradation, as well as in reducing the toxicity of organic contaminant.

(d) In comparison to other wastewater treatment methods, UV/H_2O_2 offers other advantages including zero formation of sludge during the process, apart from producing a high rate of organic pollutant removal.

(e) COD is removed efficiently via fluidized-bed Fenton process in comparison to Fenton process.

(f) Degradation of MEA waste via UV/H_2O_2 indicated that the rate of biomass acclimatization was higher in partially degraded amine in comparison to pure MEA. Biomass growth accelerates due to glycine and other degradation intermediates.

(g) Treatment of MEA via Photo-Fenton oxidation with the presence of UV light resulting to higher TOC removal percentage than that in the absence of UV light.

From the literature review on the removal of MEA via Adsorption Method, the significant information was listed:

(a) Rice husk has better oil and grease removal efficiency compared to activated carbon and sugarcane bagasse without considerable increase of the dosage.

(b) Activated carbon by sawdust absorbent exhibited higher rate of adsorption, with concentration of MEA reduced by 93%, in comparison to other absorbents, where MEA concentration remain constant or as lowest as 6%.

From the literature review on the removal of MEA via Membrane Technologies, the significant information was listed:

(a) RO membrane is practical and desirable in the removal of MEA contaminants from wastewater as it has the highest rejection separation process percentage amongst other commercial membrane.

From the literature review on the removal of MEA via Biological Treatment System, the significant information was listed:

(a) In a study on the electronic industry waste water contains TMAH, MEA, and sulphate, it was found that MEA was degraded via methanogenic pathway with sulphate reduction which proved that methanogenic treatment was applicable to MEA waste.

(b) In a sequencing batch reactor (SBR) study on the influence of inhibition and adaptation of MEA on biological degradation as well as the removal of amine, it was concluded that the removal efficiency of 9000 mg/L MEA was 92% at 10.5 days of HRT.

(c) In a study of the biodegradability of MEA in laboratory bench scale bioreactors, where it was observed that substantial levels of MEA (31,000 mg/kg) was successfully biodegraded aerobically in the bioreactors. MEA degradation products including ethanol, acetate, and ammonium at certain concentrations may completely degraded without interfering with aerobic biodegradation.

(d) To investigate the biodegradation of waste amines, a series of BOD tests and nine cases of syringe batch experiments were carried out under aerobic, micro aerobic, and anaerobic settings. Waste amines effectively decomposed with high reaction rates in all conditions mentioned, and more than 90% of amine COD was removed, according to the findings. If the pH is kept at neutral, high concentrations of amines, up to 2000 mg/l can be degraded.

(e) Another sequencing batch reactor experimental studies on the investigation on the shock loads of MEA on activated sludge treatment system shows that MEA is readily biodegraded by a mixed culture and is not inhibitory to the microbes at concentrations below 1600 mg/L COD. Beyond this threshold, MEA was inhibitory to its own degradation. MEA degraded within 15–35 °C, with 25 °C being the optimal temperature for the culture investigated. MEA degradation was slightly affected by pH ranging from 4.5 to 8.0, however, extreme pH outside the range resulted to lower rates of degradation.

From the literature review on the toxicity and corrosivity of MEA, the significant information was listed:

(a) Toxicity test using method of wells is more sensitive in comparison to the method of disc. Escherichia coli was the most sensitive at higher concentrations of MEA among the investigated bacteria. It was observed that the toxicity of MEA is higher in bacteria.

(b) Oxidation inhibitors such as EDTA and Na_2SO_3 decrease the corrosion rate, whereas, Formaldehyde slightly increased the rate of corrosion. Hence, the sequence of the rate of corrosion of MEA with the presence of inhibitors is as follow; formaldehyde > EDTA > Na_2SO_3.

To conclude, amongst the methods provided in the research study, the most common method conducted, on the removal of MEA in the removal of contaminants is via Biological Treatment Process. However, some authors agreed that the combination of 2 or more methods of removals resulting to a higher efficiency in the removal of MEA compounds, in the removal of contaminants. It was concluded that MEA is corrosive and toxic to microorganisms at lower concentrations.

References

J. Anotai et al., Treatment of TFT-LCD wastewater containing ethanolamine by fluidized-bed Fenton technology. Bioresour. Technol. **113**, 272–275 (2012)

S. Binyam, H. Mukhtar, L. Leong, Flux and rejection of monoethanolamine (MEA) in wastewater using membrane technology, in Thirteenth *International Water Technology Conference, ITWC* (2009)

R. Boopathy, Factors limiting bioremediation technologies. Biores. Technol. **74**(1), 63–67 (2000)

A. Borhan, M.M. Mat Johari, Removal of monoethanolamine from wastewater by composite reverse osmosis membrane. Jurnal Teknologi **68**(5) (2014)

C. Bradbeer, The clostridial fermentation of choline and ethanolamine I. J. Biol. Chem. **240**, 4669–4674 (1965)

BUA, Beratergremium fuer Umweltrelevante Altstoffe, Ethylene glycol, S. Hirzel Wissenschaftliche Verlagsgesellschaft Stuttgart, Germany (1994)

R.M. Davidson, Post combustion carbon capture from coal fired plants—solvent scrubbing, IEA GHG Report CCC/125, London, UK (2007)

S.B. Fredriksen, K.-J. Jens, Oxidative degradation of aqueous amine solutions of MEA, AMP, MDEA, PZ: a review. Energy Procedia **37**, 1770–1777 (2013)

M.A. Fürhacker Pressl, R. Allabashi, Aerobic biodegradability of methyldiethanolamine (MDEA) used in natural gas sweetening plants in batch tests and continuous flow experiments. Chemosphere **52**(10), 1743–1748 (2003)

G.S. Goff, G.T. Rochelle, Oxidation inhibitors for copper and iron catalyzed degradation of monoethanolamine in CO_2 capture processes. Ind. Eng. Chem. Res. **45**, 2513–2521 (2006)

G. Gottschalk, *Bacterial Metabolism*, 2nd edn. (Springer, Berlin, Germany, 1985)

S. Harimurti, I.F.M. Arief, R.M. Ramli, P.F. Khamarudin, B.K. Dutta, Biodegradability of monoethanolamine after Fenton treatment, in *Proceedings of the International Conference on Environment*, December 15–17, 2008, Universiti Sains Malaysia, Penang, Malaysia

S. Harimurti, B.K. Dutta, I.F.B.M. Ariff, S. Chakrabarti, D. Vione, Degradation of monoethanolamine in aqueous solution by Fenton's reagent with biological post-treatment. Water Air Soil Pollut. **211**, 273–286 (2010)

S. Harimurti, A. Rahmah, A. Omar, T. Murugesan, Application of response surface method in the degradation of wastewater containing MDEA using UV/H_2O_2 advanced oxidation process. J. Appl. Sci. **12**(11), 1093–1099 (2012)

A. Haritash, C. Kaushik, Biodegradation aspects of polycyclic aromatic hydrocarbons (PAHs): a review. J. Hazard. Mater. **169**(1–3), 1–15 (2009)

D. Huang, C. Hu, G. Zeng, M. Cheng, P. Xu, X. Gong, R. Wang, W. Xue, Combination of Fenton processes and biotreatment for wastewater treatment and soil). remediation. Sci. Total Environ. **574**, 1599–1610 (2017)

S.Z. Isa, *Kinetic Study of Adsorption Process Using Chitosan, Activated Carbon, and Rice Husk for Monoethanolamine (mea) Wastewater Treatment Via Batch Process*. UMP. (2014).

A. Jones, J.M. Turner, Microbial metabolism of amino alcohols. Biochem. J. **134**, 167–182 (1973)

C.W. Jones, *Applications of Hydrogen Peroxide and Derivatives*. (Royal Society of Chemistry, 2007).

S.M. Kanawade, R. Gaikwad, A. Misal, Low cost sugarcane bagasse ash as an adsorbent for dye removal from dye effluent. Int. J. Chem. Eng. Appl. **1**(4), 309 (2010)

P.N.F.M. Khamarudin, S. Harimurti, I.F.M. Arief, R.M. Ramli, B.K. Dutta, Degradation of amine based absorbent using Fenton's oxidation (ICENV, Penang Malaysia, 15–18 December 2008)

Y. Lam, R.M. Cowan, P.F. Strom, in *The Treatability of Monoethanolamine (MEA) in Nitrifying Activated Sludge*, ed. by N. Nikolaidis, C. Erkey, B.F. Smets (1999)

I.Y. Lee, N.S. Kwak, J.H. Lee, K.R. Jang, J.G. Shim, Degradation and corrosivity of MEA with oxidation inhibitors in a carbon dioxide capture process. J. Chem. Eng. Jpn. **45**(5), 343–347 (2012)

Y. Li, Biodegradation of waste amines under anaerobic, micro-aerobic and aerobic conditions. Høgskolen i Telemark (2008)

R. Liuzinas, K. Jankevicius, M. Salkauskas, R. Jakubenas, A. Paskevicius, M. Mikalajunas, Biological method for the detoxification of spent monoethanolamine solutions. Linnaeus Eco-Tech 881–888 (2007). https://doi.org/10.15626/eco-tech.2007.094

M.S. Lucas, A.A. Dias, A. Sampaio, C. Amaral, J.A. Peres, Degradation of a textile reactive azo dye by a combined chemical–biological process: Fenton's reagent-yeast. Water Res. **41**(5), 1103–1109 (2007). https://doi.org/10.1016/j.watres.2006.12.013

C.N. Maszelan, A. Buang, Monoethanolamine (MEA) wastewater treatment using photo-fenton oxidation. Appl. Mech. Mater. **625**, 792–795 (2014). https://doi.org/10.4028/www.scientific.net/amm.625.792

L. McVicker, D. Duffy, V. Stout, Microbial growth in a steady-state model of ethylene glycol-contaminated soil. Curr. Microbiol. **36**, 137–147 (1997)

A. Mohammad-Khah, R. Ansari, Activated charcoal: preparation, characterization and applications: a review article. Int. J. Chem. Tech. Res. **1**(4), 859–864 (2009)

O. Mrklas, A. Chu, S. Lunn, L.R. Bentley, Biodegradation of monoethanolamine, ethylene glycol and triethylene glycol in laboratory bioreactors. Water Air Soil Pollut. **159**(1), 249–263 (2004)

N. Muhamad, *Study on the Adsorption Process of Monoethanolamine (MEA) Wastewater Using Activated Carbon and Treated Rice Husk*. UMP. (2013)

A.A. Omar, R.M. Ramli, P. Khamaruddin, Fenton oxidation of natural gas plant wastewater. Can. J. Chem. Eng. Technol. (2010)

M.E. Razali, *Study on Batch Adsorption Process of Monoethanolamine (MEA) Wastewater Treatment Using Rice Husk and Banana Peels*. UMP (2013)

M.N. Razali, N.A.M. Salehan, M.A.M. Khairu, Feasibility study on adsorption treatment of monoethanolamine (MEA) wastewater using bio-adsorbents (n.d.)

J. Repečkienė, D. Pečiulytė, A. Paškevičius, O. Salina, K. Jankevičius, R. Liužinas, Microbiological reduction of monoethanolamine waste toxicity. J. Environ. Eng. Landsc. Manag. **19**(4), 287–295 (2010)

C. Sirtori, A. Zapata, I. Oller, W. Gernjak, A. Agüera, S. Malato, Decontamination industrial pharmaceutical wastewater by combining solar photo-fenton and biological treatment. Water Res. **43**(3), 661–668 (2009). https://doi.org/10.1016/j.watres.2008.11.013

Y.Y. Tong, *Monoethanolamine (MEA) Wastewater Treatment via Adsorption using Activated Carbon Derived from Sawdust* (2013)

K. Urasaki, H. Sumino, T. Danshita, T. Yamaguchi, K. Syutsubo, Biological treatment of electronic industry wastewater containing TMAH, MEA and sulfate in an UASB reactor. J. Environ. Sci. Health. Part A, **54**(11), 1109–1115 (2019). https://doi.org/10.1080/10934529.2019.1631655

S. Wang, J. Hovland, R. Bakke, Anaerobic degradation of carbon capture reclaimer MEA waste. Water Sci. Technol. **67**(11), 2549–2559 (2013)

Biological Organic Removals of Monoethanolamine (MEA) in an Activated Sludge System

A. N. F. Akhma, S. R. M. Kutty, L. Baloo, N. N. H. Ismail, M. A. Razali, M. A. H. M. Fauzi, N. Azmatullah, and M. R. Marzuki

Abstract

MEA is an alkanolamine used in petroleum refineries for the removal of SOUR gases from liquid hydrocarbons. However, plants treating petroleum refineries wastewater found that MEA inhibits the removals of organic compounds in the treatment system, which causes effluent chemical oxygen demand (COD) concentrations to increase. Hence, the study on the impact of MEA on the removal of organic compounds in the activated sludge system was pursued. The objectives include, to determine the impact of MEA on the removal of organic compounds, in the removal of contaminants, the rate of COD removals of organic matter in an activated sludge system and the loading of MEA which is inhibitory to the microbes in the removal of organic compounds, by varying the addition of MEA concentrations into the raw influent. Bench scale studies were conducted, where two trains comprise of reactors with an aeration tank and a clarifier, provided with sludge recycle system and were set up. Train 1 operated at both conventional aeration-activated sludge mode and extended aeration-activated sludge mode, while Train 2 operated at only extended aeration-activated sludge mode. Both influents and effluents were analyzed according to APHA methods. All sampling parameters were conducted three times a week and were measured in triplicates. Addition of MEA at various concentration of 50, 100, 500 and 1000 mg/L was made to the raw influent once the wastewater has acclimatized. The results show that the addition of 1000 mg/L MEA increased influent COD concentrations to an average of 1774 mg/L. Average COD removals in reactor A1T1 decreased with the addition of MEA, to 88.7%. However, the average COD removed/mg mlvss.day stabilized even after the addition of 100 mg/L MEA, at an average of 35.22 mg COD removed/mg mlvss.day, and 14.62 mg COD removed/mg mlvss.day, for reactor A1T1 and A1T2, respectively. Overall, effluent COD concentrations met the standard discharged limits of 120 mg/L. Both MLSS and MLVSS concentrations in reactor A1T1, A2T1 and A1T2 were stabilized throughout the study period, with MLSS/MLVSS ratio of 0.78, 0.83 and 0.84, respectively. The addition of 1000 mg/L MEA into the influent causes spikes in Sludge Volume Index (SVI) for reactors A1T1, A2T1 and A1T2 at 91 mL/g, 90 mL/g and 95 mL/g, respectively. The sludge age in reactor A1T1, A2T1 and A1T2 was maintained throughout the study, at an average of 5.4 days, 30.0 days and 30.2 days, respectively. The specific oxygen uptake rate (SOUR) declined with the addition of MEA, at an average of 5.73 mg O_2/gVSS.h., 1.77 mg O_2/gVSS.h and 1.85 mg O_2/gVSS.h, respectively, for reactor A1T1, A2T1 and A1T2, throughout the study.

Keywords

MEA • COD • COD removals • MLSS • Sludge settleability • Sludge age • Specific oxygen uptake rate and organic removals

1 Introduction

1.1 Project Background

PETRONAS Chemicals Group Bhd. comprises of a group of companies known as PCOGD, which produces a variation of petrochemical products. The wastewater generated from the refinery is currently treated via an activated sludge system in the effluent treatment system (ETS). Effluent from the process

A. N. F. Akhma (✉) · S. R. M. Kutty · L. Baloo · N. N. H. Ismail · M. A. Razali · M. A. H. M.Fauzi · N. Azmatullah
Universiti Teknologi PETRONAS, Bandar Seri Iskandar, 31750 Tronoh, Perak, Malaysia
e-mail: amera_18003186@utp.edu.my

M. R. Marzuki
PCOGD, Kerteh, Malaysia

plant flows into the equalization tank at approximately 70–80 m³/h and into the splitter box. From the splitter box, the wastewater then splits into two parallel streams, into two separate extended aeration activated sludge basin. Each stream then goes into respective clarifier (East or West) for the settling of the biomass. 200 m³ of sludge is recycled and returned from the clarifier, into the aeration tank to maintain the concentrations of biomass in the tank at approximately 4800 mg/L. The detention time of the aeration tank is approximately 24 h. The sludge age (days) is maintained by wasting from the extended aeration activated sludge basin tank at 5–8 m³/hour. The wasted sludge from the clarifier is further treated through air dilution, thickener, digester, belt press, drying bed sump and to the land farm for final disposal.

1.2 Problem Statement

Currently, the generated wastewater from the petroleum refinery is treated via an activated sludge plant in the effluent treatment system (ETS). However, ETS has been experiencing spikes in organic matters from the activated sludge effluent, where there was an amine carryover from the refinery, contributing to the increment of effluent chemical oxygen demand (COD). The increment of organic matters due to the loading of MEA in the ETS causes poor settling of biomass in the reactors. As a result, the elimination of organic compounds and contaminants with the presence of aqueous MEA in the activated sludge system was conducted through a lab bench scale-activated sludge system.

1.3 Objectives

The following are the objectives of the research:

(a) To evaluate the influence of MEA on the organic compounds removal, in eliminating pollutants in the activated sludge treatment process.
(b) To determine the MEA loading which inhibits the development of microbes in the organic compounds removal in the activated sludge treatment process, by varying the addition of MEA concentrations.
(c) To determine the removal rate of COD in the removal of organic matter in an activated sludge treatment system.

1.4 Scope of Work

150 L of raw influent sample obtained from PCOGD refinery was treated biologically via two trains of activated sludge system. The generated and treated wastewater were analyzed in accordance with APHA methods. Sampling parameters including mixed liquor volatile suspended solids (MLVSS),

mixed liquor suspended solids (MLSS), and chemical oxygen demand (COD) were measured in triplicates and conducted three times a week, for respective sampling points, to ensure results accuracy. During acclimatization phase 1, a dilution of 1:6 were made to the raw influent sample, while full strength testing was conducted during acclimatization phase 2. Once the wastewater had acclimatized, MEA was gradually added to the raw influent sample at various concentrations of 50, 100, 500 and 1000 mg/L. All reactors were monitored and maintained its biomass throughout the study, by sludge wasting.

2 Methodology

2.1 Flowchart of Project

A volume of 150L raw influent taken from PCOGD refinery was treated via bench scale-activated sludge treatment system, where two trains encompass of reactors equipped with an aeration tank, a clarifier, and provided with sludge recycling system were constructed. Once the wastewater has been treated, both influents and effluents gathered from both trains were monitored and analyzed by conducting various sampling parameters, in accordance with International Standard Methods (APHA). All data were collected and analyzed throughout all of the phases. Figure 1 displays the flowchart of the project conducted.

2.2 Setting up of Reactors

Bench scale-activated sludge system was proposed and constructed as in Fig. 2, which is utilized in the process of removing organic compounds in an activated sludge treatment system.

The reactors were fabricated with a volume of 10 L. Wastewater from PCOGD was then fed into the system at various flow rate to attain detention time of 24 h in each reactor. The biomass in the reactors was acclimatized using the biomass and wastewater from PCOGD. Sludge from the aeration tank was wasted at periodic intervals to maintain the concentration of biomass in the bioreactor, as well as maintaining the sludge age. After the treatment from the aeration tanks, the wastewater will then settle in respective to clarifier tank.

2.3 Experimental Methodology: Train 1 & Train 2

Figure 3 illustrates the configuration of two bench scale-activated sludge systems in Train 1. Reactor A1T1 was for the degradation of organic matter which operated at

Fig. 1 Flowchart of methodology

Collection 150 L of Industrial Wastewater from PCOGD

Treatment of Industrial Wastewater

Train 1   Train 2

Conventional Aeration Activated Sludge System

Extended Aeration Activated Sludge System

Extended Aeration Activated Sludge System

Sampling Monitoring (COD, MLSS, MLVSS)

Acclimatization Phase 1 & Acclimatization Phase 2

Addition of MEA at Various Concentrations

Data Collection and Analysis

Fig. 2 Dimensions of one activated sludge reactor

conventional activated sludge mode with 5 days of sludge age and a maintained MLSS concentration of 1500 mg/L, while reactor A2T1 was for nitrification, which was operated at extended activated sludge mode, with 30 days of sludge age and a maintained MLSS concentration of 4000 mg/L.

In Train 2, one bench scale-activated sludge system was constructed as in Fig. 4. Reactor A1T2 was operated at extended aeration and was used for the degradation of organic matter, providing a sludge age of 40 days and a maintained MLSS concentration at 4000 mg/L. Nitrification of the organics was expected to occur in the aeration tank.

2.4 Sampling Plan and Testing Methods

The wastewater generated and treated was analyzed in accordance with International Standard Methods (APHA), for respective sampling parameters as in Table 1. To ensure accuracy, all parameters sampling were measured in triplicates and conducted three times a week, for the respective sampling points.

Fig. 3 Schematic diagram for Train 1
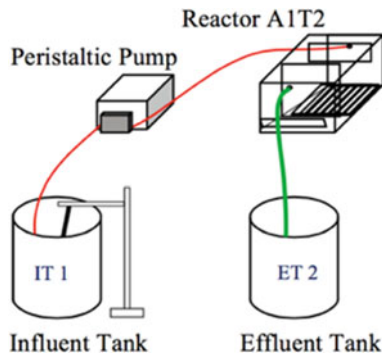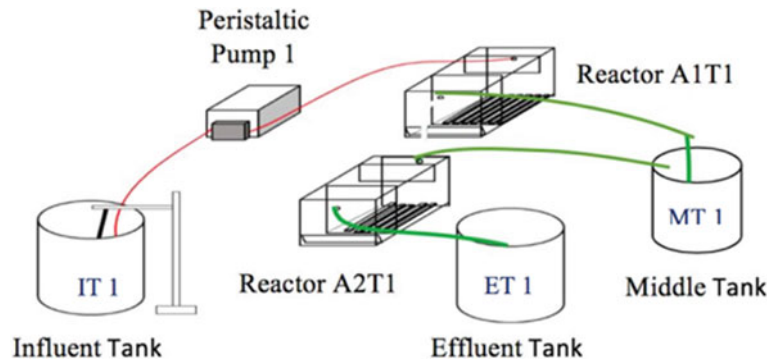
Fig. 4 Schematic diagram for Train 2

2.5 Wastewater Sampling Parameters Test Procedures

This section explains on the test procedures of sampling parameters of COD, MLSS and MLVSS, conducted throughout the study period.

2.5.1 Test Procedures for the Measurement of Chemical Oxygen Demand (COD)

2 mL of wastewater sample was pipetted and transferred into a COD vial containing potassium dichromate. The COD vial was then shaken via a touch mixer and causes exothermic reaction to occur in the vial. A blank sample was too prepared by conducting the procedures prior. The COD vial, together with a blank was then placed into the vial holder, in a preheated COD reactor at a temperature of 150 °C, for 2 h. After 2 h, the COD vials were allowed to cool in the reactor until the temperature dropped to 140 °C. At 140 °C, all

COD vials were inverted several times and further allowed the vials to sit in the reactor until the temperature of the reactor dropped to 90 °C. All COD vials were then transferred onto COD racks, allowing the COD vials to cool to room temperature. Measurements of COD were made by first selecting the program 435 COD HR or 435 COD LR from the spectrophotometer. The COD vial containing the blank sample was first cleaned using soft tissues and was then placed into the cell holder of the spectrophotometer. The reading was calibrated to 0 mg/L COD, by pressing the "zero" button. Once the spectrophotometer has been calibrated, the COD vial containing the wastewater was then cleaned and placed into the cell holder and the "read" button was pressed, which then displayed the reading of COD values in mg/L COD. All samples were shaken vigorously prior conducting the COD testing.

2.5.2 Test Procedures for the Measurement of Mixed Liquor Volatile Suspended Solids (MLVSS) and Mixed Liquor Suspended Solids (MLSS)

The glass fiber pads were pre-rinsed by allowing distilled water to pass through the filters via suction. All glass fiber pads were then placed onto separate aluminum pan using tweezers. The rinsed glass fiber pads with respective aluminum pans were then left in the drying oven at 105 °C for 24 h. After 24 h, the prepared glass fiber pads were allowed to cool in the desiccator for 15 min. After cooling, the weight of glass fiber pads together with the aluminum pan was measured via an analytic balance and the reading was recorded in milligrams. Prior conducting the measurement of MLSS and MLVSS of wastewater, a sample of 5 mL from

Table 1 Sampling parameters with respective APHA methods

Sampling parameters	APHA methods	Sampling points							
		Train 1					Train2		
		IT	A1T1	MT1	A2T1	ET1	IT	A1T2	ET2
COD	5220	✓		✓		✓	✓		✓
MLSS	2540 D		✓		✓			✓	
MLVSS	2540 E		✓		✓			✓	

the aeration tank, i.e., AITI, A2T1 and A1T2, was diluted at 1:100 in respective to conical flask. All conical flasks were then filled with distilled water up to the marked line and were shaken vigorously, to ensure the absence of settlement at the bottom of the flask.

Mixed Liquor Suspended Solids: By using tweezers, the glass fiber filters were placed on the TSS filter holder, followed by the TSS cup. A volume of 50 mL of wastewater was measured using a measuring cylinder, and the sample was poured into the TSS cup. The suction pump was on, allowing filtration of wastewater to occur. Both measuring cylinder and the TSS cup were rinsed with distilled water, at about three times to remove any biomass sticks on the walls of both apparatuses. Once the wastewater had been fully pumped out, the TSS cup was removed and the glass fiber filters containing the biomass were placed into the aluminum pan using a pair of tweezers. The glass fiber filters with the aluminum pan were then again placed into the drying oven at 105 °C for 1 h. The sample was then taken out of the drying oven and let cooled in the desiccator for 15 min. The weight of the glass fiber filters containing the biomass together with the aluminum pan was measured using an analytic balance, and the reading was recorded in milligrams. All samples were shaken vigorously before pouring onto the measuring cylinder.

Mixed Liquor Volatile Suspended Solids: The glass fiber filters with respective aluminum pan were then placed inside a 550 °C muffle furnace for at least 15 min. After 15 min, the glass fiber filters were then let cool in the desiccator for 15 min. After cooling, the glass fiber filters with respective aluminum pan were weighed via an analytical balance in milligrams.

3 Results and Discussions

3.1 Influent COD Removals Throughout the Study

Influent COD concentrations throughout the study were plotted against sampling days as in Fig. 5.

A dilution of 1:6 was made to the raw influent during acclimatization phase 1. Acclimatization phase 1 was carried out from Day 1 to Day 5, allowing the microbes in the reactors to adapt to the change in its new environment. From Day 6 to Day 10, no further dilution was made, allowing the microbes to further stabilize the organic matter. On Day 11, 1 mL of raw MEA was added into 20L influent to obtain 50 mg/L of MEA for the feed to the reactors in both trains. Throughout Day 11 to Day 19, influent COD concentrations stabilized to an average of 468 mg/L. A minimal impact was observed from the graph, as 50 mg/L of MEA was added into the influent. From Day 20 to Day 27, MEA

concentration in the influent was increased to 100 mg/L and was stabilized to an average of 585 mg/L. A slight increment on Day 25 was observed, which may be due to the addition of fresh raw wastewater samples. From Day 28 to Day 30, MEA concentration in the influent was increased to 500 mg/L. Addition of 500 mg/L of MEA increases influent COD concentrations to an average of 1210 mg/L. From Day 31 onwards, influent COD concentrations stabilized to an average of 1774 mg/L. The addition of 50 mg/L and 100 mg/L of MEA causes MEA to react with the raw influent, forming other compounds.

Auto-oxidation of MEA may have occurred in the influent tank. MEA is inhibitory to its own degradation over tested temperature within 15–35 °C with 25 °C being optimum (Lam et al. 1999). MEA biodegradation produces ethanol, ammonium and acetic acid as major breakdown products (Bradbeer, 1965; BUA, 1994; Jones and Turner, 1973; McVicker et al. 1997). Gottschalk (1985) added that acetic acid and ethanol may be broken down via methanogenesis or tricarboxylic acid cycle. Table 2 shows the average influent COD concentration throughout the study period. It was observed that influent COD increased with the addition of MEA concentrations.

3.2 Effluent COD Removals Throughout the Study

Effluent COD concentrations throughout the study were plotted against sampling days as in Fig. 6.

During the acclimatization phase 1, effluent COD concentrations varied for ET1, MT1 and ET2. During acclimatization phase 2, effluent COD concentrations varied and took 2–3 days to achieve an averaged effluent COD value of 38 mg/L, 57 mg/L and 39 mg/L for effluents from ET1, MT1 and ET2, respectively. From Day 10 onwards, it was observed that influent COD concentrations increased to an average of 468 mg/L, after the addition of 50 mg/L MEA. It was observed from Fig. 4, effluent COD concentrations for all reactors stabilized from Day 12 to an average of 29 mg/L, 51.4 mg/L and 18.6 mg/L for effluents from ET1, MT1 and ET2, respectively. From Day 20 to Day 27, addition of MEA at 100 mg/L increased influent COD concentrations to an average of 585 mg/L. Effluent COD concentrations for all reactors stabilized from Day 24 to average of 24.6 mg/L, 37.7 mg/L and 16.7 mg/L for effluents from ET1, MT1 and ET2, respectively. From Day 28 to Day 30, the concentration of MEA in the influent was strengthened to 500 mg/L. Addition of 500 mg/L MEA in the influent increased the influent COD concentrations to an average of 1210 mg/L, while effluent COD concentrations from ET1, MT1 and ET2 stabilized to an average of 68 mg/L, 115 mg/L and 61 mg/L, respectively. To
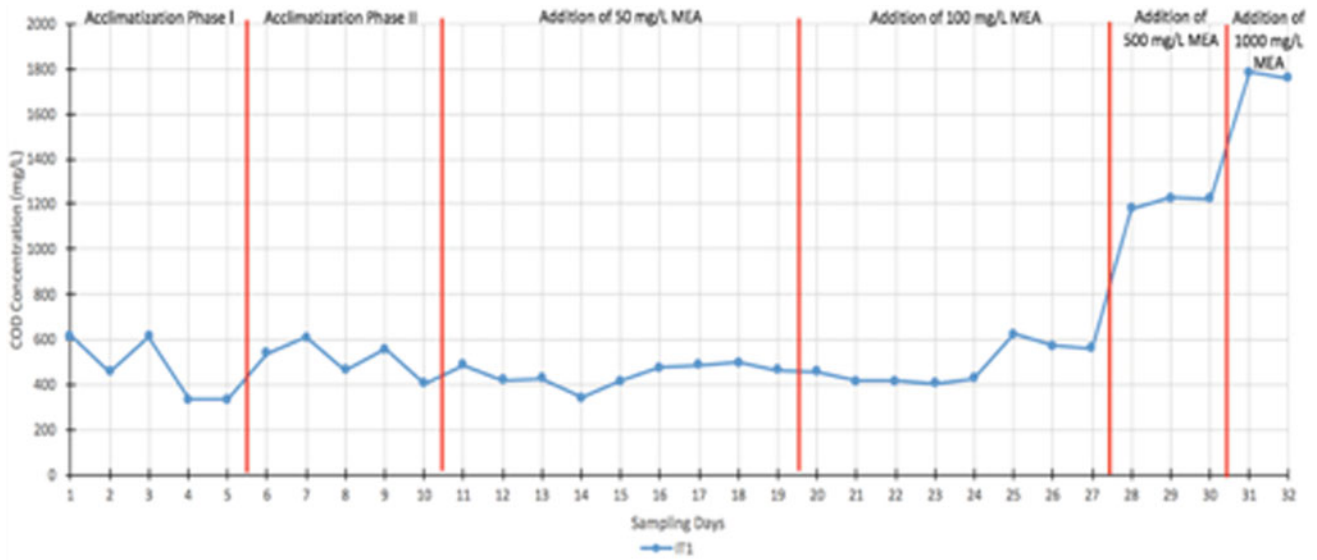
Fig. 5 COD influent versus sampling days

Table 2 MEA concentration versus average influent COD

MEA concentration (mg/L)	Average influent COD (mg/L)
50	468
100	585
500	1210
1000	1774

summarize, all effluent COD concentrations still meet the standard discharge limit of 120 mg/L. After the final addition of MEA concentration of 1000 mg/L, a spike on influent COD concentrations was observed, with an average of 1774 mg/L, while effluent COD concentrations stabilized to the average of 83.3 mg/L, 200 mg/L and 67.3 mg/L for effluents from ET1, MT1 and ET2, respectively. Effluent COD concentrations from ET1 and ET2 meet the standard discharge limit of 120 mg/L, while effluent COD concentrations of MT1 just meet the standard discharge limit of 200 mg/L. Table 3 displays the average effluent COD concentration and the average COD removals, in respective to MEA concentration throughout the study.

From Table 3, it was observed that average COD removals percentage for reactor A1T1 slightly reduced with increasing addition of MEA concentration, and vice versa for that in A2T1. The maximum COD removal rate takes approximately 30 h for partially degraded MEA while pure MEA takes 50 h (Harimurti et al. 2009).
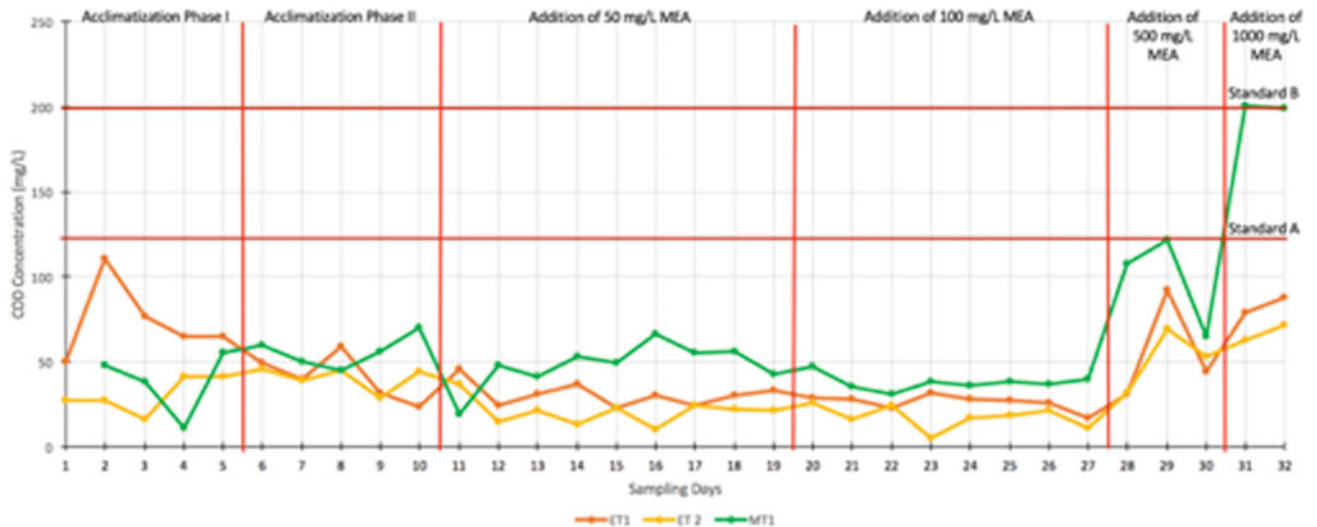
Fig. 6 COD effluent versus sampling days

Table 3 MEA concentration and average effluent COD/COD removals throughout the study

MEA concentration (mg/L)	Average effluent COD (mg/L)			Average COD removals (%)		
	ET1	MT1	ET2	A1T1	A2T1	A1T2
50	29	51.4	18.6	89.0	43.6	96.0
100	24.6	37.7	16.7	93.5	34.7	97.1
500	68	115	61	90.5	40.9	95.0
1000	83.3	200	67.3	88.7	58.4	96.2

3.3 MLSS-MLVSS Concentrations and Ratios in All Reactors Throughout the Study

Figures 7, 8 and 9 display the MLSS and MLVSS concentrations results with respective MLSS/MLVSS ratio for reactor A1T1, A2T1 and A1T2, respectively.

It was observed that MLSS and MLVSS concentrations in reactor A1T1 remained steady throughout the various phases, with MLVSS/MLSS ratio averaged at 0.78. As MEA concentration increased to 500 mg/L, MLVSS concentration dropped to 978 mg/L, indicating that the toxicity of MEA is impacting the microbes.

MLSS and MLVSS concentration in reactor A2T1 throughout the various phases with a ratio averaged at 0.83.

Decreasing trend was observed throughout the study, which may be due to the toxic impact of MEA on the biomass. Toxicity of MEA waste is minimized due to the degradation of MEA waste by microbes (Repečkienė et al. 2010). The MLVSS/MLSS ratio was 0.84 on average. The averaged MLSS and MLVSS concentrations throughout the study was given in Table 4.

3.4 COD Removals in mg COD Removed/mg MLVSS.day in All Reactors Throughout the Study

The organic removal rate in terms of COD, mg COD removed/mg mlvss.day was evaluated for all reactors in both trains. The COD removal rate was computed using the formula:

$$\text{COD removal rate} = \frac{(\text{influent COD} - \text{effluent COD}) \times \text{flowrate}}{\text{mg mlvss/day} \times \text{volume of reactor}}$$
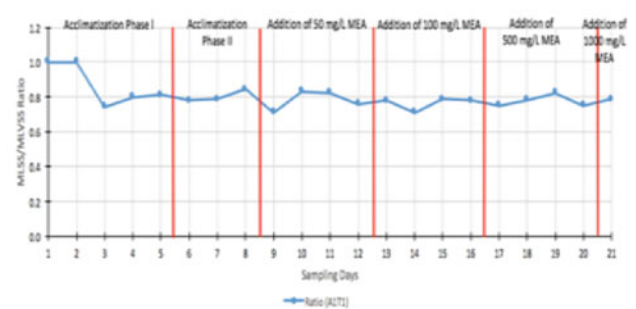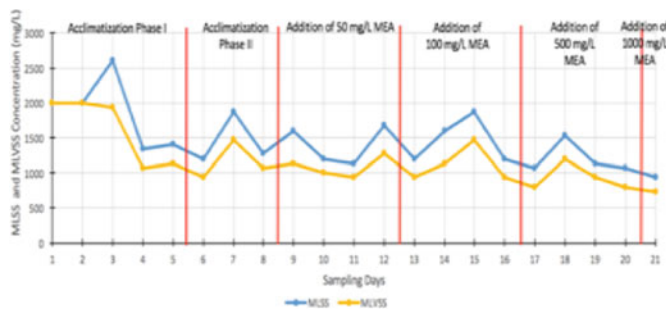
Fig. 7 MLSS-MLVSS concentration and ratios versus sampling days for A1T1
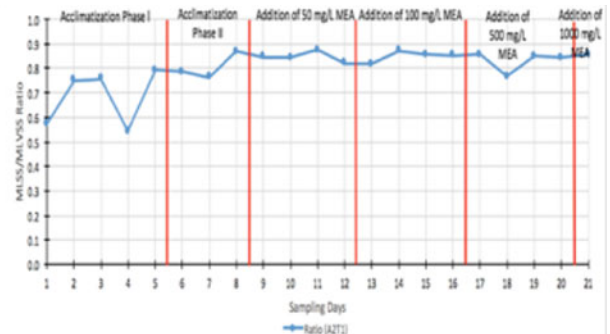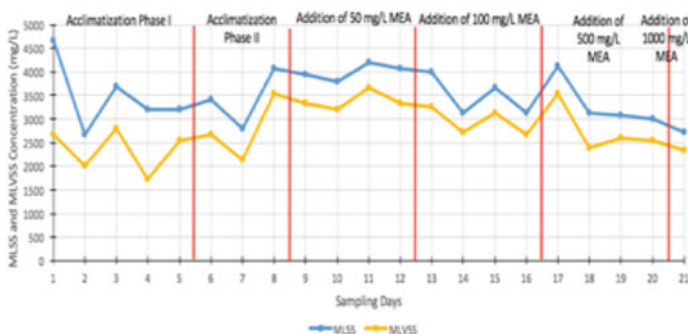
Fig. 8 MLSS-MLVSS concentration and ratios versus sampling days for A2T1
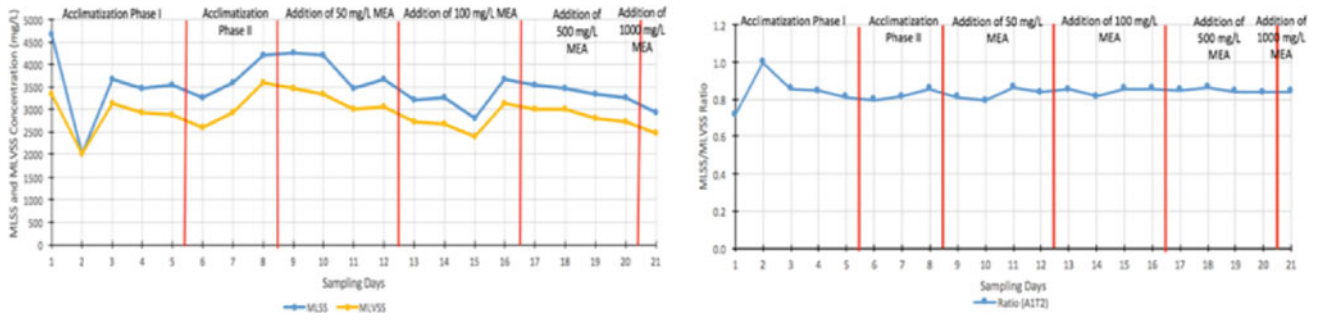
Fig. 9 MLSS-MLVSS concentration and ratios versus sampling days for A1T2

Table 4 MEA concentration versus averaged MLSS-MLVSS concentration

MEA concentration (mg/L)	Average influent COD (mg/L)					
	A1T1		A2T1		A1T2	
	MLSS	MLVSS	MLSS	MLVSS	MLSS	MLVSS
Acclimatization phase II	1567	1267			3089	2600
50	1311	1022	4000	3383	3978	3217
100	1556	1178	3311	2844	3089	2600
500	1244	978	3067	2511	3400	2883

where

Q = Flow rate of the aeration tank = 10 L/d

X = MLVSS concentration in the aeration tank (mg/L)

V = Volume of the aeration tank (10.6 L).

The results for COD removal rate day for all the reactors throughout the sampling days for Train 1 were plotted in Figs. 10 and 11 while the results for COD removal rate for all the reactors throughout the sampling days for Train 2 were plotted in Fig. 11.

It was observed that COD removal rate stabilized throughout the phases at an average of 35.22 mg COD removed/mg mlvss.day, even with the addition of 100 mg/L

MEA. However, from Day 18 onwards, COD removal rate continues to increase to an average of 160.19 mg COD removed/mg mlvss.day.

Throughout acclimatization phases, COD removal rate was insignificant, which may be due to insufficient amount of food for the microbes, as the influent was diluted. However, when the feed was given at full strength, an increased COD removal rate was observed. From Day 9 to Day 12, COD removal rate stabilized at 0.66 mg COD removed/mg mlvss.day. From Day 13 to Day 15, COD removal rate stabilized at 0.28 mg COD removed/mg mlvss.day. A decreasing trend of COD removal rate was observed from Day
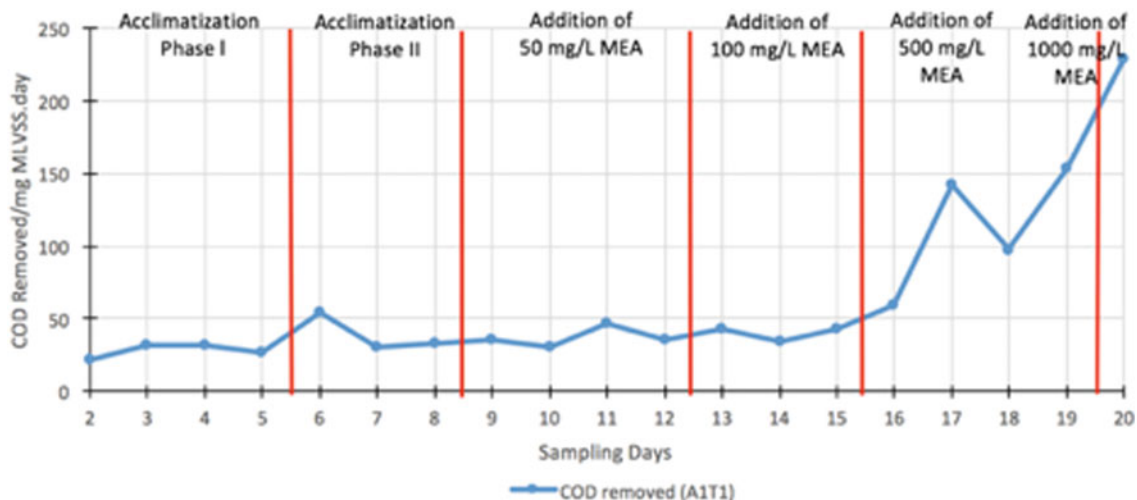
Fig. 10 COD removal rate for A1T1 versus sampling days
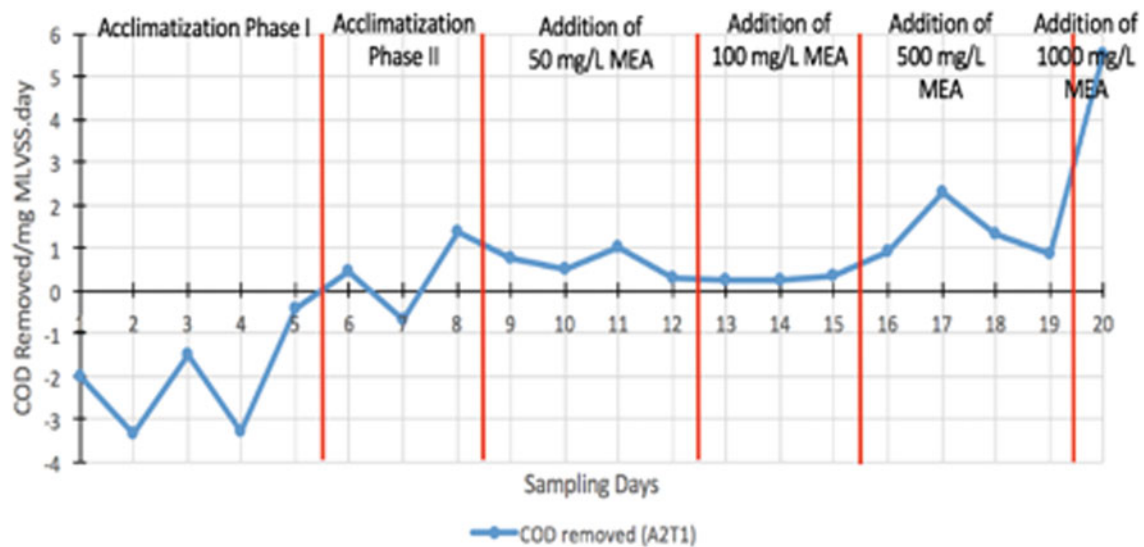
Fig. 11 COD removal rate for A2T1 versus sampling days

17 to Day 19 at an average of 1.51 mg COD removed/mg mlvss.day, after the addition of 500 mg/L MEA. This shows there is an impact of the increased MEA concentration on the COD removal rate for A2T1. A spike of COD removal rate was observed at a value of 5.54 mg COD removed/mg mlvss.day after the final addition of MEA concentration.

During acclimatization phase 1, COD removal rate stabilized at an averaged value of 16.12 mg COD removed/mg mlvss.day, from Day 2 onwards. During acclimatization phase 2, COD removal rate stabilized to an average of 15.24 mg COD removed/mg mlvss.day. From Day 11 to Day 14, the COD removal rate averaged at 15.76 mg COD removed/mg mlvss.day. Addition of 500 mg/L of MEA concentration stabilized COD removal rate from Day 17 to Day 19 to an average concentration of 42.3 mg COD removed/mg mlvss.day. Table 5 display the average COD removal rate in all reactors throughout the study.

3.5 Sludge Volume Index (SVI) Versus Sampling Days Throughout the Study

Jin, Lant and Wilen (2003) stated that SVI values of 50 mL/g to 150 mL/g may result in good sludge settleability; as in this range, filamentous bacteria may develop in low to moderate quantities. Figure 13 shows the SVI for reactors A1T1, A2T1 and A1T2 throughout the various phases.

SVI for reactors A1T1, A2T1 and A1T2 stabilized from Day 6 to Day 15, at an average of 61.2 mL/g, 67.4 mL/g and 68.1 mL/g, respectively. The best SVI values were reported at an average of 63.8 mL/g, presumably due to lower biomass concentration settling in the bioreactor system (Tsang et al. 2007). An increment was observed at Day 15 and

stabilized from Day 16 to Day 20 at an averaged SVI of 77 mL/g, 80 mL/g and 72 mL/g, for reactors A1T1, A2T1 and A1T2, respectively. A spike was observed at Day 21 for reactors A1T1, A2T1 and A1T2 after the addition of 1000 mg/L of MEA concentration, at 91 mL/g, 90 mL/g and 95 mL/g, respectively. SVI value increases, which may be due to the aging of filamentous bacteria with the increase of MLSS concentration (Alattabi et al. 2019). However, Dick and Vesilind (1969) declared that there is inconsistent connection between suspended solids concentrations with SVI, as SVI tends to remain constant as concentration increases up to a certain point. SVI continues to increase until it reaches a plateau, at which point SVI begins to drop as solids concentrations rise (Bye and Dold 1998). Sezgin (1982) observed a rise in SVI as filamentous length increased in the activated sludge treatment system. Although the presence of filamentous bacteria in the ASP is desirable, an overabundance may result to sludge settling issues (Chen et al. 2003). From Table 6, SVI remained steady with increased addition of MEA throughout the study period.

3.6 Sludge Age (Θ) Versus Sampling Days Throughout the Study

Sludge age (θ) for reactor A1T1, A2T1 and A1T2 was plotted throughout the various phases in Fig. 14.

Sludge age (θ) for all reactors was maintained throughout the study period. Reactors A1T1 and A1T2 were operated at extended aeration with the sludge age at approximately 5.2 days and 30.2 days, respectively, with a maintained MLSS of 4000 mg/L. However, reactor A2T1 was operated at conventional activated sludge system with the sludge age
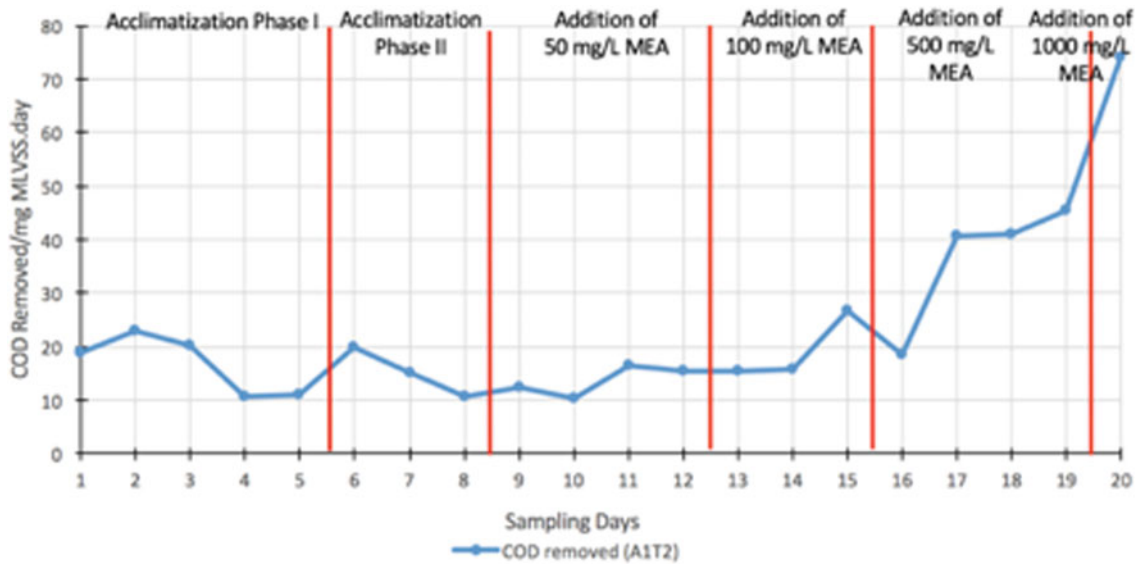
Fig. 12 COD removal rate for A1T2 versus sampling days

Table 5 MEA concentration versus average COD removal rate

MEA concentration (mg/L)	Average COD removal rate (mg COD removed/mg mlvss.day)		
	A1T1	A2T1	A1T2
Acclimatization phase II	39.20		15.24
50	36.78	0.66	13.65
100	39.82	0.28	19.34
500	125.61	1.51	42.30
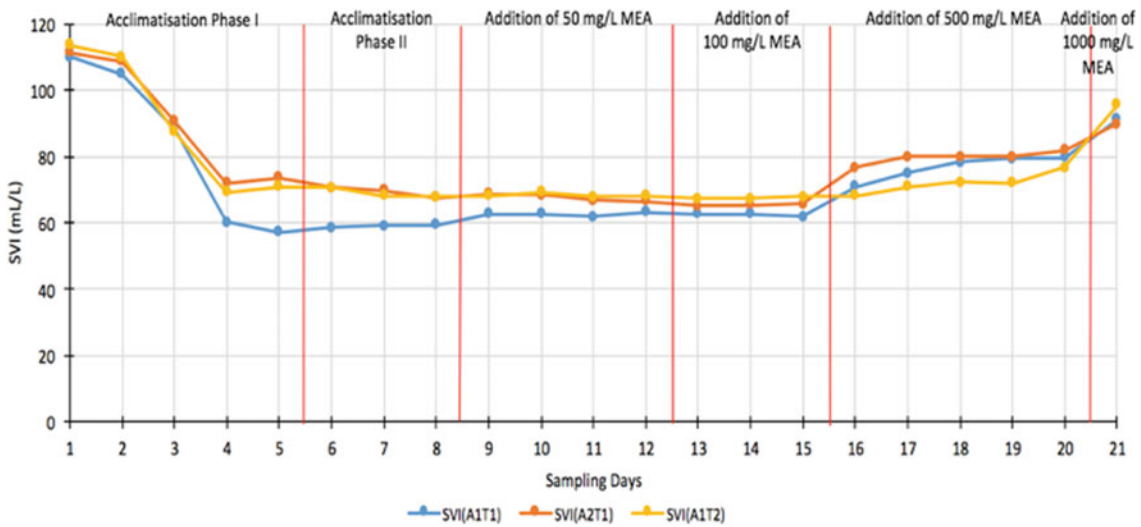
Fig. 13 SVI versus sampling days

maintained at approximately 42.3 days, with a maintained MLSS of 1500 mg/L. In another study conducted by Orhon et al. (2009), the biodegradation of peptone had an initial VSS concentration of 1865 mg/L with a sludge age of 10 days. It was discovered that after 4 h, peptone COD is decreased to a minimal level (initial COD = 564 mg/L) with a slow steady increment to a conclusive concentration of 35 mg/L, demonstrating sequential change of the

Table 6 MEA concentration versus averaged SVI

MEA concentration (mg/L)	Averaged SVI (mg/L)		
	A1T1	A2T1	A1T2
Acclimatization Phase II	59	70	69
50	62	68	68
100	62	65	67
500	77	80	72
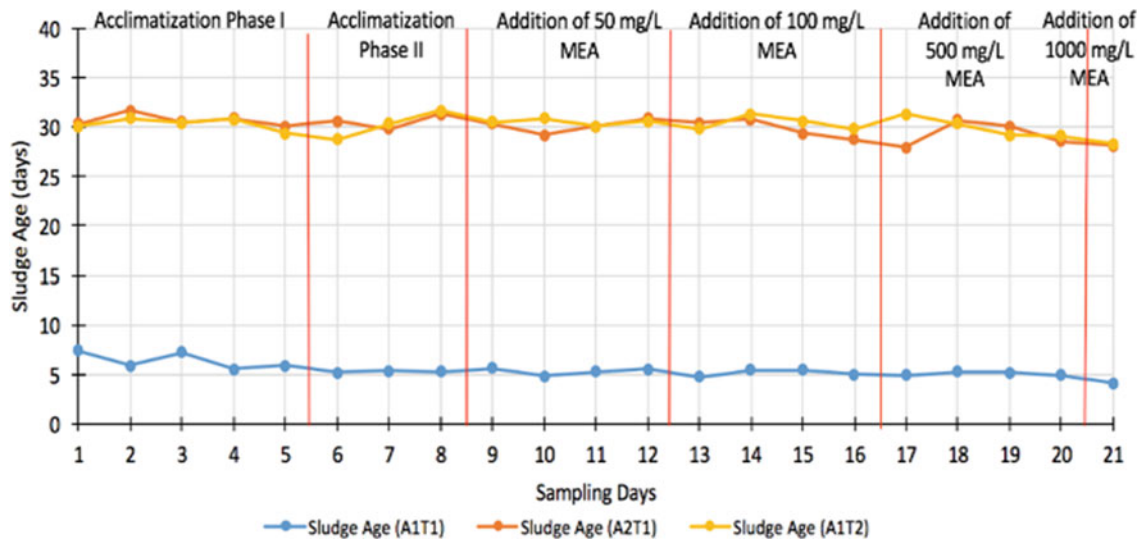
Fig. 14 Sludge age (θ) versus sampling days

Table 7 MEA concentration versus average of sludge age (θ)

MEA concentration (mg/L)	Average of sludge age (θ)		
	A1T1	A2T1	A1T2
Acclimatization Phase II	5.3	30.5	30.2
50	5.3	30.1	30.5
100	5.3	29.6	30.6
500	5.1	29.2	29.9
1000	5.1	29.8	29.5

biodegradation rate (Orhon et al. 2009). Table 7 shows the average sludge age throughout the study period.

3.7 Specific Oxygen Uptake Rate (SOUR) Versus Sampling Days Throughout the Study

The oxygen consumption rate (SOUR) is defined as the milligram of oxygen consumed per gram of volatile suspended solids (VSS) per hour. Figure 15 shows the SOUR for reactors A1T1, A2T1 and A1T2 throughout the various phases.

During acclimatization phase 1, initially the SOUR values for the reactors A1T1, A2T1 and A1T2 averaged at approximately 11.9 mg O_2/gVSS.h, 4.81 mg O_2/gVSS.h and 3.7 mg O_2/gVSS.h, respectively, toward the end of the phase. During acclimatization phase 2, SOUR values for reactors A1T1, A2T1 and A1T2 reactor averaged approximately at 12.1 mg O_2/gVSS.h, 4.6 mg O_2/gVSS.h and 3.4 mg O_2/gVSS.h, respectively. However, it can be observed that from Day 9 to Day 20, there was a gradual decreasing trend of SOUR values observed in reactors A2T1 and A1T2, with average of 1.54 mg O_2/gVSS.h and 1.74 mg O_2/gVSS.h, respectively. SOUR value in reactor A1T1 was observed to decrease significantly from Day 8 onwards with the addition of MEA. This shows that the respiration rate decreased for all reactors with increased addition of MEA. The oxygen uptake test is also useful in detecting toxicity. When toxins are present, it will depress the oxygen uptake rate and SOUR can be used to screen wastewater for toxicity. However, the toxicity of MEA has not reached its inhibitory concentration to the microbes. Amine is not inhibitory to degradation, even at high concentrations of amine at 2000 mg/L, however, amine can be degraded at neutral pH (Li 2008). The change in SOUR rate and SOUR is caused by an increase activity of microorganism in the
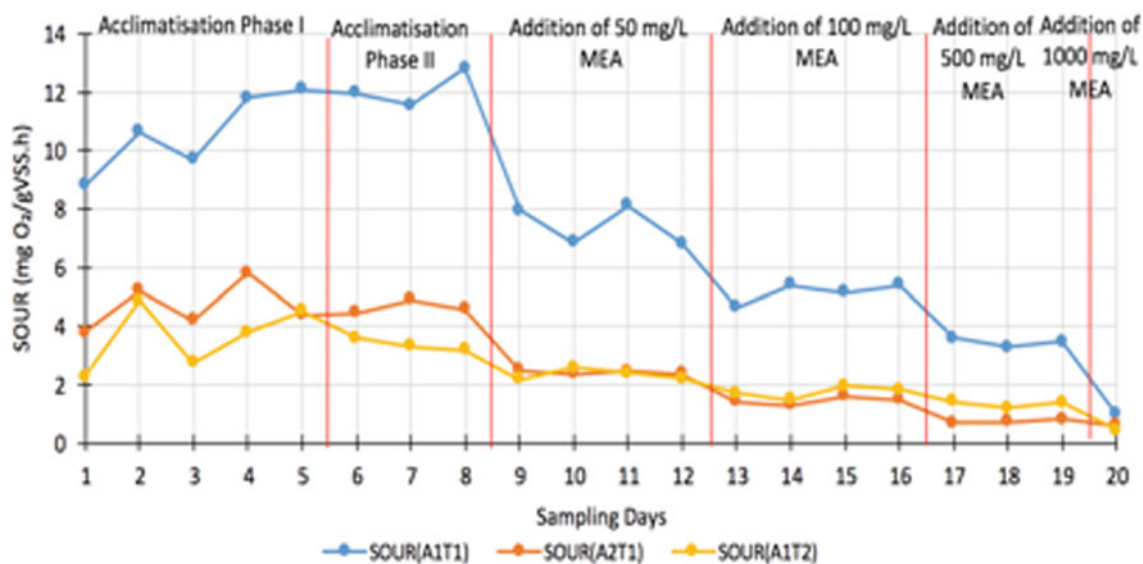
Fig. 15 SOUR versus sampling days

Table 8 MEA concentration versus average SOUR

MEA concentration (mg/L)	Average SOUR (mg O_2/gVSS.h.)		
	A1T1	A2T1	A1T2
Acclimatization Phase II	12	4.6	3.4
50	7.4	2.4	2.4
100	5.1	1.5	1.7
500	3.5	0.8	1.3

aeration system (Edwards and Sherrard 1982). In comparison with anaerobic digestion, SOUR increased as sludge recycling increased in aeration (Chen et al. 2003). According to Khursheed et al. (2015), a high SOUR rate is caused by a high activity of food oxidation. High level of SOUR might be caused by high energy demand imposed by anaerobic treatment. Table 8 displays MEA concentration against SOUR average throughout the study period.

4 Summary of the Study

The following are the summary of the research conducted:

1. The presence of MEA in all the effluent samples was not detected throughout the study period. From the study, it was concluded that MEA was degraded by the microbes in the reactor to other compounds.
2. Addition of MEA generally increased the COD in the influent, as MEA is an organic compound that consists of NH^- and OH^- which contribute toward organic nitrogen. Addition of MEA concentration also slightly reduced the average COD removals in both trains, yet, the average

COD removed/mg mlvss.day increased throughout the study in both trains.

3. Overall, effluents from both trains met the standard discharged limits although the addition of 500 mg/L MEA was made into the influent. This explains that MEA concentration has not reached inhibitory concentration levels for the microbes. Amine is not inhibitory to degradation, even at high concentrations of 2000 mg/L; however, at neutral pH, amine can be broken down (Li 2008). It was highlighted in a study that the microbes will be impacted by MEA at concentrations above 1600 mg/L. Increasing MEA concentration throughout the study increased the organics formed with reaction with MEA.
4. Overall, it was observed that SVI in all reactors has good sludge settleability. Also, sludge age in all reactors was maintained to respective sludge age and MLSS concentrations, throughout the study period.
5. Increasing MEA concentration throughout the study increased the organics formed with reaction with MEA. It was observed that with the addition of MEA, SOUR declined throughout the study period, for all reactors in both trains. This may be due to the inactivity of

microorganisms in the reactor. In Train 1, SOUR was observed to be the highest in the first reactor, A1T1, and lower toward reactor A2T1.

5 Conclusion

From the study conducted, it was concluded that the addition of MEA concentrations into the raw influents slows down the removal rate of organic compounds in the activated sludge treatment system, in the removal of contaminants. The loading of MEA concentration which inhibits the development of microbes was yet to be determined due to insufficient raw influent; hence, it is recommended that the addition of MEA concentrations above 500 mg/L in the reactors to be further evaluated. Increasing MEA concentration in the feed slightly reduced the average COD removals in both trains. However, the average COD removed/mg mlvss.day increased throughout the study for both trains. Overall, it was observed that SVI in all reactors has good sludge settleability. Increasing MEA concentration throughout the study period causes a decline in the SOUR, for all of the reactors in both trains. Overall, Train 1 performed slightly better as the impact of MEA was absorbed in the first reactor; A1T1, in comparison with Train 2.

References

A.W. Alattabi, C.B. Harris, R.M. Alkhaddar, M. Ortoneda-Pedrola, A. T. Alzeyadi, An investigation into the effect of MLSS on the effluent quality and sludge settleability in an aerobic-anoxic sequencing batch reactor (AASBR). J. Water Process Eng. **30**, 100479 (2019)

C. Bradbeer, The Clostridial Fermentation of Choline and Ethanolamine I. J. Biol. Chem. **240**, 4669–4674 (1965)

BUA, Beratergremium fuer Umweltrelevante Altstoffe, Ethylene glycol, S.Hirzel Wissenschaftliche Verlagsgesellschaft Stuttgart, Germany (1994)

C.M. Bye, P.L. Dold, Sludge volume index settleability measures: effect of solids characteristics and test parameters. Water Environ. Res. **70**(1), 87–93 (1998)

G.H. Chen, K.J. An, S. Saby, E. Broi, M. Djafer, Possible cause of excess sludge reduction in an oxic-settling anaerobic activated sludge process (OSA process). Water Res. **37**(16), 3855–3866 (2003)

R.I. Dick, P.A. Vesilind, The sludge volume index: what is it? J. Water Pollut. Control Fed. **41**(7), 1285–1291 (1969)

G.L. Edwards, J.H. Sherrard, Measurement and validity of oxygen uptake as an activated sludge process control parameter. J. Water Pollut. Control Fed. **54**(12) (1982)

M.H. Gerardi, Settleability problems and loss of solids in the activated sludge process, in *Wastewater Microbiology* (John Wiley and Sons, New Jersey USA, 2002)

G. Gottschalk, *Bacterial Metabolism*, 2nd edn. (Springer, Berlin, Germany, 1985)

S. Harimurti, B.K. Dutta, I.F.B.M. Ariff, S. Chakrabarti, D. Vione, Degradation of monoethanolamine in aqueous solution by Fenton's reagent with biological post-treatment. Water Air Soil Pollut. **211** (1–4), 273–286 (2009)

B. Jin, B.M. Wilén, P. Lant, A comprehensive insight into floc characteristics and their impact on compressibility and settleability of activated sludge. Chem. Eng. J. **95**(1–3), 221–234 (2003)

A. Jones, J.M. Turner, Microbial metabolism of amino alcohols, Biochem. J. **134**, 167–182 (1973)

C.W. Jones, *Applications of hydrogen peroxide and derivatives* (Royal Society of Chemistry, 2007)

A. Khursheed, M.K. Sharma, V.K. Tyagi, A.A. Khan, A.A. Kazmi, Specific oxygen uptake rate gradient—another possible cause of excess sludge reduction in oxic-settling-anaerobic (OSA) process. Chem. Eng. J. **281**, 613–622 (2015)

Y. Lam, R.M. Cowan, P.F. Strom, *The Treatability of Monoethanolamine (MEA) in Nitrifying Activated Sludge*, ed. by N. Nikolaidis, C. Erkey, B.F. Smets (1999)

Y. Li, *Biodegradation of waste amines under anaerobic, micro-aerobic and aerobic conditions* (Høgskolen i Telemark, 2008)

L. McVicker, D. Duffy, V. Stout, Microbial growth in a steady-state model of ethylene glycol-contaminated soil. Curr. Microbiol. **36**, 137–147 (1997)

D. Orhon, E.U. Cokgor, G. Insel, O. Karahan, T. Katipoglu, Validity of monod kinetics at different sludge ages—peptone biodegradation under aerobic conditions. Biores. Technol. **100**(23), 5678–5686 (2009)

J. Repečkienė, D. Pečiulytė, A. Paškevičius, O. Salina, K. Jankevičius, R. Liužinas, Microbiological reduction of monoethanolamine waste toxicity. J. Environ. Eng. Landsc. Manag. **19**(4), 287–295 (2010)

M. Sezgin, Variation of sludge volume index with activated sludge characteristics. Water Res. **16**(1) (1982)

Y.F. Tsang, F.L. Hua, H. Chua, S.N. Sin, Y.J. Wang, Optimization of biological treatment of paper mill effluent in a sequencing batch reactor. Biochem. Eng. J. **34**(3), 193–199 (2007)

Analysis of Garment Manufacturing Process: A Case Study (SUR Military and Civil Clothing Factory)

Tsneem Abbas and Mahmoud Hassan Onsa

Abstract

Textile industry was one of the strongest and supportive industrial sectors of economy in Sudan in the last century, but it has started to collapse in the beginning of this century, and as main derivative of textile industry there is garment industry, it can add big value to the country, and also it is an industry that is very weak in Sudan. The sustainability of garment industry depends on the productivity, that needs to monitor, analysis and improvement, therefore, the main objective of this paper is to stimulate and sustain the garment manufacturing in Sudan and as second objective is analyzing the production line of SUR Military and civil clothing factory, this paper reveals, the process of garment manufacturing and the time that it takes, the analysis is done by critical path method (CPM), based on SUR Military and civil clothing factory as case study, analyze its performance to propose an improvement based on this analysis made. The data has been collected from the case factory, through direct observation and questionnaire, of the personnel and workers. The study decelerated the importance of the production and process analysis that aids the companies or even small enterprises to improve their productivity, efficiency and optimize the time management.

Keywords

Production line process • Critical path method • Time study • Cost • Improvement

1 Introduction

One of the most important industries in the world is textile industry, it was considered one of the strongest industrial sectors and supportive of economy in Sudan since the fifties of the last century because of its significant contribution to the gross national income, there was 16 textile plant, their productivity was more than "168 million yard" per year.

Beside its contribution in national economy with added value to raw cotton it accommodated 30 thousand of labor. In the beginning of this century, this industry start to collapse and 13 factory has stopped and the productivity retreated from "168 million yard" in the last century to less than "8 million yard" in the start of this decade, on the other hand, the country's consumption of textile products increased from less than 50 million meters to more than 400 million meters (Ahmed 2016).

This sector needs rehabilitation to return to its strongest era. Textile industry involves spinning, weaving, dyeing and finishing. It attached to cotton agriculture, wool production and other textile fibers as inputs for this industry.

As a significant and main derivative of textile industry is garment industry, the garment manufacturing can add a big value to this country, beside its contribution in national income it also provides opportunities of employment.

By and large, numerous nations started their process of industrialization by focusing on labor intensive industries typically the textile industry. This industry was at the bleeding edge of ventures driving the Industrial Revolution in the United Kingdom from the mid-eighteenth to the mid-nineteenth hundreds of years. Japan is another country that took advantage of the work escalated nature of the material business to advance industrialization and the assimilation of the country's plentiful work (Fukunishi 2014).

In spite of importance of this industry and resources of our country, there is no focus on it from government or investor, also the garment industry is too poorly in our

T. Abbas (✉) · M. H. Onsa
Faculty of Engineering, University of Khartoum, Khartoum, Sudan
e-mail: tasneemabass2212@gmail.com

country, the plants of garment do not exceed five plants at this time, there is no even research are done to this sector, so it needs to develop. This paper is based on SUR Military and civil clothing factory as a case study.

This study will decelerate the importance of the analysis for production and processes, that might be help companies or even small enterprises to improve their productivity and efficiency.

2 Case Study (SUR Military and Civil Clothing Factory)

SUR Military is the main speculation of Sur International Company in Khartoum to meet the uniform requirements of Sudan Army with a limit of 600,000-sets/year. With the new extra offices, which became functional in 2016, its ability expanded to 2,000,000 sets/year. SUR Military has arrived at creation capacity to fabricate every single military adornment and gear from the rucksack and parka to socks and cordon. SUR Military is currently fit for providing items to the military and police powers of different nations in Africa and Middle East. It additionally adds to Sudan's product income (SUR Company, https://surcompany.com) and recently they add civil clothing manufacturing to the factory and its name becomes SUR Military and civil clothing factory, the civil section is new, so it needs more study; so the paper focuses on it.

2.1 Critical Path Method CPM to General Process

Critical path method a technique used to predict total project duration with diagramming. It contains a series of activities that determine the earliest time by which the project can be completed. The longest path is the determiner of the completion date because it contains the critical tasks. CPM helps in improving future planning, facilitating more effective resources management and helps avoiding problems (Critical path method, https://asana.com/resources/critical-path-method).

2.2 Manufacturing Process in SUR Military and Civil Clothing Factory

2.2.1 Inspection
It is a process that reveals if there is any damage in the fabric with using "finished inspection and roll—open-width machine". The process takes (15–20) minutes for 100 m of the fabric that usually is placed in one roll. The workers put the roll on the machine and start to monitor the fabric and if

there is any damage the worker puts a mark on the damage place. The types of damage could be in weaving, dying or printing in the shape of knots or blots.

2.2.2 Fabric Spreading
The rolls of fabric that have been inspected at the first process will convert to layers at specific long according to the order, before the fabric spreading a paper is placed on the cutting table, so that machine can move without creating any problem in the lowest ply of the fabric the spreading done manually and automatically by using cutting room technology type machine bullmer, type "compact E 600-30" During the process of spreading the workers notice the marks of damages and cut them out, then prepare the layers to cutting process.

2.2.3 Cutting
To execute a marker paper or the design of the order they use CAD-CAM and Assyst bullmer program, firstly the design is done manually then it is converted to a computer design, the cutting is done by an automatic scissor that is linked by the network of Assyst program.

2.2.4 Numbering
Numbering of cut body parts is done by sticker machine, this machine gives every single part a number that starts with the size of order and end with the number of layer that the piece is cut from it, this technique makes the sewing process easier. Then, cut pieces of body parts are checked and faulty parts are replaced by undamaged parts in same position. Then, all parts from same ply/lot of fabric of a single piece are kept together in bundle form (it is called master bundle). The master bundle is shifted to the sewing floor.

2.2.5 Sewing
It is the largest section it contains different types of sewing machines, are distributed in different lines, every line has a specific task to complete it depends on the order type and its quantity.

2.2.6 Finishing
After assembling the parts together in sewing, they are conducted to inspect for quality purpose then ironing and packing (Table 1).

In the process of fabric inspection the earliest start is 0 earliest finish time (EF) is 12 h, the shift is 8 h it needs to 1 day and 4 h to complete inspection of 4000 m that the order needs. Fabric spreading takes 4 h to 4000 m of fabric but there are two machines work at same time, therefore it needs two hours to complete the activity. Cutting needs to 4.5 h to complete, and it depends on activity B, after that Pieces go Direct to numbering process that takes 2 h, it depends on activities C. Then, to sewing process it takes

Table 1 The processes of SUR's production line to produce Jalabia Alalla

Task ID	Task	Duration (hours)	Dependency	Start		End	
				ES	LS	EF	LF
A	Inspection	12	–	–	–	11	12
B	Fabric spreading	4	A	11	12	15	16
C	Cutting	4.5	B	15	16	19.5	20.5
D	Numbering	2	C	19.5	20.5	21.5	22.5
E	Sewing	16	D	21.5	22.5	37.5	38.5
F	Finishing	2.5	E	37.5	38.5	40	41

16 h to product 1995 units of Jalabia, and it depends on activity E. The last activity is finishing, it takes 2.5 h, and it depends on activity F (Figs. 1 and 2).

3 Time Study for Sewing Process

According to the data above the production of 1995 units of Jalabia takes 41 h, and the factory operates one shift (8 h), thus the order will deliver at 5 days. The longest process is swing, therefore this paper conducted time study to it in more details (Figs. 3 and 4, Tables 2 and 3).

4 Results

4.1 Cycle Time

Cycle time is the time from pick up part of first piece to next pick up of the next piece. It had determined with stopwatch, five cycles were conducted for each operation, then the average was taken to those five cycles as standard time, the total cycle time for 28 operation equal summation of standard time over the number of operations.

$$\text{Cycle time} = \frac{\sum Xi}{N} \quad (1)$$

Cycle time for Jalabia = $\frac{21.8}{28}$ = 0.78 min.
Cycle time for trouser = $\frac{4.1}{8}$ = 0.51 min.

Duration of tasks to product 1995 unit of jalabia

■ Inspection ■ fabric spreading ■ cutting ■ numbering ■ sewing ■ finishing

7% | 31% | 5% | 11% | 5% | 41%
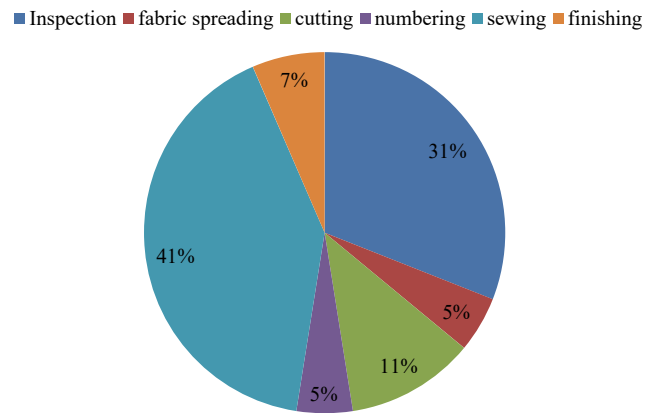
Fig. 2 The bottleneck in sewing process

4.2 Ideal Manpower

The ideal number of manpower can be calculated by the summation of standard time (CT Operator) over cycle time according to this equation:

$$\text{Ideal manpower (person)} = \frac{\sum CT \text{Operator}}{\text{cycletime}} \quad (2)$$

Ideal manpower for Jalabia = $\frac{21.8}{0.78}$ = 27.9 ~ 28 person.
Ideal manpower for trouser = $\frac{4.1}{0.51}$ = 8.03 ~ 8 person.

$$\text{Efficiency of manpower} = \frac{\text{ideal manpower}}{\text{actual allocation of manpower}} \quad (3)$$

Fig. 1 The critical path of the process

Fig. 3 The different between the actual time and standard time for Jalabia sewing process
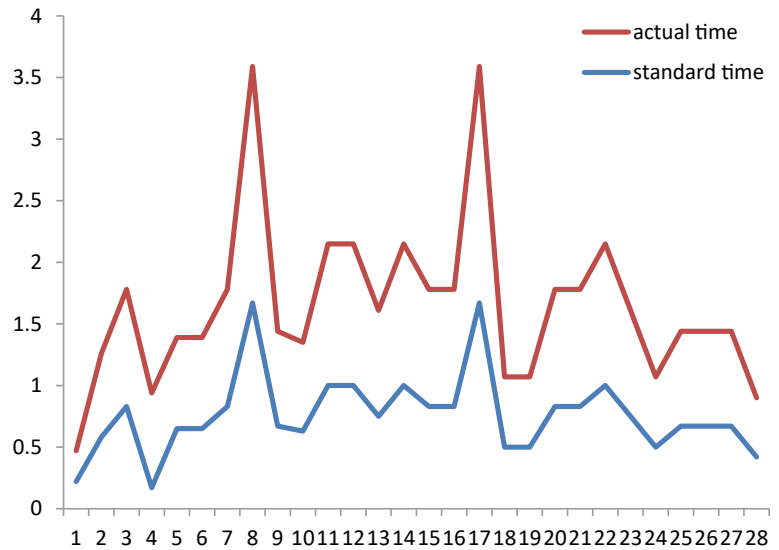
Fig. 4 The different between the actual time and standard time for trouser sewing process
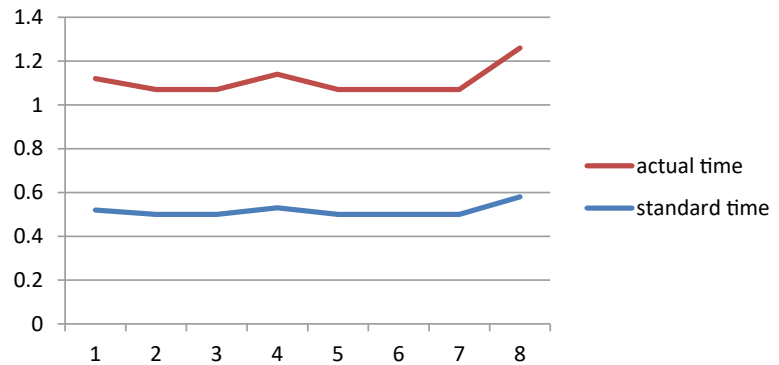
Efficiency of manpower (Jalabia) $= \frac{28}{44} = 63\%$

Efficiency of manpower $= \frac{8}{14} = 57\%$

4.3 Standard Minutes Value (SMV) and Standard Allowed Minutes (SAM)

Standard minutes value (SMV); it is a numerical value that represents the standard time of the operation in a standard work environment for qualified workers. With addition of machine allowance to those elements where machine is running and fatigue and personal needs to all elements (Ahmed et al. 2018).

$$SMV = \text{standard minutes value}$$
$$= (\text{average cycle time}) * (1 + \text{allowance}) * \text{rating} \tag{4}$$

SMV for Jalabia = 0.78 * (1 + 0.15) * 0.8 = 0.717 min.
SMV for trouser = 0.51 * (1 + 0.15) * 0.8 = 0.47 min.

Rating: is skill of operator which is observed during cycle time, it is given as 100%, 90%, 80%.

Standard allowed minutes (SAM), it is the standard operation time added to the allowance (personal allowance and company policy).

SAM = standard allowed minutes = (personal allowance + company policy) it is about 15% (Supriyadi 2019).

4.4 Production Capacity

The production capacity of a garment plant can be detected by machine (hr) capacity, line efficiency of that factory and SAM of produced item. And the accurate production capacity of a garment plant, is linked with accurate cutting room capacity, finishing room capacity.

$$\text{Production capacity} = \frac{\text{machine hour capicty} * 60 * \text{sewing line efficiency}}{\text{standard allowed minutes (SAM)}} \tag{5}$$

Table 2 The time study for Jalabia's sewing process

No	Process	Machine type	No of machine	No of person	Standard time	Actual time (SAM) = standard time + allowance (15%)
1	Hemming Chest Pocket	DDL 9000A-SH	1.0	1.0	0.22	0.25
2	Attach Chest Pocket	AP 875	1.0	1.0	0.58	0.68
3	Overlock	MO6904S	2.0	2.0	0.83	0.95
4	Joint Sides X 2	DDL 9000A-SH	2.0	2.0	0.67	0.77
5	Top Stitch Sides X 2	DDL 9000A-SH	2.0	2.0	0.65	0.74
6	Attach Side Pocket X 2	DDL 9000A-SH	2.0	2.0	0.65	0.74
7	Attach Stripe & Hemming Sleeve	DDL 9000A-SH	2.0	2.0	0.83	0.95
8	Attach Sleeve To Sides	DDL 9000A-SH	1.0	1.0	1.67	1.92
9	Over Lock Sleeve	MO6904S	1.0	1.0	0.67	0.77
10	Top Stitch Sleeve *2	DDL 9000A-SH	2.0	2.0	0.63	0.72
11	Attach Front Collar	DDL 9000A-SH	1.0	1.0	1.00	1.15
12	Attach Front Facing Right	DDL 9000A-SH	1.0	1.0	1.00	1.15
13	Attach Front Facing Left	DDL 9000A-SH	2.0	2.0	0.75	0.86
14	Attach Watch Pocket	DDL 9000A-SH	1.0	1.0	1.00	1.15
15	Attach Vertical Stripe To Back*3 Back	DDL 9000A-SH	2.0	2.0	0.83	0.95
16	Attach Horizontal Stripe To Back	DDL 9000A-SH	1.0	1.0	0.83	0.95
17	Attach Yoke To Back	DDL 9000A-SH	1.0	1.0	1.67	1.92
18	Joint Shoulder X 2	MO6904S	1.0	1.0	0.50	0.57
19	Top Stitch Shoulders + Attach Size Label	DDL 9000A-SH	1.0	1.0	0.50	0.57
20	Joint Sides/Front/Back	MO6904S	4.0	4.0	0.83	0.95
21	Top Stitch After Joint Sides	DDL 9000A-SH	3.0	3.0	0.83	0.95
22	Bottom Hemming	DDL 9000A-SH	1.0	1.0	1.00	1.15
23	Mark/Making Buttons Hole *3	LBH-1790	1.0	1.0	0.75	0.86
24	Attaching Buttons *3	LK-1903	1.0	1.0	0.50	0.57
25	Trimming/Fasting Buttons	TRIMMING TABLE	2.0	2.0	0.67	0.77
26	Pressing	Iron Veilt	2.0	2.0	0.67	0.77
27	Quality Control	QUALITY CONTROL TABLE	2.0	2.0	0.67	0.77
28	Packing	NEPO TAPLE	1.0	1.0	0.42	0.48
	Total		44	44	21.8	25.03

4.4.1 Machine Hour Capacity

Machines (hr) capacity of a garment factory can be detected by the number of sewing lines, sewing machines, and working hours per day (Production capacity in Garments Industry, https://garmentsmerchandising.com/how-to-estimate-production-capacity-of-a-garment-factory/).

Machine hour capacity = No. of sewing line in that factory × No. of machines in each sewing line × Working hours per day.

Machine hr for Jalabia = 1 * 28 * 8 = 224 h.

Machine hr for trouser = 1 * 8 * 8 = 64 h.

Table 3 Time study for trouser sewing process

No	Process	Machine	Person	Operation time (Min)	Actual Time (SAM) = Standard Time + Allowance (15%)
1	Close Front /Back /Attach Size Label	MO6904S	2	0.52	0.60
2	Hemming	DDL 9000A-SH	2	0.50	0.57
3	Inseam	DDL 9000A-SH	2	0.50	0.57
4	Attach Elastic	MO6904S	1	0.53	0.61
5	Top Stitch Elastic	DDL 9000A-SH	2	0.50	0.57
6	Trimming	TRIMMING TABLE	2	0.50	0.57
7	Pressing	Iron Veilt	2	0.50	0.57
8	Quality Control	Q-CONTROL TABLE	1	0.58	0.68
	Total		14	4.1	4.74

4.4.2 Line Efficiency

Line efficiency is a process utilized by industrial engineers to produce garments. It is usually done by estimating the efficiency of a line. It is equal output multiply by SMV over working minutes.

$$\text{Line efficiency} = \frac{\text{output} * \text{standard minutes value (SMV)}}{\text{working minutes}} * 100 \tag{6}$$

Line efficiency of Jalabia = $\frac{450*0.717}{8*60} * 100 = 67\%$

Line efficiency of trouser = $\frac{450*0.47}{8*60} * 100 = 44\%$

Then the production capacity will be as follow:

Production capacity for Jalabia = $\frac{224*60*0.67}{25.03} = 359.79$ ~ 360 piece per day.

Production capacity for trouser = $\frac{64*60*0.44}{4.74} = 356.4$ ~ 456 piece per day.

5 The Cost

The cost typically refers to the total cost of making product which includes the raw materials and other expenses, cost plays vital role in garment industry, so it needs to be considered (Table 4).

6 Discussion

SUR company cares about the quality standards which is good, but it needs to adjust the processes to meet those standards, the first problem is in inspection process, there is one machine to inspect fabric, so it takes 31% of the production time. To make the production process faster needs to bring more machines. In sewing process that take 41% of the production time; the time study decelerates that; the cycle time to produce one unit is 0.78 min for Jalabia and 0.47 min for trouser, the overall rating of manpower is 80%. The manpower utilization is 63% for Jalabia and 57% for trouser which are low the number of manpower is more than needed, the line efficiency for Jalabia is 67% and for trouser is 44%, the company needs to increase the efficiency by increase the SMV. And by increasing the line efficiency the production capacity will increase.

The total cost is 8,054,649 SDG and the revenue is 1,208,197 SDG, which is too low compared to total cost, if the company decrease 25% of manpower and increase the sales price to 30% the revenue will be 2,403,795 SDG.

7 Conclusion

This study decelerates many problems in the processes of production that need to fix, following there are some improvements that may be contributed in enhancing the productivity and increase the efficiency of line production.

Number of machines in inspection process need to be more than one. The plant has modern machines but their using is not efficient, thus the efficient use of those machines can increase the productivity to (20–30%). And definitely for best use systematic training will be required to manpower. The wages of manpower are too weak, so the company needs to increase the wages and link them with performance to make workers more motivated. Also to deliver the orders faster the company should add another shift. To gain better revenues the company needs to improve the efficiency of manpower utilization, and to increase the sales price to more than 25%.

Table 4 The total cost of Jalabia production

		Consumption	Unit price	Cost for one unit (SDG) = consumption * unit price
Fabric description	Plain 65% poly—35% cotton	4 MT	900	3600
Accessories description	100% poly thread	0.111 MT	243	26.97
	Elastic garter w:3 cm	0.45 MT	107	48.15
	Button 15 mm	2 MT	85	170
Packing	Packing carton 600 * 400 * 400	0.04 Pcs	1350	54
	Poliprapen circular strip	0.00016 kg	152	0.02
	Transparent packing tapew:4 cm	0.00036 roll	156	0.06
	Plastic bag 55 * 35 cm	1 Pcs	51	51
Total				3950.2

Total material cost for 1995 units = 1995 * 3950.2 = 7,880,649 SDG

Average labor cost = 3000 SDG
Total labor cost = 3000 * 58 = 174,000 SDG

Total cost = Total material cost + Total labor cost = 8,054,649 SDG
The sales price is 15%
The revenue = 8,054,649 * 0.15 = 1,208,197 SDG

References

H.A.M. Ahmed, Textile industry in Sudan, Sudan University of Science and Technology, Sudapedia (2016)

M. Ahmed, T. Islam, G. Kibria, *Estimation of the Standard Minute Value of Polo Shirt by Work Study* (2018)

Critical path method. https://asana.com/resources/critical-path-method

T. Fukunishi, T. Yamagata, *The Garment Industry in Low-Income Countries* (2014)

Production capacity in Garments Industry. https://garmentsmerchandising.com/how-to-estimate-production-capacity-of-a-garment-factory/

S. Supriyadi, *Analysis of Work Load and Total Operator Needs on Final Inspection of Work Station* (2019)

SUR Company. https://surcompany.com

2D Finite Element Simulation of Steady-State Groundwater Flow Using MATLAB

Marwa Suliman Omer and Abdelrahman ELzubier Mohamed

Abstract

In this paper, we try to obtain a numerical solution for finite element which is formulated for steady-state groundwater flow discretized by using triangular element grid. Then, a MATLAB program is deveoped for this purpose to get primarily the unknown potential function at the triangular elements nodes. The Simulation of Finite element Field problems MATLAB Program was developed and implemented, as a check and test of nodal potential value. The program SFFP was applied for solution of a two-dimensional porous medium problem, fluid flow problem, and body exposure to a heat source problem. In the meantime, results obtained when compared with published data, found very close with maximum percentage difference of 0.22%. Thus, SFFP was applied to groundwater flow beneath a coffer dam problem of known results as a case study; for verification, a comparison of the results was obtained with a maximum percentage difference of 1.32%. This verifies the accuracy of SFFP results.

1 Introduction

As stated by Hinton and Owen (1979) finite element field problem is the situation in which only one degree of freedom exists at each nodal point. In particular, the so-called quasi-harmonic equation which has wide applicability in many branches of engineering and physics is considered. In this way, a finite element program which is developed to solve the two-dimensional quasi-harmonic equation system can be employed to analyze several problems of engineering interest. According to Zienkiewicz et al. (2013) examples of field problems, such as heat conduction, groundwater potential, torsion of shafts, seepage, lubrication of bearings and irrotational fluid flow can be solved when using quasi-harmonic equation. As had been shown by Moaveni (2008) based on time, there are two modes of groundwater flow: steady-state and transient groundwater flow. As had been stated by Bathe (1996) the main characteristic of steady-state problem is that the system response does not change with time. As had been presented by Hinton and Owen (1979) and Wang and Anderson (1982) Galerkin's method and the finite element technique are so frequently combined in computer solution of groundwater flow programs that the two have become particularly synonymous. Galerkin's method is based on a particular principle of weighted residual which is determined directly by governing partial differential equation without need to the physical quantity resort.

Reilly (1984) developed a computer program to evaluate radial flows. Adeboye et al. (2013) presented 2D flow non-homogenous Laplace equation hydorolic conductivity and piezometric head. Kulkani (2018) developed a Eulerian–Lagrangian formulation using numerical models to evaluate groundwater pollution which considered as a challenge of obtaining precise and stable numerical solution. Igboekwe (2014) in his paper finite element method of modeling solute transmit in groundwater flow studied movement of water solute from the surface to aquifer using finite element analysis and reviewed of analytical methods and numerical methods (finite deference and finite element). Jansser and Hemker (2004) presented regional models for large or long-term projects, analytical and numerical models, restrictions of analytical models and advantages of

M. S. Omer (✉)
Roads, Bridges, and Drainage Corporation, Khartoum, Sudan
e-mail: marwasuliman27@gmail.com

A. E. Mohamed
Sudan University of Science and Technology, Khartoum, Sudan

numerical models, and advantages of finite elements with triangular grid. Rouhani (2007) presented a finite element numerical solution for groundwater models discretized by triangular element grid using an object-oriented approach. Kalantari et al. (2018) modeled Birjand aquifer in two dimensions by the isogeometric analysis using four-point Gauss integration method.

In this paper, a numerical solution for finite element is formulated for steady state groundwater flow evaluated by grid of triangular element. Then, a MATLAB program is deveoped for this purpose to get firstly the unknown potential function at the triangular elements nodes. The Simulation of Finite element Field problems MATLAB Program (SFFP) was developed and implemented, as a check and test of nodal potential value.

2 Methodology

In this part, all the indispensable numerical solution and theoretical expressions stages for solution of quasi-harmonic equation are presented. Then, these steps were coded, and the simulation of SFFP was developed and implemented.

The fluid flow through a soil in two dimensions is governed by the equation:

$$\frac{\partial}{\partial x}\left(k_x \frac{\partial \emptyset}{\partial x}\right) + \frac{\partial}{\partial y}\left(k_y \frac{\partial \emptyset}{\partial y}\right) + Q = 0 \qquad (1)$$

Present the biharmonic equation and its solution.
Where:
$\emptyset \equiv$ The potential function.
$k_x, k_y \equiv$ Permeability coefficients.
The boundary conditions (B.Cs):

(A) Specified at nodal point

$$\emptyset = \emptyset p \qquad (2a)$$

(B) Loading boundary

$$k_x \frac{\partial \emptyset}{\partial x} n_x + k_y \frac{\partial \emptyset}{\partial y} n_y + q + \alpha(\emptyset - \emptyset_a) = 0 \qquad (2b)$$

D.E

$$\frac{\partial}{\partial x}\left(k_x \frac{\partial \emptyset}{\partial x}\right) + \frac{\partial}{\partial y}\left(k_y \frac{\partial \emptyset}{\partial y}\right) + Q = 0$$

which is the quasi-harmonic equation with:

$$Q = S - \frac{dV}{dt}$$

$$\alpha = q = 0$$

and B.C^s. $\emptyset = \emptyset p = 0$.
$S \equiv$ Rate of fluid injection per unit volume.
$\frac{dV}{dt} \equiv$ Rate of volume change per unit volume.

The Galerkin's Method

Employing Galerkin's weighted residual process, assuming a solution $\emptyset$ results in residuals as:

$$e_A = \frac{\partial}{\partial x}\left(k_x \frac{\partial \emptyset}{\partial x}\right) + \frac{\partial}{\partial y}\left(k_y \frac{\partial \emptyset}{\partial y}\right) + Q \neq 0 \qquad (3a)$$

From the D.E.

$$e_B = k_x \frac{\partial \emptyset}{\partial x} n_x + k_y \frac{\partial \emptyset}{\partial y} n_y + q + \alpha(\emptyset - \emptyset_a) \neq 0 \qquad (3b)$$

From the B.C^s, the weighted residuals:
$\int_A e_A w_A dA + \int_{SB} e_B w_S dS = 0$

$$\int_A \left[\frac{\partial}{\partial x}\left(k_x \frac{\partial \emptyset}{\partial x}\right) + \frac{\partial}{\partial y}\left(k_y \frac{\partial \emptyset}{\partial y}\right) + Q\right] w_A dA$$
$$+ \int_{SB} \left[k_x \frac{\partial \emptyset}{\partial x} n_x + k_y \frac{\partial \emptyset}{\partial y} n_y + q + \alpha(\emptyset - \emptyset_a)\right] w_S dS = 0. \qquad (4)$$

Integrating each term by parts, choosing weight $w = w_A = w_S$, and arranging results in week integral form as:

$$-\int_A \left[\frac{\partial w}{\partial x} k_x \frac{\partial \emptyset}{\partial x} + \frac{\partial w}{\partial y} k_y \frac{\partial \emptyset}{\partial y} + wQ\right] dA$$
$$+ \int_{SA} \left[k_x \frac{\partial \emptyset}{\partial x} n_x + k_y \frac{\partial \emptyset}{\partial y} n_y\right] w dS - \int_{SB} [q + \alpha(\emptyset - \emptyset_a)] w dS = 0 \qquad (5)$$

Finite Element Representation of Weak Form

Approximately, the function $\emptyset$ and weight using shape function N_i for a finite element discretization with n nodes substituting in week form gives:

$$-\int_A \left[\left(\frac{\partial N_i}{\partial x} k_x \frac{\partial N_j}{\partial x} + \frac{\partial N_i}{\partial y} k_y \frac{\partial N_j}{\partial y}\right)\emptyset_j - N_i Q\right] dA + x_i$$
$$- \int_{SB} N_i \left[q - \alpha\emptyset_a + \alpha \sum_{j=1}^{n} N_j \emptyset_j\right] dS = 0 \qquad (6)$$

Rearranging gives:

$$\left[\int_A \sum_{j=1}^{n}\left(\frac{\partial N_i}{\partial x}k_x\frac{\partial N_j}{\partial x}+\frac{\partial N_i}{\partial y}k_y\frac{\partial N_j}{\partial y}\right)dA+\alpha\sum_{j=1}^{n}N_j\emptyset_j\right]\emptyset_j$$
$$=\int_A N_iQdA-\int_{SB}N_i[q-\alpha\emptyset_a+]dS+x_i \tag{7}$$

$$i,j \equiv \text{ from 1 to } n$$

In which:

$$x_i=\sum_{j=1}^{n}\int_{SB}\left[k_x\frac{\partial N_j}{\partial x}n_x+k_y\frac{\partial N_j}{\partial y}n_y\right]\emptyset_j N_i dS$$

That represents constrains (reactions).
Equation (7) can be written as:
OR:

$$\{k^e\}\{\emptyset^e\}=\{f^e\} \tag{8}$$

where:

The element stiffness matrix is:

$$\{k^e\}=\int_A\sum_{j=1}^{n}\left(\frac{\partial N_i}{\partial x}k_x\frac{\partial N_j}{\partial x}+\frac{\partial N_i}{\partial y}k_y\frac{\partial N_j}{\partial y}\right)dA+\alpha\sum_{j=1}^{n}N_j\emptyset_j \tag{9a}$$

The element nodal load vector is:

$$\{f^e\}=\int_A N_iQdA-\int_{SB}N_i[q-\alpha\emptyset_a+]dS+x_i \tag{9b}$$

Evaluation of the Triangular Element Properties

Finite element grid using simple triangular element (Fig. 1) is convenient to approximate arbitrary-shaped regions with small deviations. Based on Eq. (8), the triangular element is formulated as follows:
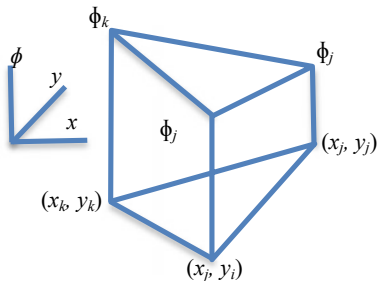
Fig. 1 Nodal values of the potential function for a triangular element

- The potential function within any point at triangle is given in terms of the shape functions and nodal potential values as follows:

$$\{\emptyset^e\}=\sum_{i=1}^{3}N_i\emptyset_i^e=\{N_1N_2N_3\}\{\emptyset_1^e\emptyset_2^e\emptyset_3^e\} \tag{10}$$

where the shape functions N_1, N_2 and N_3 are:

$$N_1=\frac{1}{2A}(a_1+b_1x+c_1y)$$
$$N_2=\frac{1}{2A}(a_2+b_2x+c_2y) \tag{11}$$
$$N_3=\frac{1}{2A}(a_3+b_3x+c_3y)$$

and A is the element area.

- The element stiffness matrix is then given from Eqs. (9a), (10), and (11) by:

$$\{k^e\}=\{k^e\}_I+\{k^e\}_{12}+\{k^e\}_{23}+\{k^e\}_{31} \tag{12}$$

In which:

$$\{k^e\}_I=\sum_{i=1}^{n}\sum_{j=1}^{n}\frac{1}{4A}(k_xb_ib_j+k_yc_ic_j)$$
$$=\frac{k_x}{4A}\{b_1b_1b_1b_2b_1b_3b_2b_1b_2b_2b_2b_3b_3b_1b_3b_2b_3b_3\}$$
$$+\frac{k_y}{4A}\{c_1c_1c_1c_2c_1c_3c_2c_1c_2c_2c_2c_3c_3c_1c_3c_2c_3c_3\} \tag{13}$$

and

$$\{k^e\}_{12}=\frac{\alpha S_{12}^e}{6}\{210120000\} \tag{14a}$$

$$\{k^e\}_{23}=\frac{\alpha S_{23}^e}{6}\{000021012\} \tag{14b}$$

$$\{k^e\}_{31}=\frac{\alpha S_{12}^e}{6}\{201000102\} \tag{14c}$$

- Element nodal load vector, neglecting x_i, is given from (9b) and (11) as:

$$\{f^e\}=\{f^e\}_Q+\{f^e\}_{c12}+\{f^e\}_{c23}+\{f^e\}_{c31} \tag{15}$$

where:

$$\{f^e\}_Q = \frac{QA}{3}\{111\} \tag{16a}$$

$$\{f^e\}_{c12} = -\frac{(q - \alpha\emptyset_a)S_{12}^e}{2}\{110\} \tag{16b}$$

$$\{f^e\}_{c23} = -\frac{(q - \alpha\emptyset_a)S_{23}^e}{2}\{011\} \tag{16c}$$

$$\{f^e\}_{c31} = -\frac{(q - \alpha\emptyset_a)S_{31}^e}{2}\{101\} \tag{16d}$$

Groundwater flow:

The fluid flow:

$$\frac{\partial}{\partial x}\left(k_x \frac{\partial h}{\partial x}\right) + \frac{\partial}{\partial y}\left(k_y \frac{\partial h}{\partial y}\right) + Q = 0 \tag{17}$$

$h \equiv$ Pressure head.

In case of steady-state groundwater flow:

$$Q = S - \frac{dV}{dt} \tag{18}$$

$$\alpha = q = 0$$

Based on the above formulation and B.Cs, an adopted modular process with a separate subroutine will be utilized to perform the main operation. These subroutines are then called in sequence by a main or master program.

3 Results

The program SFFP was applied for solution of a two-dimensional porous medium problem, fluid flow problem, and body exposure to a heat source problem. In the meantime, the results obtained were compared with published data as follows:

3.1 Case One: Two-Dimensional Porous Medium

Sandy soil region with two-dimensional shown in the adapted Fig. 2 (Logan 2007), it is required to measure the potential distribution. The tension (fluid head) on the left part is a constant equal to 10.0m, and that on the right part is 0.0. The upper and lower sides are impervious. The impervious are $k_{xx} = k_{yy} = 25 \times 10^{-5} \frac{m}{s}$. Unit thickness is assumed. The results obtained using SFFP are presented in

Fig. 2 Two-dimensional porous medium
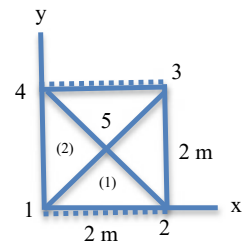
Table 1 and compared with solution presented by Logan (2007).

As can be seen from Table 1, the nodal potential obtained using SFFP completely agrees with the known published result with no difference.

3.2 Case Two: Two-Dimensional Fluid Flow Problem

The fluid flow problem shown discretized in Fig. 3—which is adapted from Logan (2007)—has the top and bottom parts impervious, whereas the right side has a constant head of 3cm and the left side has a constant head of 4cm. The nodal potential result obtained using SFFP is presented in Table 2 and compared with solution presented by Logan (2007).

The compression shows complete agreement between the two results.

As can be seen from Table 2, the result obtained using SFFP completely agrees with the known published result with no difference.

Table 1 Two-dimensional porous medium results

Node number	Nodal potential value(cm)		Difference %
	Logan (2007)	SFFP solution	
1	10.0000	10.0000	0.00
2	0.0000	0.0000	0.00
3	0.0000	0.0000	0.00
4	10.0000	10.0000	0.00
5	5.0000	5.0000	0.00
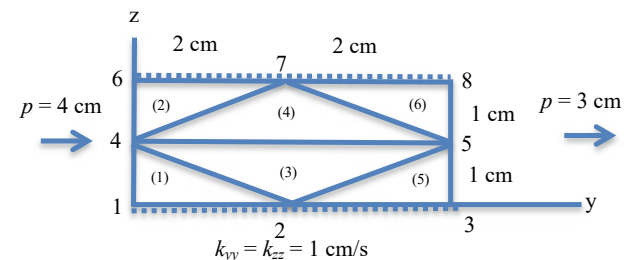
Fig. 3 Two-dimensional fluid flow problem

Table 2 Two-dimensional fluid flow problem results

Node number	Nodal potential values (cm)		Difference %
	Logan (2007)	SFFP solution	
1	4.0000	4.0000	0.00
2	3.5000	3.5000	0.00
3	3.0000	3.0000	0.00
4	4.0000	4.0000	0.00
5	3.0000	3.0000	0.00
6	4.0000	4.0000	0.00
7	3.5000	3.5000	0.00
8	3.0000	3.0000	0.00

Table 3 Body with two-dimensional exposure to a heat source results

Node number	Nodal temperature values (°C)		Difference %
	Logan (2007)	SFFP solution	
1	180.0000	180.0000	0.00
2	180.0000	180.0000	0.00
3	100.0000	100.0000	0.00
4	100.0000	100.0000	0.00
5	153.0000	153.3333	0.22

As can be seen from Table 3, the result obtained using SFFP closely agrees with the known published result with a maximum percentage difference of 0.22%.

Fig. 4 Two-dimensional body subjected to a heat source

3.3 Case Three: Body with Two-Dimensional Exposure to a Heat Source

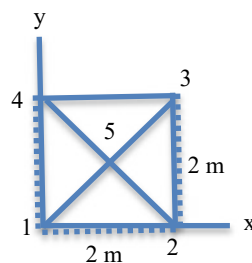For the body with two-dimensional shown in in the adapted Fig. 4 (Logan 2007), it is required to measure the distribution of temperature. The temperature of the upper part of the body is maintained at 100 °C. The body is isolated on the other sides. A uniform heat source of Q = 1000 $\frac{W}{m^3}$ acts over the whole plate, as shown in the figure. A constant thickness of 1 m is assumed. Let $k_{xx} = k_{yy}$ = 25 W/(m °C).

We need attention just for the left half of the body, because we have a vertical plane of the symmetry passing through the body 2 m from both the left and right portions. This vertical plane can be considered as isolated boundary. The finite element model is shown in the adapted Fig. 5 (Logan 2007). The results obtained using SFFP are presented in Table 3 and compared with solution presented by Logan (2007).

Fig. 5 Discretized body of Fig. 4

4 Discussion

This case study focused on the flow of groundwater beneath a coffer dam which had been solved by using a potential formulation as done by Hinton and Owen (1979). The geometry of the model is evident in Fig. 6 (Hinton and Owen 1979). It is supposed that boundary ABC is impervious (no leakage) as is the sheet pile wall EFG. The pressure head in this case is the difference in height between AG and DF which is 3 units. Arbitrarily setting $\emptyset = 0.0$ along DF, since the flow speeds depend only on the gradient of $\emptyset$, then $\emptyset = 3.0$ along AG. Along ABC and on either side of the sheet pile wall, it is required that $\frac{\partial \emptyset}{\partial n} = 0$ also symmetry conditions along CD require $\frac{\partial \emptyset}{\partial n} = 0$ on this part. These boundary conditions are shown in Fig. 6. The equi-potential lines obtained by Hinton and Owen (1979) are also shown in the same figure.

The finite element mesh employed for the case study using SFFP is illustrated in Fig. 7. Figure 8 presents the equi-potential lines obtained using SFFP.

Referring to Figs. 6 and 8, the results show very close agreement. To confirm this, the values of nodal potential of five randomly selected nodes are presented and compared with the solution presented by Hinton and Owen (1979) in Table 4.

Results shown in Table 4 are in very close agreement with a maximum percentage difference of 1.32% (mainly due to the interpolation of the reference results). If SFFP results are approximated to two decimals as those of the reference, the results are almost identical (maximum percentage difference = 0.36%). This verifies the accuracy SFFP results.
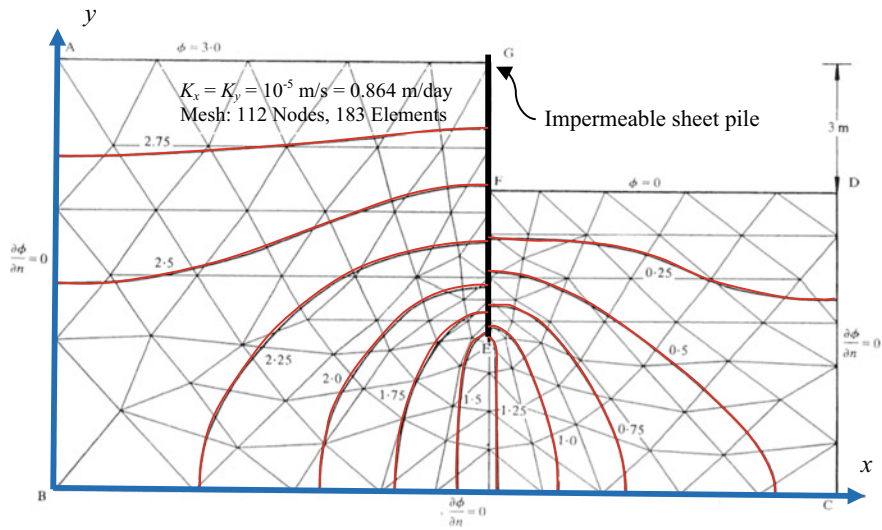
Fig. 6 Groundwater flow beneath a coffer dam showing equi-potential lines
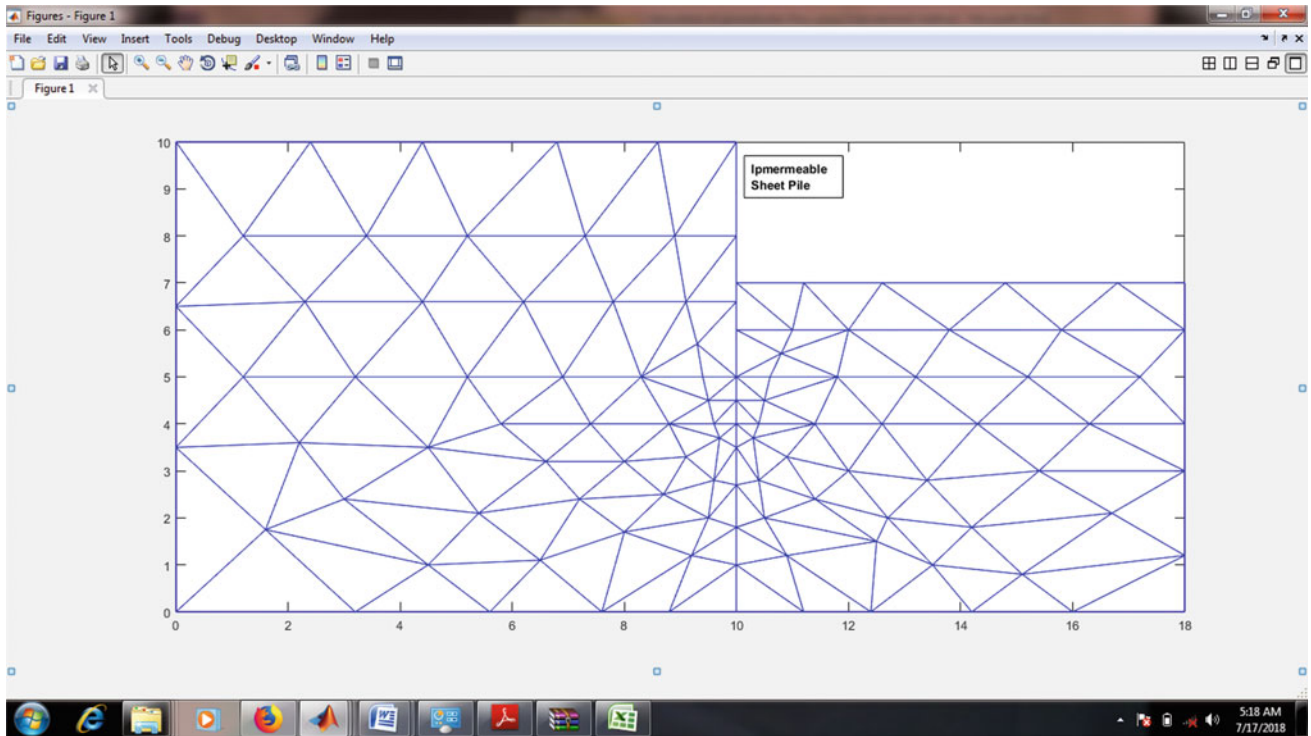
Fig. 7 Finite element mesh employed for the case study using SFFP
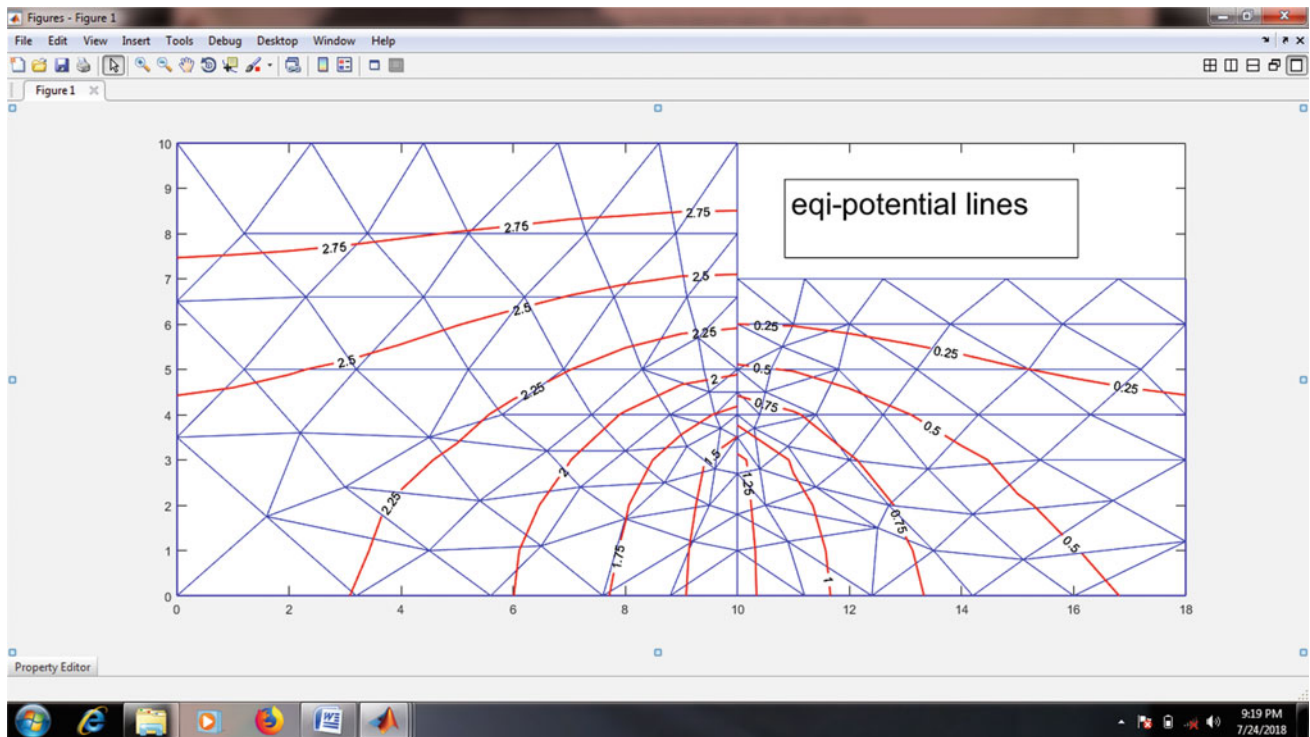
Fig. 8 Groundwater flow beneath a coffer dam showing equi-potential lines obtained using SFFP

Table 4 Comparison between SFFP and Hinton and Owen (1979) Nodal potential values

Node Number	Nodal potential values (m)		Difference %
	Hinton and Owen (1979)	SFFP solution	
11	2.25	2.2505	00.02
22	2.75	2.7417	−00.30
33	1.75	1.7473	−00.15
65	0.53	0.5307	00.13
99	0.25	0.2467	−01.32

5 Conclusions

From the result presented in this paper, the finite element solution of quasi-harmonic equation was formulated for steady-state groundwater flow. Then MATLAB was used to develop SFFP for solution of quasi-harmonic equation. SFFP was implemented, and its results accuracy verified by comparing with known results. The comparison showed very close agreement between results with a maximum difference of 0.22%. SFFP program was applied to a groundwater flow beneath a coffer dam problem as a case study. The results obtained using SFFP were in close agreement with the published results with a maximum difference of 1.32%.

References

K.R. Adeboye, M.D. Shehu, A. Ndanusa, *Finite Element Discretization and Simulation of Ground Water Flow System, IOSR-JM*, vol. 5, issue 6, pp. 54–61 (2013)

K.J.F. Bathe, *Finite Element Procedures* (Prentice Hall, New Jersey, 1996)

E. Hinton, D.R.J. Owen, *An introduction to finite element computational procedures*. Great Britain, Redwood Burn (1979)

M.U. Igboekwe, *Finite Element Method of Modeling Solute Transport in Groundwater Flow, PJST*, vol. 15

G. Jansser, K. Hemker, *Groundwater Models as Civil Engineering Tools*, FEM-MODFLOW, Czech Republic (2004)

M. Kalantari, A. Akbarpour, M. Khatibinia, Numerical modeling of groundwater flow in unconfined aquifer in steady state with isogeometric method. Modares Civil Eng. J. (M.C.E.J) **18**(3), 195–206 (Persian, 2018)

N.H. Kulkarni, A new numerical model coupling modified method of characteristics and garkin finite element method for simulation of solute transport in groundwater flow system. AQUADEMIA Water Environ. Technol. (2018)

D.L. Logan, *A first Course in The Finite Element*, United States, Chris Carson (2007)

S. Moaveni, *Finite Element Analysis: Theory and Application with ANSYS*, 3rd edn (Pearson Prentice Hall, United States of America, 2008)

T.E. Reilly, *A Galerkin's Finite Element Flow Model to Predict the Transient Response of a Radially Symmetric Aquifer*. U.S. Geological Survey Water Supply Paper2198 (1984)

A.L.K. Rouhani, 2D modeling of groundwater flow using finite element method in an object-oriented approach, in *IMWA Symposium, Water in Mining Environment*, Italy (2007)

H.F. Wang, M.P. Anderson, *Introduction to Groundwater Flow Modeling: Finite Difference and Finite Element Method*, San Francisco (1982)

O.C. Zienkiewicz, R.L. Taylor, J.Z. Zhu, *A Multidimensional Finite Element Method* (Butterworth-Heinemann, Amsterdam, Boston, 2013)

Integration Evaluation of the Universal Integrated Wi-Fi Controller from Buildings to Agricultural Applications

Fawaz Mohamed and Sharief Babikir

Abstract

The control over a Wi-Fi network that uses a microcontroller with a built-in Wi-Fi module can be considered one of the most recent technologies of the Internet of Things (IoT). Nevertheless, most of the available researches on Wi-Fi controllers is dedicated to a specific application. This paper aims to extend the integration evaluation of our designed and implemented universal integrated Wi-Fi controller with multiple applications from smart buildings to smart agricultural applications. The proposed system is based on Ep8266 NodeMCU with a built-in Wi-Fi module. The digital inputs, the digital outputs, and the analog input of the Wi-Fi module are redesigned to be suited for various voltage levels. The design was implemented and was successfully tested with integration evaluation for multiple applications. The first considered application was the controlling and managing of residential buildings and commercial buildings. In this paper, the integration evaluation is extended with the application of controlling a virtual farm or greenhouse model using the Blynk IoT cloud system with smartphones. For input to output (End to end) control path without relays, the total minimum time response is about 18 us and with relays is about 10 ms. For Wi-Fi radio channel, the maximum distance for the open environment was estimated to be 375 m with a bandwidth of 1Mbps and Round-Trip Time Delay (RTD) of about 30.87 ms. For good signal conditions, the throughput was evaluated to be from 4.5 to 14.9 Mbps for various configurations of the communication channel.

Keywords

Wi-Fi controller • Internet of Things (IoT) • Universal integration • Smart buildings • Smart farms

1 Introduction

The Internet of Things (IoT) deals with the control over communication networks for different applications of different fields such as buildings, agricultural, and industrial fields. Nevertheless, it can be organized into two research domains: which are control applications (Sarhan 2020, Singh and Saikia 2016, Umarov et al. 2019, Srivastava et al. 2018; Wenbo et al. 2015; Khan et al. 2018; Malathi et al. 2017; Panchal et al. 2020, Saputra and Y. Lukito 2017, Kodali et al. 2016, Peter et al. 2019, Hutabarat et al. 2018, Yıldız and Burunkaya 2019, Shareef et al. 2018, Li et al. 2009, Hlaing et al. 2017, López-Vargas et al. 2019); and networking protocols (Kodali and Soratkal 2016, Wen and Wang 2018, Wang et al. 2017, Khanchuea and Siripokarpirom 2019).

The research in control applications concerns with developing prototype models for a specific application using microcontrollers with Wi-Fi modules: such as farm and irrigation as in (Singh et al. 2016, Umarov et al. 2019, Srivastava et al. 2018, smart-home control in generals, specified items of smart-home control as in Wenbo et al. 2015, Khan et al. 2018, Malathi et al. 2017, Panchal et al. 2020, Saputra and Lukito 2017); and smart home security as in (Kodali et al. 2016, Peter et al. 2019, Hutabarat et al. 2018). Other researches; as in (Yıldız and Burunkaya 2019, Shareef et al. 2018, Li et al. 2009, Hlaing et al. 2017, López-Vargas et al. 2019); consider the measuring and monitoring of power and energy of the household.

Most of the proposed designs of these researches share the same concepts concerning the interfacing of the controller with the sensors and actuators for the application under study and providing locally or remotely communicated control through Wi-Fi and smartphones or personal computers. Nevertheless, these researches take fewer concerns about the networking protocols and information technology servers.

F. Mohamed (✉) · S. Babikir
University of Khartoum, Khartoum, Sudan
e-mail: fawaz.fathi@oiu.edu.sd

In comparison, we can see that each work has developed its controller to be intergraded with the chosen application rather than multi-application. Almost all of the results of the previous researches under this group consider just the successful implementation and integration with its related one application. On the other hand, the objective of this research is to design and implement a universal Wi-Fi controller that can be integrated with multiple applications (Mohamed and Babikir 2022).

2 Design and Implementation of the Proposed Universal Wi-Fi Controller

2.1 General System Architecture

Figure 1 shows the block diagram of our proposed universal Wi-Fi controller, which is based on the ESP8266 controller with a built-in Wi-Fi module (Mohamed and Babikir 2022).

2.2 Design Specifications and Parameters

The design specifications and parameters are determined according to the requirements of the target applications and their related sensors and actuators.

The buildings and agricultural applications are considered as slow dynamic processes such as temperature control, humidity control, moistures control, turning on or off electrical load, which also have fewer precision requirements.

For example, the insulated environment of buildings and Greenhouses has large time constants for their temperature control on the order of minutes of about 1–5 min. When compared with free air space which has temperature–time constant on the order of seconds, of about 1 s with a bandwidth of 1 Hz. Accordingly, it is common to use on–off control for the Greenhouse climate control or the buildings' HVAC systems rather than PID feedback regulators as an example. The sampling rate and control algorithms are required to be 10–20 times faster than the controlled process, which implies that the controller has to support 20 Hz or 50 ms processing speed as a minimum.

For analog input units, rather than those slow dynamic processes, there may be requirements to measure the AC voltage and current of the main utility, which has 50 Hz and requires a 500 Hz–1 kHz sampling rate. For buildings and agricultural applications, the analog signals have a large voltage range that requires less resolution such as 8–10bits and a wide input voltage range, from 3.3 V to 10 V.

For the digital input unit of the system, the highest speed requirements that can be faced are for serial data interfacing with sensors. These serial communication protocols include: 1-wire protocol, which is used with some temperature and humidity sensor units such as DH11; the Wiegand protocol, which is used with RFID card reader; and the IR protocols which are used with Infrared IR receiver. The minimum pulse widths for each of these protocols are 20 us, 20 us, and 104 us, respectively. The voltage of digital input sensors can be 3.3, 5, 12, 24 V.

Accordingly, the minimum pulse width that requires the digital input unit to support is 20 us as maximum time response. This specification, on the other hand, will support other pulsing sensors such as a water flow meter for agricultural applications that have a maximum frequency of 225 Hz for 30 L per minute for some types such as the POW110D3B Model.

For digital output units, rather than slower dynamics for turning on or off the electrical loads, there may be need to

Fig. 1 Block diagram of the proposed system
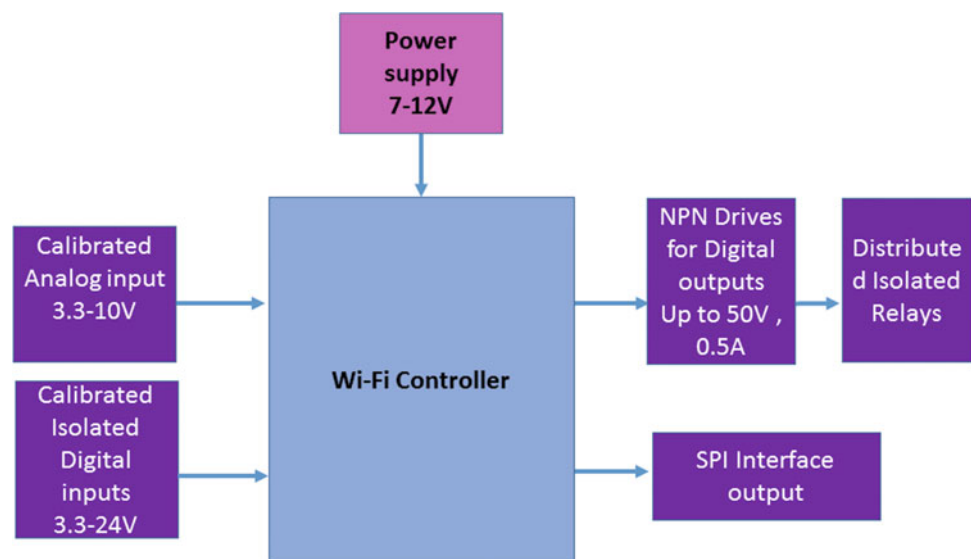
trip automatic air circuit breaker for over current/voltage protection, which requires time response less than or equal to 100 ms.

The voltage of digital output interfacing can be 3.3 V or 5 V to interface with other controllers; or 5 V, 12 V, or 24 V to interface with external actuators such as DC relays, TRIAC, or SCR which can be used to actuate larger loads or actuators such as contactors, motors.

For the Wi-Fi radio communication channel, the maximum distance requirements can be found for an open environment of the Greenhouses to be about 200 m, which can be doubled or increased with other access points.

The maximum round trip time delay constraint is required when a remote cloud server is used, in addition to its monitoring task, as computational central controller and the Wi-Fi controllers is used as distributed input/output I/O units. This requires the maximum round trip time delay to be 10 to 20 times less than the time constant of the controlled plant to neglect its effect. For the 1 s temperature–time constants the maximum round trip time delay is required to be less than or equal to 50 ms.

Table 1 summarizes the requirements for various input and output units of the proposed system.

2.3 Implementation

The system includes four digitally isolated inputs that can be calibrated with a signal conditioning circuit for a wide input voltage range (3.3–24 V); as well as different types for binary sensors such as NPN-transistor output type, PNP transistor output type, or normal switches. In addition to that, the controller has an analog input, which can be calibrated with a signal conditioning circuit for a wide input voltage range (3.3–10 V).

Furthermore, the controller contains seven digital outputs with a relay drive with up to 50 V and 0.5A, which is

Table 1 The requirements for various input and output units of the proposed system

System unite	Sampling rate (kHz)/time response (ms) requirements	Voltage range (V)/ distance (m) requirements
Controller	$\leq$ 50 ms	–
Digital input	$\leq$ 20 ms	3.3–24 V
Digital output	$\leq$ 100 ms	3.3–24 V
Analog input	$\geq$ 1 kHz	3.3–10 V
Wi-Fi channel	RTD $\leq$ 50 ms	$\geq$ 200 m for open area

isolated from loads with distributed relays. In addition, a serial peripheral interface (SPI) socket is used to interface with other sensors or modules that support it.

The design was implemented as a hardware prototype, which is demonstrated in Fig. 2 (Mohamed and Babikir 2022).

3 Integration Evaluation with Smart Building Applications

In our previous work as in (Video documentation of Wi-Fi Controller Integration with Smart Home Applications 2018, Video documentation of Wi-Fi Controller Integration with Access Control Applications of Smart Buildings 2018, Mohamed and Babikir 2022), the system was evaluated for integration with multiple applications of the smart buildings.

The first application of the smart building was the controlling of residential buildings loads with an embedded web server on the Wi-Fi controller and web browser on smartphones. The second one concerned integration with the RFID remote access control application of commercial buildings.

3.1 Integration with Smart Home Applications

On the hardware level, the main Wi-Fi controller is interfaced through distributed outputs relays with lamps, a traditional fan, and an evaporative cooler, as shown in Fig. 3.

On the software level, the Wi-Fi controller is programmed as an embedded HTTP web severer with embedded Hypertext Markup Language (HTML)/JavaScript page, to control and monitor different loads as shown in Fig. 4. For more information, a video demonstration can be found on (Video documentation of Wi-Fi Controller Integration with Smart Home Applications 2018).

3.2 Integration with Access Control Applications

On the hardware level, the Wi-Fi controller is interfaced with two RFID readers with serial Wiegand protocol through its digital inputs; likewise, the Wi-Fi controller is interfaced with LEDs through its digital outputs drive to emulate the gate door actuators as shown on Fig. 5.

On the software level, the Hercules Ethernet Converter SETUP utility was used to emulate the remote access control server with User Datagram Protocol (UDP) protocol as shown in Fig. 6. For more information, a video demonstration can be found on (Video documentation of Wi-Fi Controller Integration with Access Control Applications of Smart Buildings 2018).

Fig. 2 **a** The implementation of
the main controller board and
distributed board. **b** Bottom view
of the main controller board

(a)   (b)
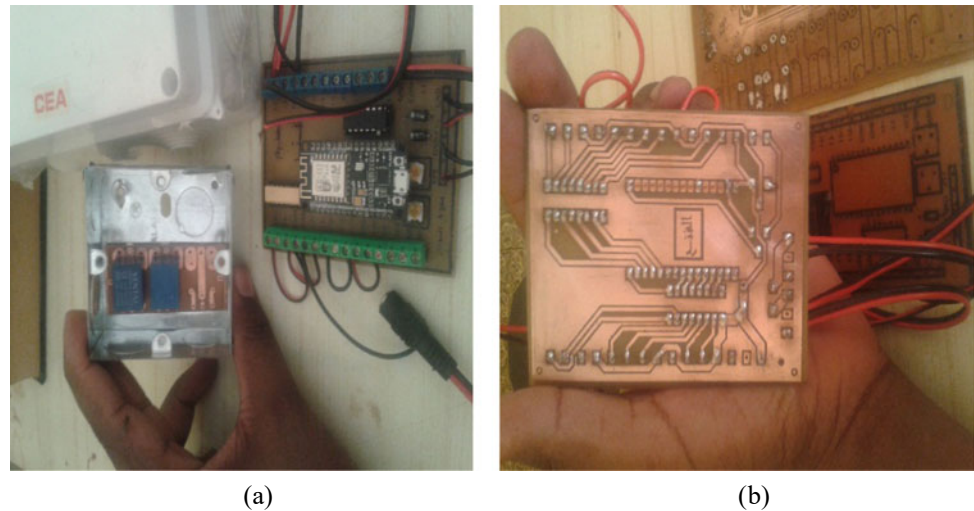
Fig. 3 **a** The main Wi-Fi
controller board is combined with
a 12 V power supply. **b** The
distributed relays board is
installed on the same box of a
manual switch

(a)   (b)
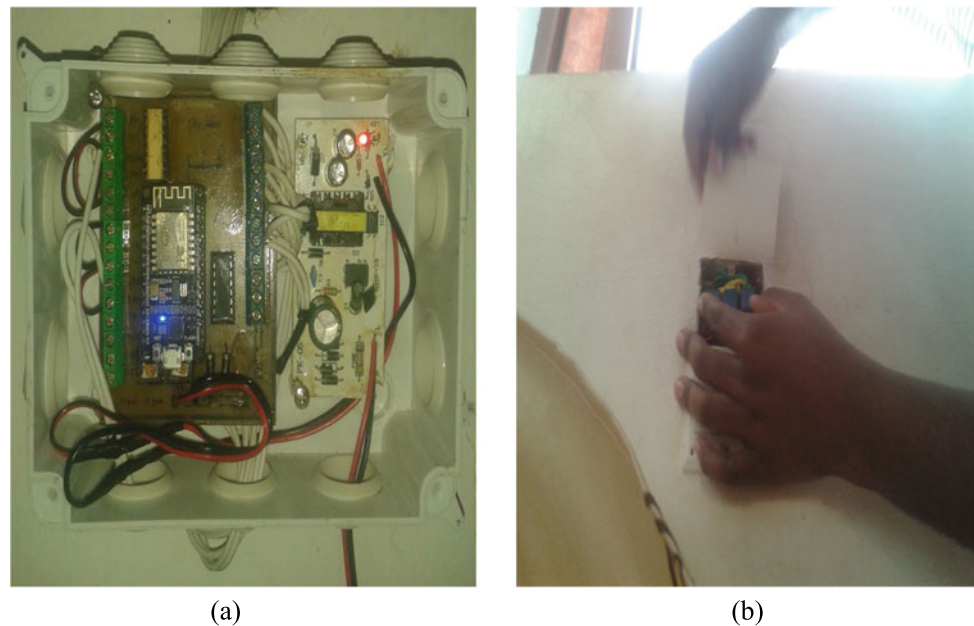
4 Integration Evaluation with Smart Farms and Green House Applications

In this paper, the integration evaluation is extended with the application of controlling a virtual farm or greenhouse model using the Blynk IoT cloud system with smartphones.

The Blynk cloud server is used as a broker between Blynk client app on a smart mobile phone and IoT controller as ESP8266, in addition to that the Blynk server has cloud computing capability as an option; so it can perform some controlling tasks like the controller such as scheduled actions or event conditional actions based on sensor readings.

Figure 7a shows the Blynk client app on a smart mobile phone configured for a virtual farm model to monitor temperature, humidity, and moisture; and to perform direct conditional event actions accordingly. These conditional event actions include the switching of fan of the evaporative cooler, and the pump of the evaporative cooler according to the temperature and the humidity levels; and the switching of the irrigation valves according to the soil moister level. In addition to that to perform a scheduled operation of irrigation valves.

Figure 7b illustrates the interfacing of the Wi-Fi controller with various sensors and actuators: such as temperature sensor, humidity sensor, moisture sensor, irrigation valves, and the fan and pump of the evaporative cooler. The actuators are emulated with LED for modeling purposes. For more information video demonstrations can be found on (Video documentation of Wi-Fi Controller Integration with Smart Farms and Green House Applications 2018).

Fig. 4 **a** Embedded HTML/JavaScript page with a smartphone web browser. **b** Example of controlling different residential buildings loads
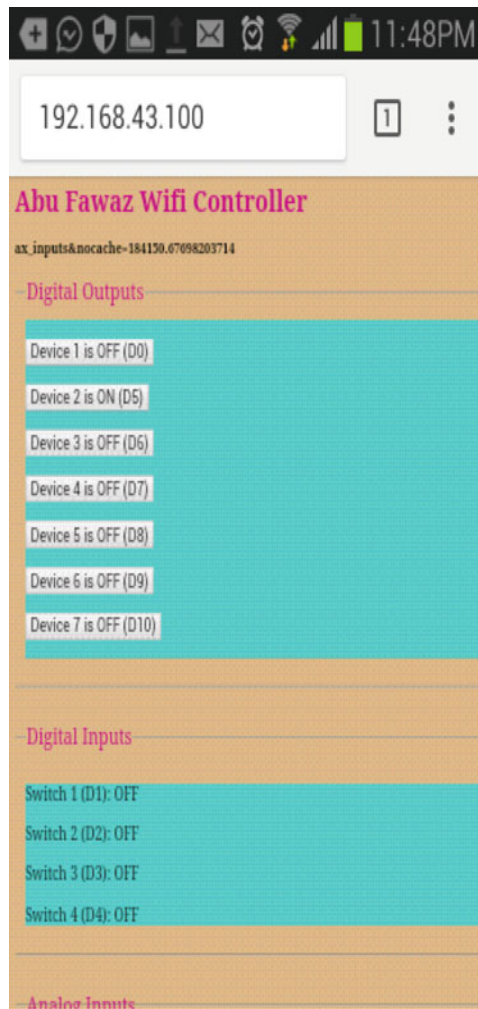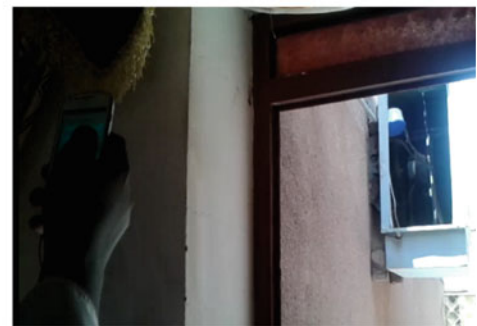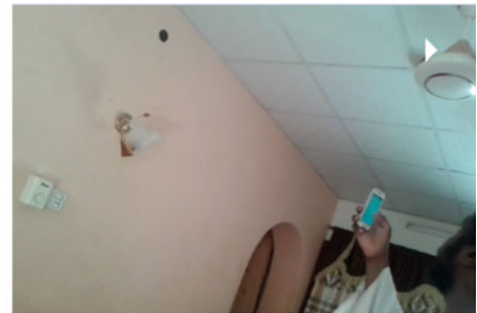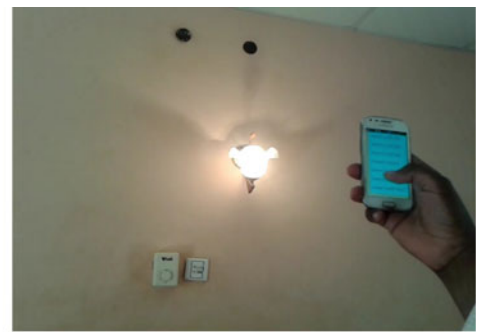
(a)   (b)

Fig. 5 **a** The Wi-Fi controller is interfaced with RFID readers with serial Wiegand protocol through its digital inputs. **b** The Wi-Fi controller is interfaced with LEDs through its digital output drives to emulate the gate door actuators

(a)   (b)

Fig. 6 a The authorized RFID card data are sent from the Wi-Fi controller to the access control server. **b** The authorized opening command is sent from the access control server to the Wi-Fi controller

(a)   (b)

Fig. 7 a Shows the Blynk client app on a smart mobile phone configured for a virtual farm model. **b** The interfacing of Wi-Fi controller with various sensors and actuators of virtual farm model

(a)   (b)

```
//timer to send the sensed real data as Flags regularly to blynk cloud server
BlynkTimer timer;
void sendFlagToServer() {
int chk;
// Read the real data of temperature, moisture and humidity  and writes them to Blynk Flags
  chk = DHT.read(DHT11_PIN);
    Blynk.virtualWrite(V0, DHT.humidity);
    Blynk.virtualWrite(V1, DHT.temperature);
    Blynk.virtualWrite(V2, analogRead(A0));
}

void setup()
{

 //connect with local Blynk cloud server
   Blynk.begin(auth, ssid, pass,IPAddress(192,168,43,44), 8442);
   // Setup a function to be called every second
   // Flags timer to send the sensed real data regularly
  timer.setInterval(2000L, sendFlagToServer);
}

void loop()
{
   // run the Blynk service routine to send and receive the on-off signals..
   //..for digital input and output for each pin
   Blynk.run();
   // run the Flag timer service routine to send and receive the real numerical data
   timer.run();
}
```

Fig. 8 The pseudo-code for the smart farm application

The programing codes and algorithms which is implemented on the microcontroller chips differ according to the target applications. Figure 8 shows the pseudo-code which is used as an algorithm on the ESP8266 chip for this application.

5   Performance Evaluation

Although this paper is intended for application integration evaluation, the performance can be estimated from the datasheet of the individual components of the system, the valuable previous research papers on the field with our, and our modeling and verified measurements if it is necessary.

5.1   Direct Digital Input to Digital Output Response Time

The total minimum response time of the designed Wi-Fi controller can be determined with modeling from the tested specifications of the datasheet of its units.

ESP8266 MCU with FPU + DSP processor has a 2.294 MHz I/O toggle rate, 290 kHz GIPO's inv. loop rate, and 113.40 DMIPS (Ivkovic and Ivkovic 2017).

For the input to output (End to end) control path without relays through the controller, the dominant unit is the digital input unit with PC847, so the total minimum time response is estimated to be about 18 us.

On the other hand, for the input to output (End to end) control path with relays, the dominant unit is the relays; so the total minimum time response is estimated to be about 10 ms.

This total response time can increase if the processing time of the Wi-Fi controller's program or other external processing units, which can be measured with the internal MCU's timer, is greater than the stated minimum response time (Mohamed and Babikir 2022).

5.2   Distance for the Wi-Fi Channel

The datasheet of ESP8266 provides the output power of the transmitter and the bandwidth of the Wi-Fi channel in Mbps with its related receiver's sensitivity in dBm as shown in Fig. 9.

Nevertheless, the datasheet doesn't provide other parameters such as the max distance, time delay, and throughput because they depend on the environmental conditions.

Fig. 9 The Wi-Fi Radio
Characteristics of ESP8266

Parameters	Min	Typical	Max	Unit
Input frequency	2412	-	2484	MHz
Output impedance	-	39+j6	-	Ω
Input reflection	-	-	-10	dB
Output power of PA for 72.2 Mbps	15.5	16.5	17.5	dBm
Output power of PA for 11b mode	19.5	20.5	21.5	dBm
Sensitivity				
DSSS, 1 Mbps	-	-98	-	dBm
CCK, 11 Mbps	-	-91	-	dBm
6 Mbps (1/2 BPSK)	-	-93	-	dBm
54 Mbps (3/4 64-QAM)	-	-75	-	dBm
HT20, MCS7 (65 Mbps, 72.2 Mbps)	-	-72	-	dBm

There are valuable efforts, such as in (Barai et al. 2017), to measure the distance in meter with its received signal strength in dBm; but these measurements are taken for the open space environment only from 0.3 m with −55dBd to 10 m with −88 dBm.

Although the maximum distance that is related to the sensitivity of about -98dBm is not measured, the interpolated model equation is developed with the curve fitting technique with an average error level of 8.32%. So, the maximum distance can be estimated to be about 375 m for −95 dBm.

The distance of 15 m can be considered as approximated maximum distance for the indoor environment as agreed with our measurements, which can be related to a sensitivity of −98dBm approximately.

For other environments, the empirical COST Hata model, as in (Singh 2012), can be utilized; although it is developed for base stations with a height above 30 m. For our estimation, the mobile and base stations are assumed to be with 2 m height, 20 dBm transmitter power, 1 dB antenna gain for COST Hata model calculation as in (Table 2).

5.3 Throughput and Time Delay of the Wi-Fi Channel

For the actual throughput, there are other valuable efforts, as in (A simple throughput test for ESP8266 based on iperf by Pansila 2021); these works concluded that for good signal conditions with RTOS SDK 2.2; the ESP8266 has throughput from 4.5 Mbps to 7.2 Mbps for Tx/Rx TCP with a buffer size of 1440 * 2, and from 10.5 Mbps to 14.9 Mbps for Tx/Rx UDP with buffer size of 1460.

The TCP throughput can be increased to 13 Mpbs when downloading four simultaneous files from ESP8266 when acts as a server, as indicated in (ESP8266 TCP Server Speed Test by Pratik PandaJ 2021).

Moreover, there are valuable efforts in (Mesquita et al. 2018) to measure the roundtrip time delay (RTD) in milliseconds (ms) for different distances in meter; but the measurements are taken for indoor environments only from 1 m with 6.8 ms to about 15 m with 30.87 ms before losing the connection retransmission with 99%. The time delay of 30.87 ms can be related to the maximum distance of other environments, because it depends on the minimum sensitivity of −98dBm.

Table 2 The estimated max. distance of the Wi-Fi channel for different environments

Experimental model	The approximated maximum distance in meter
ESP8266 open space environment	375
ESP8266 indoor environment	15
COST hata medium city/suburban (1500–2400 MHz)	150
COST hata large city (1500–2400 MHz)	120

6 Discussion

The ability of the Wi-Fi controller to universally integrate with multiple applications originates from the nature of the input and output units of the design.

The interfacing features of the input and output units include: the calibrated digital and analog input units; the distributed relay boards that can be integrate into parallel existing boxes of load switches; the possibility of using drives of output units without relays; and the integration with any networked program applications of smartphones,

computers, servers, and cloud systems with various communication protocols.

Although the proposed design is implemented and is tested for a limited number of applications, the principle can be generalized. In turn, this enables the successful implementation of universal integration with the proposed cost-effective design.

7 Conclusions

In summary, the results prove the concepts of universal integration of the Wi-Fi controller with smart applications. This universal integration can be accomplished with the proper design of interfacing units.

The proposed Wi-Fi controller system is considered the first release of the universal integrated programmable controller project. Despite the success of the system integration with smart buildings and farms, the global integration process with applications of other fields may require other treatments for the interfacing units.

References

A simple throughput test for ESP8266 based on iperf by Pansila. https://github.com/pansila/ESP8266-Iperf-Test. Accessed on 30 Nov 2021

S. Barai, D. Biswas, B. Sau, Estimate distance measurement using NodeMCU ESP8266 based on RSSI technique, in *Proceedings of 2017b IEEE CAMA*, Tsukuba, Japan (2017), pp. 170–173. https://doi.org/10.1109/CAMA.2017.8273392

Blynk IoT Platform. https://www.blynk.io. Accessed on 31 Dec 2021

ESP8266 TCP Server Speed Test by Pratik PandaJ. http://iot-bits.com/esp8266-tcp-server-speed-test/. Accessed on 30 Nov 2021

W. Hlaing, S. Thepphaeng, V. Nontaboot, N. Tangsunantham, T. Sangsuwan, C. Pira,Implementation of WiFi-based single-phase smart meter for Internet of Things (IoT), in *2017 International Electrical Engineering Congress (iEECON)*, Pattaya, Thailand (2017), pp. 1–4

D.P. Hutabarat, S. Budijono, R. Saleh, Development of home security system using ESP8266 and Android smartphone as the monitoring tool, in *IOP Conference Series: Earth and Environmental Science*, vol. 195, no. 1 (IOP Publishing, 2018), p. 012065

J. Ivkovic, J.L. Ivkovic, Analysis of the performance of the new generation of 32-bit Microcontrollers for IoT and Big Data Application, in *Proceedings of the International Conference on Information Society and Technology (ICIST)*, Kopaonik, Serbia (2017)

A. Khan, A. Al-Zahrani, S. Al-Harbi, S. Al-Nashri, I.A. Khan, Design of an IoT smart home system, in *2018 15th Learning and Technology Conference (L&T)*, Jeddah, Saudi Arabia, (2018), pp. 1–5

K. Khanchuea, R. Siripokarpirom,A multi-protocol IoT gateway and WiFi/BLE sensor nodes for smart home and building automation: design and implementation, in *2019 10th International Conference of Information and Communication Technology for Embedded Systems (IC-ICTES)*, Bangkok, Thailand (2019), pp. 1–6

R.K. Kodali, S. Soratkal,MQTT based home automation system using ESP8266, in *2016 IEEE Region 10 Humanitarian Technology Conference (R10-HTC)*, Agra, India (2016), pp. 1–5

R.K. Kodali, V. Jain, S. Bose, L. Boppana, IoT based smart security and home automation system, in *2016 International Conference on Computing, Communication, and Automation (ICCCA)*, Greater Noida, India (2016), pp. 1286–1289

L. Li, X. Hu, W. Zhang, Design of an ARM-based power meter having WIFI wireless communication module, in *2009 4th IEEE Conference on Industrial Electronics and Applications*, Xi'an, China (2009), pp. 403–407

A. López-Vargas, M. Fuentes, M. Vivar, IoT application for real-time monitoring of solar home systems based on Arduino™ with 3G connectivity. IEEE Sens. J. **19**(2), 679–691 (2019)

M. Malathi, A. Gowsalya, M. Dhanushyaa, A. Janani, Home automation on ESP8266. SSRG Int. J. Comput. Sci. Eng. 2348–8387 (2017)

J. Mesquita, D. Guimarães, C. Pereira, F. Santos, L. Almeida, Assessing the ESP8266 WiFi module for the Internet of Things, in *2018 IEEE 23rd International Conference on Emerging Technologies and Factory Automation*

F. Mohamed, S. Babikir, Universal integrated Wi-Fi controller for smart building applications. Eng. J. **12** (University of Khartoum, 2022)

A. Panchal, D. Jadhav, S.P. Aspalli, IOT home automation using ESP8266 with voice commands of hindi language. Int. Res. J. Mod. Eng. Technol. Sci. **2**, 814–819 (2020)

J.S.P. Peter, S. Selvakumar, H. Pandit, P. Aggarwal, Home automation and home security using Arduino and ESP8266 (IoT). Int. J. Innov. Technol. Explor. Eng. **8**(7), 39–42 (2019)

L.K.P. Saputra, Y. Lukito, Implementation of air conditioning control system using REST protocol based on NodeMCU ESP8266, in *2017a International Conference on Smart Cities, Automation & Intelligent Computing Systems (ICON-SONICS)*, Yogyakarta, Indonesia (2017), pp. 126–130

Q.I. Sarhan, Systematic survey on smart home safety and security systems using the arduino platform. IEEE Access **8**, 128362–128384 (2020)

H. Shareef, M.S. Ahmed, A. Mohamed, E. Al Hassan, Review on home energy management system considering demand responses, smart technologies, and intelligent controllers. IEEE Access **6**, 24498–24509 (2018)

Y. Singh, Comparison of Okumura, Hata and COST-231 models on the basis of path loss and signal strength. Int. J. Comput. Appl. **0975–8887**(11), 59 (December 2012)

P. Singh, S. Saikia,Arduino-based smart irrigation using water flow sensor, soil moisture sensor, temperature sensor, and ESP8266 WiFi module, in *2016 IEEE Region 10 Humanitarian Technology Conference (R10-HTC)*, Agra, India (2016), pp. 1–4

P. Srivastava, M. Bajaj, A.S. Rana, Overview of ESP8266 Wi-Fi module based smart irrigation system using IoT, in *2018 Fourth International Conference on Advances in Electrical, Electronics, Information, Communication, and Bio-Informatics (AEEICB)*, Chennai, India (2018), pp. 1–5

A. Umarov, M. Kunelbayev, M. Satymbekov, G. Turken, B. Alimbayeva, K. Imanzhanova, L. Duisembayeva, Microclimate monitoring system for a home greenhouse as part of ESP32, in *International Conference on Renewable Energy & Emerging Technologies (ICREET)* (2019)

Video documentation of Wi-Fi controller integration with access control applications of smart buildings (2018). https://youtu.be/mEjUEJmGS7o

Video documentation of Wi-Fi controller integration with smart farms and green house applications (2018). https://youtu.be/ceO3dtkUGPs

Video documentation of Wi-Fi controller integration with smart home applications (2018). https://youtu.be/Yg8vo4eWkzQ

M. Wang, S. Qiu, H. Dong, Y. Wang, Design an IoT-based building management cloud platform for green buildings, in *2017 Chinese Automation Congress (CAC)*, Jinan, China (2017), pp. 5663–5667

X. Wen, Y. Wang, Design of smart home environment monitoring system based on Raspberry Pi, in *2018 Chinese Control and Decision Conference (CCDC)*, Shenyang, China (2018), pp. 4259–4263

Y. Wenbo, W. Quanyu, G. Zhenwei, Smart home implementation based on Internet and WiFi technology, in *2015 34th Chinese Control Conference (CCC)*, Hangzhou, China (2015), pp. 9072–9077

S. Yıldız, M. Burunkaya, Web-based smart meter for general purpose smart home systems with ESP8266, in *2019 3rd International Symposium on Multidisciplinary Studies and Innovative Technologies (ISMSIT)*, Ankara, Turkey (2019), pp. 1–6

Adobe Construction in Nineteenth-Century Citadels in Morocco: Mechanical and Soil Characteristics

Omar Khtou, Issam Aalil, and Mohamed Aboussaleh

Abstract

The characteristic architecture in the oases of southeastern Morocco is that of raw earth construction. This is done through two techniques: rammed earth and adobe. This work is carried out with the aim of preserving this ancestral know-how by studying a construction dating back two centuries. The first step is to characterize a soil extracted from the remains of an old building, the grain size and plasticity of the soil showed that it was not very clayey and moderately plastic and that it was suitable for earth construction. Secondly, the study focuses on the mechanical resistance of blocks extracted from the remains studied; the result obtained satisfies all the standards. In order to characterize the durability of the adobe, we made samples of the earthen bricks with a similar soil and the study showed good durability of the adobe construction. The raw earth is a material that can stand in time, and finally, the reusability of the earth material from old buildings has been studied; the results have shown that raw earth is a perfectly reusable material, which makes it the ideal ecological material.

Keywords

Vernacular construction • Adobe • Soil characteristics • Mechanical characteristics

1 Introduction

For thousands of years, construction has been done exclusively with local materials. If we take the example of the Great Wall of China, we can see that it adapts throughout its course to the nature of the ground on which it is built. Thus, we find parts built of stone on the rock, earth on the earth, and sometimes even sand in some desert parts. Given the size of the territory crossed by this building, it was built using local materials in order to limit the transport of the extraction area to that of the construction site. Exploiting local materials to build your home is a universal behavior. And often, land is the only material available. Studies estimate that "at least 30% of the world's population lives in earthen buildings and 17% of buildings inscribed on UNESCO's World Heritage List are earthen architectural works" (Anger and Fontaine 2009), considering that raw earth construction is widely distributed around the world.

For more than a thousand years, the material of choice for construction in the oases of southeastern Morocco has been the raw earth (Mellaikhafi et al. 2021). These oases are recognized by the presence of various large fortresses known as ksar (or ksour in plural). These constructions represent an architectural part of the national heritage and also of the UNESCO world heritage such as the ksar ait Benhadou. El Khorbat ksar, located near Tinejdad City, is an example of vernacular architecture tackled in many studies (Gil Piqueras and Rodríguez Navarro 2019). These constructions were made using two main techniques: rammed earth and adobe. The rammed earth technique consists of tamping damp earth in a formwork. The earth is poured into a formwork in layers. Adobe is a raw earth brick shaped by hand or in a wooden mold in a plastic state and air-dried. This is often reinforced with straw fibers.

Earth construction provides thermal compliance in an arid climate, which is cold in winter and very hot in summer. It reduces cooling and heating energy requirements through heat storage capacity of the rammed earth materials, which is beneficial to the environment (Mellaikhafi et al. 2021). In addition, raw earth is a material with low gray energy and its operation meet environmental requirements. However, the use of this material faces many obstacles as the non-uniformity unlike cement concrete: the material changes

O. Khtou (✉) · I. Aalil · M. Aboussaleh
Laboratory of Sciences and Engineering, ENSAM, Moulay Ismail University, 50000 Meknes, Morocco
e-mail: omar.khtou@gmail.com

enormously from one region to another and from one deposit to another.

This work focuses on raw earth used in the city of Tinjedad, located in a southeastern oasis of Morocco, to characterize the material used in more than 200 years old building in the ksar of gardmit and compare it to the standards, then the mechanical resistance of several blocks extracted from old constructions was measured and compared to standards, which made it possible to draw conclusions regarding the durability of the earth material. The reusability of the earth was also studied by reusing the earth from old constructions to make new adobes.

The soil used for this study is extracted in the city of Tinejdad, in the central-eastern part of the Kingdom of Morocco, a region known for its traditional earthen citadel architecture.

2 Experimental Methodology

2.1 Raw Earth Characterization

Initially, the study was interested in the characterization of the nature of the soil used in the making of three blocks extracted from several walls of the old citadel (ksar) of gardmit in the municipality of Tinejdad in the southeast from Morocco.

Granulometry

The particle size analysis is carried out in two phases:

The first, the particle size analysis by sieving with water (standard NF P 94–056): It gives the particle size repair of the elements whose diameter is greater than 80 microns. The different sieves are weighed after immersion for 24 h in water and drying of the different sieve oversizes (Mellaikhafi et al. 2021).

The second phase, particle size analysis by sedimentation (standard NF P 94–057): It concerns the fraction of the soil less than 80 microns and as its name indicates it uses the principle of sedimentation that takes place in a standardized tube of 2 L of distilled water. The principle of the test is based on Stokes' law (Mellaikhafi et al. 2021).

Plasticity

This test is carried out on the fraction less than 400 μm and consists in varying the water content of the material in order to assess its consistency (Mellaikhafi et al. 2021). The test is carried out in two phases and in accordance with Standard NF P 94–051: A first phase in which the water content is sought for which a groove made in a soil placed in a cup

of imposed characteristics closes when the latter and its content are subjected to repeated shocks. In a second phase, we look for the water content for which a roll of soil, of fixed size is made manually, cracks. The Atterberg limits correspond to the thresholds of passage from the solid state to the plastic state: the plastic limit PL, and from the plastic state to the liquid state: the liquidity limit Ll. The interval between these two limits defines the extent of the domain of plasticity: plasticity index PI.

The methylene blue test (BV)

The aim of this test is to characterize the specific surface of the clay fraction of a material. The result of the test depends directly on the nature and the amount of this fraction in the material, it tells us about the sensitivity of the clay to water and therefore about its swelling shrinkage properties.

The test is carried out on the fraction of particles with a diameter of less than 5 mm. It consists of measuring, by assay, the amount of methylene blue that can be adsorbed by a material suspended in water and with permanent stirring. The method consists of an injection, in the aqueous bath containing the test sample, of elementary doses of 5 cm^3 of a solution of methylene blue. The adsorption of the blue is checked one minute after each addition, by performing a task with a glass rod on a filter paper. The resulting stain consists of a dark blue nucleus and a transparent halo, indicating that the injected blue is fully adsorbed and the test is negative. When the halo begins to turn blue, adsorption is allowed to take place. If after five minutes the halo persists, the degree of adsorption saturation is reached and the test is positive. The total quantity of methylene blue solution used is recorded.

2.2 Mechanical Test Plan and Samples

This study is interested from a mechanical point of view to the compressive strength, three samples (W1, W2, and W3) were extracted from three blocks of old walls; these samples went through a concrete saw to make bricks of 10×10 10cm; the test is performed using a press with a capacity of 3000 kN; in accordance with the standard NF P 18-406, the loading speed is 300 N/min.

Then, in order to study the durability of the raw earth construction, bricks (B1, B2, and B3) were shaped from earth extracted from the same area and having characteristics very similar to the earth constituting the studied walls.

2.3 Reusability

The construction in raw earth is certainly an ecological solution, and here the study consists in going even further in

this aspect of the earth material, by reusing the earth extracted from an old construction.

Then, in order to study the reusability of the raw earth construction, bricks (R1, R2, and R3) were shaped from the old wall's earth.

Then the results are compared with those obtained with raw earth extracted from deposits on site.

3 Results and Discussion

3.1 Raw Earth Characteristics

Tables 1 and 2 show the characteristics of the raw earth used in three old walls "W1", "W2", "W3" and the raw earth extracted from deposit on site "N".

The results of the particle size analysis indicate that the soil in the old walls contains between 12 and 16% gravel, approximately 60% sand, 15% silt and between 12 and 16% clay. The Atterberg limits are, respectively, between 21.3 and 23.5%, for the liquidity limit; between 12.9 and 14.8% for the plastic limit; and between 8.4 and 9.3% for the plasticity index.

And with regard to the earth mined on-site from the on-site deposit, the particle size analysis indicates that the soil contains approximately 13% gravel, 63% sand, 12% silt, and 12% clay. The Atterberg limits are, respectively, 20% for the liquidity limit, 12.7% for the plasticity limit, and 7.5% for the plasticity index. Based on the LPC (Magnan 1980) and USCS (ASTM Committee D-18 on Soil and Rock 2017) soil classification, the different soils used are classified as clayey sand. These floors meet the requirements of Moroccan regulations for earthquake-resistant earth constructions for adobe, with the exception of the liquidity limit

which is below the minimum threshold of 25% (RPCT: the Moroccan earthquake-resistant earth construction regulation 2011).

3.2 Mechanical Characteristics

The mechanical characterization of the adobe samples was carried out to characterize and compare the mechanical resistance to compression of different bricks, those of the old walls W1, W2, and W3, those built from the earth extracted from the deposit in the same zone B1, B2, and B3. The various samples meet the required compressive strength, and the most demanding standard, being the New Mexico code, imposes a minimum compressive strength of 2 MPa (Code 2015).

The figure shows the compression resistances of the different bricks. The bricks extracted from the old walls: W1, W2, and W3. Bricks made with raw earth extracted from the on-site deposits B1, B2, and B3, and bricks made by reusing soil from old walls R1, R2, R3 (Fig. 1).

4 Conclusion

The purpose of this research was first to study the raw earth used for traditional construction in the Moroccan southeast, used more than 200 years ago, it meets the requirements of the Moroccan standard, and the resistance to the compression of different blocks extracted from old walls meets different standards. The study then concerned the durability of the material by comparing the compressive strengths of old "W" bricks with new "N" bricks, and the results obtained showed that the earthen material retains good compressive

Table 1 Raw earth granulometry

	Gravel (20–2 mm)	Coarse sands (2–0.2 mm)	Fine sands (0.2–0.06 mm)	Silt (0.06–0.02 mm)	Fine Silt (0.02–0.002 mm)	Clay (< 0.002 mm)
% "W1"	12	25	35	7	8	13
% "W2"	10	28	31	6	9	16
% "W3"	13	31	30	6	8	12
% "N"	13	30	33	5	7	12

Table 2 Raw earth characteristics

	Fine content (%)	Liquidity limit (%)	Plasticity limit (%)	Plasticity index (%)	Methylene blue value
"W1"	28	22.5	13.2	9.3	2.88
"W2"	31	23.5	14.8	8.7	2.92
"W3"	26	21.3	12.9	8.4	2.8
"N"	24	20.2	12.7	7.5	2.75

Fig. 1 Compressive strength of different bricks
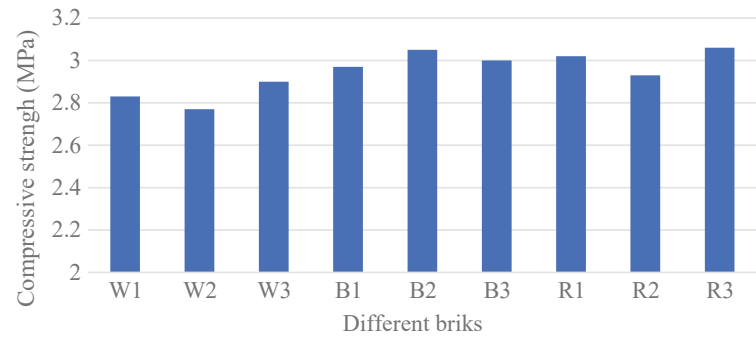
strength after two centuries. The research finally treated the reusability of raw earth used in these same walls, it was reused for making bricks, these bricks were then compared with bricks constructed from a very similar earth deposit, and this comparison showed that the earth material is perfectly reusable.

References

R. Anger, L. Fontaine, Bâtir en terre, du grain de sable à l'architecture, éditions Belin. *Cité des sciences et de l'industrie, Parigi* (2009)

ASTM Committee D-18 on Soil and Rock, Standard Practice for Classification of Soils for Engineering Purposes (Unified Soil Classification System) 1. ASTM Int. (2017)

N.M.A. Code, New Mexico earthen building materials code. Santa Fe, NM (2015)

M.T. Gil Piqueras, P. Rodríguez Navarro, Restoration of the Sidi Bou Guertif Marabout, El Khorbat, Morocco. Loggia, Arquitectura & Restauración **32**, 60–73 (2019)

J.P. Magnan, Geotechnical classification of soils. (1) note on the LCP classification. Bulletin de Liaison des Lab des Ponts et Chaussees **105**

A. Mellaikhafi, A. Tilioua, H. Souli, M. Garoum, M.A.A. Hamdi, Characterization of different earthen construction materials in oasis of south-eastern Morocco (Errachidia Province). Case Stud. Constr. Mater. **14**, e00496 (2021)

RPCT: the Moroccan earthquake-resistant earth construction regulation (2011)

Adsorption of Abattoir Wastewater Contaminants by Coconut Shell-Activated Carbon

Ibrahim Mohammed Lawal, Usman Bala Soja,
Abdulhameed Danjuma Mambo, Shamsul Rahman Mohamed Kutty,
Ahmad Hussaini Jagaba, Gasim Hayder, Sule Abubakar,
and Ibrahim Umaru

Abstract

Abattoir wastewater composition depends on type and number of animals slaughtered, as well as the process's water requirements. As a result, it must be treated before being discharged in order to preserve the environment. The utilization and efficacy of activated coconut shell derived from agricultural waste for the removal of some recalcitrant target contaminants in abattoir wastewater were explored in this study. The use of this adsorbent as a potential replacement for advanced treatment methods was examined in a batch test. The maximum adsorption capacity was determined by varying adsorbent dosages at 25, 30, 35, 40, 45 and 50 g and at reaction time of 24, 48, 72, 96 and 120 hr. At 24 hr contact time, the pH ranged between 6.7 and 8.0. The optimum dosage, reaction time and percentage removal of electrical conductivity (30 g/l, 120 hr, 56.57%), ammonia (50 g/l, 48 hr, 61.55%), colour (50 g/l, 120 hr, 78.6%), total suspended solid (45 g/l, 24 hr, 26.64%) and chemical oxygen demand (50 g/l, 24 hr, 73.28%), respectively. From the results obtained, adsorption efficiency improved as adsorbent dosage was increased albeit at different reaction time. Hence, low-cost adsorbent such as coconut shell can be used as an alternative and cost-effective treatment technique for abattoir wastewater for a safe disposal.

1 Introduction

Abattoir effluent falls under the category of "severe industrial" waste. It contains a lot of suspended solids. The wastewater is highly pretentious, rapidly decomposes and allows for environmental pollution. Blood from slaughtered animals, rumen solids, undigested food, feathers, flesh pieces and bone fragments are all found in abattoir wastewater according to reports (Elumalai et al. 2017).

Wastewater generated in abattoirs can account for as much as 80% of the total water consumed in the slaughter-house processes. The reuse of treated wastewater is an excellent option in a wide range of applications, including agriculture, industrial processes, surface water management and groundwater recharge (Elewa et al. 2022). The health threat posed by the discharge of the aforementioned large volume of effluents into receiving water, and the surrounding environment has had an adverse impact on the environment (Saeed et al. 2021a).

The most frequently used conventional methods for treating abattoir wastewaters are screening, sedimentation, coagulation–flocculation, filtration and activated sludge biological processes. Numerous researchers have investigated methods for treating abattoir wastewater, including

I. M. Lawal (✉)
Department of Civil and Environmental Engineering,
University of Strathclyde, Glasgow, G1 1XJ, UK
e-mail: Ibrahim.lawal@strath.ac.uk

I. M. Lawal · A. H. Jagaba · S. Abubakar · I. Umaru
Department of Civil Engineering, Abubakar Tafawa Balewa
University, Bauchi, Nigeria
e-mail: Ibrahim.lawal@strath.ac.uk

U. B. Soja
Department of Civil Engineering, Federal University Dutsin-Ma,
P.M.B. 5001, Dutsin-Ma, Katsina State, Nigeria

U. B. Soja · A. D. Mambo
Department of Civil Engineering, Nile University of Nigeria,
Abuja, Nigeria

S. R. M. Kutty · A. H. Jagaba
Department of Civil and Environmental Engineering, Universiti
Teknologi PETRONAS, Perak Darul Ridzuan, Malaysia

G. Hayder
Department of Civil Engineering, College of Engineering,
Universiti Tenaga Nasional (UNITEN), 43000 Kajang,
Selangor Darul Ehsan, Malaysia

aerobic and anaerobic biological systems, as well as hybrid systems. For abattoir wastewater treatment, anaerobic treatment systems are a better option. Abattoir wastewater has been successfully treated through the methods listed. Anaerobic treatment removes a lot of COD, BOD and SS while also producing a usable energy source in the form of methane gas. Anaerobic treatment generates very little sludge and eliminates the need for chemical pre-treatment. However, agro-based coconut shell was considered a waste product and therefore investigating the feasibility of its usage as a non-conventional treatment method for wastewater provides a disposal solution for the coconut processing industry, and it is almost completely free. Total suspended solids (TSS), fats and colloids are frequently removed from abattoir effluents via physicochemical processes such as dissolved air flotation and coagulation–flocculation units (Al-mahbashi et al. 2022). However, it is not advisably recommended as greenhouse gases are emitted during the process.

It has been observed that non-biodegradable contaminants are a serious health and environmental hazard, and secondary methods cannot be used to remove them. To remove these pollutants, tertiary/advanced wastewater treatment methods like ion exchange, precipitation, membrane separation, electrolysis and adsorption can be used. But methods are capital intensive and necessitate a high level of skills, and thus, few end-users actually use these methods. Adsorption technology's low cost, simplicity, versatility and robustness have made it a popular method for removing pollutants. Adsorbent selection is critical to the success of the adsorption process. A variety of adsorbents can be used to remove pollutants from industrial wastewater, for example, adsorbent materials such as activated carbon, silica gel and activated alumina. Regrettably, most of these adsorption media are prohibitively expensive. In addition, inconvenient separation, low adsorption capacity, high preparation costs, non-recyclability, low yield, chemical precipitation, toxic sludge generation and a significant amount of processing temperatures for their activation are some of the other drawbacks of this technology (Hussaini Jagaba et al. 2019).

Because of its cost-effectiveness, low energy consumption, non-corrosiveness, relatively simple technological procedure, and ability to work over a wide temperature and pressure range, adsorption has emerged as a potential technology for sequestration and CO2 collection (Jagaba et al. 2020, 2021a; Ghaleb et al. 2020).

Activated carbon is non-graphite microcrystalline carbon (Nasara et al. 2021). When wood or other materials are heated to high temperatures in an airless environment to release trapped gases, the result is a highly porous form of activated carbon, which is a fine black powder with no odour or taste (Jagaba et al. 2021c). When heated with an oxidizing agent or other chemicals to break it down into a powder, it can be activated to improve its ability to absorb gases, liquids or dissolved substances (adsorbents) on the surface of its pores (Jagaba et al. 2022a).

Coconut shell is the primary source of activated carbon in the gold mining industry due to its high carbon concentration, mechanical strength, low ash content, high yield, resistance to attrition and low cost. Although any carbonaceous material can be converted into activated carbon, it has been reported that coconut shells provide a high-quality vapour-adsorbent carbon (Qiu et al. 2021). The adsorbent made from coconut shell and other natural materials is cost-effective and durable. Coconut shell contains 33.61% of cellulose, 36.51% of lignin, 29.57% of pentosans and 0.61% of ash (Al-Dhawi et al. 2020).

The objective of this study is to investigate the efficacy of coconut shell-activated carbon in treating abattoir wastewater effluent from a meat factory in Bauchi, Nigeria, and to establish the kinetics of organic pollutants adsorption. Aspects of the chemical activation of coconut shell to produce activated carbon are also studied. The study will seek to provide a baseline and guide for locally produced activated carbon to reduce wastewater treatment costs for local industries, but also serves as a pathway to boost local content and improve the nation's gross domestic product (GDP), by reducing reliance on expensive processes has justified the effort of the research.

2 Materials and Methods

Experimental Materials

Various instruments and reagents were used to collect, preserve, characterize and analyse the wastewater samples before, during and after treatment. A kiln, calorimeter, an evaporator dish, a sample cell, a beaker, a measuring cylinder, a pH metre, digital metre, a pipette, nitric acid, zinc chloride and chlorine are among the materials utilized in this study.

Water Sample collection

The quality of data on wastewater chemical, physical and biological elements is influenced by sample collection and analysis. The wastewater was collected at the discharge point of the Bauchi Meat Factory during the washing period of the slaughtered animals. Two samples were taken, rinsed in distilled water and collected in 1-L airtight plastic sampling bottles (Make-Tarsons) (Yu et al. 2015). This was done to ensure that micro-organisms in water received oxygen and to determine the presence of anions and cations at each water point. Filtered samples were filled to the brim of the bottle with 0.45 mm membrane and stored (Jagaba et al. 2021c)

according to standard methods for water analysis as prescribed by the EPA (Noor et al. 2021). The samples were taken in ice bags for storage and analysis (Saeed et al. 2021b).

Preparation of activated carbon

Coconut shells were gathered, split into little pieces and cleaned with tap water before being used. After that, it was dried for 15 days. To remove moisture and other volatile impurities, the dried coconut shell components were oven dried for 24 h at 150 °C. The coconut shell was crushed and sieved into a 300–700 µm size range. It was then activated with $ZnCl_2$ to achieve a 100% Impregnation ratio (500 gm dry precursor was thoroughly combined with 3000 ml concentrated $ZnCl_2$ solution containing 500 gm $ZnCl_2$). It was thoroughly mixed and kept for 24 h to properly soak $ZnCl_2$ onto its surface. The slurry was heated for 24 h at 100 °C in the oven (Ghaleb et al. 2021). The dehydration reagent $ZnCl_2$ was utilized in this investigation to reduce the carbonization temperature during chemical activation, preventing tar formation and promoting carbon char (Baloo et al. 2021; Jagaba et al. 2022b).

Muffle furnaces were used to keep the chemically impregnated samples in a galvanized iron pipe of specific dimensions. Under a nitrogen flow rate of 120 cm3 min-1 STP, materials in the furnace were heated to a final carbonization temperature of 650 °C. This was done for an hour at 650 °C. Then it was cooled completely with a continuous flow of nitrogen gas. Various organic and mineral matters were removed from the dried material by washing it 2–3 times with 0.5 N HCl and afterwards with warm distilled water. Afterwards, the solution had to be rinsed with cold water in order to neutralize the sample. Finally, the sample was dried for 24 h in a 100 °C oven before being sealed in an airtight container (Sule Abubakar et al. 2016).

Analysis and analytical methods

Standard techniques were used to test the wastewater samples for pH, electric conductivity (EC), COD, colour, TSS, turbidity, ammonia (NH4), nitrogen and phosphate (Nasiru et al. 2016).

Chemical Oxygen Demand

This study used the HACH method to assess COD. Four HACH test tubes were made with potassium dichromate (KD), distilled water and concentrated sulphuric acid. The first sample served as a blank, while others were utilized for the sample run (Hussaini Jagaba 2018). A dilution factor of 50 was used to dilute the samples. The first test tubes would be filled with distilled water (2 mL) as a blank, and

the remaining three test tubes were filled with 2 mL of diluted sample. After two hours of refluxing each for test tube mixture, calorimetrically, the oxidant used up in the sample was determined. The COD was determined using the DR 6000 spectrophotometer. In this case, the COD reduction efficiency (%) is the ratio of the difference between COD initial abattoir wastewater discharged and final COD of abattoir wastewater discharge after treatment to the initial COD of abattoir wastewater discharged.

pH (APHA Standard Method 4500)

Standard procedure was followed for the initial and subsequent pH tests (Jagaba et al. 2021b). The pH of the abattoir wastewater sample was measured with HQ440d HACH pH metre before and after treatment. The initial pH for coagulation was determined using sulphuric acid and sodium hydroxide solutions.

For TSS (Standard procedure 2540D), filtration was done with 5 mL raw wastewater sample. On the other hand, to shear bigger particles, the sample was agitated at high speed with a magnetic stirrer. A stopwatch was used to time the flow of the filtering of the sample water. Before transferring the filter to the aluminium weighing dish, a desiccator was employed to balance the temperature.

Below is the formula used to calculate the TSS concentration:

$$TSS\left(\frac{mg}{1}\right) = \frac{1000 * (A - B)}{\text{volume of Sample in ml}} \quad (1)$$

where

A = the weight of the sample and the filter, in milligrams
B = weight of the filter, in milligrams.

Colour (USEPA, Method 8025)

The raw colour of abattoir wastewater was measured using a DR 6000 HACH spectrophotometer by the standard platinum-cobalt method for both the influent and effluent. Two test tubes were prepared to analyse the colour: the first was filled with deionized water and used as a control, while the second test tube was filled with diluted wastewater sample. A procedure number 125, which corresponds to 465 nm wavelength colour measurement, was selected after inputting both test tubes into the cell holder, pressing zero for control and reading the second test tube's colour, which contained the wastewater sample (Jagaba et al. 2021b).

Batch Adsorption Study and Procedure

At temperatures between 24 and 27 °C, batch adsorption studies were conducted to obtain the equilibrium data
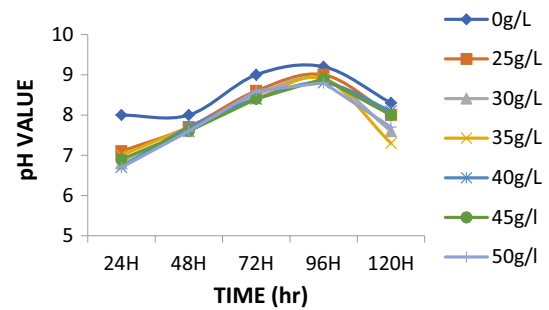
needed for the wastewater/effluent treatment system's design and operation. A series of 2-L containers were used for equilibrium studies. Each container held 2000 ml of effluent and was placed in a flocculate-control assembly. A known amount of adsorbent (25, 30, 35, 40, 45 and 50) g/l was added into each container with the exception of one known sample used as control sample (effluent sample without adsorbents) and all were well-labelled. For the desired time periods, the containers were covered and agitated intermittently (24, 48, 72, 96 and 120 h). On the basis of preliminary experiments, the contact time and other conditions (e.g. adsorbent dosage) were chosen. pH, COD, BOD, TSS, turbidity, electric conductivity, ammonia, chlorine, phosphate, sodium, phosphate, colour, total suspended solid, total solids and nitrogen were all determined after the solutions were separated from the adsorbent.
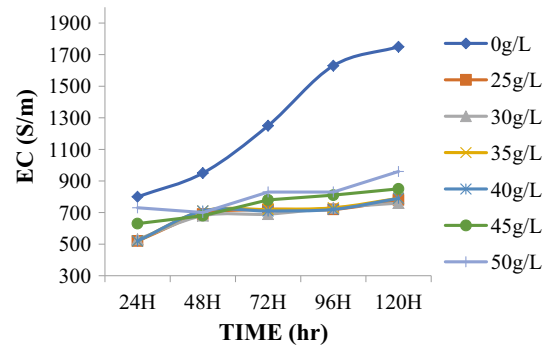
3 Results

The result of the target contaminants of the abattoir wastewater sample was presented in Table 1 and was used as control test for the adsorption study to investigate the efficacy of the coconut shell-activated carbon at different dosage and reaction time throughout the batch experiment. The effect of the ACS carbon at different dosage and reaction time for the selected target contaminants in this study is shown in Figs. 1, 2, 3, 4 and 5.

Fig. 1 Influence of pH on ACS adsorption

Fig. 2 Effect of EC on ACS adsorption
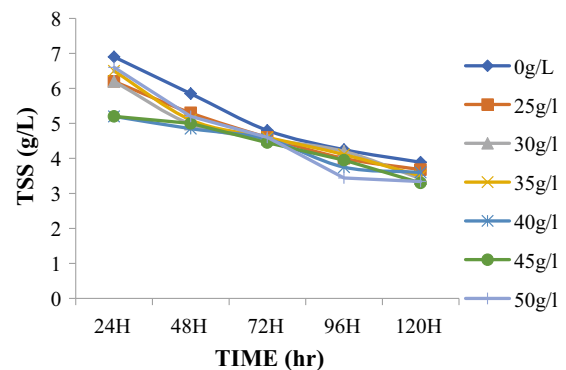
Fig. 3 Effect of TSS on ACS adsorption
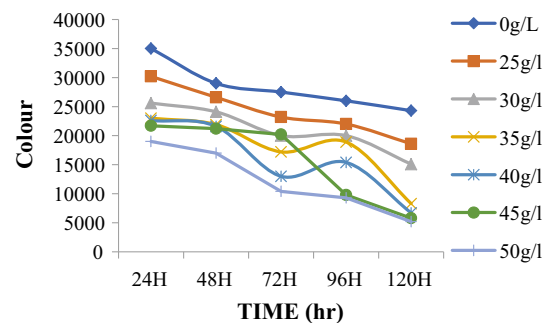
Fig. 4 Effect of colour on ACS adsorption

Table 1 Raw slaughterhouse effluent characteristics

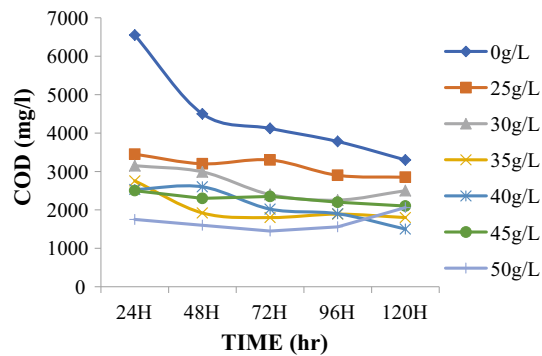| Parameters	Effluent from a slaughterhouse
pH	8.0
Turbidity (NTU)	6030
Total Dissolved Solid (ppm)	530
Electric Conductivity (Siemens/m)	800
COD (mg/l)	6550
BOD (mg/l)	1400
NH_4 (mg/l)	74.7
Chlorine Cl (mg/l)	69.5
Phosphate PO_4 (mg/l)	21
Sodium (mg/l)	268
Potassium (mg/l)	316
Colour (mg/l)	35,000
Total suspended solid	6.9
Total solids	536.9
Nitrogen	58

Fig. 5 Effect of COD on ACS adsorption

4 Discussion

The batch experiment's examined data revealed that the pH of the wastewater sample increases with reaction and peaked at 96 h with a sudden drop in pH. The minimum pH value of 6.7 was at 24 h.

The electrical conductivity of the sampled wastewater achieved a 56.57% removal at 120 h and optimum dosage of 40 g/l from 1750 Ms/m to 760 Ms/m.

Total suspended solid removal efficiency was 26.64% at 24 h and at optimum dosage of 45 g/l from 6.9 g to 5.2 g.

Colour removal efficiency was 78.6% at 120 h and at optimum dosage of 50 g/l which showed a sudden drop from 24,300 mg to 5200 mg.

Chemical oxygen demand removal efficiency was 73.28% at 24 h and at optimum dosage of 50 g/l with an initial value of 6550 mg/l to a final value of 1750 mg/l.

However, the removal kinetics was measured but study related to the dynamics of the reactions pathway was not studied. Therefore, the results of the analysed sample indicate the removal efficiency increased with dosage of the activated coconut shell carbon.

5 Conclusions

The physicochemical properties of some of the recalcitrant target parameters in the wastewater were determined. Activated coconut shell was used as an adsorbent in batch adsorption experiments for 24, 48, 72, 96 and 120 h at various dosages of 25, 30, 35, 40, 45 and 60 g/l to determine the optimum pH concentration and percentage removal of recalcitrant target parameters in wastewater.

The percentage removal of the various parameters measured, though sometimes sinusoidal, increases with an increase in dosage of activated coconut shell, according to the experimental results. The optimum dosage is defined as the smallest amount of adsorbent required to achieve maximum adsorption.

Coconut shell-activated carbon has proven to be useful in the treatment of abattoir wastewater to a certain level before safe disposal. Furthermore, the adsorbent's reaction time and dosage were found to influence the results for each parameter tested. Some of the results were found to be sinusoidal at different retention time and dosage. But almost all the target parameters like pH, electrical conductivity, total suspended solid, colour and chemical oxygen demand were found to have higher efficiency of removal at higher concentration of the adsorbent at adsorbent dose of 50 g/l.

References

N.S. Al-Dhawi, S.R.M. Kutty, N.M.Y. Almahbashi, A. Noor, A.H. Jagaba, Organics removal from domestic wastewater utilizing palm oil clinker (POC) media in a submerged attached growth systems. Int. J. Civil Eng. Technol. (IJCIET) **11**(6), 1–7 (2020)

N. Al-mahbashi et al., Column study for adsorption of copper and cadmium using activated carbon derived from sewage sludge. Adv. Civil Eng. **2022**, 1–11 (2022). https://doi.org/10.1155/2022/3590462

L. Baloo et al., Adsorptive removal of methylene blue and acid orange 10 dyes from aqueous solutions using oil palm wastes-derived activated carbons. Alex. Eng. J. **60**(6), 5611–5629 (2021). https://doi.org/10.1016/j.aej.2021.04.044

K. Elewa, A. Belal, O. El Monayeri, A.F. Tawfic, Application of metal-organic framework (Zn-Ph-D CP) for copper ion removal from aqueous solution. Ain Shams Eng. J. **13**(5), 101670 (2022). https://doi.org/10.1016/j.asej.2021.101670

V. Elumalai, K. Brindha, E. Lakshmanan, Human exposure risk assessment due to heavy metals in groundwater by pollution index and multivariate statistical methods: A case study from South Africa. Water (Switzerland), **9**(4) (2017). https://doi.org/10.3390/w9040234

A.A.S. Ghaleb, et al., Anaerobic co-digestion for oily-biological sludge with sugarcane bagasse for biogas production under mesophilic condition, in *IOP Conference Series: Materials Science and Engineering*, vol. 991, no. 1 (2020). https://doi.org/10.1088/1757-899X/991/1/012084

A.A.S. Ghaleb et al., Sugarcane bagasse as a co-substrate with oil-refinery biological sludge for biogas production using batch mesophilic anaerobic co-digestion technology: effect of carbon/nitrogen ratio. Water (switzerland) **13**(5), 1–23 (2021). https://doi.org/10.3390/w13050590

A. Hussaini Jagaba, Wastewater treatment using alum, the combinations of Alum-Ferric Chloride, Alum-Chitosan, Alum-Zeolite and Alum-*Moringa Oleifera* as adsorbent and coagulant. Int. J. Eng. Manag. **2**(3), 67 (2018). https://doi.org/10.11648/j.ijem.20180203.13

A. Hussaini Jagaba, S. Abubakar, M. Abdu Nasara, S. Muhammad Jagaba, H. Mohammed Chamah, I. Mohammed Lawal, Defluoridation of drinking water by activated carbon prepared from *Tridax*

Procumbens plant (A Case Study of Gashaka Village, Hong L. G. A., Adamawa State, Nigeria). Int. J. Comput. Theor. Chem. **7**(1), 1 (2019). https://doi.org/10.11648/j.ijctc.20190701.11

A.H. Jagaba, et al., Derived hybrid biosorbent for zinc(II) removal from aqueous solution by continuous-flow activated sludge system. J. Water Process Eng. **34**(January), 101152 (2020). https://doi.org/10.1016/j.jwpe.2020.101152

A.H. Jagaba et al., Degradation of Cd, Cu, Fe, Mn, Pb and Zn by Moringa-oleifera, zeolite, ferric-chloride, chitosan and alum in an industrial effluent. Ain Shams Eng. J. **12**(1), 57–64 (2021a). https://doi.org/10.1016/j.asej.2020.06.016

A.H. Jagaba et al., Evaluation of the physical, chemical, bacteriological and trace metals concentrations in different brands of packaged drinking water. Eng. Lett. **29**(4), 1552–1560 (2021b)

A.H. Jagaba, et al., A systematic literature review on waste-to-resource potential of palm oil clinker for sustainable engineering and environmental applications. Materials **14**(16) (2021c). https://doi.org/10.3390/ma14164456

A.H. Jagaba, S.R.M. Kutty, G.H.A. Salih, A. Noor, M.F.U. Md Hafiz, N.S.A. Yaro, A.A.H. Saeed, I.M. Lawal, Palm oil clinker as a waste by-product: utilization and circular economy potential, in *Elaeis guineensis*, ed. by H. Kamyab (IntechOpen, Malaysia, 2022a), p. 25

A.H. Jagaba et al., Kinetics of pulp and paper wastewater treatment by high sludge retention time activated sludge process. J. Hunan Univ. Nat. Sci. **49**(2), 242–251 (2022b)

M.A. Nasara, I. Zubairu, A.H. Jagaba, A.A. Azare, Assessment of non-revenue water management practices in Nigeria (a case study of bauchi state water and sewerage cooperation) assessment of non-revenue water management practices in Nigeria (a case study

of bauchi state water and sewerage cooperation). Am. J. Eng. Res. (AJER) **10**(5), 390–401 (2021)

A. Nasiru, C. Osakwe, I.M. Lawal, A.U. Chinade, Assessment of physicochemical parameters and heavy metals in gombe abattoir wastewater. Am. J. Eng. Res **5**(3), 64–69 (2016)

A. Noor, et al., Kinetic modelling of nutrient removal of petroleum industry wastewater remediation, in *2021 Third International Sustainability and Resilience Conference: Climate Change* (2022), pp. 216–220. https://doi.org/10.1109/ieeeconf53624.2021.9667961

B. Qiu, X. Tao, H. Wang, W. Li, X. Ding, H. Chu, Journal of analytical and applied pyrolysis biochar as a low-cost adsorbent for aqueous heavy metal removal: a review. J. Anal. Appl. Pyrol. **155**(February), 105081 (2021). https://doi.org/10.1016/j.jaap.2021.105081

A.A.H. Saeed et al., Pristine and magnetic kenaf fiber biochar for cd2+ adsorption from aqueous solution. Int. J. Environ. Res. Public Health **18**(15) (2021a). https://doi.org/10.3390/ijerph18157949

A.A.H. Saeed, et al., Modeling and optimization of biochar based adsorbent derived from Kenaf using response surface methodology on adsorption of CD2+. Water (Switzerland) **13**(7) (2021b). https://doi.org/10.3390/w13070999

A.H.J. Sule Abubakar, A.A.A. Latiff, I.M. Lawal, Aerobic treatment of kitchen wastewater using sequence batch reactor (SBR) and reuse for irrigation landscape purposes. Am. J. Eng. Res. (AJER) **5**(5), 23–31 (2016)

L. Yu et al., Microbial community structure associated with treatment of azo dye in a start-up anaerobic sequenced batch reactor. J. Taiwan Inst. Chem. Eng. **54**, 118–124 (2015). https://doi.org/10.1016/j.jtice.2015.03.012

Vehicular Network Spectrum Allocation Using Hybrid NOMA and Multi-agent Reinforcement Learning

Lina Elmoiz Alatabani, Rashid A. Saeed, Elmustafa Sayed Ali,
Rania A. Mokhtar, Othman O. Khalifa, and Gasim Hayder

Abstract

The recent years have seen a proven impact of the reinforcement learning use in many applications which showed tremendous success in solving many decision-making paradigms in machine learning. Most of the successful applications involves the existence of more than one agent, which makes it fall into the multi-agent category, taking autonomous driving as an example of these applications. We know that today's Internet of Vehicles (IoVs) consists of multi-communication patterns which work efficiently in keeping all the IoV network components connected. With regards to sharing the frequency spectrum, applying Non-Orthogonal Multiple Access (NOMA) communication built over deep deterministic policies gradients (DDPG) scheme to cope with the rabid erratic channels conditions due to fast mobility nature of vehicles network has proven promising results. In this paper the framework of NOMA communication-based DDPG and multiple agent reinforcement learning approach (MARL) are discussed in brief, and then, the performance evaluation of DDPG scheme compared with MARL and random spectrum allocation approaches for vehicular network spectrum and resources allocation is analysed.

Keywords

Spectrum allocation • V2V communications • Hybrid NOMA • Reinforcement Learning • MARL • DDPG • Random allocation

1 Introduction

In the process of enhancing the driving experience in terms of safety and traffic efficiency in Internet of Vehicle (IoV) framework, vehicle-to-everything (V2X) have been recognized as an essential technology which provide connectivity to the IoV network. Many connection mechanisms have been proposed but cloud-based cellular network has more advantages when it comes to coverage range and computation (Abdelgadir and Saeed 2020; Liang et al. 2019). There are two connection modes in V2X communications, they are vehicle-to-infrastructures (V2I) and vehicles-to-vehicles (V2V). These communication modes are utilized to carry IoV application such as traffic monitoring which will require frequency in the use of V2X server using high throughput V2I networks, besides the real times delivery of safety related messages using V2V communications (Duan et al. 2020; Alawi et al. 2014; Liu et al. 2020).

In general, vehicle networks may suffer from several impairments, especially in variable communication media, such as path loss, time-selective wireless channels, in addition to shadowing and multiple interference to multiple vehicles. Therefore, the radio spectrums are allocated in such a way that it helps to improve the communication performance by efficiently exploiting the wireless channels (Abdelgadir et al. 2018). There are a number of methods and

L. E. Alatabani (✉) · R. A. Saeed · E. S. Ali
Department of Electronics Engineering, Sudan University of Science and Technology (SUST), Khartoum, Sudan
e-mail: lina.alatabani@gmail.com

E. S. Ali
Department of Electrical and Electronics Engieering,
Red Sea University (RSU), Port Sudan, Sudan

R. A. Saeed · R. A. Mokhtar
Department of Computer Engineering, College of Computers and Information Technology, Taif University,
P.O. Box 11099 Taif, 21944, Saudi Arabia

O. O. Khalifa
Department of Electrical and Computer Engineering,
Faculty of Engineering, International Islamic University Malaysia, Gombak, Malaysia

G. Hayder
Department of Civil Engineering, College of Engineering,
Universiti Tenaga Nasional (UNITEN), 43000 Kajang,
Selangor Darul Ehsan, Malaysia

techniques that have been proposed aims to improve the IoV spectrum allocations.

Most of the previous methods follow the approach of formulating an improvement in spectrum allocation problem to obtain an optimal solution based on the differences between goal performance and complexity (Liu et al. 2020). In vehicle networks, optimization methods require that they must be activated several times when any change in the channel and network topology occurs, which leads to increased operating costs. AI techniques contribute to provides a unique solution to improve spectrum allocation methods especially those related to channel, energy and spectrum management for communications between different vehicle networks (Eltahir et al. 2016). For example, the reinforcement learning (RL) can be used to allocate energy into a distributed channel for inter-vehicle communication in V2V networks within the constraints of V2V link latency and interference effect.

The RL agent enables to interact with IoV environment and related with each V2V link. The IoV environmental characteristics can be defined as a set of V2V and V2I link channel information, by the RL, in addition to learns the policy to select the channel power as an action according to the channel info, like the remaining traffic amount, latency, and interference level. The agent related to V2V link helps to observes the IoV environmental states, and take decisions according (Aoki et al. 2020). This approach is considered as an optimal decision policy for spectrum allocations based on RL scheme.

Multi V2V channels enables for sharing links with pre-occupied V2I channels enables to provide enrich services requirement in vehicles network. For such purpose, there is a need to a scheme able to provides maximum V2I links capacity with intelligent power allocation. Through this motivation, the paper presents and evaluates the performance of the most recent efficient scheme that enables to allocating resources and managing the channels spectrum according to the different communications and bandwidth capacities required in vehicle networks (Li and Guo 2019a). The evaluated scheme is based on NOMA and deep deterministic policies gradients which considered to provide higher V2V communications throughput and ensures acceptable latency for spectrum sharing and power transmission control. The paper evaluates the proposed scheme with various other related techniques and discusses its comparative performance.

The reminder of the sections of this manuscript are arranges in this sequence, Sect. 2, we discussed the closed related work. Section 3 presented the research approach for spectrum allocation by using multiple agent reinforcement learning and the NOMA based on deep deterministic policies gradients (DDPGs) approach. Section 4 shows the simulation model and parameters, and the results and discussions is Sect. 5.

2 Related Works

In Liang and Ye (2020) the sharing of spectrum and resources for in vehicles network challenges using multiple agent reinforcement learning is investigated, where number of vehicles-to-vehicles (V2Vs) link reutilize the spectrum frequencies which is pre-occupied by vehicles-to-infrastructures (V2Is) link. Rapid channels change in high vehicular mobility environment prevent the network capabilities of gathering precise instant channels status data at the base station (BS) for central spectrum allocation and management. The paper modelled based on the sharing the spectrum resources as a multiple agents' reinforcement learning issue, which is resolved by utilizing a deep Q-networks fingerprint approach that is acquiescent to a decentralized model and implementations.

Authors in Yi-Han et al. (2020) review the resources management and allocations challenges in vehicular networks by using and employed non-orthogonal multiple-access (NOMA) technique is investigated, where aim to use the spectrum frequencies sharing that is pre-occupied by the vehicle-to-infrastructures devices (V2Is). In answer the author modelled the spectrum and other resources allocation issue using a distributed Discrete driven time and Finite-states Markov decisions procedures (DFMDPs), in which distribution decision are achieved by multi-agent that does not has whole and complete networks data.

In Zhang et al. (2020), authors proposed a deep reinforcement learning based on decentralized selection mode and V2Xs cellular network resources allocation communications to focus on the challenges occurring from QoS requirement and the untrustworthyV2V link. By utilizing Markov decisions procedures (MDPs) along with the DRL-based distributed procedure to ensure reliability and an efficient outage probability is measured in the reward functions.

In Li and Guo (2019b) two distributed spectrum allocations based on actor critic framework is proposed which are trained in a centralized environment and executed in a decentralized manner. Learning by using user's historical data, actions, and policies in order to decrease the time taken for the learning process and the computational complexity. The proposed methodology also transfers the complex training processes to the base stations (BSs) to reduce the computation complexity caused by algorithm execution.

Authors in Yi-Han (2020), investigates in the methods used to solve the resources allocation issues in vehicular communications. The authors provide a mechanism based on multi-agent Deep Deterministic Policies Gradients (DDPGs), enable to improves the resource allocation in vehicles-to-vehicles (V2Vs) communication. They used NOMA technologies to share frequency spectrum and pre-allocate it to

vehicles-to-infrastructures (V2Is) networks. The results present that the proposed approach gives maximum sum-rate of V2Is networks and ensuring the reliability and latency requirements of safety the critical data transmissions.

In Muhammad et al. (2020), the researchers presented a method for allocating spectrum resources to IoV services based on cloud computing infrastructure. The authors presented a method for using a machine learning (ML) approach to resource management by predicting network traffic at the edge in vehicle networks. The proposed method allows for smart resource allocation that helps save energy while ensuring the optimization of the various vehicle communication services resources.

3   Vehicular Network Spectrum Allocation

Vehicle networks provide a number of services related to smart cities and self-driving, which require satisfactory quality-of-services (QoSs) and quality-of-user-experiences (QoE), which is are the criteria's that is difficult to obtain due to the limiting factors of vehicle communication channels in the event of errors or congestion. According to that, it is very important to allocate the use of available wireless network resources in a very efficient manner. This section presents a brief concept of the NOMA scheme, and two methods used in this paper with the aim of improving resource allocation in V2V networks.

3.1   Non-orthogonal Multiple Access (NOMA) Communication

In 5G wireless communications, NOMA provides a potential benefits in radio access when compared to the OFDMA. NOMA enables to enhance the spectrum efficiency, in addition to reduce latency for massive communication networks (Zhao et al. 2016). IN NOMA, many users can share the same resources at the same, frequency, time, and space which provides a means of ability to be applied for 5G communications, and in IoT as well.

NOMA enables number of users to use the same resources, which causes interference between communication systems, but the use of resource management techniques and reduce interference, especially in dense networks, helps to overcome these problems. There are two types of current NOMA schemes, which are known as the energy field NOMA and NOMA Coding Domain. Power level provides levels that allow multiple users to send the signals by sharing the frequency code resources at same time so that the power level is determined by the user based on his channel gain (Noura et al. 2021).

As an example, in case of multiple users with a single base station, the transmitted signal from the base station to the users is formed as superposition coded signal as follows:

$$\text{Signal} = \sqrt{p_1}x_1 + \sqrt{p_2}x_2 + \ldots \sqrt{p_n}x_n \tag{1}$$

where x_1, x_2, and x_n preprepresent the the transmitted signals from the BS to users, p_1, p_2, and p_3 are the the transmit power for users.

Particularly, the system power is predefined based on adopted power allocation. The receive signal is depends on, the gain of channel between the base station and users, the Gaussian noise, in addition to the interferences and power spectral density. By applying NOMA, a highly spectrum-efficient can be achieved which improved the system throughput (Amer et al. 2021). Moreover, NOMA power allocation enables the communication system to balancing between the users fairness and throughput.

3.2   Multi-agent Reinforcement Learning

As for the demanding and fast varying nature of vehicular networks, considering spectrum access design which consists of both vehicles-to-vehicles (V2Vs) and vehicles-to-infrastructures (V2Is) connectivity as presented in Fig. 1, the V2I generally provides connection for all vehicles to the base stations (BSs) or BSs road side units (RSUs). While V2V usually provides direct connection within the neighbouring vehicle. Focussing on the vehicles-to-everything V2X structure provided by the 3rd Generations Partners Project (3GPP), which is supported by 5G networks because of the high bandwidth demand of V2X communications (Canese et al. 2021).

On the Internet of Vehicles (IoV) structure, multiple V2Vs channels try to share scarcity spectrum resources which is reallocated by V2Is channels. For the nature of IoV which can be explained as multi-agent environment, came the need for the application of Reinforcement Learning RL upon this type of environment, i.e. "high mobility" (Budhiraja et al. 2021). By which each V2Vs channels are acting as agent interconnects with the unknown network environments to gain experience. Thus, V2Vs agents cooperatively inspect the unknown environment and clarify resources allocations and power control schemes with the consideration of their own observations.

The RL frameworks of modelling for the IoV environment can be firstly described by the single-agent formulation. The fundamental elements those can be used to describe the relationship between the agents and environment are, state, actions, and reward. The configuration of the environment is provided by the state, and the options of agents achieved by action which interact to modify the

Fig. 1 IoV network elements
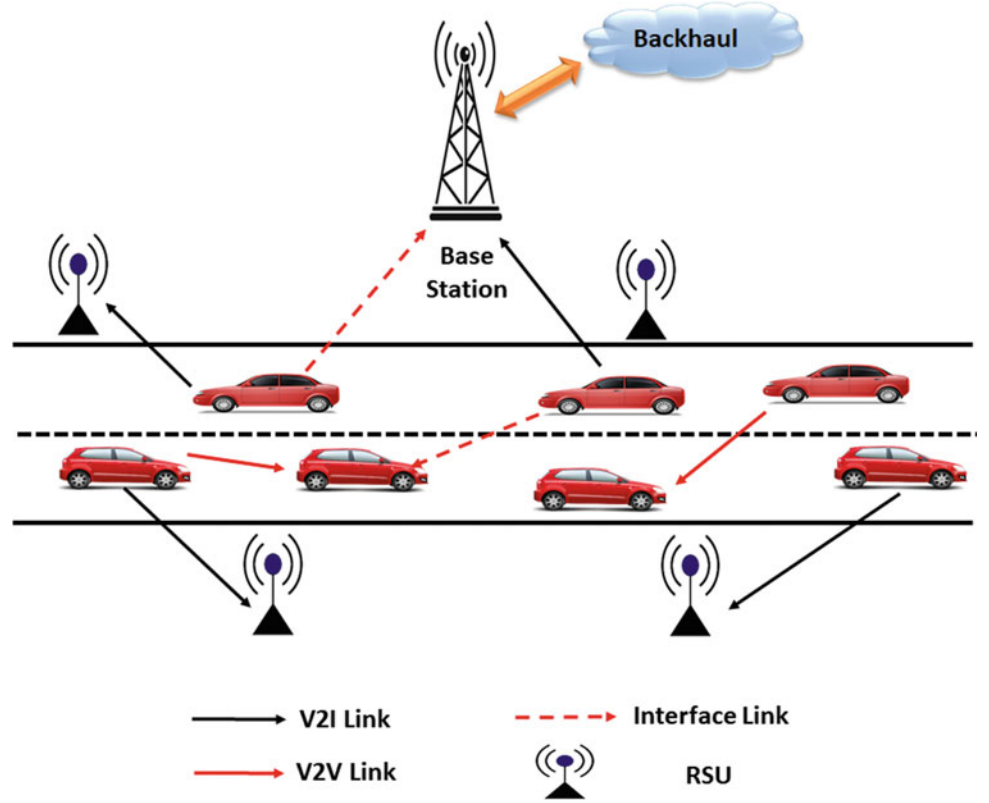
environment (Palanisamy 2020). The signal used to define the agent task is a reward, acting to motivates the agent to take actions after sensing the environments.

The best selected action can be determined due to the policy adopted by agent. For optimal policy, a return value Rt is used overtime horizon T for a finite length and non-finite time as follows (Hu and Li 2021):

$$R = \sum_{i=0}^{T-t-1} \gamma^i r_{t+i+1}; \text{ finite time horizons} \quad (2)$$

$$R = \sum_{i=0}^{\infty} \gamma^i r_{i+1}; \text{ non-finite time horizons} \quad (3)$$

where r_t is the reward received by the agent at the time-step t. γ is a discounted factor between 0 and 1. If we denotes the policy by π, the value function of the state action can be calculated as follows:

$$Q_\pi(s,a) = E[Rt \mid St = s, a_t = a, \pi] \quad (4)$$

For multi-agent framework, Markov Games is considered as a main framework for decision-making with multiple agents. The Markov Game enables to use multiple agents to interact with shared environment and with each other. It's an extension of Markov decision process (MDP) that helps to describing the probability of a state transition (Hu and Li 2021). The multiple agent reinforcement learning have different denied models according to stochastic games and Markov decision process in addition to Nash equilibrium.

The multi-agent RL methods have two stages, the learning or training stage and the execution stage (Moubayed et al. 2020). The learning phase is centralized, while the implementation stage is distributed, meaning that in the training stage the network performances oriented recompense can be accessed by each single V2Vs agents, which them alters its action towards and optimum policy through updating its deep Q-Networks (DQNs) (Alawi et al. 2012). While in the execution stage local observations of the environment is collected by each V2V agent and then an action is chosen conferring to the trained DQNs on a scales of time with small-scale channels fading (Jameel).

The components of the multi-agent RL model is described as follows:

(a) **States and Monitoring**: In the multi-agent RL MARL the sharing of resource issue can be seen as all V2Vs channels k act and agent trying to explore the unknown environment (Eltahir et al. 2013). The issue can be modelled mathematically as: at each coherent time t step we give the present state's environment the V2Vs channel k receive and monitor Z of the environment, gk [m] is power gain for V2Vs channel and gk[m] is power gain for V2Is channel.

(b) **Action Space**: The sharing of vehicular spectrum and channels resources is concluded at the sub-band spectrum selections by which each sub-band is pre-occupied by V2Is channels, and power transmission in which the given model chose to limit down the power control options to 4 levels for the sake of ease of practise (Liu and Shoji 2019). There for the action space dimension is $4 \times M$ where M represents disjoints sub-band which the spectrum is broken into.

(c) **Reward Design**: RL has appealing qualities when it comes to resolving the problem with difficult to optimize objectives, which is the reward model flexibility (Ali et al. 2021). In the V2Xs spectrum allocation issues the objectives are to enhance the sum V2Is throughput which enhancing the probability of success for V2Vs channels within a given constraint of time T which can also be modelled mathematically.

(d) **Learning Algorithm**: Focussing on episodic configuration where each episode expands the V2Vs data delivery and throughput at constraint of time T, each episode is starting with a random selection power transmission for vehicular link channel status and a full V2Vs data packet size B that takes until the end of time T (Moon et al. 2020).

3.3 NOMA Communications-Based DDPG Framework

Today's IoV applications are rapidly developing, the need to meet the QoS requirements has also grown as a result, all in which for the purpose of giving the best driving experience for users in terms of efficiency, security, and other QoS requirements. This has extracted the attention of researchers in order to deliver the required service with the best qualities and standards (Bai et al. 2019; Khan et al. 2019; Alatabani et al. 2020). 3GPP partners have initiated project to deal with divers V2X QoS requirement by utilizing the discussed devices-to-devices (D2D) communication with long-terms evolutions (LTEs) and 5G cellular networks, D2D communications has shown great results in terms of meeting the QoS requirements in V2X and at the same time supporting for high mobility, there for D2D-based non-orthogonal multi-access (NOMA) communications is considered for resource allocation which enhances latency and other QoS requirements (Qiu et al. 2020; Vaezi et al. 2019; Ahmed et al. 2020).

Resource allocation-based deep learning model is proposed and shown promising results. The Discrete-time and finite-state Markov decision process (DFMDP) model which can be described as a tuple (S, A, p, r) in which S represents infinite states set, A is a finite set of actions, p is a probability of transmission for states to s', and r is the obtained reward after an action is implemented (Vaezi et al. 2019). However, the model has limitations when it comes to processing tasks in continuous action space. There for an enhancement has been done and a new model has been proposed using Deep Q-learning (DQL) instead of the original QL algorithms. The multi-agent Deep Deterministic Policy Gradient (DDPG) goal model is to look for the optimal policies for resource allocation for V2X with the goal of selecting appropriate bands of spectrum and power transmission that satisfies QoS requirement (Zhang et al. 2020). Although Deep Reinforcement Learning algorithms are superior to the conventional Q-learning but still it cannot handle continuous action space. Therefore, DDPG algorithm used deep neural networks DNN to learn competitive policies and overcome the limitations.

4 System Model and Parameters

The network model is considering for cellular-based vehicular communication enables to provides links for both V2Vs and V2Is networks. In network scenario, all transceivers rely on the use of NOMA technology to improve spectrum efficiency and reuse it in V2I communications for the uplink spectrum. The assumptions also consider the mutual interferences between V2Is and V2Vs networks. The multi-agent RL-based resources allocation is considered in the scenarios as a mechanism enables to access scarcity spectrum shared by V2Is channels. The use of multiple V2V agents enable to collect and extracts the environment information for spectrum sharing, allocations, and power control approaches based on their own observations of the environment state.

The simulation model is based on the vehicles network consists of four V2V and V2I channels with carrier frequency 2 GHz based on the urban case defined by 3 GPP TR 36.885. The description of network according to the 3GPP TR36.895 is consider the M V2I channels are begin by M vehicles and the K V2Vs channels are designed among all vehicles with its surrounding neighbours. Table 1 shown the main simulations parameters for network evaluation scenario.

5 Results and Discussion

The simulation results present the evaluation performance of various spectrum allocation schemes for vehicular network compares with multi-agent reinforcement learning (MARL). First the comparison of MARL with random baseline and single-agent RL model (SARL) is shown in Fig. 2. In Fig. 3, the performance evaluation between the DDPG and related resource allocations are observed.

Table 1 Simulations parameters settings

| Parameters	Values
Vehicles mobility model	Urban case
V2Is channels M channel	4
V2Vs channels N channel	4
Carrier frequencies	2 GHz
Bandwidth per channel	4 MHz
Base station antenna height	25 m
Base station antenna gain	8dBi
Vehicle's antenna	1.5 m
Vehicle's antenna gain	3dBi
Vehicle's receiver NF (noise figure)	5 dB
Vehicles speeds	36 km/h
V2I transmission power	23dBm
V2V transmission power	5, 10, 23, − 100 dBm
Noise power	− 114 dBm
V2V payload size B	$[1,2,3,\ldots] \times 1060$ bytes
Latency constraint of V2V payload delivery	100 ms
Shadowing distribution of V2I communications	Lognormal
Shadowing distributions of V2V communications	Lognormal
fading	Rayleigh

As shown in Fig. 2, the results of the performance evaluation for MARL are compared with random baseline and SARL schemes based on the payload size of each V2V communication. It is noticeable that the MARL scheme gives higher performance compared to other methods, as it can optimally distribute the spectrum to the sub-bands and have the ability to control the transmission power and maintain the continuity of V2V communications. However, the increasing of each V2V connection payload to approximately 6Mbits, will decrease the network throughput by up to 90%. Compared to other methods, MARL have the ability to ensure the reliability and latency requirement of V2Vs channels in a high-traffic vehicles networks. When the load size increases,

the performance of both the random and the SARL schemes are closed, while the MARL method maintains the high performance, which ensures the latency V2V communication and the high capacity of the network throughput.

As can be seen in Fig. 3, it found that the growth in the vehicles number leads to a reduction in the network throughput for V2I communications in general. This drawback is due to the interference between V2V and V2I communications when the number of vehicles are increased. This will lead to decreasing in communication rate and throughput in V2I networks. When looking at the DDPG mechanism, it found that, the DDPG gives highest throughput of V2I networks compared to other methods due

Fig. 2 MARL model performance evaluation
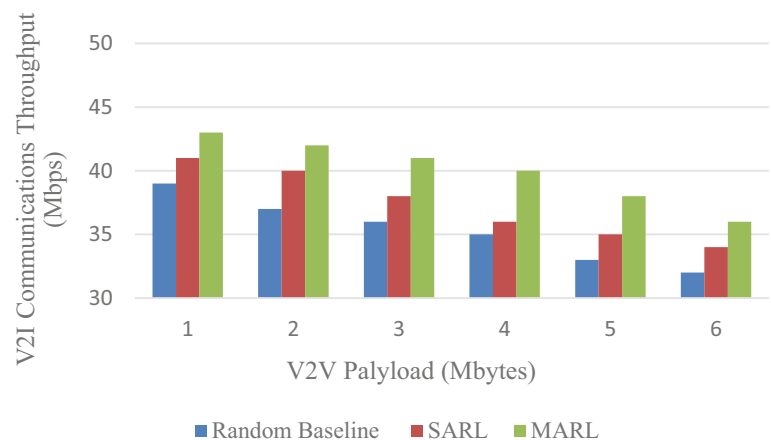
Fig. 3 DDPG model
performance evaluation
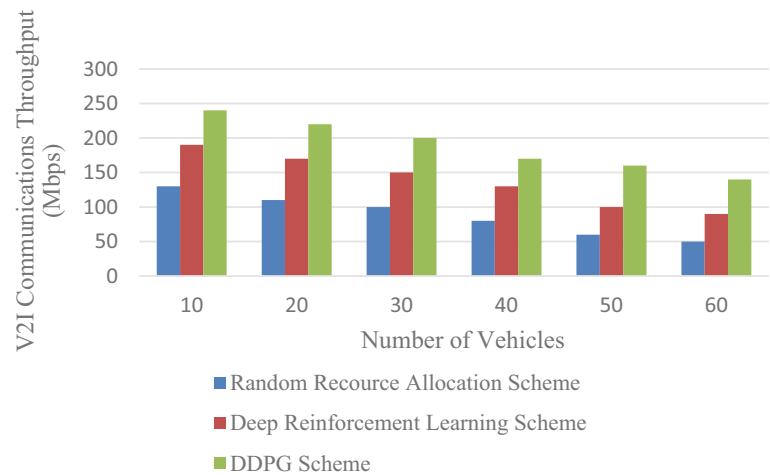
to its ability to allocate optimal resources at a high rate. When compared to other schemes, it found that the random resources sharing and allocations approach gives the least performance because of the random resource allocation method, which increases the interferences among V2Is and V2Vs channels. Also, the use of deep reinforcement learning can improve performance significantly more than random scheme, however, it can unable to gives optimal resource allocation because of continuous states of transmission powers.

6 Conclusion

The important of the topic under study is to optimally allocate resources and spectrum for V2Xs communication underlying cellular network. Current researchers are studying ways to enhance the performance of IoV networks using artificial intelligence in general and deep learning to be specific. A prospect research would be to look at this problem and combine techniques and models together to have the optimum system that is efficient and with excellent performance in the high demanding environment of IoV for the main aim of giving the best driving experience to users within the IoV network.

References

M. Abdelgadir, R.A. Saeed, Evaluation of performance enhancement of OFDM based on cross layer design (CLD) IEEE 802.11p standard for vehicular ad-hoc networks (VANETs), city scenario. Int. J. Sig. Process. Syst. **8**(1) (2020)

M. Abdelgadir et al., Cross layer design approach for efficient data delivery based on IEEE 802.11P in vehicular ad-hoc networks (VANETS) for city scenarios. Int. J. Ad Hoc Netw. Syst. (IJANS) **8** (4) (2018)

R.S. Ahmed; E.S. Ali, R.A. Saeed, Machine learning in cyber-physical systems in industry 4.0. in *Artificial Intelligence Paradigms for Smart Cyber-Physical Systems,* ed. by A.K. Luhach, A. Elçi (IGI Global Book Publisher, 2020)

L.E. Alatabani, E.S. Ali, R.A. Saeed, Deep learning approaches for IoV applications and services. *Intelligent Technologies for Internet of Vehicles* (Springer, 2020)

M. Alawi, R. Saeed, A. Hassan, O. Khalifa, in *Internet Access Challenges and Solutions for Vehicular Ad-Hoc Network Environment*, IEEE International Conference on Computer & Communication Engineering (ICCCE2012), 3–5 July 2012, Malaysia (2012)

M.A. Alawi, R.A. Saeed, A.A. Hassan, R.A. Alsaqour, Simplified gateway selection scheme for multi-hop relay vehicular ad hoc network. Int. J. Commun. Syst. **27**(12), 3855–3873 (2014)

E.S. Ali, M.K. Hasan, R. Hassan, R.A. Saeed, M.B. Hassan, S. Islam, N.S. Nafi, S. Bevinakoppa, *Machine Learning Technologies for Secure Vehicular Communication in Internet of Vehicles: Recent Advances and Applications*. J. Secur. Commun. Netw. (SCN) **2021** (2021)

A., Asmaa, A.-M. Ahmad, S. Hoteit, Resource allocation for downlink full-duplex cooperative NOMA-based cellular system with imperfect SI cancellation and underlaying D2D communications. Sensors **21**(8), 2768 (2021). https://doi.org/10.3390/s21082768

S. Aoki et al., *Cooperative Perception with Deep Reinforcement Learning for Connected Vehicles*. arXiv (2020)

Z. Bai, W. Shangguan, B. Cai, L. Chai, in *Deep Reinforcement Learning Based High-level Driving Behavior Decision-making Model in Heterogeneous Traffic*. Chinese Control Conference (2019)

I. Budhiraja, N. Kumar, Deep reinforcement learning based proportional fair scheduling control scheme for underlay D2D communication. IEEE Internet of Things J. **8**(5) (2021)

L. Canese et al., Multi-Agent reinforcement learning: a review of challenges and applications. Appl. Sci. **11**, 4948 (2021). https://doi.org/10.3390/app11114948

W. Duan, J. Gu, M. Wen, G. Zhang, Y. Ji, S. Mumtaz, Emerging technologies for 5G-IoV networks: applications, trends and opportunities. IEEE Netw. **34**(5) (2020)

A.A. Eltahir, R.A. Saeed, M.A. Alawi, An enhanced hybrid wireless mesh protocol (E-HWMP) protocol for multihop vehicular communications. 2013 Int. Conf. Comput. Electr. Electron. Eng. (ICCEEE) 1–8 (2013)

A.A. Eltahir, R.A. Saeed, A. Mukherjee, M.K. Hasan, Evaluation and analysis of an enhanced hybrid wireless mesh protocol for vehicular ad-hoc network. EURASIP J. Wirel. Commun. Netw. (1), 1–11 (2016)

B. Hu, J. Li, An edge computing framework for powertrain control system optimization of intelligent and connected vehicles based on curiosity-driven deep reinforcement learning. IEEE Trans. Indust. Electron. **68**(8) (2021)

F. Jameel et al., Efficient mining cluster selection for blockchain-based cellular V2X communications. IEEE Trans. Intell. Trans. Syst. (Early Access)

H. Khan, A. Elgabli, S. Samarakoon, M. Bennis, C.S. Hong, Reinforcement learning based vehicle-cell association algorithm for highly mobile millimeter wave communication. IEEE Trans. Cognitive Commun. Netw. **5**(4) (2019)

Z. Li, C. Guo. *Multi-Agent Deep Reinforcement Learning based Spectrum Allocation for D2D Underlay Communications*. arXiv (2019a)

Z. Li, C. Guo. Multi-Agent deep reinforcement learning based spectrum allocation for D2D underlay communications. IEEE Trans. Vehicular Technol. (2019b)

L. Liang, H. Ye, Deep-Learning-Based wireless resource allocation with application to vehicular networks. Proc. IEEE **108**(2) (2020)

L. Liang et al., Spectrum sharing in vehicular networks based on multi-agent reinforcement learning. IEEE J. Select. Areas Commun. **37**(10), 2282–2292 (2019)

W. Liu, Y. Shoji, Edge-Assisted vehicle mobility prediction to support V2X communications. IEEE Trans. Vehicular Technol. **68**(10) (2019)

Y. Liu, Z. Jiang, S. Zhang, S. Xu, Deep reinforcement learning-based beam tracking for low-latency services in vehicular networks. arXiv 2020

Z. Liu et al., *Joint Optimization of Spectrum and Energy Efficiency Considering the C-V2X Security: A Deep Reinforcement Learning Approach*. arXiv (2020)

S. Moon et al. Deep learning-based channel estimation and tracking for millimeter-wave vehicular communications. J. Commun. Netw. (2020)

A. Moubayed, A. Shami, P. Heidariy, A. Larabi, R. Brunner, *Edge-enabled V2X Service Placement for Intelligent Transportation Systems*. arXiv (2020)

A. Muhammad, T.A. Khan, K. Abbass, W.-C. Song, in *An End-to-end Intelligent Network Resource Allocation in IoV: A Machine Learning Approach*, 2020 IEEE 92nd Vehicular Technology Conference (VTC2020-Fall), (2020), pp. 1–5. https://doi.org/10.1109/VTC2020-Fall49728.2020.9348842

H.N. Noura, R. Melki, A. Chehab, Efficient data confidentiality scheme for 5G wireless NOMA communications. J. Inf. Secur. Appl. **58**, 102781 (2021), ISSN 2214-2126. https://doi.org/10.1016/j.jisa.2021.102781

P. Palanisamy, in *Multi-Agent Connected Autonomous Driving using Deep Reinforcement Learning*". IEEE 2020 International Joint Conference on Neural Networks (IJCNN), Glasgow, UK (2020)

H. Qiu et al., Secure V2X communication network based on intelligent PKI and edge computing. IEEE Netw. **34**(2) (2020)

M. Vaezi, R. Schober, Z. Ding, H. Vincent Poor, Non-Orthogonal multiple access: common myths and critical questions. IEEE Wirel. Commun. **26**(5) (2019)

Y.-H. Xu et al., Deep deterministic policy gradient (DDPG)-based resource allocation scheme for NOMA vehicular communications. IEEE Access (2020)

X. Zhang, M. Peng, S. Yan, Y. Sun, Deep reinforcement learning based mode selection and resource allocation for cellular V2X communications. IEEE IoT J. (2020)

X. Zhang et al., Deep reinforcement learning based mode selection and resource allocation for cellular V2X communications. IEEE Internet of Things J. **7**(7) (2020)

Y. Zhao, K. Liu, K. Chai, Y. Chen, M. Elkashlan, J. Alonso-Zarate, NOMA-based D2D communications: towards 5G. 2016 IEEE Glob. Commun. Conf. (GLOBECOM) (2016) pp. 1–6. https://doi.org/10.1109/GLOCOM.2016.7842024

Social Internet of Things (SIoT) Localization for Smart Cities Traffic Applications

Razan A. M. Elnour, Elmustafa Sayed Ali, Ibtihal Yousif, Rashid A. Saeed, Rania A. Mokhtar, Gasim Hayder, and Othman O. Khalifa

Abstract

In recent years, many applications have appeared that use GPS systems extensively, especially in GPS data-based traffic monitoring systems for phones and smart vehicles as well. These systems help to provide information about movement, speed, geographical location, and some other information related to traffic. Currently, these systems interact with social networks (SNS) on several platforms to communicate between people to share different spatial and temporal information on social networking platforms such as Twitter, Facebook, WhatsApp, and Instagram. These systems can also provide users with information such as weather, traffic details, and several changes in smart cities. Many statistics show that there is massive activity in the use of social networks and benefit from them as sources of many information and exploration for some events related to places in real time. By analyzing social communication data using the machine learning technique (ML), the SNS can achieve the concept of the social Internet of things (SIoT). The concept of localization is social networking platforms allow obtaining location information for different objects through wireless sensor networks for both indoor and outdoor environments. This paper presents an explanation of technical details of localization in the social Internet of things (SIoT) and some applications in which the concept of localization is used.

R. A. M. Elnour · I. Yousif
Department of Electronics Engineering, Sudan University of Science and Technology (SUST), Khartoum, Sudan

E. S. Ali (✉)
Department of Electrical and Electronics Engineering, Faculty of Engineering, Red Sea University (RSU), Port Sudan, Sudan
e-mail: elmustafasayed@gmail.com

R. A. Saeed · R. A. Mokhtar
Department of Computer Engineering, College of Computers and Information Technology, Taif University,
P.O. Box 11099 Taif, 21944, Saudi Arabia

G. Hayder
Department of Civil Engineering, College of Engineering, Universiti Tenaga Nasional (UNITEN), 43000 Kajang, Selangor Darul Ehsan, Malaysia

O. O. Khalifa
Department of Electrical and Computer Engineering, Faculty of Engineering, International Islamic University Malaysia, Gombak, Malaysia

O. O. Khalifa
Libyan Centre for Engineering Research and Information Technology, Bani Waleed, Libya

1 Introduction

Traffic congestion is one of the most verified cases through social networks to decide on avoiding traffic congestion, which leads to an increase in traffic times and trips with the accumulation of queues of vehicles. Most vehicle owners interact through social media platforms to know the general traffic situation in cities and to read data that shows cases of severe congestion. Traffic becomes more complex than the number of vehicles, which becomes a heavy burden on transportation departments. For example, the New York State Department of Transportation issued a report in 2019 showing the average base speed in the city, as it was observed to slow by 30% in the city center (Joseph et al. 2015).

Severe traffic congestion can lead to severe congestion over time, which can have negative effects on society, the economy, and the environment, such as severe fuel consumption, additional labor costs, and unexpected accidents (Karam and Mohamed 2012). Some techniques that help reduce congestion are used, such as the use of smart traffic methods that use traffic monitoring sensors and cameras to

read the movement of vehicles and analyze the recorded data for traffic evaluation and upgrade (Alnazir et al. 2021).

Some applications can interact with social platforms, such as the real-time navigation application, which collects information related to traffic, analyzes the data, and then works to produce information that helps people decide to avoid traffic congestion (Elbasheir et al. 2021). Many smart objects such as cameras and sensors are connected via the Internet and linked to software and platforms on a network cloud that enables users to benefit from the information collected through these smart devices, thus achieving the concept of the SIoT.

There are other applications, such as Google Maps and Waze, able to provide information on actual traffic by making use of data taken from smartphone GPS systems, and analysis software such as those used in Google, which collects data through Android phones, where each Android user acts as a source of data and using intelligent algorithms predict traffic congestion by analyzing the number and speed of Android users (Alatabani et al. 2021).

Although these methods provide reports about traffic by analyzing phone data, they are not accurate due to the lack of direct participation of users in preparing these reports. These platforms usually work well, but the information provided by Google Maps does not use social media channels (see Fig. 1). Therefore, it is necessary to take advantage of social media platforms as an important source of traffic accident monitoring data, which will greatly help in producing more accurate traffic reports (Alatabani et al. 2021).

2 Localization Methods on the Social Internet of Things

The interaction between the IoT and social networks plays an important role in creating some applications and models of the social Internet of things (SIoTs) framework as shown in Fig. 2. This type of network provides communication platforms for establishing social relationships to share common interests and better services to users (Ahmed et al. 2022). The process of localization is related to the scenarios and conditions that relate to the objects of social networks and the nodes of the IoT. Several hardware-based methods and different performance metrics can enable to provide localization for social networks.

A. Social Media

The social networking system focuses on the structure and identification of social networks over the Internet for those who share their interests and activities and who are interested in browsing the activities of others. These networks are used to do business and share data (Ahmed et al. 2022).

Social networks are reliable and provide many services according to their experiences, understanding values, and needs. The important potential services benefits are:

Reliable advertising through social networks recommended by friends and neighbors.
Obtaining valuable information about users by the organizations through Social networks, by monitoring the user's activities and this social network feature improves advertising effects.

B. Social Sensors

Localization techniques are used with the event-based tool in social networks (SN) allowing the discovery of special events (e.g., social gatherings, detours, hazards), and providing an atmosphere of the neighboring environment through text-to-speech feedback (Hassan et al. 2022). These technologies have the potential to feel the neighborhood to a user who represents a current state that is updated frequently through social media messages sent by humans acting as sensors, called "social sensors." They operate within platforms that enhance the global perception of the environment from situational feedback through event summaries. These concepts can be used to support mobility for visually impaired users as they provide awareness of the surroundings (available services, obstacles, or hazards) for the blind user. A sensor unit with inertial and ultrasonic sensors is hosted on the user for user localization, and sensor network nodes are installed in their environment for interaction (Ando et al. 2010).

## 3 Localization Applications on the Social Internet of Things

This section presents the different applications of these social IoT application systems in different fields, which correspond, to localization methods to provide the required social IoT application functionality. Localization potential is a trend for a society highly connected to the rapidly growing Internet of things as a tool that defines sensors, machines, vehicles, and mobile devices. Object data localization must be available.

### 3.1 Vehicular Social Network (VSN)

In the applications of vehicular traffic, it was found that the increasing volume of vehicular traffic within cities constantly threatens to increase congestion significantly (Mona et al. 2021a). To counter this problem, a vehicle social network (VSN) infrastructure as shown in Fig. 3 can be built in

Fig. 1 Social IoT model
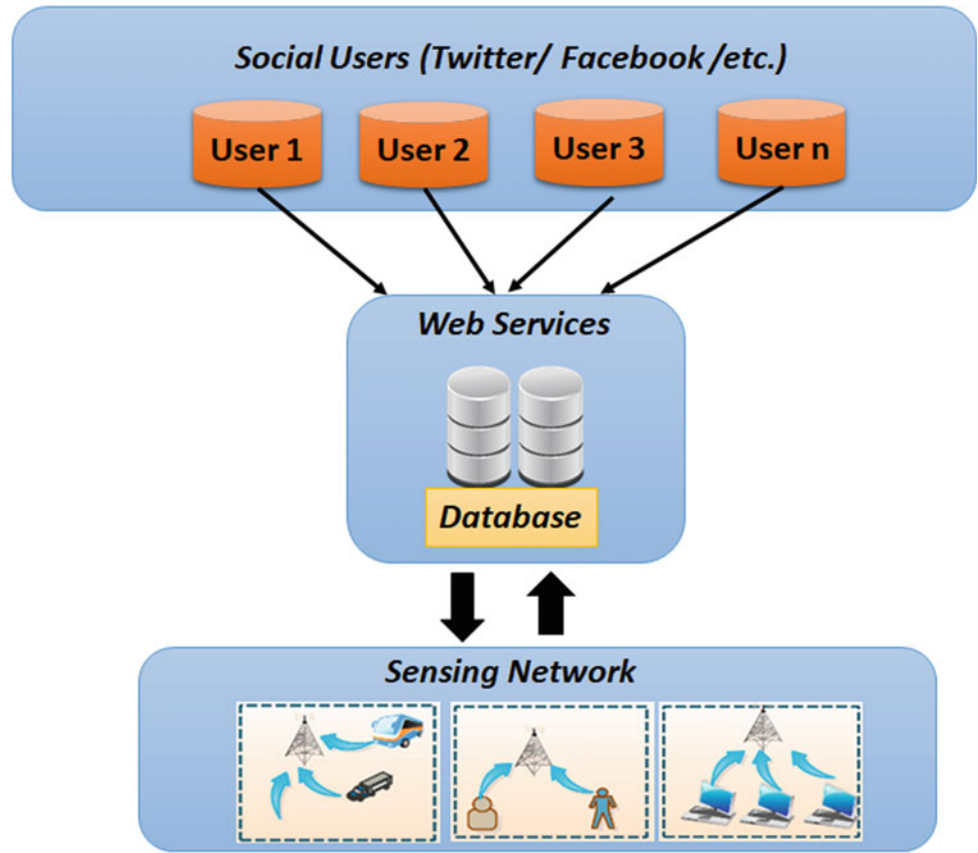
**Fig. 2** Framework of social network localization
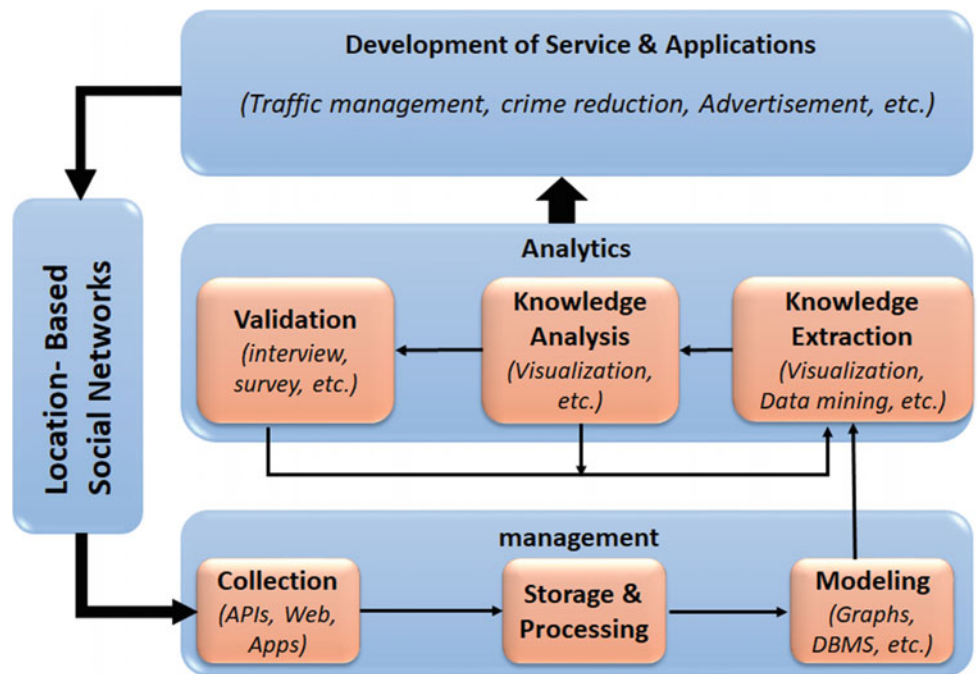
which the flow of traffic is monitored throughout the day utilizing sensors, cameras, and massive data-gathering devices. This infrastructure enables the extraction of data and analysis of it by VSN algorithms such as support vector machine (SVM) gives traffic feedback supported by policies to provide load traffic planning (Roman et al. 2018).
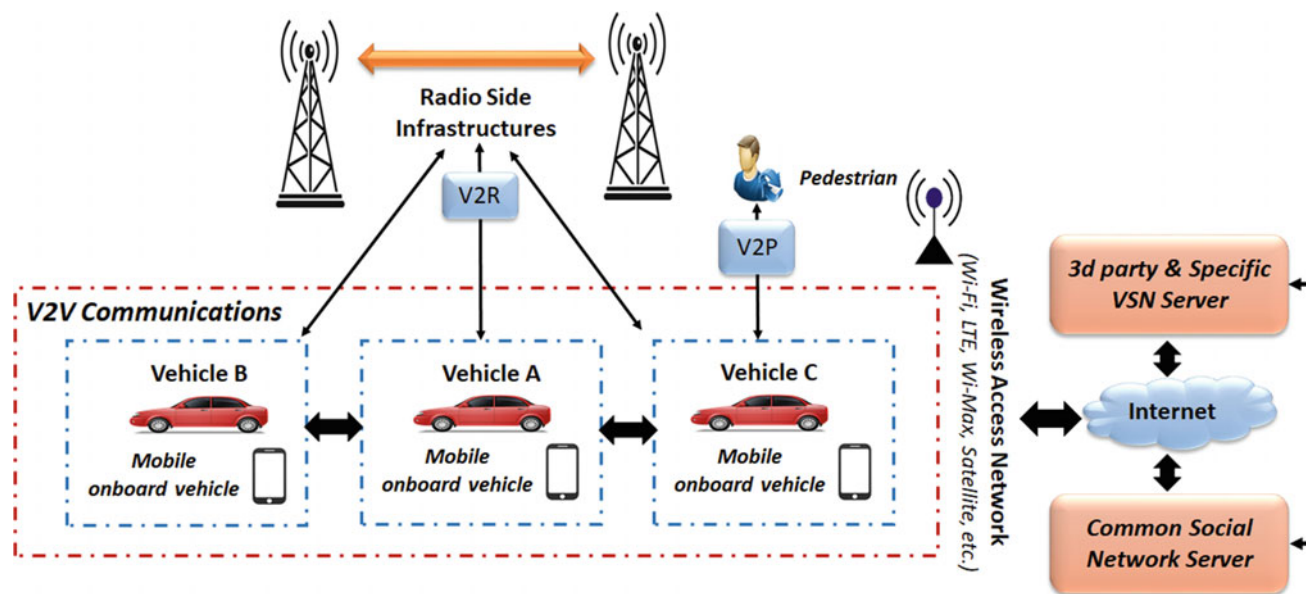
Fig. 3 Physical architecture of VSNs

A. VSN Extraction Data

The data is collected for various vehicle applications and intelligent transportation systems to detect street parking using a mobile sensor, which works well with normal on-street parking where parked vehicles must move alongside streets and detectors on external lanes. Extract road lane information from various sources including GPS and advanced driving assistance systems that assist in detecting lane markings using deep learning (Yang and Srini 2016).

B. VSN Algorithms

AI algorithms use the processes of detecting the movement of Moro and the paths of drivers; an example of this is the use of the alert path algorithm on the intelligence of the ant path (Ali et al. 2021). The support vector machine (SVM) can also be used for short-term traffic analysis with route data to classify congestion conditions and measure critical congestion rates. These classes are used to predict the future traffic situation and to analyze and record accident evidence from vehicle sensors for future investigation to provide an adequate data source about traffic behavior supervision once implemented (Dia and Thomas 2011; Nguyen 2010).

C. VSN policies

Various crowdsourcing structures and employment policies are used that contribute to the application of crowdsourcing data to the urban traffic problem (Shekhar and Setty 2015).

Some studies focused on the problem of real-time route planning in urban cities by building models to detect anomalies with the tested vehicles and then selecting the most comfortable route based on the data collected.

It also can build route-planning algorithms to improve urban navigation under traffic congestion, based on fuel consumption. In smart urban design, mobile users and vehicles can complete different tasks from different locations at the same time through VSN exploitation and crowdsourcing (Ahmed et al. 2021). For example, location-based query tasks and auto-sensing tasks can provide VSN members with necessary information about the traffic network in real time.

3.2 Mobile Social Network MSN

Mobile social networks (MSNs) enable interactions among users who have the same interests and similar goals that are exchanged by using mobile devices and interacting via virtual social networks, promoting the use of mobile applications and the use of existing social networks to create communities of service discovery and collaboration (Rehman et al. 2021). At the same time, social networks take advantage of the various technologies in smartphones and can access any information or social behaviors in any region. Social networks can analyze the user relationships to define structures and interactions between them or related to organizations for improving the mobile interactions and enhancing the provided services by networks (Mona et al. 2021b). Figure 4 shows the physical architecture of MSNs.
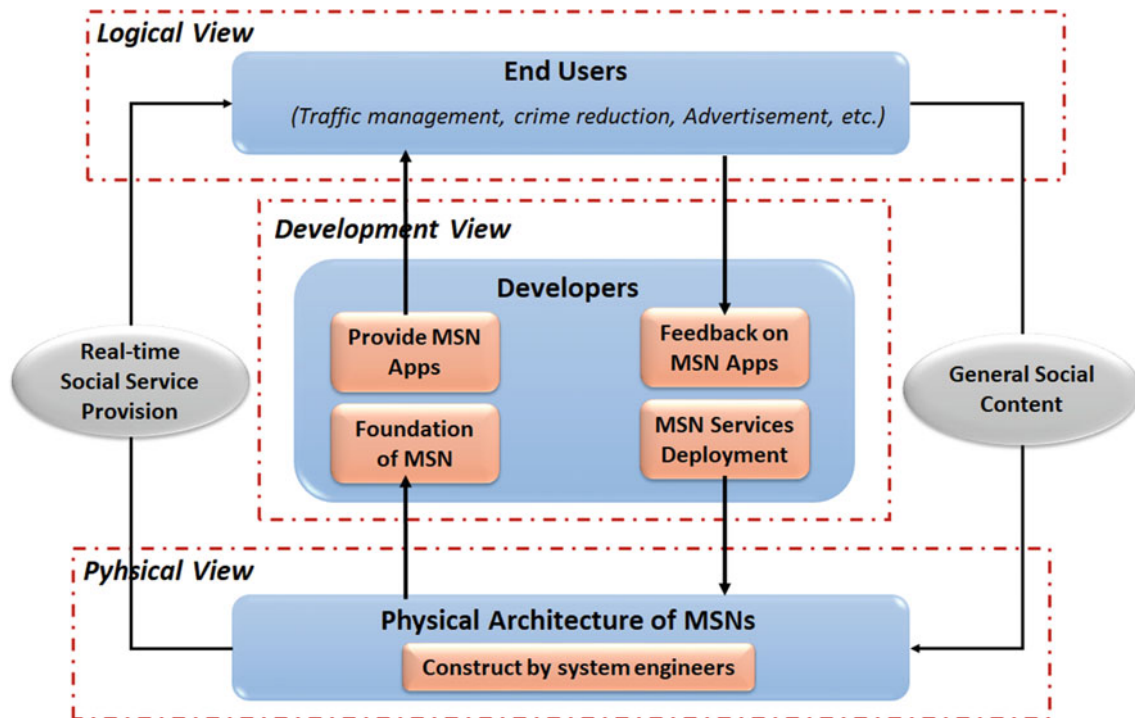
Fig. 4 Physical architecture of MSNs

MSN uses mobile networks to support the concept of the web in real time and take the capabilities advantage of modern devices such as smartphones, GPS capabilities, and sensor units (cameras, accelerometers, gravity sensors, etc.) to enhance traditional social networks with additional features, such as location awareness, the ability to asynchronous interaction, and the ability to capture different active social information (Shekhar et al. 2016). According to the capabilities of MSN, it can provide different and modern services in many aspects that are explained as follows.

A. Interaction of Opportunistic Social

MSNs enable users in mobile virtual community networks to obtain information about close contacts or meet and get to know new people by obtaining location information (He et al. 2013).

B. Educational and Scientific Purposes

Scientists and researchers can use MSNs to share knowledge anytime, anywhere, and to help groups expand their knowledge base and flexibility in organizing. It can also provide platforms for expanding practical discussions (He et al. 2013).

C. Government

For government agencies, MSN is a fast and convenient tool that enables governments to obtain the latest input from the public and provide timely information and helps improve government services and public policymaking (Zhang et al. 2017).

3.3 Natural Language Processing in Social Media

Social media NLP acts as a massive unsupervised data source to enable efficient text processing of social networking data flowing over the Internet. The work was expanded by scanning for the presence of noise in social media texts. Understandably, extracting and analyzing such a huge source of data is fraught with numerous challenges and limitations (Yang et al. 2012).

Some notable examples include work where knowledge from social media has been used in relational mining and relative reporting mining to mine correlations between information and negative feedback from any user-contributed social media content. It is also possible to analyze the information that is recorded during natural disasters and measure the sentiments of individuals about the events that are expressed in posts on social media platforms. (Humphreys 2010).

A. Redundancy Check

Duplicate posts can happen because tweets and posts are recreated by users. The regular expression method is used to

check randomly received publishing sections against existing sections for similar string patterns (Monné 2009). By measuring the percentage of patterns, and matching, repetitive posts are ignored.

B. Storage of Data

Posts that have passed the repeat test are stored systematically. Data from the content of posts is stored keeping the publisher's username and publication period for the post (Tang et al. 2016). Other information related to the number of tweets, posts, and comments made by the user and the identification of data accumulation levels is stored.

3.4 Vehicles Traffic Analysis

Social media can provide solutions for vehicle traffic forecasting relatively. The social media network tools with Web 2.0 can provide a method to monitor the increased traffic flow in a particular area. Social media tools enable observation of the tweet rate coming from the drivers or other users to indicate vehicle traffic congestion in a dedicated area where short-term traffic improvement techniques through social media posts help to analyze the traffic (Imran et al. 2015).

Mechanisms can also be used to mine data from various social media posts to monitor traffic conditions entering and leaving several lanes or port paths. Traffic can be predicted by using integrated sensors in vehicles or placed on highways, with the tweets that are posted on social networks regarding the traffic in that area. The interaction between sensor information and Twitter analysis on congestion can extract highly reliable traffic information by building a framework for an integrated system that integrates social media data with smart vehicle and traffic systems (Ni et al. 2014). The integrated system must be able to classify the data collected from social networks and sensors and analyze it intelligently through artificial intelligence algorithms capable of verifying the data in addition to the capabilities of checking geographical locations and analyzing the behavior of users to take an optimal decision for traffic management.

A. Location Identification

Traffic congestion is analyzed with the help of a geographic filter for posts, which enables us to know the origins of posts related to the congestion area. Entries can come from people who are not physically present in the traffic congestion area. To solve this problem, all the prepositions in the sentence are selected (for example, in, in, on, etc.) and as soon as the prepositions are selected, the words are sent immediately. After it is successful, it is sent to the Google Maps API

(Supriy et al. 2014). The API returns geo-coordinates if the query is within a city traffic region perimeter, then stores that location and the corresponding timestamp among posts, and keeps track of names of locations mentioned in a given post.

B. Analysis of Users Sentiments

Emotions analysis is used for all users who post comments related to traffic congestion. The information is analyzed and collected in a database containing a dictionary of words related to sentiment classification. Each word in the posts is neatly categorized against the database to find out both positive and negative comments (Mona et al. 2020). A positive sign is shown for the word with a positive emotional rating and the opposite for a negative rating. This process helps to verify the accuracy of the information provided by the users (Green and Larasati 2014).

C. Route Optimization

The feeling generated for each post submitted by the user with the advantage of its connection to the port area is placed in a table containing some information, such as the user's feelings about a particular traffic area in specific periods, in addition to previous special events of traffic congestion in a particular area (Kayastha et al. 2011). All this information is used in the process of training the Google Maps API and developing guidelines to avoid a pre-registered area that can make the user feel passive in a certain period. (Eshmawi et al. 2022; Nahla et al. 2021; Rajput et al.).

4 Localization Problem in SIoT Infrastructure

Studies are comparing smartphone-based traffic monitoring systems with the mobile social network (MSN) (Bellavista et al. 2012; Salih et al. 2020; Hasan et al. 2022; Grosenick 2012), which is used as an effective way to monitor traffic in major cities around the world. By comparison, it turns out that any such system must be a "collective resource" where a large number of users contribute information to the system and get the results simultaneously (Hasan et al. 2022). Thus, the use of location data for mobile phones constitutes a large number of motorists, along with the features already available in the Google Maps API and location services, it is possible to create a versatile system for monitoring traffic (Aswathy et al. 2022). However, the number of features and information available with Google Maps and the location service varies from country to country.

Recently, researchers have been interested in investigating an emerging concept, vehicle social networks (VSN) (Saeed et al. 2022), which effectively exploit data availability, particularly in urban areas. Using VSN, vehicles

can establish relationships with their peers and other devices based on shared interests (Mikolov et al. 1301). This greatly empowers existing intelligent transportation systems (ITS) with additional intelligence and enables new applications associated with traffic safety and traffic efficiencies, such as accident reporting or warnings related to slippery roads. The navigation methods currently in use, such as Google Maps navigation (Anatabine et al. 2022), Waze navigation, and shortest path solutions rely on historical data, statistical records, and human input (Mansour et al. 2022).

5 Conclusion

The problem of traffic congestion is more and more evident due to the lack of adequate infrastructure in poor countries and due to the increasing number of vehicles. Traffic congestion causes high fuel consumption and increases the cost of communication in addition to environmental pollution. The traffic congestion wastes a large number of working hours and increases production costs. Moreover, it causes problems for law enforcement agencies, firefighters, medical teams, or paramedics leading to an increase in crimes as well as loss of life. Advances in satellite technology and artificial intelligence in guiding vehicles from highly congested roads to less congested roads in smart cities. The use of self-driving vehicles has high potential in collecting the data required to know the density of traffic on different roads, which can be integrated with social media data analysis platforms to determine the best ways to reach them in a faster and smarter way.

References

M.Z. Ahmed, A.H.A. Hashim, O.O. Khalifa, R.A. Saeed, R.A. Alsaqour, A.H. Alkali, Connectivity framework for rendezvous and mobile producer nodes using NDN interest flooding. Int. Congr. Adv. Technol. Eng. (ICOTEN) **2021**, 1–5 (2021)

Z.E. Ahmed, M.K. Hasan, A.A. Hashim, R.A. Saeed, R.A. Mokhtar, S.P. Singh, T.M. Ghazal, in *Optimization Procedure for Intelligent Internet of Things Applications*, 2022 International Conference on Business Analytics for Technology and Science (ICBATS) (2022), pp. 1–6. https://doi.org/10.1109/ICBATS54253.2022.9759065

L.E. Alatabani, E.S. Ali, R.A. Saeed, Deep learning approaches for IoV applications and services. in *Intelligent Technologies for Internet of Vehicles. Internet of Things (Technology, Communications, and Computing)*, eds. by N. Magaia, G. Mastorakis, C. Mavromoustakis, E. Pallis, E.K. Markakis (Springer, Cham, 2021)

E.S. Ali, M.K. Hasan, H. Rosilah, R.A. Saeed, M.B. Hassan, S. Islam, N. Shaker, S. Bevin, Machine learning technologies for secure vehicular communication on internet of vehicles: recent advances and applications. Wiley-Hindawi, J. Secur. Commun. Netw. (SCN) **2021** ((2021). https://doi.org/10.1155/2021/8868355

A. Alnazir, R.A. Mokhtar, H. Alhumyani, E.S. Ali, R.A. Saeed, S. Abdel-khalek, Quality of services based on intelligent IoT WLAN MAC protocol dynamic real-time applications in smart cities. Comput. Intell. Neurosci. **2021**(2287531), 20 (2021). https://doi.org/10.1155/2021/2287531

L. Anatabine, E.S. Ali, R.A. Mokhtar, R.A. Saeed, H. Alhumyani, M. K. Hasan, Deep and reinforcement learning technologies on internet of vehicle (IoV) applications: current issues and future trends. J. Adv. Transport. **2022**(1947886), 16 (2022)

B. Ando, S. Baglio, S. La Malfa, V. Marletta, A sensing architecture for mutual user-environment awareness case of study: a mobility aid for the visually impaired. IEEE Sens. J. **11**(3), 634–640 (2010)

R.H. Aswathy, P. Suresh, M.Y. Sikkandar, S. Abdelkhalek, H. Alhumyani et al., Optimized tuned deep learning model for chronic kidney disease classification. CMC-Comput. Mater. Continua **70**(2), 2097–2111 (2022)

P. Bellavista, A. Corradi, M. Fanelli, L. Foschini, A survey of context data distribution for mobile ubiquitous systems. ACM Comput. Surv. **44**(4) (2012), 24

H. Dia, K. Thomas, Development and evaluation of arterial incident detection models using a fusion of simulated probe vehicle and loop detector data. Inf. Fusion **12**(1), 20–27 (2011)

M.S. Elbasheir, R.A. Saeed, A.A.Z. Ibrahim, S. Edam, F. Hashim, S.M.E. Fadul, A review of EMF radiation for 5G mobile communication systems. IEEE Asia-Pacific Conf. Appl. Electromagn. (APACE) **2021**, 1–6 (2021). https://doi.org/10.1109/APACE53143.2021.9760689

A.A. Eshmawi, H. Alhumyani, S.A. Khalek, R.A. Saeed, M. Ragab et al., Design of automated opinion mining model using optimized fuzzy neural network. CMC-Comput. Mater. Continua **71**(2), 2543–2557 (2022). https://doi.org/10.32604/cmc.2022.021833

N. Green, S.D. Larasati, Votter corpus: a corpus of social polling language. in *LREC* (2014), pp. 3693–3697

S. Grosenick, *Real-Time Traffic Prediction Improvement Through Semantic Mining of Social Networks*, Ph.D. dissertation, University of Washington (2012)

M.K. Hasan, R.A. Saeed, S.A. Alsuhibany, S. Abdel-Khalek, An empirical model to predict the diabetic positive using stacked ensemble approach. Front. Public Health **9**, 792124 (2022). https://doi.org/10.3389/fpubh.2021.792124

M.K. Hasan, T.M. Ghazal, R.A. Saeed, B. Pandey, H. Gohel, A. Eshmawi, S. Abdelkhalek, A. Mahmoud, A review on security threats, vulnerabilities, and countermeasures of 5G enabled Internet-of-Medical-Things. IET Commun. **16**, 421–432 (2022). https://doi.org/10.1049/cmu2.12301

M.B. Hassan, M.K. Hasan, E.S. Ali, R.A. Saeed, R.A. Mokhtar, O.O. Khalifa, A.H.A. Hashim, in *Performance Evaluation of Uplink Shared Channel for Cooperative Relay based Narrow Band Internet of Things Network*, 2022 International Conference on Business Analytics for Technology and Science (ICBATS) (2022), pp. 1–7. https://doi.org/10.1109/ICBATS54253.2022.9758935

J. He, W. Shen, P. Divakaruni, L. Wynter, R. Lawrence, in *Improving traffic prediction with tweet semantics*, Proceedings of the Twenty-Third International Joint Conference on Artificial Intelligence (2013)

L. Humphreys, in *Mobile Social Networks and Services*, Proceedings of Social Computer, Concepts, Methodology, Tools Application, vol. 1 (2010), pp. 283–293

M. Imran, C. Castillo, F. Diaz, S. Vieweg, Processing social media messages in mass emergency: a survey. ACM Comput. Surv. (CSUR) **47**(4), 67 (2015)

S.L. Joseph et al., Being aware of the world: toward using social media to support the blind with navigation. IEEE Trans. Human-Mach. Syst. **45**(3), 399–405 (2015). https://doi.org/10.1109/THMS.2014.2382582

A. Karam, N. Mohamed, in *Middleware for Mobile Social Networks: A Survey*, Proceedings of 45th HICSS (2012), pp. 1482–1490

N. Kayastha, D. Niyato, P. Wang, E. Hossain, Applications, architectures, and protocol design issues for mobile social networks: a survey. Proc. IEEE **99**(12), 2130–2158 (2011)

R.F. Mansour, H. Alhumyani, S.A. Khalek, R.A. Saeed et al., Design of cultural emperor penguin optimizer for energy-efficient resource scheduling in green cloud computing environment. Cluster Comput. (2022)

T. Mikolov, K. Chen, G. Corrado, J. Dean, *Efficient Estimation of Word Representations in Vector Space*. arXiv preprint arXiv:1301.3781

B.H. Mona, E.S. Ali, R.A. Mokhtar, R.A. Saeed, S. Bharat, NB-IoT: concepts, applications, and deployment challenges, in *LPWAN Technologies for IoT and M2MApplications*, eds. by S. Bharat, M. Zennaro (Elsevier, 2020), ISBN: 9780128188804

B.H. Mona, Ali, E.S. Ahmed, R.A. Saeed, Machine learning for industrial IoT systems. in *Handbook of Research on Innovations and Applications of AI, IoT, and Cognitive Technologies*, eds. by J. Zhao, V. Vinoth Kumar (IGI Global, Hershey, PA, 2021a), pp. 336–358. https://doi.org/10.4018/978-1-7998-6870-5.ch023

H.B. Mona, E.S. Ali, R.A. Saeed, Intelligent Internet of things in wireless networks. Telecommunications, Intelligent Wireless Communications, Chap. 6 (2021b) pp. 135–162

L.M.V. Monné, A survey of mobile social networking, current internet Trent. Helsinki Univ. Technol., Espoo, Finland, TKK Technical Reports in Computer Science and Engineering (2009)

N. Nahla, M.K. Hasan, M. Imran, R.A. Saeed, A. Khairul, Z. Ariffin, E. S. Ali, R.A. Mokhtar, I. Shayla, E. Hossain, M. Arif, A systematic review on cognitive radio in low power wide area network for industrial IoT applications. MDPI, Sustainability (2021). https://doi.org/10.3390/su13010338

H. Nguyen, Mobile social network and its open research problems. Dept. of Comput. Sci. Univ. Houston, Houston, TX, USA (2010)

M. Ni, Q. He, J. Gao, Using social media to predict traffic flow under special event conditions, in *The 93rd Annual Meeting of Transportation Research Board* (2014)

B.U. Rehman et al., Joint power control and user grouping for uplink power domain non-orthogonal multiple access. Int. J. Distrib. Sens. Netw. (2021). https://doi.org/10.1177/15501477211057443

C. Roman, R. Liao, P. Ball, S. Ou, M. de Heaver, Detecting on-street parking spaces in smart cities: performance evaluation of fixed and mobile sensing systems. IEEE Trans. Intell. Transp. Syst. **19**(7), 22342245 (2018)

M. Saeed, R.A. Saeed, R.A. Mokhtar, H. Alhumyani, E.S. Ali, A novel variable pseudonym scheme for preserving privacy user location in 5G networks, Secur. Commun. Netw. **2022**(7487600), 11 (2022)

R. Salih; S.A. Mahbub, R.A. Mokhtar, E.S. Ali, R.A. Saeed, IoE design principles and architecture, in *Internet of Energy for Smart Cities: Machine Learning Models and Techniques* (CRC Press Publisher, 2020). https://doi.org/10.4018/978-1-7998-5101-1

H. Shekhar, S. Setty, in *Disaster Analysis Through Tweets*, 2015 International Conference on Advances in Computing, Communications, and Informatics (ICACCI), IEEE (2015), pp. 1719–1723

H. Shekhar, M. Uma, S. Setty, *Vehicular Traffic Analysis from Social Media Data*, B.V. Bhoom College of Engineering and Technology (BVBCET), KLE Technological University Hubballi, KLE Technological University Hubballi, Conference Paper (2016). https://doi.org/10.1109/ICACCI.2016.7732281

M. Supriy, A. Septiani, R. Hakim et al., Mining the traffic conditions via Twitter based on rough set theory, in *International Seminar on Innovation in Mathematics and Mathematics Education* (Department of Mathematics Education Faculty of Mathematics and Natural Science Yogyakarta State University, 2014)

L. Tang, X. Yang, Z. Dong, Q. Li, CLRIC: collecting lane-based road information via crowdsourcing. IEEE Trans. Intell. Transp. Syst. **17**(9), 25522562 (2016)

C. Yang, P. Srini, Life satisfaction and the pursuit of happiness on Twitter. PLoS ONE **11**(3), e0150881 (2016)

K. Yang, X. Cheng, L. Hu, J. Zhang, Mobile social networks: state-of-the-art and a new vision. Int. J. Commun. Syst. **25**(10), 1245–1259 (2012)

J. Zhang, J. Fan, Z. Luo, Generating multi-destination maps. IEEE Trans. vis. Comput. Graph. **23**(8), 19641976 (2017)

An Evaluation of the Factors Affection the Potential for Biomass Upgrading for Energy Use in Malaysia

Abdelhalim Abobker Adam and Gasim Hayder

Abstract

Malaysia's rapid urbanization and economic development along with extensive growth in population led to increased energy demand. With the emerging environmental concerns, looking for viable alternatives to secure the energy demand and mitigate the greenhouse gas emissions simultaneously conveyed the attentions toward biogas utilization and extraction from different organic wastes. The concept of "waste to wealth" is crucial in dealing with various harmful wastes when being dumped instantly to Malaysia landfills, those such as effluent derived from palm oil mills, garden wastes, sewage sludge, food waste, animal manure, and landfill. Thus, either mitigation of threats or valorization of the wastes via biogas generation can be achieved through intensive utilization of anaerobic digestion. For instance, each day in the country 15,000 tons of food is wasted, if treated and utilized properly has the potential to fulfill the energy demanded as it is considered to be 10 times the early consumption, adding to the environmental positive impacts. Therefore, introduction of new polices that promote and encourage the utilization of renewable energy technologies along with adaptation of newly emerging enhancements, are of the Malaysian government's target to reduce the over dependency on the depleted resources. Thus, it is necessary to incorporate significant factors affecting biogas generation for the purpose of energy generation in the country. The current paper assesses the existing biomass treatment technologies based on their effectiveness, evaluates the feedstocks for the purpose of anaerobic digestion based on their organic contents and economic analysis, reviews the biogas to biomethane technologies (evaluation based on economic analysis), and lists most important policies that qualify the incorporation of renewable energy technologies for energy mix targets. Results show that palm oil mill effluent and food wastes have highest potential to produce biogas compared to other feedstocks where co-digestion is preferable for more desired results, additionally, the economic analysis depicts that the palm oil mill effluent still the most favorable followed by the food wastes in term of short payback period, high internal rate of return, and high net present value.

Keywords

Biomass feedstock • Anaerobic digestion • Treatment technologies • Upgrading technologies • Policies

1 Literature Review

To meet with the ever-increasing demand of fuel due to the rapid increase in population in Malaysia, searching for a cleaner energy production is crucial in order to address the GHG along with maintain and increase the development rate in the country. Thus, AD is proven to be a good method of converting the various feedstocks available in Malaysia into Biogas. The following literature review confirms the strong correlation between the (treatment & upgrading technology used, different feedstocks utilized and the government policies available) and the purity and amount of Biogas produced.

2 AD Treatment and Upgrading Technologies Availability

Biogas production through anaerobic digestion AD technologies with different configurations ranging from conventional to more cleaner technologies Chan et al. (2019)

A. A. Adam (✉)
College of Graduate Studies, Universiti Tenaga Nasional (UNITEN), 43000 Kajang, Selangor, Malaysia
e-mail: abdo9116@gmail.com

G. Hayder
Department of Civil Engineering College of Engineering, Universiti Tenaga Nasional (UNITEN), 43000 Kajang, Selangor, Malaysia

discussed the current technologies used in treating effluent derived from palm oil mills considering biochemical oxygen demand BOD set by the department of environment as a framework, besides problems and challenges deter mill owners from having biogas plants in the mills. Chan advocates that in order to achieve zero discharge of mill effluent concept, there are two advanced technologies namely expanded granular sludge bed and anaerobic–aerobic bioreactor. Both technologies distinguished by the degree of effluent treatment and methane generation efficiency along with their ability to produce biofertilizer out of the treated effluent. Besides, all palm oil mill sites are expected to acquire biogas production technologies whenever financial and other aiding supports took place by the government in the future. Though, Chan failed to note the upgrading technologies and was limited to only one feedstock. The article aids the current paper with the zero discharge technologies. More recently, Lim et al. (2021a) reviewed on existed biogas technologies in Malaysia, the scalable technologies with additional configurations, and conducted a socio-economic analysis in light of the biogas to energy concept, along with particular emphasis on the waste management system. The article stresses that, regarding the AD technology scalability, there is a strong correlation between the digester size and biogas yield, thus scaling up increases the digester dimensions and the potential of efficiency reduction is found besides, the article drags the attention toward the main purposes of the polices imposed by the government which represented in the elevation of the residences' awareness regarding the negative impact of direct food disposal on health and shrinking landfills. On the other hand, Lim's survey showed that the existence of food waste separation is limited only to 28% of the participants in the study. However, the study neglected the cost and parameters associated with the upgrading technologies and the feedstocks. The article contributes to the current study on the biogas treatment & upgrading technologies and the policies imposed by the government. In addition, Sun et al. (2015) systematically reviewed the current level of biogas cleaning and upgrading technology, including product purity and contaminants, methane recovery and loss, upgrading efficiency, and capital and operating expenses. In addition, the potential use of biogas and the resulting gas quality requirements are thoroughly explored. Sun claims that there are still significant inconsistencies in data on methane loss and energy use, for example. Furthermore, over-pursing high quality or overlooking biogas quality might result in excessive costs additionally, cryogenic separation, in-situ upgrading, hydrate separation, and biological approaches are some of the most recent advancements in biogas upgrading technology however, they are still in development, and the majority of the material available has come from laboratory or pilot tests. Nevertheless, Sun paid little attention to CO_2

separation and utilization. The article contributes with the biogas upgrading technologies evaluation based on the economic aspect such as operational costs and other related parameters.

3 Feedstock Suitability

Feedstocks such as POME is well explored in Malaysia with considerable amount of research articles, however other biomass types proven to have high potential of been treated by AD and thus yield high amount of biogas. Lim et al. (2021b) evaluated prospective feedstocks with high potential of biogas yield with anaerobic digestion AD, based on their tendency to be treated via AD, amount of methane extracted from each, and scale up & economic analysis. Lim claims that there are six feedstocks proven to be treated using anaerobic digestion technologies however, after examining their respective characteristics collected from various sources, some of the feedstocks require improvement, such as pH correction and co-digestion due to their C/N ratios not being in the optimum range, in order to increase the AD process efficiency. Both FW and POME have proven to be economical and exhibited methane yields of up to 0.5 L for each gram volatile solid, while landfill leachate had the lowest methane output of 0.12 L for each gram volatile solid. The modified Gompertz model was chosen as the best kinetic model for AD and can be utilized in the scale-up analysis. Nevertheless, Lim disregarded considering co-digestion of different feedstocks simultaneously to increase the biogas yield. The article qualifies the current paper with the evaluation of the potential feedstocks from different sides. Furthermore, these studies reviewed the various feedstocks used. Hanum et al. (2019) evaluated the utilization of sewage sludge for biogas extraction in Malaysia, as well as barriers faced while boosting anaerobic digestion and co-digestion of one or two substrates when treating sewage sludge. Additionally, the paper outlined impediments that suppress sewage sludge utilization such as financial, policy barrier, and technical requirements along with the characteristic of the Malaysia's sewage sludge as well counted as a factor of suitability. Hanum contends that while Malaysia has a diverse spectrum of biomasses suitable for co-digestion, mixing food waste with the sewage sludge in a co-digestion process may be more reliable solution to overcome mono-digestion disadvantages. Thus, food waste is advised to be added as a co-substrate for improving the process' performance while also assisting Malaysia in addressing its growing food waste problem. However, the article overlooked other substrates to be treated with the SS and was limited to the FW. The article provides a base for further evaluation the SS based on the provided characteristics. While Hanif et al. (2020) reviewed on producing

electricity from biogas-derived FW and conducted a techno-economic analysis in smart city based on sustainability and eco-friendly. Aside from that, Tan et al. (2014) reviewed evaluation of three methods used for municipal solid waste treatment in Taman Beringin as a case study namely AD, incineration, and landfill gas recovery system (LFGRS) under the environmental, economic, energy requirements, and lesser carbon emissions. Tan claims that incineration is the best option for municipal solid waste treatment, due to the facts that it is more cost-effective and environmentally feasible option followed by AD. It was considered that waste-to-energy WTE alternatives, in particular, could be a viable option for reducing GHG emissions while maintaining economic viability through by-product manufacturing. The article contributes by emphasizing on the AD as a good option for Landfill treatment rather than the conventional one. Additionally, conversely Abdeshahian et al. (2016) reviewed on the potential of animal manure and assessed the biogas production from animal and poultry farms in Malaysia. The article advocates that due to the low-cost of animal and poultry wastes, they considered as important sources for renewable energy such as biogas generation, furthermore the total animal waste produced in 2012 from farm animals and slaughterhouses was around 24.28 million tons. Adding to that, the cumulative biogas extracted from cattle was around 4589.493 million m^3/year, equivalent to 8.27×10^9 kWh/year of energy generation. The article contributes significantly on the evaluation of animal manure considering economic values under certain governmental polices.

4 Polices

There are several polices have been imposed by the government in Malaysia, the introduced polices affected the renewable energy RE sector potential in the country by qualification or suppression. Bong et al. (2017) reviewed and evaluated substantial renewable energy governmental frameworks in Malaysia, with in-depth discussion of significant rules surrounding solid waste management for the purpose of establishing biogas production from municipal solid waste effectively. Bong emphasizes that biogas has a network with a lifecycle of three phases: feedstock phase, process of the biogas production, and usage phase. Numerous critical stages were discovered within each phase. The analysis's objective was to ascertain the function of existed policies, scarcity of governmental support, and impediments

encountered. Additionally, several plans, such as National Renewable Energy Policy 2010 and Action Plan for instance, have embedded long-term strategic moves such as encourage outsiders to invest in RE industry, nurture and develop human capital, and cross-sector coordination. The article contributes significantly to the current work with the policies and incentives available. No doubt that with the industrialization and urbanization cause for more energy demand, however the fossil fuel used caused rapid increase in GHG emissions. Thus, biomass is the most promising source of energy therefore, developing and utilizing greener technologies for treatment that save cost, increase methane yield, and reduce the methane losses is crucial. Furthermore, more cost-efficient upgrading technologies that enhance the biomethane produced without losses is needed. Additionally, searching for feedstocks with high potential of biogas, less energy demanding in treatment process, and have high organic matters for fermentation microorganisms to increase the digestion process is crucial, along with favorable government policies that encourages the local residences, investors, and organizations to invest and utilize the wasted resources for sustainable development and environmental considerations.

References

P. Abdeshahian et al., Potential of biogas production from farm animal waste in Malaysia. Renew. Sustain. Energy Rev. 714–723 (2016)

C.P.C. Bong et al., Review on the renewable energy and solid waste management policies towards biogas development in Malaysia. Renew. Sustain. Energy Rev. 988–998 (2017)

Y.J. Chan et al., Palm oil mill effluent (POME) treatment-current technologies, biogas capture and challenges. Green Energy Technol. 71–89 (2019)

M. Hanif et al., Economic feasibility of smart city power generation from biogas produced by food waste in Malaysia via techno-economic analysis. Earth Environ. Sci. 476 (2020)

F. Hanum et al., Treatment of sewage sludge using anaerobig digestion in Malaysia: current state and challenges. Front. Energy Res. 1–6 (2019)

Y.F. Lim et al. Review of biowastes to energy in Malaysia: current technology, scalability and socioeconomic analysis. Clean. Eng. Technol. 1–13 (2021a)

Y.F. Lim et al., Evaluation of potential feedstock for biogas production via anaerobic digestion in Malaysia: kinetic studies and economics analysis. Environ. Technol. 1–15 (2021b)

Q. Sun et al., Selection of appropriate biogas upgrading technology-a review. Renew. Sustain. Energy Rev. 521–532 (2015)

S. Tan et al., Economical and environmental impact of waste-to-energy (WTE) alternatives for waste incineration, landfill and anaerobic digestion. Energy Procedia 704–708 (2014)

Multilevel Authentication in Smart Online Classroom Attendance

Nazhatul Hafizah Kamarudin, Jong Joon Siong, Mahmud Iwan Solihin, and Gasim Hayder

Abstract

This project presents a prototype of a multilevel authentication in smart online classroom attendance. The scope of this project includes some steps. It begins with conceptual design of a multilevel authentication for students' attendance in the online classroom application. The system generates a student unique identity for the first-level authentication followed by a biometric authentication for student verification. Overall, the development of a multilevel authentication scheme for the online classroom is presented in this paper. The prototype can authenticate the student unique identity and biometric authentication for student verification. In addition, the designed smart system prototype is also able to store the student attendance and sending back to the lecturer.

Keywords

Multilevel authentication • Face recognition • Online classroom attendance • Smart system

1 Introduction

In 2020, the global coronavirus pandemic has prompted many universities to transition to online learning in a hurry instead of attending physical classes face to face. The scope of the project is to design a multilevel authentication in smart online classroom attendance. The project is designed for demonstration and presentation.

Attendance management is important to everyone in organizations including educational institutions. Institutions require tracking of people as a mean to maintain their presence and performance. Particularly in universities or schools, monitoring attendance of their students during classes/lectures become a challenging task. Manual attendance checking especially in a large class tends to produce errors and time-consuming process. To overcome, an efficient web-based application attendance management system is designed to track students' activities in the classroom. This paper deals with the application of the biometric recognition in personal authentication enabling the development of this technology to be used in various area. The physical or behavioral characteristics can be implemented based on a biometric system, for example, iris, voice, fingerprints, and face (Uike et al. 2020).

Software and hardware components are required to establish a biometric-based attendance system. Most of the literature review only addresses the hardware types utilized in various projects. These include the applications of microcontroller platform, biometric sensors, communication channels, database storage, and other components. Based on some literatures, microcontroller modules have been applied in biometric-based attendance systems (Uike et al. 2020; Miran 2014; Seng and Haidi 2019; Arunraja et al. 2019; Nandhini et al. 2019; Waingankar et al. 2018; Suresh et al. 2019; Odabi and Jonathan 2015; Rivandi et al. 2019; William et al. 2019; Astuti et al. 2021).

A facial recognition is a biometric innovation that includes deciding if the facial picture of some random individual matches any facial picture put away in the information base. Different variables (like outward appearances, maturing, and even light) may cause variations to the picture. It is hard to consequently take care of this issue. Among various biometric acknowledgment advances, facial acknowledgment may not be the most solid innovation.

N. H. Kamarudin · J. J. Siong · M. I. Solihin (✉)
Faculty of Engineering, Technology and Built Environment, UCSI University, No. 1, Jalan Menara Gading, UCSI Heights (Taman Connaught), Cheras, 56000 Kuala Lumpur, Malaysia
e-mail: mahmudis@ucsiuniversity.edu.my

G. Hayder
Department of Civil Engineering, College of Engineering, Universiti Tenaga Nasional (UNITEN), 43000 Kajang, Selangor Darul Ehsan, Malaysia

However, it has a bigger number of benefits than other acknowledgment advances. It is generally utilized in security and access control, criminology, police control, and office attendance frameworks (Miran 2014).

This paper presents a case study on prototyping for a face recognition-based attendance system for educational institutions. The design and inspiration of the prototype is the work published in Odabi and Jonathan (2015). The system is using a camera module, 16 Gb Micro SD card class 10 with OpenCV and Numpy through Python to complete the requirements. The steps involved in the system are to initiate the opening Python script and then to create a dataset of the student by entering the ID number. After that, a picture of the class is taken, and the recognizer Python file is initiated. Finally, if the face is matched, the responding name with present status is marked in the Excel file with the current data and time.

2 Prototype Design

The project hardware involves a webcam to do the biometric authentication, and software part will be developed using Python. A three-level authentication scheme for the online classroom attendance is introduced. The first level authenticates the students name and ID. Second level is one-time password (OTP) authentication; i.e., the OTP will be sending to the student email for authentication. Lastly, the third level is a biometric authentication which is face recognition. The student must upload the photo through phone or webcam to

the software; after the software has matched the data, the attendance will be taken and sent though email of the lecturer (see Figs. 1 and 2).

For the first-level authentication, it utilizes graphical user interface (Python GUI) which is an arrangement of intuitive visual parts for computer programming. It uses *Tkinter* library in Python (see Fig. 3). The system has been designed to authenticate the students name, ID, and even biometric. So, form to register is required to store the student information in order to do for the authenticate as shown in Fig. 4.

The second-level authentication utilizes the Python email API to do the email OTP authentication. There is the list of the port numbers for developer as reference to set up a SMTP server. Python has *smtplib* module which is used to send the emails. As *smtplib* is in built module, no need to install it separately.

Third-level authentication is a biometric authentication which is using the Python OpenCV to do the face recognition. The expression "Computer Vision (CV)" is regularly utilized and heard in artificial intelligence (AI) and deep learning (DL) applications. The term basically alludes to enabling computer to see the world like people. The entire cycle includes picture procurement, screening, examination, recognizable proof, and data extraction.

Face recognition usually entails locating a face in an image, assessing facial features, comparing to known faces, and making an educated guess. Face location is the first step. For cameras, the face location is a fantastic factor. When the camera can intuitively select faces, it can verify that all of the faces are focused before taking the picture.

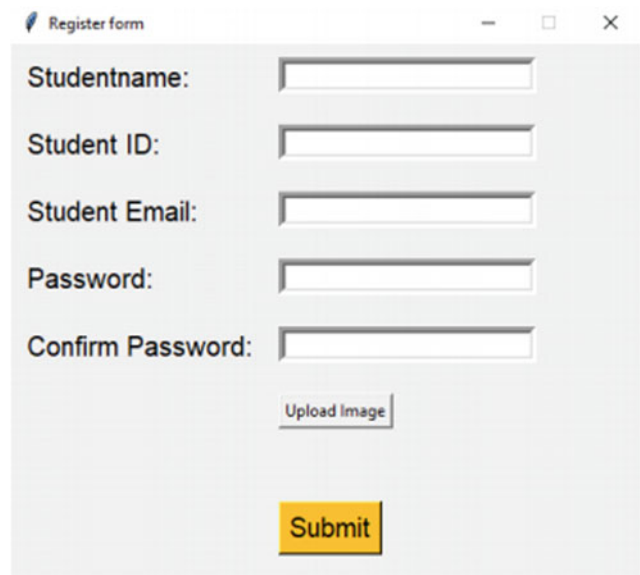**Fig. 1** Flow of the data for class attendance
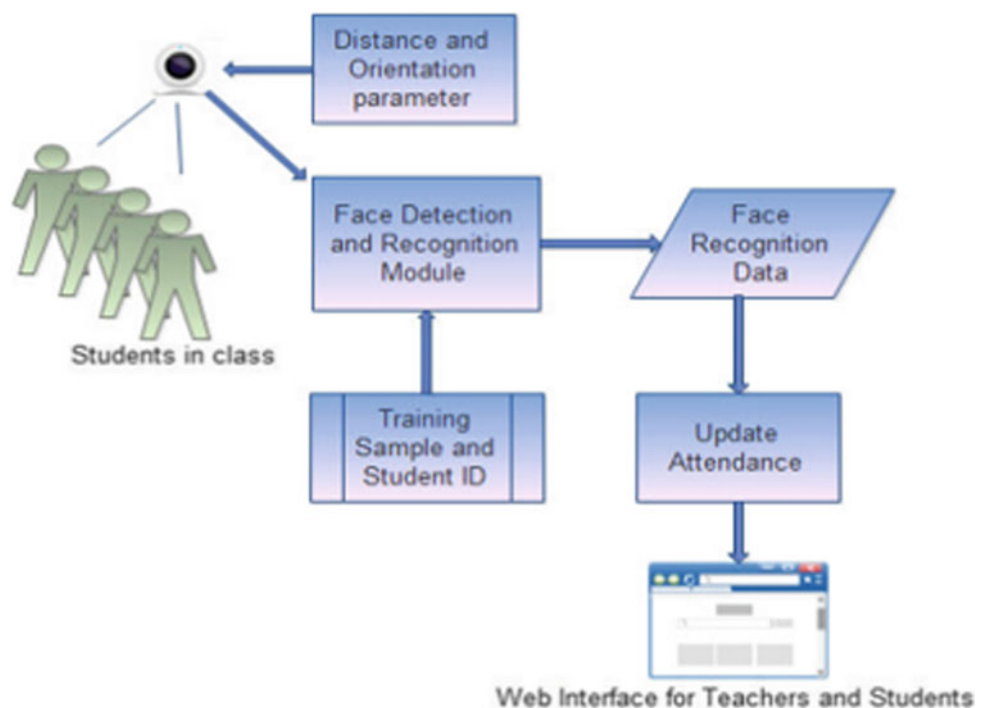
Fig. 2 Conceptual diagram of the authentication system
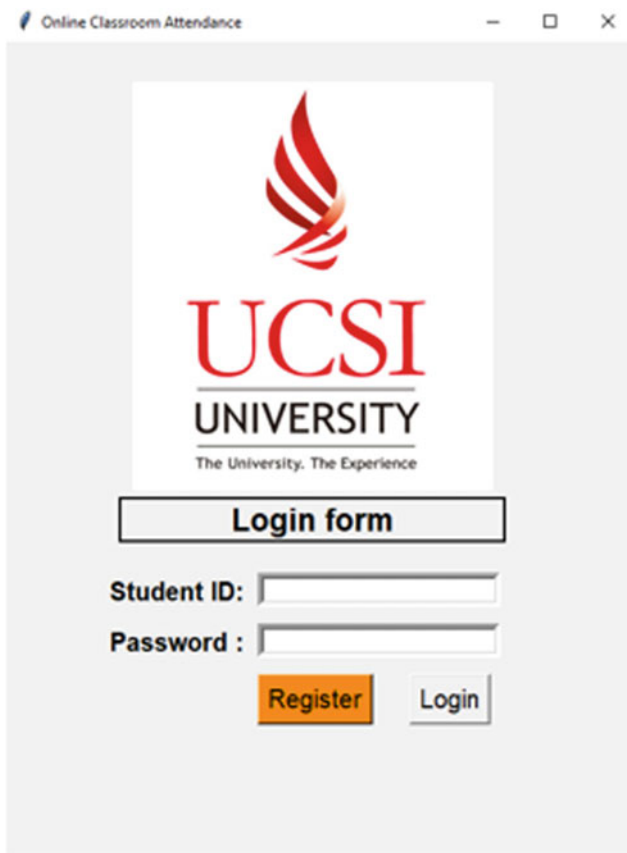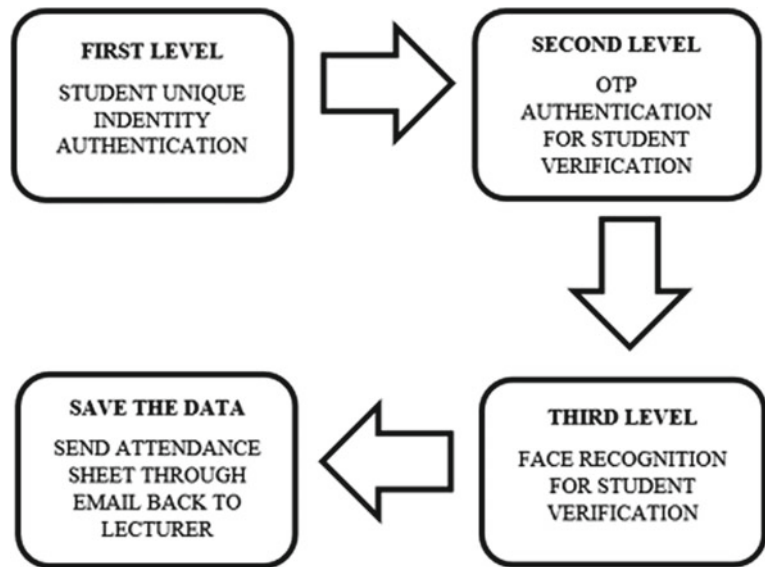
Fig. 3 Login page developed using Tkinter GUI

Fig. 4 Using Tkinter GUI to create a registration page

Secondly, after secluded the countenances in the picture, the subsequent phase is to take care of the issue of the appearances where turned headings appear to be unique to a computer. To take care of the headings issue, one can utilize a calculation called face milestone assessment. This needs to produce 68 explicit focused spots that exist on each face as shown in Fig. 5.

The third stage is to encode the faces. The simplest way to deal with face recognition is to just think about the obscure face that appears in sync two with each of the photographs of people who have been successfully identified. To get the 128 estimations for each face, run the face photos through their pre-trained model.

Finally, the encoding must be decoded to reveal the individual's name. To create a classifier that can use estimates from another test image and determine which realized individual is the closest match. Running this classifier takes milliseconds, after which the classifier will provide the individual's name.

Fig. 5 68 Landmarks on face

3 Software Flow Diagram

The first level authenticates the students name and ID. The second level is OTP authentication. The third level is a biometric authentication which is face recognition. The student must upload the photo through phone or webcam to the software. After the software has matched the data, the attendance will be taken and sent through email of the lecturer. The following figures (Figs. 6, 7, and 8) show the overall software flow diagram in the system.

4 Results for Face Recognition

In the system, the third-level authentication is a biometric authentication using face recognition. Here, the student is required to open their webcam. Then the system will scan for the face and match with the database; if the student face is not in the database, the system will show "unknow." The system will only take attendance when it matches the face with the system database. After the attendance is taken, the system will automatically send it to the lecturer. Figure 9 shows the successful face recognition phase. After the face is matched, the mark attendance function will generate the attendance for the student as shown in Fig. 10. It is noted that the accuracy of the face recognition depends on OpenCV module performance itself. We have not fully tested and evaluated the accuracy in this report.
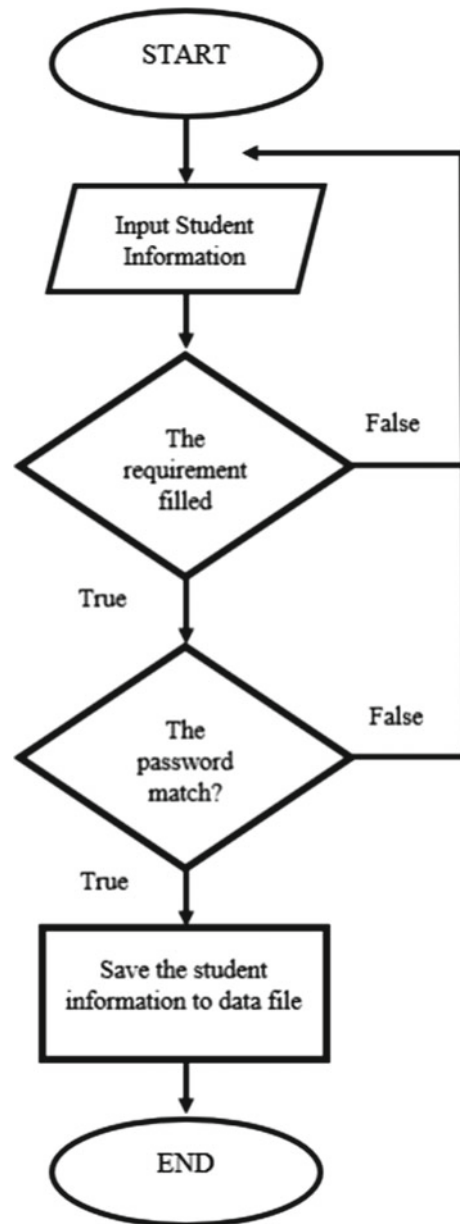

Fig. 6 Flowchart for registration

5 Discussions

This project prototype is using third-level authentication which includes student unique identity authentication, email OTP authentication, and biometric authentication using face recognition.

Currently, the system runs independently which requires student to open the system to take attendance and then open Microsoft team for online lecture. By combining the system
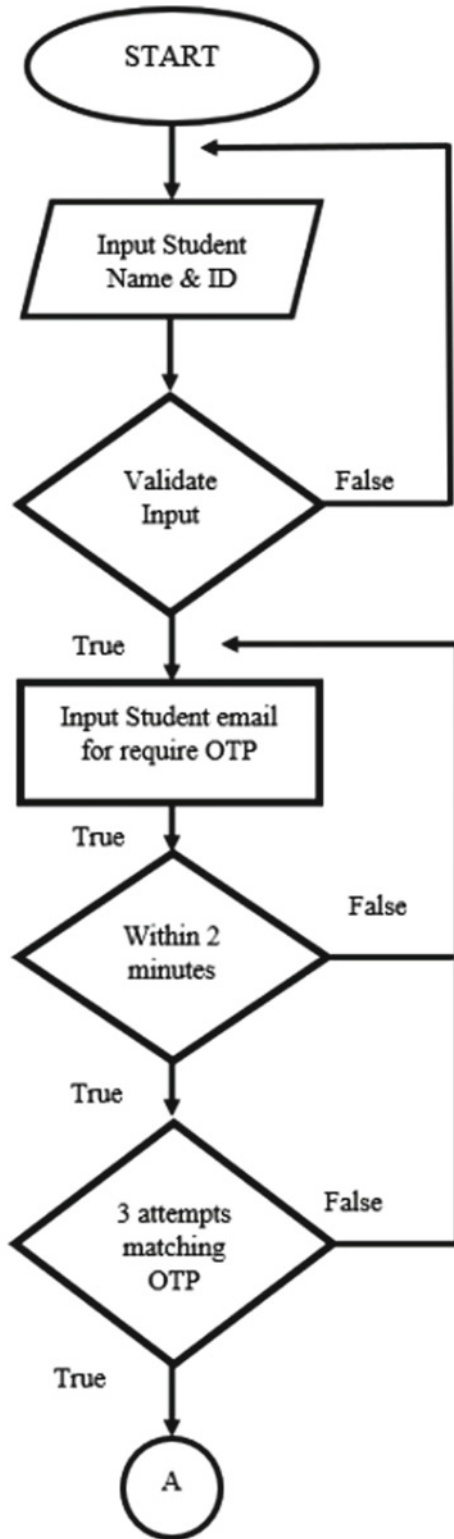
Part A

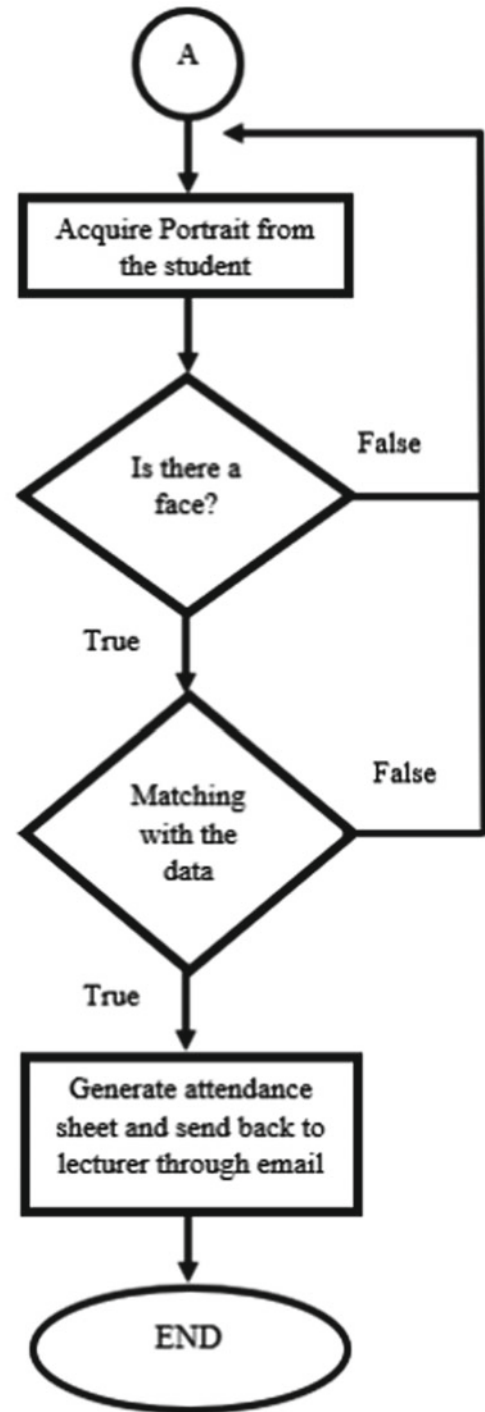**Fig. 7** Part-A flowchart of the authentication system

Part B

Fig. 8 Part-B flowchart of the authentication system

attendance can be directly sent to the lecturer through Microsoft team. Based on the design, the discrepancy between this project and the projects in literature review can be viewed. For example, in terms of cost, the project in literature review is more expensive than project prototype due to the method used. For instance, spending extra money on GPS and fingerprint modules for each student is not a

with Microsoft Team, for example, students can work more conveniently without having to open two different software applications, and the database can be more secure. The

Fig. 9 System detects faces and
matches with the database
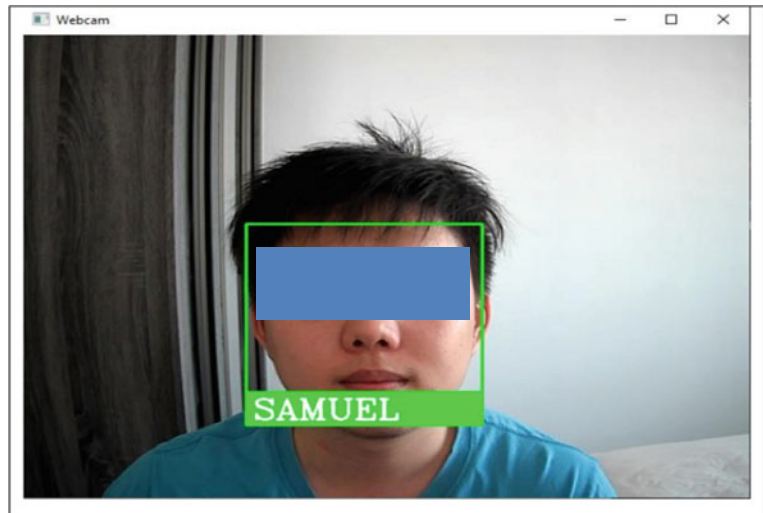
Fig. 10 Generated attendance in Excel sheet

wise choice. Therefore, the project considers the cost efficiency by choosing a webcam for face recognition, which students can use for lectures, final exams, meeting, etc.

References

A. Arunraja, G.M. Rajathi, S. Mathumitha, Smart attendance system using Esp8266. Int. J. Sci. Technol. Res. **08**(09), 1–6 (2019)

W. Astuti, S. Tan, M. I. Solihin, R. S. Vincent, B. Michael, Automatic voice-based recognition for automotive headlights beam control. Int. J. Automot. Mech. Eng. **18**(1), 8454–8463 (2021). https://doi.org/10.15282/IJAME.18.1.2021.05.0640

H.M.B. Miran, Attendance checking system using quick response code for students at the university of sulaimaniyah. J. Math. Comput. Sci. **10**, 189–198 (2014)

R. Nandhini, N. Duraimurugan, S.P. Chokkalingam, Face recognition based attendance system. Int. J. Eng. Adv. Technol. **08**(3S), 1–4 (2019)

O.I. Odabi, E.O. Jonathan, Automatic attendance and mobile learning system in sensor-enabled heterogeneous and dynamic university environment. West Afr. J. Ind. Acad. Res. **13**(01), 29–34 (2015)

P. Rivandi, A. Winda, D. Satrio, M.I. Solihin, in *Automotive Start–Stop Engine Based on Fingerprint Recognition System*, E3S Web Conference, vol. 130 (2019), p. 01022. https://doi.org/10.1051/e3sconf/201913001022

C.H. Seng, I. Haidi, Biometric-based attendance tracking system for education sectors: a literature survey on hardware requirements. Hindawi J. Sens. **7410478**, 25 (2019)

V. Suresh, S.C. Dumpa, C.D. Vankayala, H. Aduri, J. Rapa, Facial recognition attendance system using Python and OpenCV. J. Softw. Eng. Simul. **05**(02), 18–29 (2019)

S.P. Uike, M.P. Tambakhe, C.S. Dakhore, A.G. Waghade, Smart student attendance management system. Int. Res. J. Eng. Technol. **07**(02), 1–4 (2020)

A. Waingankar, A. Upadhyay, R. Shah, N. Pooniwala, P. Kasambe, Face recognition based attendance management system using machine learning. Int. Res. J. Eng. Technol. **05**(06), 1–7 (2018)

L. William, A. Winda, D. Satrio, T. Sofyan, M. Iwan Solihin, in *Automotive Start-Stop Engine Based on Face Recognition System*, E3S Web Conference, vol. 130 (2019), p. 01020. https://doi.org/10.1051/e3sconf/201913001020

The Effect of Groundnut Shell Ash and Metakaolin on Geotechnical Properties of Black Cotton Soils

Ibrahim Umaru, Mustapha Mohammed Alhaji, Ahmad Hussaini Jagaba, Shamsul Rahman Mohamed Kutty, Ibrahim Mohammed Lawal, Sule Abubakar, and Usman Bala Soja

Abstract

Groundnut shell ash (GSA) and metakaolin (MK) were investigated for their stabilizing prospects in highly expansive clay soils due to the rising cost of traditional stabilizers and the need for cost-effective utilization of waste materials for useful engineering applications (black cotton soil). The natural soil's index qualities revealed that it belongs to A-7-6 in the AASHTO classification system and CH in the USCS classification system. This implied that the soil is unsuitable for most engineering purposes. The natural soil's liquid limit and plasticity index values of 60.2% and 30.1%, respectively, which indicated that the samples were malleable. The soaked CBR for natural soil is 1.67%, but it rises to 3.26% when 10% GSA and 10% MK are added. This value fell short of the recommended CBR values for pavement materials. The samples' durability measured based on their resistance to strength loss, fell short of the recommended strength by 80%. This concludes that the groundnut shell ash and metakaolin cannot be used as standalone for stabilization of black cotton soil. However, when compared to the un-stabilized soil, the strength of UCS increased from 128.03 kN/m^2 to 482 kN/m^2 after 28 days of curing.

1 Introduction

Black cotton soil (BCS) is problematic soils which are not good for engineering use, such as road and building construction. In other words, they are very good and fertile for all agricultural purposes. Expansive soils are widespread in semi-arid climatic zones around the world, when yearly evaporation surpasses precipitation, and can be seen anywhere on the planet (Dukare et al. 2016). In some regions of the world, these soils are termed "black cotton soil". Cotton grows well on them, hence the name and black cotton soils come in a variety of colours. The prevalence of montmorillonite, according to Kankia et al.(2021a), dominates the mineralogy of this soil, which is marked by considerable volume changes from wet to dry seasons and likewise. In the summer, black cotton soil deposits reveal a common pattern of fissures. Cracks that measured 70 mm broad and over 1 m deep have been recorded, with high deposits extending up to 3 m or more. Bitumen, lime, and cement are the three most used stabilizers for expanding clays (Jagaba et al. 2019a).

In twenty-first century, attentions of researcher have been shifted from the use of traditional stabilizers (cement, lime, bitumen, etc.) to the use of huge agricultural waste generated from the processing of agricultural products that constitutes problem in the environment. Waste utilization from agricultural material is aimed at reducing the cost of procuring cement and other traditional stabilizers and for the

I. Umaru · A. H. Jagaba · I. M. Lawal (✉) · S. Abubakar
Department of Civil Engineering, Abubakar Tafawa Balewa University, Bauchi, Nigeria
e-mail: Ibrahim.lawal@strath.ac.uk

M. M. Alhaji
Department of Civil Engineering, Federal University of Technology, Minna, Nigeria

A. H. Jagaba · S. R. M. Kutty
Department of Civil and Environmental Engineering, Universiti Teknologi PETRONAS, Perak Darul Ridzuan, Malaysia

I. M. Lawal
Department of Civil and Environmental Engineering, University of Strathclyde, Glasgow, G1 1XJ, UK

U. B. Soja
Department of Civil Engineering, Federal University Dutsin-Ma, Dutsin-Ma, P.M.B. 5001 Katsina State, Nigeria

advancement of engineering practice (Kankia et al. 2021b). Some researchers (Kankia et al. 2021a; Vasavi et al. 2016; Reddy and Rani 2013; Saeed et al. 2021a, 2021b) look into the possibility of using agricultural waste to stabilize the qualities of expansive problematic soils. Their findings reveal that wastes have a desired effect when used alone or in combination with lime or cements.

Groundnut is one of the economic crops produce in Nigeria since 1950. It ranked the sixth in the world's oil seed crops producing 48–50% oil contents followed by protein of 26–28% and lastly carbohydrate, minerals, and vitamins of 11–27%. India produces the most groundnuts in the world, followed by China and Nigeria (Jagaba et al. 2019b). Globally, 20 million hectares of land are utilized for groundwater farming each year and 10% of that are situated in Nigeria. All six north eastern states, four largely populated north western states, and three north central states are among Nigeria's biggest producers (Ng et al. 2021).

The use of solid waste (groundnut shell ash) dumping for soil stabilization is an important practice that has a number of environmental benefits (Ghaleb et al. 2020). All solid and semi-solid materials abandoned by the community are referred to as solid waste. Indiscriminate solid waste management has negative consequences for the environment, perhaps leading to infectious disease outbreaks and epidemics. The excessive reliance on industrially made soil enhancing chemicals (cement, lime, and bitumen, for example) has maintained the cost of stabilizing a road high. This has hampered the ability of developing countries to provide roadways to suit the needs of its rural areas, who make up a substantial proportion of their population. Furthermore, the World Bank has invested on research targeted at reutilizing industrial by-products (Noor et al. 2021a).

According to Nasara et al. (2021), groundnut shell ash (GSA) can be used as a soil remediation agent, particularly in engineering projects with unstable soil, where it can be used as an alternative for deep/raft foundations, saving money and energy. The utilization of agro-based wastes as raw materials has served as an option to reduce environmental pollution levels. Field residues and processing residues are two types of agricultural residues. Field residues are leftovers from crop harvesting that remain on the field. Leaves, stalks, seed pods, and stems make up this group. Process residues, on the other hand, are residues that remain after the crop has been processed into substitute precious resources. Groundnut shells are agricultural wastes derived from groundnut milling (Jagaba et al. 2021a). Metakaolin (Jagaba et al. 2021c) is a highly pozzolanic substance made by calcining kaolin at 700 °C. As a result, the goal of this research is to investigate the viability of agricultural wastes (groundnut shell ash—GSA) in variable percentages and metakaolin in a constant percentage to stabilize black cotton soils.

2 Materials and Methods

2.1 Materials

2.1.1 Soil

The black cotton soil utilized was sourced from Kwandon town in Deba Local Government Area of Gombe State, which is located in North-Eastern part of Nigeria, using a disturbed sample method during the rainy season. The soil was excavated to a depth of 1 m, a portion of the excavated material was wrapped in nylon to acquire the natural moisture content of the soil, and the leftover soil was stored in bags and taken for laboratory analysis. The soil was air dried first before pulverizing.

2.1.2 Groundnut Shell Ash

The groundnut shell ash was sourced locally in Minna, Niger State, Nigeria. It was oven dried at room temperature and then burned at 600–700 °C to produce the ash (GSA). The ash produced was sieved with sieve no. 212 μm. The oxide composition groundnut shear ash (GSA) of Alabadan et al. (Al-dhawi et al. 2020) was adopted as shown in Table 1.

2.1.3 Metakaolin

Kaolin for production of metakaolin was obtained from Alkaleri L. G. A of Bauchi State. It was burned at temperatures ranging from 600 to 700 °C in a kiln at industrial design department at A. T. B. U. Bauchi, the metakaolin was allow to cool before grinding and was sieved using sieve no. 212 μm. The oxide composition of metakaolin of Umar et al. (Jagaba et al. 2021c) was adopted (Table 2).

2.2 Methods

Laboratory test on the black cotton soil and groundnut shell ash/metakaolin mixture was done in accordance with BS1377 (Noor et al. 2021b) standard. Various proportions of 2%, 4%, 6%, and 8% of GSA and 10% metakaolin were

Table 1 Oxide composition of groundnut shell ash

Oxide	Concentration (%)
CaO	8.66
SiO_2	15.92
Al_2O_3	6.73
Fe_2O_3	1.93
MgO	4.72
$K_2O + Na_2O$	6.12
SO_3	6.40
CO_3	6.02

Source Al-dhawi et al. (2020)

Table 2 Oxide composition of metakaolin

Property	Concentration (%)
Al_2O_3	34.2
SiO_2	53.7
K_2O	0.932
CaO	0.513
TaO_2	5.97
V_2O_3	0.23
Cr_2O_3	0.057
MnO	0.061
Fe_2O_3	3.84
NiO	0.071
CuO	0.030
ZnO	0.009
Ga_2O_3	0.088
Total	100

Source Jagaba et al. (2021b, 2021c)

mixed with BCS and the subsequent experiments carried out on the blended mix.

2.2.1 Atterberg Limits Test

The laboratory test was carried out in accordance with Osinubi et al., (Saeed et al. 2021c), and the liquid limit (LL), plastic limit (PL), and plasticity index (PI) of SSA/lime stabilized BCS were determined in the laboratory. Varying percentages of SSA (2%, 4%, 6%, and 8%) with 10% fixed metakaolin were added to BCS by dry weight of soil.

2.2.2 Soil Compaction Test

The soil compaction test was done in accordance with British Standard 1377 (Noor et al. 2021b). The goal was to assess how compacted dry density and soil moisture content were related. The typical proctor light weight compaction efforts were used for this study (BSL). The soil was compacted in a mould of volume 100 cm^3 with 2.5 kg rammer weight and a drop of 304.8 mm in three layers with twenty-seven (27) blows for each layer. The related OMC and MDD were calculated using a graph of moisture content vs dry density. The method was repeated by adding 2%, 4%, 6%, and 8% SSA to the natural BCS, along with 10% metakaolin.

2.2.3 Strength

California bearing ratio (CBR) and unconfined compressive strength (UCS) values were determined using strength tests on a black cotton soil-groundnut shell ash-metakaolin mixture. For curing, the compacted CBR specimens were tightly sealed in plastic bags to prevent moisture loss owing to evaporation. The composites optimum moisture content was used to cast and cured by enclosing every sample in polythene material bags to thwart moisture loss prior to actual testing in full compliance with the Nigerian General Specification (1997), while specimens for unconfined compressive strength (UCS) were prepared at their respective optimum moisture content and curing by wrapping each sample in polythene material bags to prevent moisture loss. In the instance of UCS, the sample was cured for 7, 14, and 28 days. Another set of soil sample was cured for 7 days under comparable circumstances before being properly withdrawn, de-waxed, and totally submerged in water for seven (7) days before being tested for UCS.

2.2.4 Durability

The soil stabilized specimens' durability was assessed using a dip in water test to determine resistance to loss of strength, instead of the wet-dry and freeze–thaw tests recommended by ASTM (Ghaleb et al. 2021), which are ineffective in tropical circumstances. The resistances to loss of strength were calculated as a ratio of the 14-day UCS value of cellophane-cured specimens to the 7-day UCS value of cellophane-cured specimens, opened and submerged in water for further 7 days.

3 Results and Discussions

3.1 Index Properties

Table 3 summarizes the results of index properties performed on natural soil. The black cotton soil was classed as an A-7-6 clayey soil by the AASHTO Classification System. According to the Unified Soil Classification System, USCS (Ghaleb et al. 2021), the soil was classed as inorganic clay soil of high plasticity "CH" with LL and PI values of 60.2 and 30.1%, respectively. As a result, the outcomes obtained fall short of the industry norm for most engineering projects.

3.2 Atterberg Limit

3.2.1 Liquid Limit

Figure 1 depicts the effects of GSA and MK on the black cotton soil's LL. After an initial drop at 2% GSA and 10% MK content, the LL increased as the groundnut shell ash and metakaolin concentration increased. The conclusion is consistent with (Nasara et al. 2021). When the structure of a soil at its LL undergoes a change that results in a marked decline in repulsive forces, its strength increases to the point where more moisture is required to bring the soil to its dynamic shear strength. This did tend to raise the LL of the soil-GSA ash and MK mixture from 60.2% at no GSA and MK content to 58.4% at 10% GSA and MK content each. The first
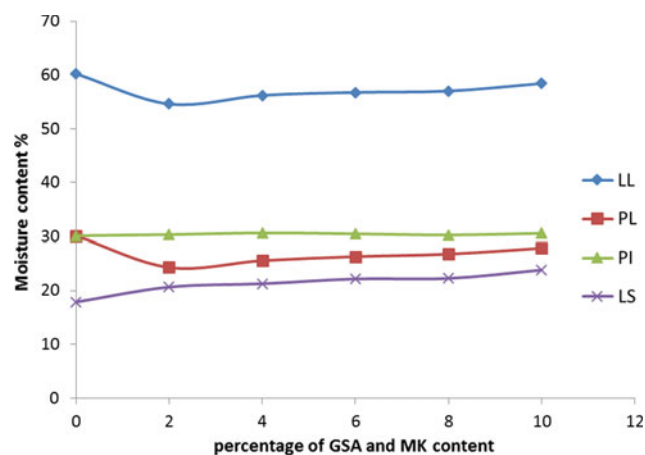
Table 3 Properties of untreated black cotton soil

Property	Value/description
Natural moisture content	30.57%
Specific gravity	2.28
Percentage passing BS sieve No. 200	83.85%
Liquid limit	60.2%
Plastic limit	30.1%
Plasticity index	30.1%
Linear shrinkage	17.86%
AASHTO classification	A–6
Unified soil classification system	CH
Maximum dry density (MDD)	1.40 Mg/m^3
Optimum moisture content (OMC)	27.5%
Unconfined compressive strength	128.03 kN/m^3
California bearing ratio soaked	1.67%
California bearing ratio (unsoaked)	2.20%
Colour	Dark grey

decline in the LL could be attributed to the influence of dilution of clay content in the mix, along with a decrease in the diffused double layer. The rise in the LL between 2% GSA and 10% MK and 10% GSA and 10% MK could be consistent with the observation that each increase in GSA and MK introduced more pozzolanic chemicals from the ash, which required more water to complete hydration.

3.2.2 Plastic Limit

Figure 1 depicts the variance in the BCS's PL as a function of GSA and MK concentration. The addition of GSA and MK led to the reduction in the PL of treated soils. The study by Nasara et al. (2021) obtained results contrary to the trend in this research. According to the report, the PL of the BCS rose due to flocculation attributed to the prevalence of free lime in the fly ash. However, the free lime level in GSA and MK is insufficient to exceed the PL, and so no such change was detected. Sharp reduction in the PL (24.29%) was observed at 2% GSA and 10% MK. That's because the amount of soil to be flocculated dropped as the proportion of GSA and MK in the mix rose, and the finer particles of GSA and MK may be assimilated in the voids of flocculated soil. As a result, the amount of water trapped in the pores decreased, lowering the PL.

3.2.3 Plasticity Index

Figure 1 depicts the variation in plasticity index of the samples after addition of varied percentages of GSA and a fixed proportion of MK. The inclusion of GSA and MK raises the BCS's plasticity index, as shown in the graph. The plasticity index at no GSA content was 30.1% and as stabilizer content was increased to 4% GSA and 10% MK, a peak value of 30.61% was recorded. The rise in PI was most likely caused by a lack of Ca^{2+}, which is needed to replace the weakly bound ions in the clay structure, and therefore, flocculation did not take place as reported by Nasara et al. (2021). Instead, there was an increase in the fine fraction which absorbed more water and became more plastic.

3.2.4 Linear Shrinkage

The soil natural linear shrinkage was 17.86%; a rise was observed to a peak value of 23.81% as depicted in Fig. 1. The rise in the linear shrinkage after adding GSA and MK could be attributed to lack of flocculation and agglomeration as explained earlier and hence the mixture contained finer materials which exhibited more shrinkage characteristics.

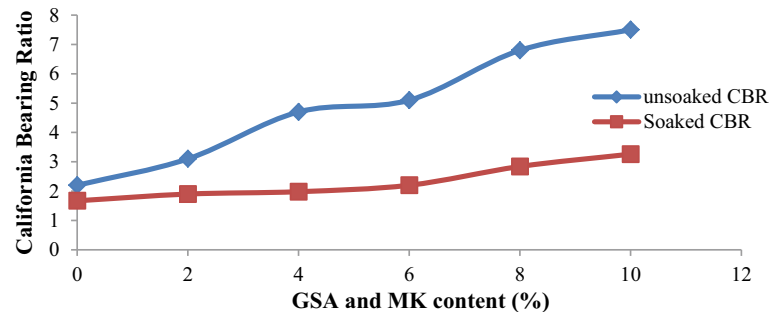**Fig. 1** Variations of Atterberg limit with GSA and MK content

Fig. 2 Variation of MDD with GSA and MK content
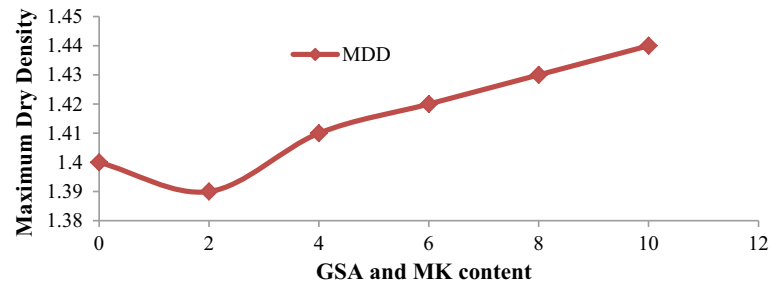
Fig. 3 Variation of optimum moisture content with GSA and MK content
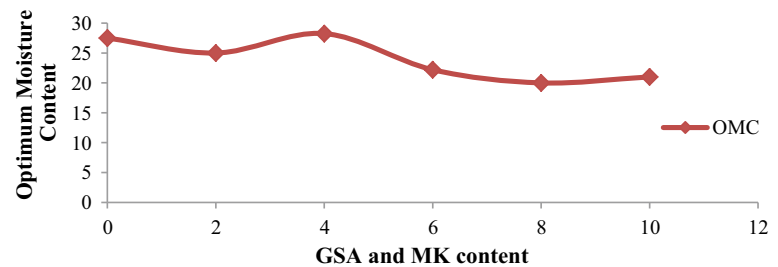
Fig. 4 Variation of CBR with GSA and MK content

3.3 Compaction Parameters

3.3.1 Maximum Dry Density

On the black cotton soil, the fluctuation of the maximum dry density (MDD) with GSA and MK content is displayed in Fig. 2. For 0% GSA, the maximum dry density was 1.4 Mg/m^3 and on addition of GSA and MK, a decrease in MDD was observed to a value of 1.39 Mg/m^3 at 2% GSA and 10% MK. Further, increase in GSA content led to rise in MDD to a maximum of 1.44 Mg/m^3 at 10% GSA and 10% MK as reported by Nasara et al. (2021). The initial decrease in MDD could be attributed in part to the flocculation and agglomeration of clay particles filling larger areas, resulting in a reduction in MDD (Khan et al. 2015). The subsequent increase in MDD is predominantly related to ion exchange.

3.3.2 Optimum Moisture Content

The OMC for sample without GSA is 27.5%, and consecutive increases in OMC to a value of 28.25% at 4% GSA and 10% MK content, as shown in Fig. 3. Further, addition of groundnut shell ash and metakaolin led to a reduction in the

OMC to 20% at 8% GSA and 10% MK as explained by Moses and Osinubi (Abubakar et al. 2016a) and finally, increase of OMC to 21% was observed at 10% GSA and 10% MK blend mix. The first increases in OMC could be attributed to the different cations and clay mineral particles' increased desire for water to conduct hydration process. The decrease in OMC from 8% GSA to 10% MK was due to self-desiccation, in which all available water molecules were used up in the hydration reaction, resulting in decreased hydration and incomplete hydration, which harmed the OMCs.

3.3.3 California Bearing Ratio

Figure 4 depicts the variation in CBR with GSA and MK content. According to Ijimdiya, the addition of GSA and MK content resulted in an increase in CBR (Nasara et al. 2021). Although the increase is still required this could also be linked to the insufficient quantity of CaO present in the GSA and MK. The peak soaked CBR value of 3.26% was obtained at 10% GSA and 10% MK this value fell short of the specification requirement for base and sub-base materials

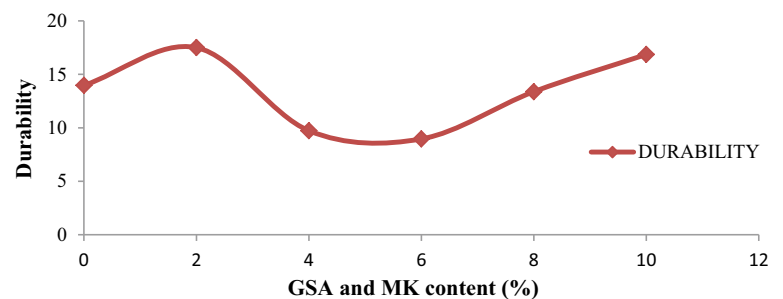**Fig. 5** Variation of USC with GSA and MK content
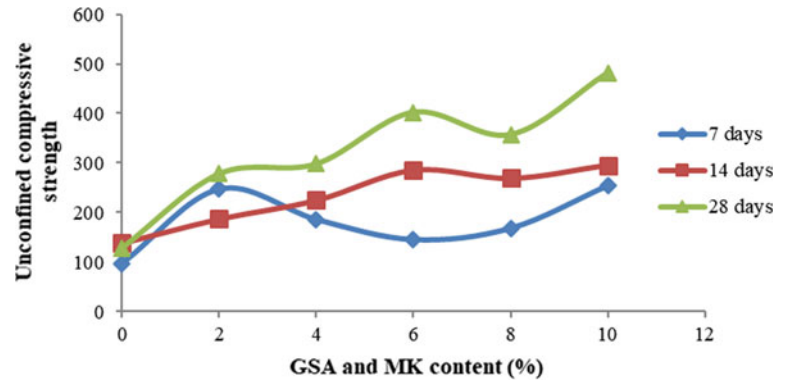
(Abubakar et al. 2016b). The peak CBR value was attained at 10% GSA and MK content each with a CBR value of 7.5% for the unsoaked condition depicted in Fig. 4. Notably, it has very little effect on the CBR value of black cotton soil, which is in line with the findings of other studies (Noor et al. 2021a; Jagaba 2022).

3.3.4 Unconfined Compressive Strength

Figure 5 shows the effect of adding groundnut shell ash and metakaolin to black cotton soil, as well as their UCS values and the fluctuation of UCS with increasing curing time. It is observed in Fig. 5 that on addition of 4% GSA and 10%MK, there was a decrease in the UCS of the mixture. The reasons for the decrease could be as a result of insufficient CaO in the GSA which is required for the stabilization of the BCS. However, at 10% GSA and 10% MK, there were increased values of UCS recorded. It is possible that the higher UCS is due to the existence of enough calcium oxide for stability. At curing periods of 7, 14, and 28 days, UCS values at 10% GSA and 10% MK mixture increased to 254, 295, and 482 kN/m^2, respectively. The time-dependent strength gain action and pozzolanic reactivity of the free lime content of GSA and MK are responsible for the increasing trend of compressive strength with curing time. The increase in compressive strength is due to adequate water, which aided the hydration process linked to the reaction of black cotton soil, groundnut shell ash, and metakaolin. These result in secondary cementitious compounds (Lawal et al. 2021).

3.3.5 Durability

Figure 6 depicts the effect of adding groundnut shell ash and metakaolin on soil durability. At 10% GSA and 10% MK content, the maximal durability value for resistance to strength loss was 18.8%. The soil stabilized specimens' durability was assessed using a dip in water test to determine resistance to strength loss, instead of the wet-dry and freeze–thaw tests mentioned in Ghaleb et al. (2021), which are ineffective in tropical conditions. The resistances to strength loss were calculated as a ratio of the 14-day UCS value of cellophane-cured specimens to the 7-day UCS value of unsealed cellophane-cured specimens submerged in water for further seven (7) days. According to George and Karibo, the GSA failed to meet the minimal durability criteria for application in pavement construction (Jagaba et al. 2021d).

4 Conclusions

The results obtained from this study have led to the following conclusions.

The soil is highly plastic and classified as A-7-6 subgroup of the AASHTO classification. Adding GSA and MK significantly improves the index properties, compaction, and strength characteristics of black cotton soil examined. It increases the MDD of the soils with decrease in the corresponding values of optimum moisture content.

Fig. 6 Variation of durability with GSA and MK content

The plastic limit of the soils decreases, while linear shrinkage increases with the addition of GSA and MK. The UCS of these soils increases upon the addition of GSA and MK. Soil properties were enhanced at 28 days curing period.

The peak CBR (soaked) value at 10% GSA and 10%MK failed to satisfy the country's specification for base and sub-base materials. Conversely, GSA and MK cannot be used as a standalone stabilizer for road construction work. However, it is recommended that GSA and MK can be used more profitably as an admixture with conventional or traditional stabilizers such as lime and cement.

References

S. Abubakar, I.M. Lawal, I. Hassan, A.H. Jagaba, Quality water analysis of public and private boreholes (a case study of Azare Town, Bauchi, Nigeria). Americal J. Eng. Res. **5**(2), 204–208 (2016a)

S. Abubakar, A. Latiff, I.M. Lawal, A.H. Jagaba, Aerobic treatment of kitchen wastewater using sequence batch reactor (SBR) and reuse for irrigation landscape purposes, 5(5), 23–31 (2016b)

B.N. Al-dhawi, S.R. Kutty, N.M. Almahbashi, A. Noor, A.H. Jagaba, *Organics Removal from Domestic Wastewater Utilizing Palm Oil Clinker (POC) Media in A Submerged Attached Growth Systems* (2020)

S. Dukare, P. Barad, M. Gupta, P. Barad, in *Effect of rubber Tyre Shread on Properties of Black Cotton Soil*. International Conference on Science and Technology for Sustainable Development (ICSTSD), pp. 2348–8352 (2016)

A. Ghaleb et al., in *Anaerobic Co-Digestion For Oily-Biological Sludge with Sugarcane Bagasse for Biogas Production Under Mesophilic Condition*, IOP Conference Series: Materials Science and Engineering, vol. 991, no. 1 (IOP Publishing, 2020), p. 012084

A.A.S. Ghaleb et al., Sugarcane bagasse as a co-substrate with oil-refinery biological sludge for biogas production using batch mesophilic anaerobic co-digestion technology: effect of carbon/nitrogen ratio **13**(5), 590 (2021)

A.H. Jagaba et al., Effect of environmental and operational parameters on sequential batch reactor systems in dye degradation. in *Dye Biodegradation, Mechanisms and Techniques*, eds. by S.S. Muthu, A. Khadir (Sustainable Textiles: Production, Processing, Manufacturing & Chemistry. Springer, Singapore, 2022)

A.H. Jagaba et al., Stabilization of soft soil by incinerated sewage sludge ash from municipal wastewater treatment plant for engineering construction **2**(1), 32–44 (2019a)

A.H. Jagaba et al., Defluoridation of drinking water by activated carbon prepared from tridax procumbens plant (A Case Study of Gashaka Village, Hong LGA, Adamawa State, Nigeria) **7**(1), 1 (2019b)

A.H. Jagaba et al., Palm oil clinker as a waste by-product: utilization and circular economy potential (2021a)

A.H. Jagaba et al., A systematic literature review on waste-to-resource potential of palm oil clinker for sustainable engineering and environmental applications **14**(16), 4456, (2021b)

A.H. Jagaba, S. Kutty, M. Fauzi, M. Razali, M. Hafiz, A. Noor, in *Organic and Nutrient Removal from Pulp and Paper Industry Wastewater By Extended Aeration Activated Sludge System*, IOP Conference Series: Earth and Environmental Science, vol. 842, no. 1 (IOP Publishing, 2021c), p. 012021

A.H. Jagaba, S.R.M. Kutty, G. Hayder, E. H. Onsa Elsadig, I. M. Lawal, K. Sayed, S. Abubakar, I. Hassan, I. Umaru, I. Zubairu, M.A. Nasara, U.B. Soja, Evaluation of the physical, chemical, bacteriological and trace metals concentrations in different brands of packaged drinking water. Eng. Lett. **29**(4) (2021d)

M.U. Kankia et al., Performance of fly ash-based inorganic polymer mortar with petroleum sludge ash **13**(23), 4143 (2021a)

M.U. Kankia et al., Optimization of cement-based mortar containing oily sludge ash by response surface methodology **14**(21), 6308 (2021b)

S.U. Khan, A. Noor, I.H. Farooqi, GIS application for groundwater management and quality mapping in rural areas of District Agra, India **4**(1), 89–96 (2015)

I.M. Lawal, D. Bertram, C.J. White, A.H. Jagaba, I. Hassan, A. Shuaibu, Multi-Criteria performance evaluation of gridded precipitation and temperature products in data-sparse regions. Atmosphere **12**, 1597 (2021)

M.A. Nasara, I. Zubairu, A.H. Jagaba, A.A. Azare, Y.M. Yerima, B. Yerima, Assessment of Non-Revenue Water Management Practices in Nigeria (A Case Study of Bauchi State Water and Sewerage Cooperation) (2021)

J. Ng, D. Wong, S. Kutty, A. Jagaba, in *Organic and Nutrient Removal for Domestic Wastewater Treatment Using Bench-Scale Sequencing Batch Reactor*, AIP Conference Proceedings, vol. 2339, no. 1 (AIP Publishing LLC, 2021), p. 020139

A. Noor, S. Kutty, L. Baloo, N. Almahbashi, V. Kumar, A. Ghaleb, in *Bio-kinetics of organic removal in EAAS reactor for co-treatment of refinery wastewater with municipal wastewater*, IOP Conference Series: Materials Science and Engineering, vol. 1092, no. 1 (IOP Publishing, 2021a), p. 012068

A. Noor, S.R. Kutty, N.M. Almahbashi, V. Kumar, A.A. Ghaleb, B.N. Al-Dhawi, Integrated submerged media extended aeration activated sludge (ISmEAAS) reactor start-up and biomass acclimatization. J. Hunan Univ. Nat. Sci. **48**(9) (2021b)

C.N.V. Reddy, K.D. Rani, Potential of shredded scrap tyres in flexible pavement construction. Indian Highways **41**(10) (2013)

A.A.H. Saeed et al., Pristine and magnetic kenaf fiber biochar for Cd^{2+} adsorption from aqueous solution **18**(15), 7949 (2021a)

A.A.H. Saeed et al., in *Removal of Cadmium (II) from Aqueous Solution by Rice Husk Waste*, 2021b International Congress of Advanced Technology and Engineering (ICOTEN), IEEE, pp. 1–6 (2021b)

A.A.H. Saeed et al., Modelling and optimization of biochar-based adsorbent derived from Kenaf using response surface methodology on adsorption of Cd2+ **13**(7), 999 (2021c)

B.S. Vasavi, D.S.V. Prasad, A.C.S.V. Prasad, Stabilization of expansive soil using crumb rubber powder and cement. Int. J. Innovative Res. Technol. **2**(8), 26–31 (2016)

Stabilization of Lateritic Soil with Scrap Tyre Crumb Rubber

Mohammed Tasiu Ibrahim, Kolawole Juwonlo Osinubi,
Saeed Yusuf Umar, Abimiku Joshua, Ahmad Hussaini Jagaba,
and Usman Bala Soja

Abstract

Non-lateritic soils are commonly used for construction purposes. However, due to the variability of the properties of the soil, it does not meet the design requirement. In this study, non-lateritic soil sample was taken from a borrow pit in Dungulbi, Bauchi State Nigeria. The materials were characterized and then stabilized with scrap tyre crumb rubber (STCR) in concentration of 1, 2, 3, 4, and 5% by dry weight of the soil for various sizes of scrap tyre crumbs rubber (STCR) in the range (i.e. 0.212, 2.36, 3.35, and 4.75 mm). The test conducted on the non-lateritic soil-STCR includes compaction using three energies level and durability. The results obtained indicate a general decrease in both optimum moisture content (OMC) and maximum dry density (MDD) as the STCR contents increases. For all the three different compaction energy levels used, the durability decreased with increase in the STCR content. The BSL compactive efforts resulted in higher durability values than the samples compacted using BSH and WAS compactive efforts. The highest durability obtained with the BSL compaction effort could be attributed to decrease in compressibility which is believed to be caused by lower compaction energy and less orientation of adjacent particles during compaction.

1 Introduction

Soil stabilization is the mechanical or chemical modification of one or more engineering qualities of soil to make it suitable for usage (James and Pandian 2016; Dukare et al. 2016; Kankia et al. 2021a). The term "soil modification method" refers to a slight change in the qualities of the soil. The term "modification" in this context refers to a slight alteration in soil qualities (Jagaba et al. 2019a). However, soil stabilization methods are utilized to decrease the compressibility as well as permeability of soil mass in earthwork, enhance its shear strength, and raise the bearing capacity of foundation soils by changing the soil engineering characteristics enough to let field construction to take place (Kankia et al. 2021b; Vasavi et al. 2016; Reddy and Rani 2013; Saeed et al. 2021a). Stabilization differs from modification in that the additive reaction produces a significant amount of long-term strength gain.

The development of new engineering materials with regulated properties from unconventional source materials has the potential of providing the sustainability of many engineering projects (Saeed et al. 2021b). Portland cement is among the most often utilized additions in soil stabilization for different kinds of granular soils (Jagaba et al. 2019b). With a greater emphasis on engineering for sustainable development currently, there is a need to test a wide range of practical applications for waste material disposal and pass on the practical information for proper implementation (Ng et al. 2021). Every year, millions of tonnes of trash tyres are produced due to the growing number of cars on the road around the world. A limited amount of scrap tyres is used for a variety of purposes, including floor mats, tarred road

M. T. Ibrahim · S. Y. Umar · A. H. Jagaba (✉)
Department of Civil Engineering, Abubakar Tafawa Balewa University, Bauchi, Nigeria
e-mail: ahjagaba@gmail.com

K. J. Osinubi
Department of Civil Engineering, Ahmadu Bello University, Zaria, Nigeria

A. Joshua
Department of Civil Engineering, Federal Polytechnic Bauchi, Bauchi, Nigeria

U. B. Soja
Department of Civil Engineering, Federal University Dutsin-Ma, P.M.B. 5001, Dutsin-Ma, Katsina State, Nigeria

construction, and shoe production locally. The remaining significant amount of scrap tyres are illegally dumped in various parts of the country.

The beneficial use of wastes does not only decrease their negative effect on the environment but also reduce the cost of disposal, preserve, and protect the environment as well as proffer solution to problems associated with the soils of low shear strength (Ghaleb et al. 2020; Noor et al. 2021a). Therefore, this study evaluates the properties of a non-lateritic soil treated with scrap tyre crumbs rubber of different sizes when used as a road construction material.

2 Materials and Methods

2.1 Materials

2.1.1 Lateritic Soil

The bulk disturbed sampling approach was used to get the soil sample for this study from a borrow pit at Dungulbi along Bauchi-Gombe Road. The soil samples were collected at a depth of 1.5–2.0 m to avoid using topsoil and ensure non-inclusion of organic matter. Samples were taken in big racs, with a small amount used for determining the natural moisture content put in a polythene bag and secured to prevent moisture loss during transport to the soil laboratory (Nasara et al. 2021; Jagaba et al. 2021c). The samples were air-dried, and large lumps were crushed and passed through BS No. 4 sieve.

2.1.2 Scrap Tyre Crumb Rubber

The scrap tyre was collected from a dumping site in Bauchi state, Nigeria. Crumb rubber was obtained from cutting scrap tyres into small chips manually shredded to sizes that include 4.75, 3.35, 2.36, and 0.212 mm was prepared using machine.

2.2 Methods

2.2.1 Compaction

The British Standard Light (standard Proctor, BSL), West African Standard (intermediate, WAS), and British Standard Heavy (modified Proctor, BSH) compaction methods were utilized (Jagaba et al. 2021a, 2021d; Al-dhawi et al. 2020; Noor et al. 2021b). The BSL compaction equals 595.96 kJ/m^3 of ASTM D 698-12 compaction energy, whereas the WAS compaction equals 993.26 kJ/m^3 of ASTM D 698-12 compaction energy. Table 1 lists the features of the compaction methods used.

At ambient temperature, the laterite was allowed to dry before being pulverized into small enough pieces to pass through a sieve with a 4.76 mm opening. 315 mixes were created by adding STCR in stepwise concentrations of 0, 1 to 5% weight of soil. The moisture level of the mouldings used to prepare the samples varied from 10 to 15%. The per cent STCR control mix was called C0—0STCR, while the other five mixes were labelled C1—1STCR, C2—2STCR, C3—3STCR, C4—4STCR, and C5—5STCR, respectively, to reflect the levels of STCR addition to the soil by weight. Three specimens were produced and compacted for each percentage addition of STCR. The MDD (Qd$_{max}$) and the average of OMC (W$_{opt}$) were calculated.

2.2.2 Durability

The soil specimens made by combining non-laterite soil with 1 to 5% STCR were used in the durability test. For each % of STCR, three samples were made. First, dried soil was combined with different STCR %. To get the mixture's moisture content up to the stipulated ideal moisture level, a suitable amount of water equal to the OMC was added. By static compression, the mixes were remoulded into conventional moulds of 38 mm Ø and 80 mm length to the necessary maximum dry density as per BS 1377: 1990: part 5. (Saeed et al. 2021c; Ghaleb et al. 2021). The compacted samples were cured for seven days at 90–100% relative humidity and then placed in a closed desiccator partially filled with water at room temperature for 5 h before being weighed and measured. The specimens were then heated in a 70 °C oven for 43 h before being retrieved. Specimens were weighed, and their measurements were measured once more. The process outlined above constitutes one wetting and drying cycle (48 h). The specimens were placed in desiccators once again. The specimens are dried at 110 °C and weighed after 12 cycles of testing to establish the oven-dry weight of the specimens. After the 12 cycles of testing, the data acquired allowed for the calculation of volume and moisture changes in the specimens. Each cycle's weight loss

Table 1 Characteristics of compaction methods used

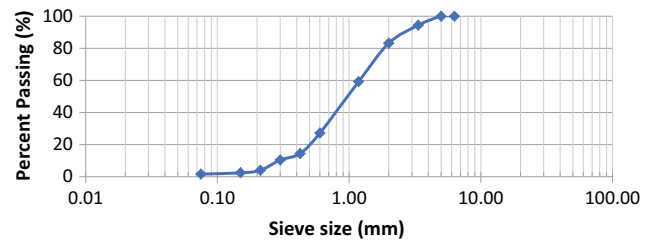| Compaction method	Volume of mould (cm^3)	Weight of rammer (kg)	Height of fall (cm)	Number of layers	Numbers of blows	Work done (kJ/m^3)
BSL	1000	2.5	30	3	27	596
WAS	1000	4.5	45	5	10	993
BSH	1000	4.5	45	5	27	268

is calculated independently after each wetting and drying (Khan et al. 2015; Abubakar et al. 2016a).

3 Results and Discussion

3.1 Characterization of Materials

Table 2 summarizes the results of classification tests performed on natural soil. Physical observation revealed that the soil is reddish brown in colour. The particle size disperse curve shown in Fig. 1 depicts a well-graded soil. The soil classifies as A–2–7(0) and GW using the AASHTO ASTM D3282-09 soil classification system and USCS ASTM D2487-11, respectively (Abubakar et al. 2016b; Jagaba et al. 2022; Lawal et al. 2021; Jagaba et al. 2021b). These classification systems show that the soil is coarse sand of low plasticity (Tables 3 and 4).

Fig. 1 Size distribution curve for soil sample

Table 2 Soil characteristics

Property	Quantity
% Passing No. 200 sieve (%)	1.6
Moisture content (%)	9.7
LL (%)	51.0
PL (%)	26.7
PI (%)	2.4.3
Linear shrinkage	11.4
Specific gravity	2.61
AASHTO classification	A-2–7 (0)
USCS	GW
Group index	0
Percentage fine sand fraction	2.4
Percentage medium sand fraction	20.0
Percentage coarse sand fraction	60.8
Percentage fine gravel fraction	16.8
MDD (Mg/m^3)	
BSL	1.81
WAS	1.82
BSH	1.83
Optimum moisture content (%)	
BSL	14.4
WAS	13.8
BSH	13.6
Unsoaked California bearing ratio (%)	
BSL	35.6
WAS	38.6
BSH	46.8
Soaked California bearing ratio (%)	
BSL	10.7
WAS	13.1
BSH	21.0
Colour	Reddish Brown

Table 3 Index properties of scrap tyre crumb rubber stabilized soil

S/No	Mix proportion (%)		Linear shrinkage	Index properties (%)		
	Soil	STCR	W_S (%)	W_L	W_P	I_P
1	99	1	10.90	44.3	21.1	23.2
2	98	2	10.71	43.8	20.8	23.0
3	97	3	10.43	43.1	20.4	22.7
4	96	4	10.14	43.0	20.4	22.6
5	95	5	10.00	41.8	20.3	21.5

Table 4 XRF results of the natural non-lateritic soil

Oxides composition	Concentration (%)
SiO_2	65.97
Al_2O_3	23.27
Ti_2O	0.71
Fe_2O_3	7.03
K_2O	1.06
MgO	ND
Na_2O	0.12
MnO	0.02
CaO	0.44
ZnO	ND
NiO	ND
SrO_3	0.03
Cr_2O_3	ND
S	0.01
P	ND
NbO_2	0.01
MoO_2	0.03
Zr_2O	0.02
SbO	ND
Cd_2O	0.02
Ag_2O	0.01
LOI	–

3.2 Compaction characteristics

Figures 2, 3, 4 and 5 describe the correlation between moulding water content and dry density for various soil-STCR combinations. MDD reduced in general when the STCR replacement level increased. The MDD of soil mixtures was projected to reduce as the STCR component in the combination increased from 1 to 5%. The impacts of the numerous percentage replacement rate on moisture content demonstrate a convergent behaviour that could be likened to STCR's low water absorption capacity. The inclusion of STCR with a specific gravity of 1.17 did result in mixtures with lower specific gravity, which inevitably leads to a reduction dry density. It is evident from the plot of the OMC and MDD; the best results were achieved using British Standard Heavy. As the STCR replacement level increased, the moisture content decreased which is an indication of better performance.
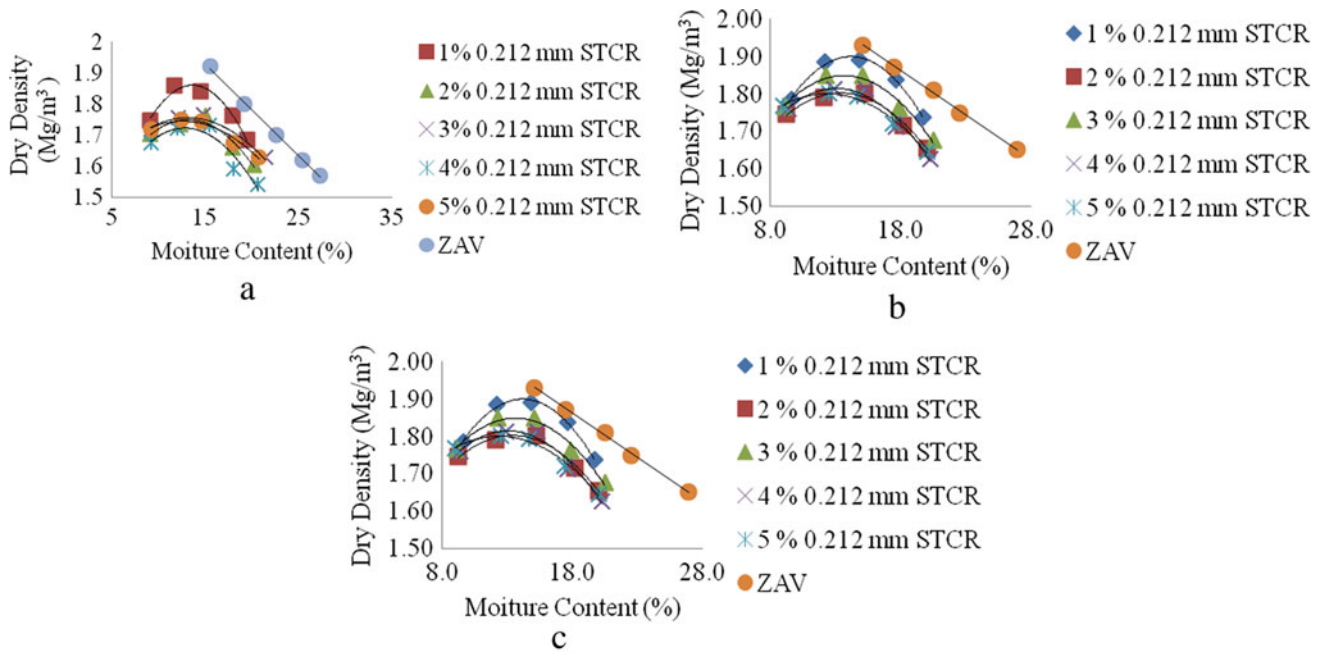
Fig. 2 Moisture–density relationship of non-lateritic soil stabilized with 0.212 mm STCR for: **a** BSL, **b** WAS, **c** BSH compaction
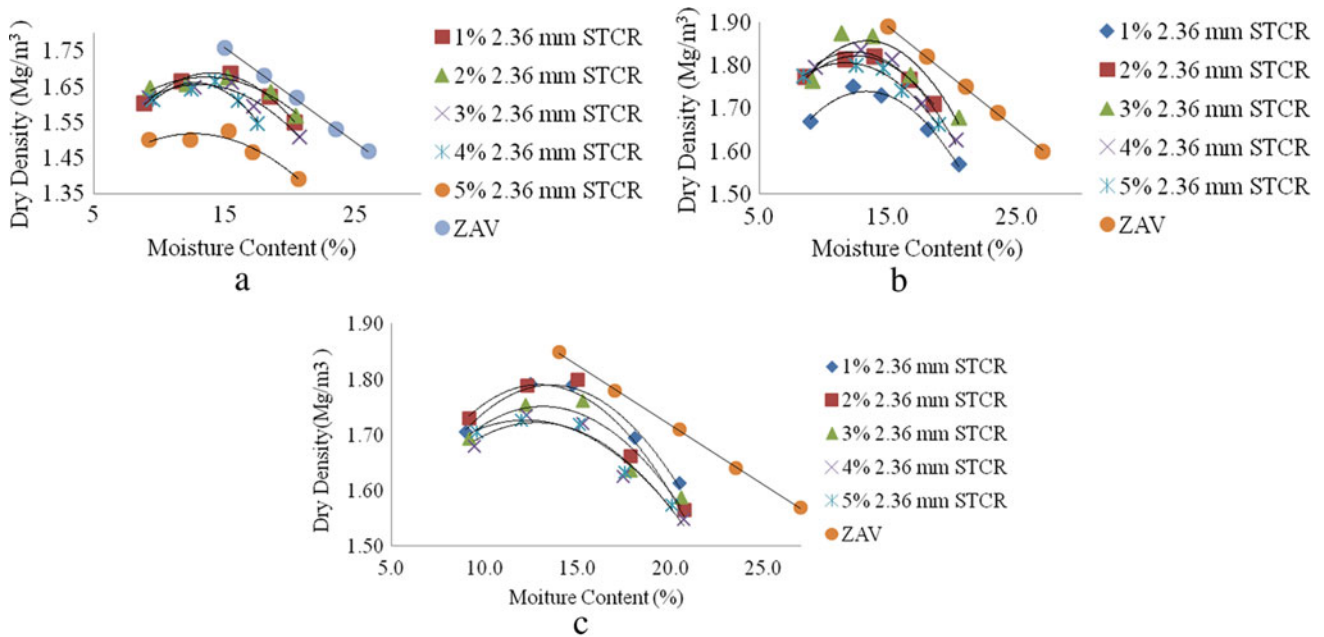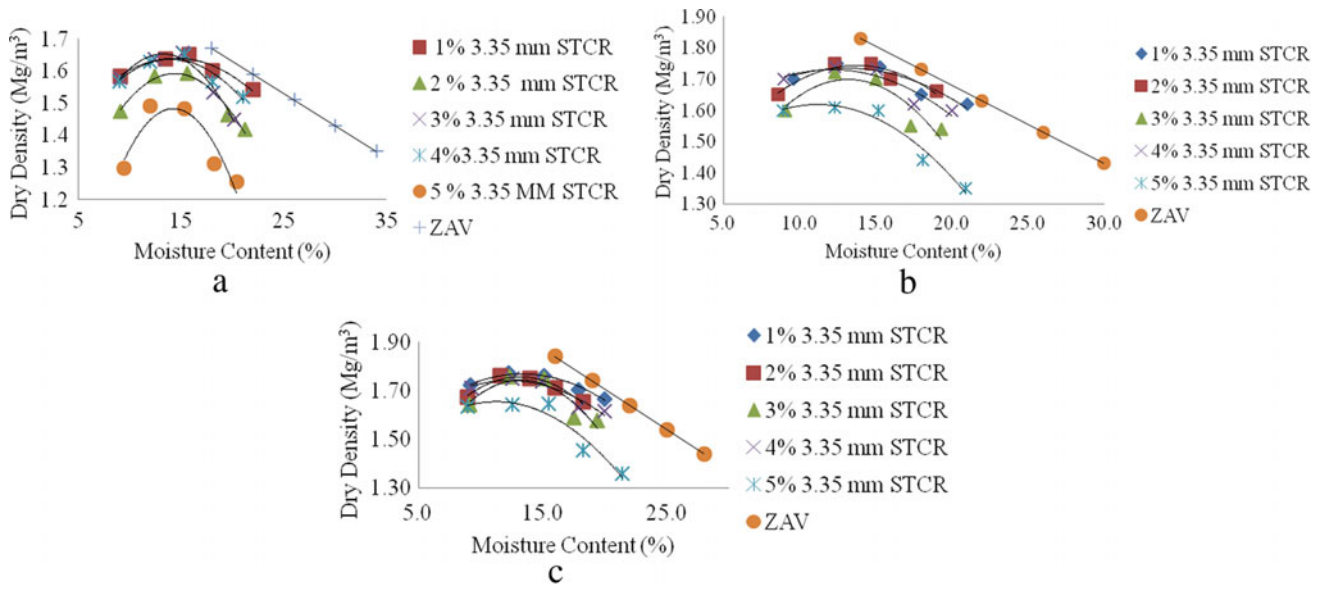

Fig. 3 Moisture–density relationship of non-lateritic soil stabilized with 2.36 mm STCR for: **a** BSL, **b** WAS, **c** BSH compaction

3.3 Durability

The variation of durability with various percentage of STCR content after compacting the sample at OMC using BSL, WAS and BSH compaction energies showed that the durability of non-laterite soil decreases with increase in percentage of STCR and also decrease as circles of wetting and drying increase. The resilience of all three distinct compaction energy levels employed reduced as the STCR content rose. However, the peak durability values recorded after the 12

Fig. 4 Moisture–density relationship of non-lateritic soil stabilized with 3.35 mm STCR for: **a** BSL, **b** WAS, **c** BSH compaction
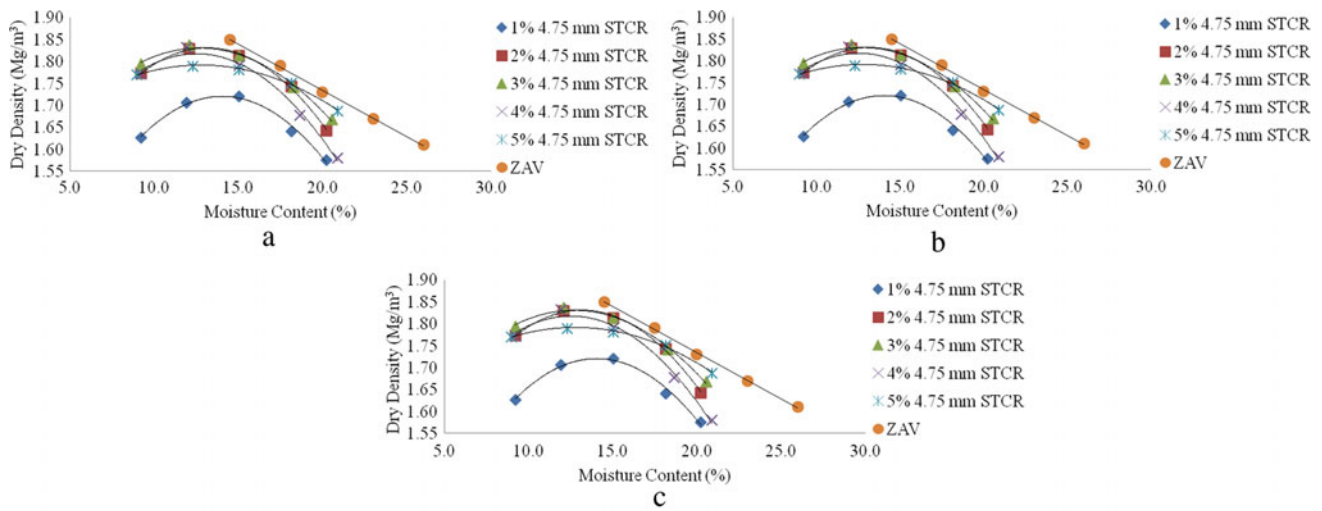
Fig. 5 Moisture–density relationship of non-lateritic soil stabilized with 4.75 mm STCR for: **a** BSL, **b** WAS, **c** BSH compaction

cycles of wetting and drying are 3.46%, 2.63%, 2.49%, and 2.45% at 1% STCR content for 0.212, 2.36, 3.35, and 4.75 mm STCR size using BSL compaction effort as shown in Tables 5, 6, 7 and 8. The specimens compacted employing BSL compactive efforts had greater durability values than those compacted using WAS and BSH compactive efforts. The maximum durability was achieved with the BSL compaction effort, which is thought to be due to a decrease in compressibility produced by reduced compaction energy and less orientation of nearby particles during compaction.

Table 5 Durability test results of non-laterite soil stabilized with STCR (BSL)

Circles	1% 0212 STCR		2% 0.21 STCR		3% 0.212 STCR		4% 0.212 STCR		5% 0.212 SICR	
	W	D	W	D	W	D	W	D	W	D
1.	2.60	0.13	2.45	0.01	2.43	0.00	2.41	0.03	2.35	0.00
2.	2.63	0.11	2.23	0.00	2.22	0.11	2.35	0.01	2.33	0.00
3.	2.60	0.11	2.06	+0.01	2.07	0.13	2.22	0.14	2.20	0.00
4.	1.92	0.10	1.39	+0.14	2.04	0.10	2.00	0.15	1.98	0.13
5.	1.15	0.64	1.94	0.28	1.95	0.06	1.89	0.06	1.85	0.06
6.	−0.60	0.65	−0.24	0.30	1.97	0.05	1.85	−0.03	1.80	0.03
7.	0.64	0.34	0.63	0.35	1.14	0.03	1.88	−0.21	1.79	0.01
8.	0.11	−0.14	0.60	0.25	1.11	−0.14	1.57	−0.19	1.80	0.00
9.	0.09	−0.28	−0.14	−0.14	1.03	−0.20	1.32	0.06	1.30	0.00
10.	0.31	−0.11	−0.10	−0.15	0.95	−0.22	0.64	0.07	1.00	0.00
11.	0.01	0.10	0.10	−0.18	0.65	−0.64	0.71	−0.17	0.60	0.00
12.	0.02	0.00	0.06	−0.38	0.64	1.7	0.60	−0.06	0.32	0.00

Node W = wetting, D = drying

Table 6 Durability test results of non-laterite soil stabilized with STCR (WAS)

Circles	1% 0.212 STCR		2% 0.212 STCR		3% 0.212 STCR		4% 0.212 STCR		5% 0.212 STCR	
	W	D	W	D	W	D	W	D	W	D
1.	2.53	0.65	2.51	0.00	2.50	0.00	2.41	0.00	2.40	0.97
2.	2.41	0.10	2.40	0.00	2.38	1.05	2.33	0.00	2.36	0.19
3.	2.30	0.00	2.25	0.64	2.51	1.21	−2.38	0.00	2.13	0.25
4.	1.90	−0.13	2.00	0.78	2.30	0.95	−2.45	0.71	2.17	−0.03
5.	1.00	0.10	1.85	1.00	1.91	−0.65	−0.64	0.63	1.85	0.15
6.	0.85	0.00	1.65	1.05	−1.95	−0.55	0−.65	0.48	1.75	−0.29
7.	−0.71	0.00	−1.13	−0.64	−2.00	0.64	1.05	−0.01	1.69	−0.33
8.	0.64	0.06	−1.65	0.13	−2.31	0.13	0.95	−0.14	1.53	−0.35
9.	0.12	−0.13	−1.78	0.06	1.09	0.11	−0.35	−0.28	0.64	−0.38
10.	−0.11	0.06	0.64	−0.11	0.95	0.06	−0.45	−0.32	0.64	0.01
11.	0.06	0.00	−0.13	0.11	−0.64	0.03	0.13	−0.38	1.05	0.01
12.	0.06	0.00	−1.63	0.11	−0.75	0.00	0.11	−0.39	0.48	0.00

Node W = wetting, D = drying

4 Conclusions

From the result of the investigation carried out within the scope of the study, the following inference in the context of utilizing STCR in soil stabilization can be drawn:

- The non-lateritic soil used for this study is classified as A–2–7 (0) and GW using the AASHTO ASTM D3282-09 soil classification system and USCS ASTM D2487–11, respectively. The LL and PL were found to be 51.0 and 26.7%, respectively, and the corresponding plasticity index is 24.3% which is confirmed that the soil is low plastic soil.
- An increase in STCR content led to the reduction of OMC and MDD
- The investigated STCRs are promising materials to enhance the geotechnical qualities of non-laterite soils

Table 7 Durability test results of non-laterite soil stabilized with STCR (BSH)

Circles	1% 0.2.12 STCR		2% 0.2.12 STCR		3% 0.2.12 STCR		4% 0.212 STCR		5% 0.2.12 STCR	
	W	D	W	D	W	D	W	D	W	D
1.	2.49	0.0	2.46s	0.0	2.41	0.0	2.41	0.13	2.11	0.12
2.	2.45	0.0	2.25	0.0	2.40	0.0	2.39	0.15	2.36	0.13
3.	2.42	1.00	2.04	0.0	2.20	0.11	2.19	0.64	1.98	0.11
4	2.00	0.45	−0.79	1.03	2.11	0.20	2.10	0.28	1.90	−0.3
5.	1.17	0.35	−0.2	0.38	1.39	0.13	1.55	0.14	1.95	0.10
6.	−0.65	0.09	0.62	−0.6	1.21	0.10	1.39	0.25	0.08	−0.3
7.	0.11	−0.13	0.13	0.13	1.20	0.09	1.20	−0.28	0.25	−0.2
8.	0.10	0.10	0.07	−0.10	0.91	0.06	1.19	−0.14	0.20	0.06
9.	0.64	−0.10	0.06	−0.10	0.64	0.05	1.00	0.11	0.17	0.03
10.	0.00	0.13	0.4	0.23	0.60	0.03	0.20	−0.06	−0.28	0.02
11.	0.00	0.23	0.35	0.13	0.55	0.02	0.4	0.00	−0.30	0.01
12.	−0.11	0.00	0.30	−0.26	0.00	0.01	0.00	0.00	−0.14	0.00

Node W = wetting, D = drying

Table 8 Durability test results of non-laterite soil stabilized with modified STCR (BSL)

Circles	1% 2.36 STCR		2% 2.36 STCR		3% 2.36 STC3.		4% 2.36 STCR		5% 2.36 STCR	
	W	D	W	D	W	W	W	D	W	D
1.	3.46	0.0	3.35	0.07	3.23	0.06	3.19	0.04	3.14	0.00
2.	3.35	0.50	3.30	0.06	3.20	0.06	3.15	0.03	3.05	0.00
3.	3.17	0.39	3.00	0.11	2.96	0.06	3.00	0.01	2.97	0.01
4.	3.13	−0.26	3.13	0.13	2.91	0.11	2.87	0.01	2.85	0.01
5.	2.66	−0.19	2.64	0.25	2.62	−0.11	2.60	−0.01	2.64	0.00
6.	2.62	−0.06	2.60	0.55	2.56	−0.13	2.54	−0.11	2.50	0.00
7.	2.52	0.06	2.13	0.15	2.35	0.01	2.40	0.14	2.11	0.01
8.	2.14	0.13	2.00	0.11	2.15	0.03	2.25	−0.23	2.30	−0.01
9	2.00	−0.66	1.85	−0.06	2.00	−0.01	1.96	−0.28	1.93	−0.01
10.	1.85	0.06	1.75	−0.11	1.97	−0.13	1.90	−0.30	1.75	−0.06
11.	1.74	−0.06	1.69	0.00	1.85	0.23	1.70	0.01	1.49	−0.11
12.	1.65	0.06	1.45	0.00	1.65	−0.30	1.39	0.00	1.20	0.00

Node W = wetting, D = drying

with low plasticity. 3% of STCR content was observed to yield maximum improvement.

References

S. Abubakar, I.M. Lawal, I. Hassan, A.H. Jagaba, Quality water analysis of public and private boreholes (a case study of Azare Town, Bauchi, Nigeria). Americal J. Eng. Res. **5**(2), 204–208 (2016a)

S. Abubakar, A.A.A. Latiff, I.M. Lawal, A.H. Jagaba, Aerobic treatment of kitchen wastewater using sequence batch reactor (SBR) and reuse for irrigation landscape purposes **5**(5), 23–31 (2016b)

B.N. Al-dhawi, S.R.M. Kutty, N.M. Almahbashi, A. Noor, A.H. Jagaba, *Organics Removal from Domestic Wastewater Utilizing Palm Oil Clinker (POC) Media in A Submerged Attached Growth Systems* (2020)

S. Dukare, P. Barad, M. Gupta, P. Barad, in *Effect of Rubber Tyre Shread on Properties of Black Cotton Soil*. International Conference on Science and Technology for Sustainable Development (ICSTSD) (2016), pp. 2348–8352

A. Ghaleb et al., in *Anaerobic co-digestion for oily-biological sludge with sugarcane bagasse for biogas production under mesophilic condition*, IOP Conference Series: Materials Science and Engineering, vol. 991, no. 1 (IOP Publishing, 2020), p. 012084

A. Ghaleb et al., Sugarcane bagasse as a co-substrate with oil-refinery biological sludge for biogas production using batch mesophilic anaerobic co-digestion technology: effect of carbon/nitrogen ratio **13**(5), 590 (2021)

A.H. Jagaba et al., Stabilization of soft soil by incinerated sewage sludge ash from municipal wastewater treatment plant for engineering construction **2**(1), 32–44 (2019a)

A.H. Jagaba et al., Defluoridation of drinking water by activated carbon prepared from tridax procumbens plant. *A Case Study of Gashaka Village Hong LGA, Adamawa State, Nigeria* **7**(1), 1 (2019b)

A.H. Jagaba, S.R.M. Kutty, M. Fauzi, M. Razali, M. Hafiz, A. Noor, in *Organic and nutrient removal from pulp and paper industry wastewater by extended aeration activated sludge system*, IOP Conference Series: Earth and Environmental Science, vol. 842, no. 1 (IOP Publishing, 2021a), p. 012021

A.H. Jagaba, S.R.M. Kutty, G. Hayder, E.H. Onsa Elsadig, I.M. Lawal, K. Sayed, S. Abubakar, I. Hassan, I. Umaru, I. Zubairu, M.A. Nasara, U.B. Soja, Evaluation of the physical, chemical, bacteriological and trace metals concentrations in different brands of packaged drinking water. Eng. Lett **29**(4) (2021b)

A.H. Jagaba et al., *Palm Oil Clinker as a Waste By-Product: Utilization and Circular Economy Potential* (2021c)

A.H. Jagaba et al., A systematic literature review on waste-to-resource potential of palm oil clinker for sustainable engineering and environmental applications 14(16), 4456 (2021d)

A.H. Jagaba et al., Effect of environmental and operational parameters on sequential batch reactor systems in dye degradation. in *Dye Biodegradation, Mechanisms and Techniques. Sustainable Textiles: Production, Processing, Manufacturing & Chemistry. Springer, Singapore*, eds. by S.S. Muthu, A. Khadir (2022)

J. James, P.K. Pandian, Industrial wastes as auxiliary additives to cement/lime stabilization of soils. Adv. Civil Eng. (2016)

M.U. Kankia et al., Performance of fly ash-based inorganic polymer mortar with petroleum sludge ash **13**(23), 4143 (2021a)

M.U. Kankia et al., Optimization of cement-based mortar containing oily sludge ash by response surface methodology **14**(21), 6308 (2021b)

S.U. Khan, A. Noor, I.H. Farooqi, GIS application for groundwater management and quality mapping in rural areas of District Agra, India **4**(1), 89–96 (2015)

I.M. Lawal, D. Bertram, C.J. White, A.H. Jagaba, I. Hassan, A. Shuaibu, Multi-criteria performance evaluation of gridded precipitation and temperature products in data-sparse regions. Atmosphere **12**, 1597 (2021)

M.A. Nasara, I. Zubairu, A.H. Jagaba, A.A. Azare, Y.M. Yerima, B. Yerima, *Assessment of Non-Revenue Water Management Practices in Nigeria* (A Case Study of Bauchi State Water and Sewerage Cooperation, 2021)

J. Ng, D. Wong, S.R.M. Kutty, A.H. Jagaba, in *Organic and nutrient removal for domestic wastewater treatment using bench-scale sequencing batch reactor*. AIP Conference Proceedings, 2021, vol. 2339, no. 1 (AIP Publishing LLC, 2021), p. 020139

A. Noor, S.R.M. Kutty, L. Baloo, N. Almahbashi, V. Kumar, A. Ghaleb, in *Bio-kinetics of organic removal in EAAS reactor for co-treatment of refinery wastewater with municipal wastewater*, IOP Conference Series: Materials Science and Engineering, vol. 1092, no. 1 (IOP Publishing, 2021a), p. 012068

A. Noor, S.R.M. Kutty, N. Almahbashi, V. Kumar, A.A.S. Ghaleb, B. N. Al-Dhawi, Integrated submerged media extended aeration activated sludge (ISmEAAS) reactor start-up and biomass acclimatization. J. Hunan Univ. Nat. Sci. **48**(9) (2021b)

C.N.V. Reddy, K.D. Rani, Potential of shredded scrap tyres in flexible pavement construction. Indian Highways **41**(10) (2013)

A. Saeed et al. (2021a) Pristine and magnetic kenaf fiber biochar for Cd2+ adsorption from aqueous solution **18**(15), 7949

A. Saeed et al., in *Removal of Cadmium (II) from Aqueous Solution by Rice Husk Waste*, 2021 International Congress of Advanced Technology and Engineering (ICOTEN), IEEE (2021b), pp. 1–6

A. Saeed et al., Modelling and optimization of biochar-based adsorbent derived from Kenaf using response surface methodology on adsorption of Cd2+ **13**(7), 999 (2021c)

B.S. Vasavi, D.S.V. Prasad, A.C.S.V. Prasad, Stabilization of expansive soil using crumb rubber powder and cement. Int. J. Innovative Res. Technol. **2**(8), 26–31 (2016)

Reducing Energy Consumption in Lighting Systems Using Smart and IoT-Based Control Method

Shahad Al-juaid, Rawan Al-zahrani, Lujain Al-talahi, Ghadeer Majly, and Rania Mokhtar

Abstract

The energy conservation and remote monitoring are essential for smart building automation. The paper introduces smart lighting control system that aims to help in reducing energy consumption for occupants. The system focuses on three strategies for managing the lighting system: daylight harvesting, occupancy sensing, and childcare. Therefore, the system implements photosensing, motion, and sound detection to state light status. The system provides both local control and IoT-based remote control for the different gadgets. The system relay in the future (IoT/IoE) technology to provide energy sustainability, automation, control, and management level led by the user.

Keywords

Internet of things • Internet of everything • Lighting control • Photosensing • Motion detection • Sound detection

1 Introduction

The care for the environment pushes toward using green energy sources and energy conservation. Energy efficiency is one of the most important technical challenges of our time (Salih Abdalla et al. 2020). Lighting and environment monitoring have tremendous potential in improving living standards. In KSA, the energy consumption by the lighting system is estimated as 17% of electricity use, while the global average is estimated as 15%. This shows that lighting is a major area that needs deploying of energy-saving techniques and efficient usage methods in both indoor and outdoor environment ("Energy Saver Identifier"; Anjali et al. 2017; Abo-Zahhad et al. 2015; Fazal et al. 2019).

A report by the department of energy in USA also shows that 15% of an average building's electricity is consumed by the lighting system. Therefore, household switched to LED lighting which result in about 225$ saves in energy costs annually (Akanksha et al. 2021). Lighting control is gaining great importance with respect to the growing demands for energy reservation and versatility to sustain visual need. Manual controls of lighting system and environmental factor are subject to human error, human may forget to shut off light during non-working hours, when the space becomes unoccupied, or during daytime (Mokhtar and Saeed 2011).

Several studies have been conducted in the field of energy saving such as automatic room light controller with visitor counter (Saeed et al. 2014; Abbas Alnazir et al. 2021; Dafalla et al. 2021), and this study implements home automation with a bidirectional counter. In (Saeed et al. 2012a), wireless sensor networks are used for implementing an energy monitoring and management system for buildings. In this work, an efficient load management is proposed energy management system (EMS) is designed to reduce the consumption of the energy by the consumers at the peak load hours. This results in reduction of the carbon emissions of the household. IoT is being vital role in today's smart systems (Mokhtar and Saeed 2011; Saeed et al. 2012b, 2019a, 2019b, 2021a; Mokhtar et al. 2010; Musa et al. 2021). An IoT-based Smart Building Management System using Arduino is proposed in Saeed et al. 2021b. The study focuses on the present concept of smart building automation system based on Arduino. Table 1 compares these related studies.

2 Smart Lighting Control System

This paper introduces a design of smart lighting control system based on IoT with consideration of energy conservation, to achieve acceptable automated level of energy

S. Al-juaid · R. Al-zahrani · L. Al-talahi · G. Majly · R. Mokhtar (✉)
Taif University, Al Hawiyah, Taif, 26571, Saudi Arabia
e-mail: ramohammed@tu.edu.sa

Table 1 Comparison of related works

No	System	Controller	Applications	Merits
1	NB-IoT technology for smart medical system (Energy Saver Identifier)	Android mobile	Facilitates the registration of the patients and enables medical staff to complete their work easily	Time efficient Effort efficient
2	An automated room light controlling with visitor counter (Fazal et al. 2019)	Microcontroller	Room Light Control and Visitor Counter	Low cost
3	Using wireless sensor networks to implement an energy monitoring and management system (Akanksha et al. 2021)	Arduino Uno	Energy control based on WSN	Energy-efficient Highly scalable
4	Building energy management system based on microcontrollers (Mokhtar and Saeed 2011)	Microcontroller	Energy Management System	Low cost

saving, sustainability, and operational cost savings (Ahmed et al. 2020). Lighting control is implemented based on three strategies: daylight harvesting, occupancy sensing, and childcare. Utilizing these approaches together is almost typical for every building whether its residential, commercial, or industrial buildings to reduce energy consumption. The system therefore consists of:

1. **Motion-controlled light**: This part includes motion sensor, which detect human motion, the sensor works based on movement of human in or out of the sensors range and detect the move and send a signal in its port to the controller. Then the system triggers the light ON/OFF accordingly (Saeed et al. 2015). The motion sensor used is PIR, "Passive Infrared," "Pyroelectric," or "IR motion" sensor. This is small, inexpensive, low-power, easy-to-use sensor. The motion detection is suitable for corridor parts of the building, and it also helps in the night security if an unexpected motion is detected (Mokhtar et al. 2015).

2. **Photo-controlled light**: This part includes photosensor, to detect luminosity (visible light) to detect whether the place has enough light or not (Saeed 2011). Then the system triggers the light ON/DIMM/OFF accordingly. The photosensor used is a photoresistor, the photoresistor is a light-dependent resistor (LDR), or photo-conductive cell which is a passive element that reduces the resistance with regard to the amount of luminosity (light) that received on the sensitive surface of the resistor (Mokhtar et al. 2021). Photosensing satisfies the control aspects for the outdoor lights or for area where visible light of the sun exists.

3. **Sound-controlled light**: This part includes sound sensor, which detects human sound, almost always used to detect whether a child is crying or screaming. Then the system triggers the light ON/OFF accordingly (Saeed and Mokhtar 2012).

Based on the value sent by the sensor, the controller decides the action need to be taken and send the right value in the specific output port. Therefore, the light bulb is controlled based on real need of the place. The system conceptual model is shown in Fig. 1.

2.1 Simulation Setup

Logical view: In the logical workspace the component of the system and the network are built and connected, here the development platform is MCU virtual card which provide similar environment to Arduino. The connection of the devices is done based on their nature digital or analog. Light and detector devices for each strategy are selected as "things," to demonstrate the IoT, and these devices are therefore equipped by network connection possibility. The light is equipped by Ethernet port or with WLAN (Baykas et al. 2012).

In the other hand, a simple network is implemented, that is local LAN of the building, consisting of a wireless router to connect to an IoT server, which is used as the remote registration server for the things (Ahmed et al. 2015). Devices are connected to the registration server, and the user can monitor the sensor and control the light from any Internet-connected device in the local or cellular network. Figure 2 illustrates the simulation of the system in the logical view.

The left side of the figure demonstrates the local control while the right side demonstrates the IoT frame of the system. IoT devices (things), motion detector, sound frequency detector, and network-enabled lights are connected to the remote registration server (Saeed et al. 2021b) which is configured as shown in Fig. 3. Conditions are configured for devices in the server as shown in Fig. 4.
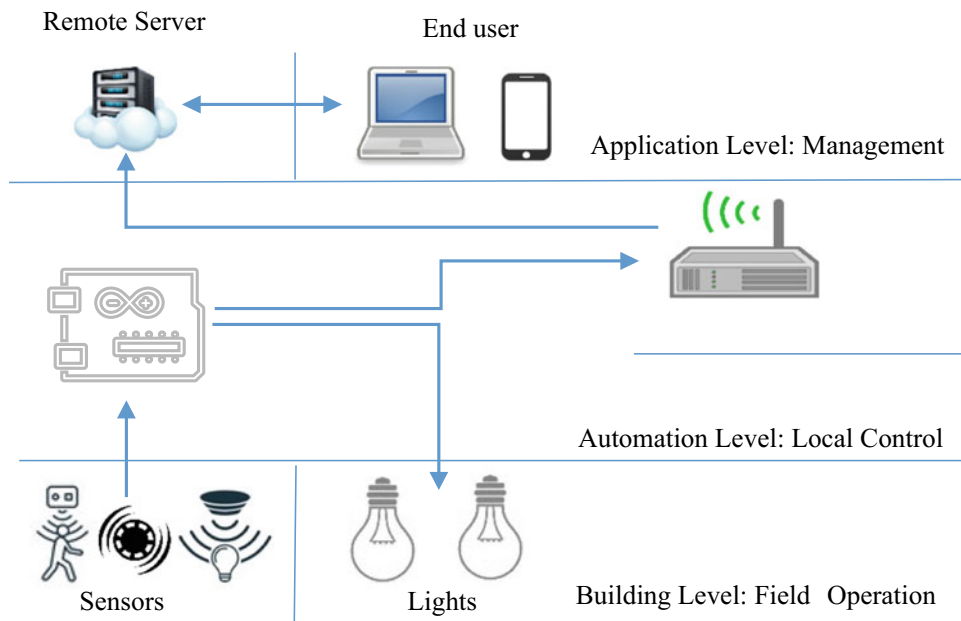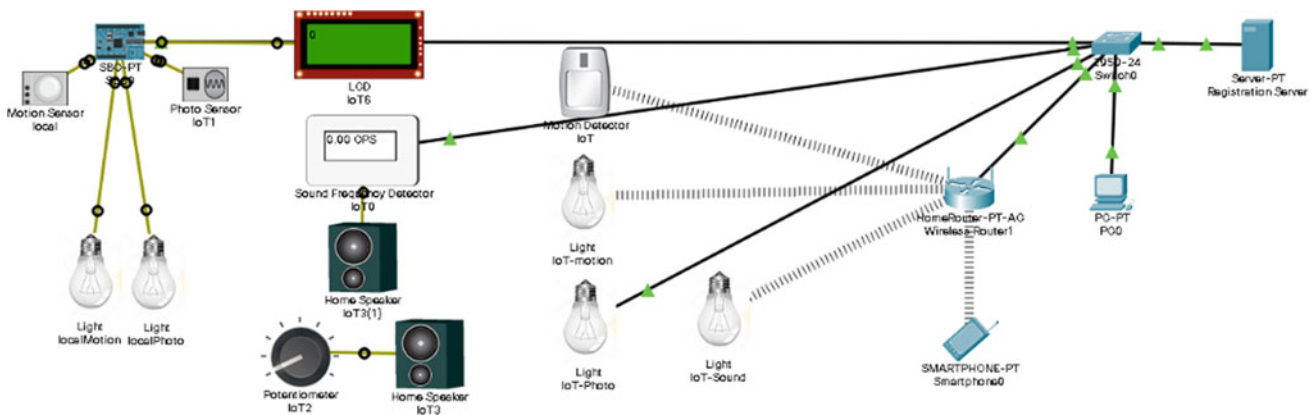
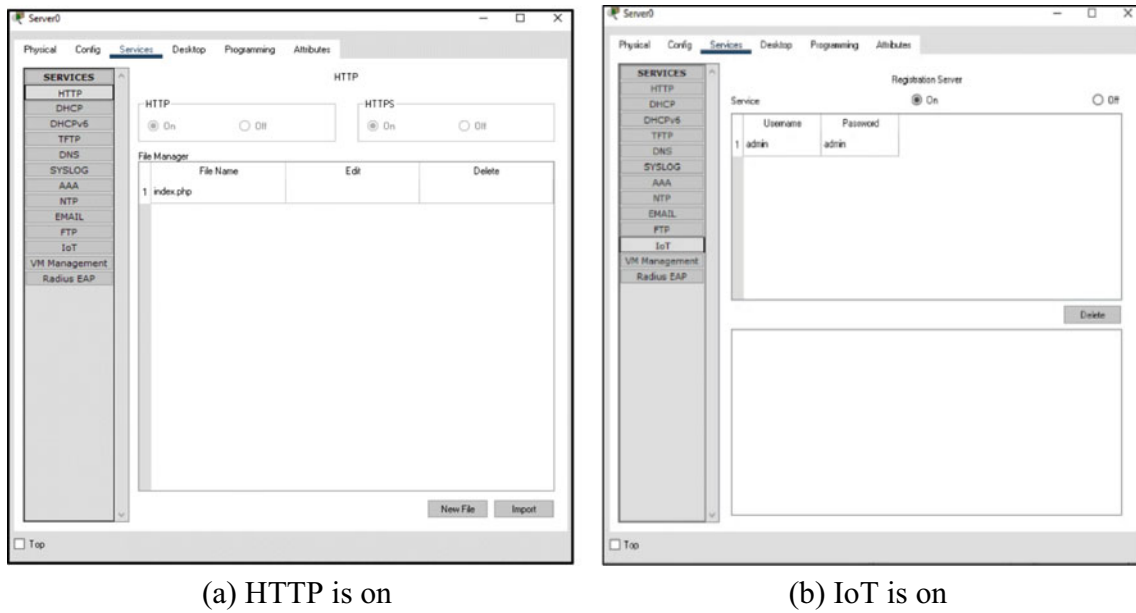**Fig. 1** System model

Fig. 2 System design and simulation

3 Results

3.1 Motion-Controlled Light

Figure 5 illustrates the result for motion-controlled light: When a target moves, the motion is detected at the local motion sensor and the motion detector. Based on the sensor value that was sent to the SBU card, the card set the motion-controlled light that connected to the SBU to ON. On the other hand, when the motion detector (things) detects a motion the IoT server triggers the network-connected motion-controlled light ON.

3.2 Photo-Controlled Light

For photo-controlled light, light is detected from the simulation real-time environment, which provide visible light (sunlight) phenomena based on daytime as shown in Fig. 6. When low light detected by the photosensor the light is set to DIM (Mokhtar et al. 2013), when enough light is detected by the photosensor the light is set OFF; however only when the delectated light is very low, or no light detected the light is set to ON as shown in Fig. 7.

(a) HTTP is on   (b) IoT is on

Fig. 3 Registration server configuration

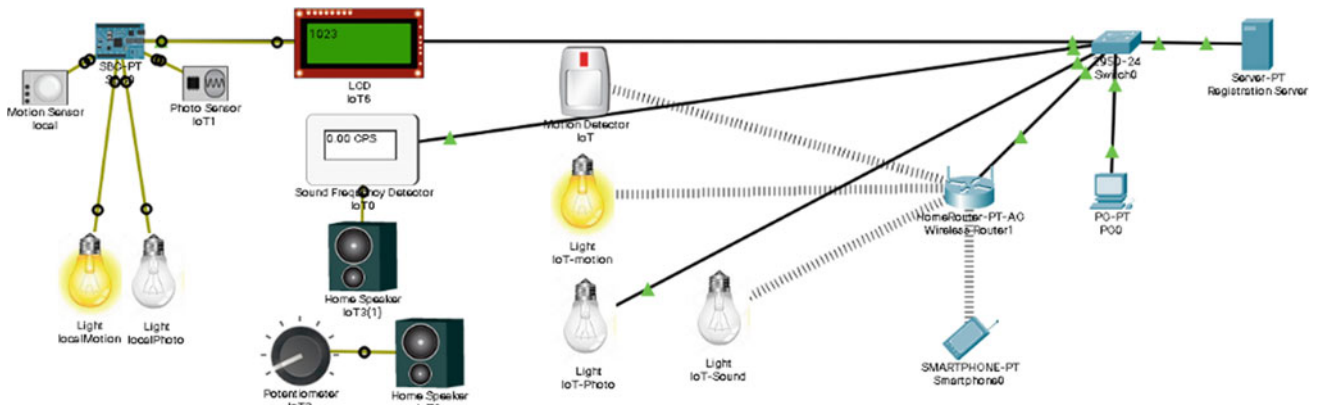**Fig. 4** IoT server—device condition setting
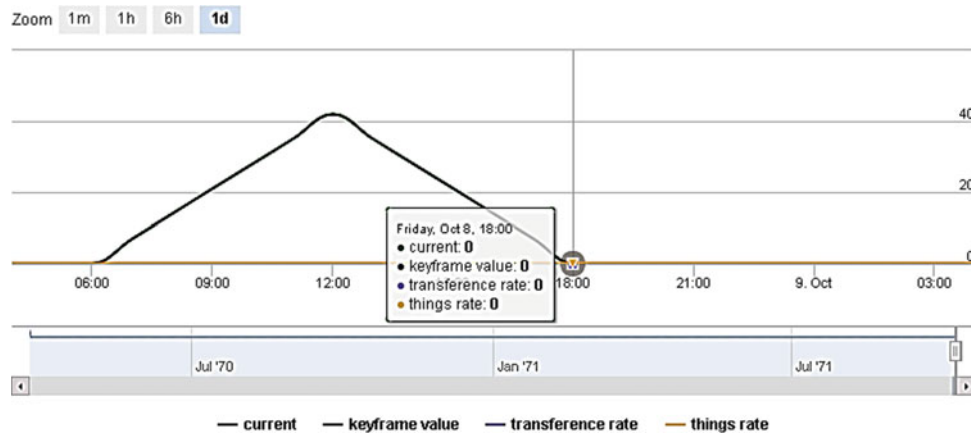

Fig. 5 Motion-controlled light

Fig. 6 Simulation real-time environment, visible light (sunlight) phenomena
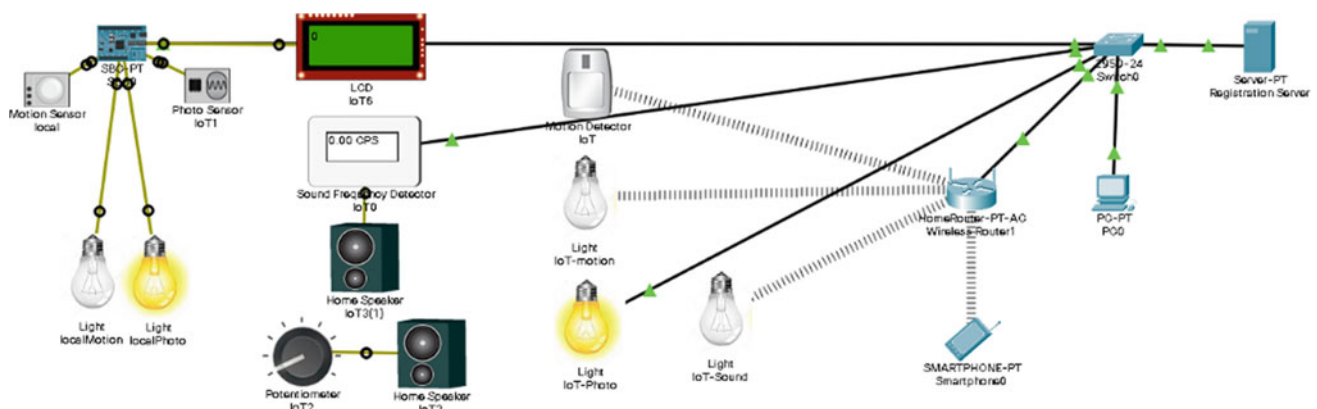

Fig. 7 Photosensing, no light detected the light bulb is set to ON

3.3 Sound-Controlled Light

For sound-controlled light, a potentiometer fed the speaker to produce sound. The frequency of the sound is detected by sound frequency detector that is connected to the IoT server, once a sound is detected the sound-controlled light is set to ON as shown in Fig. 8.

3.4 Remote Monitoring

All devices that are connected to the IoT server can be monitored and controlled from the end user device. The statues of the devices are accessible through HTTP protocol in server as shown in Fig. 9.

4 Discussion

Lighting control is essential enabling method for adopting green and sustainable energy sources, such as solar panel. Lighting control helps avoid energy waste (Hassan et al.

2021, 2020; MDPI, Sustainability 2021). The methodology of the proposed system aims to implement lighting control that helps the energy conservation for smart home, and smart building automation to monitor and control the lighting system. The lighting control aim to save energy by ensuring no light is left ON when it is not required (Salih Ahmed et al. 2021).

5 Conclusions

In this paper, three lighting control strategies were proposed to ensure proper use of lighting systems as well as reduce energy waste. These include photosensing, occupancy, and childcare strategies. The system is designed as local control system as well as IoT-based control and mentoring system. The result of the system operation shows that for the energy used by lighting system can be reduced significantly by using such light control methods.
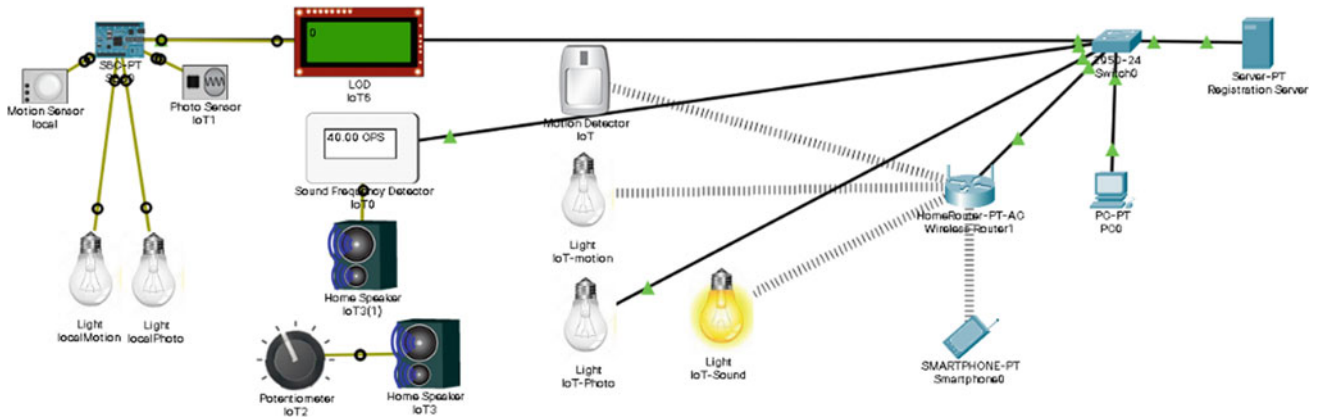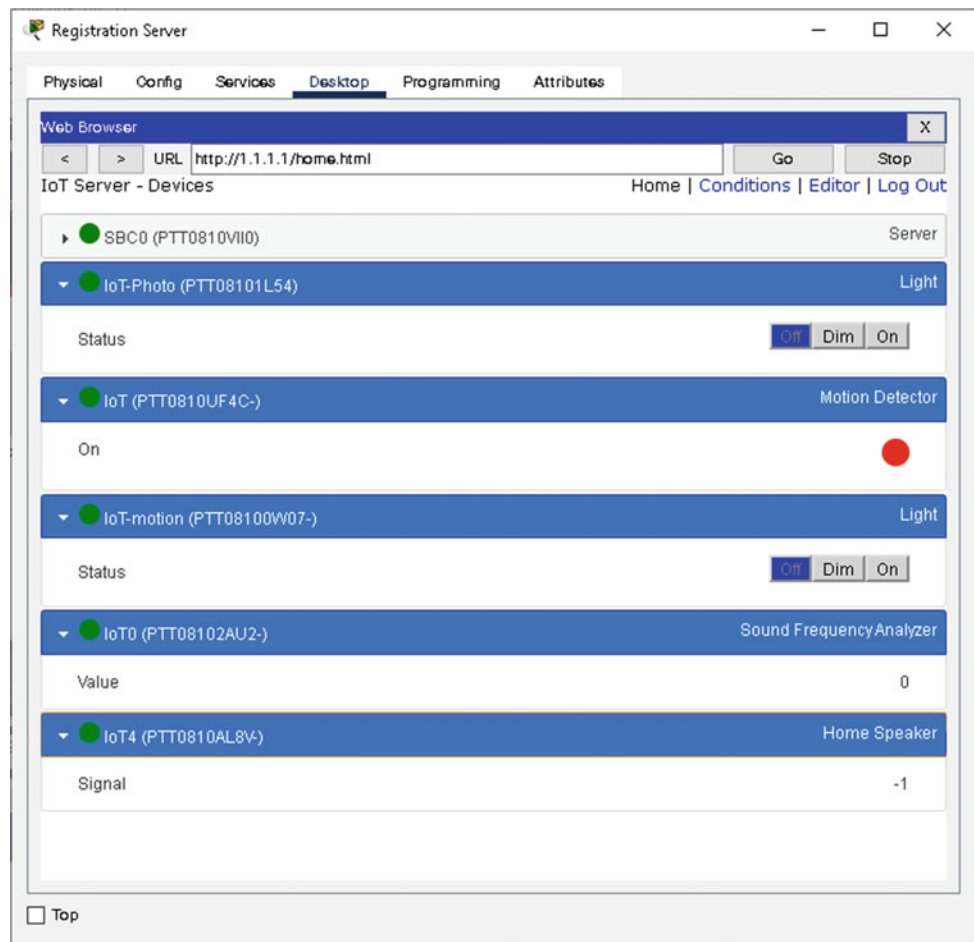
Fig. 8 Sound-controlled light is set to ON

Fig. 9 IoT server devices

References

A. Alnazir, R.A. Mokhtar, A. Hesham, E.S. Ali, R.A. Saeed, S. Abdel-khalek, Quality of services based on intelligent IoT WLAN MAC protocol dynamic real-time applications in smart cities. Computat. Intell. Neurosci. **2021**(2287531), 20 (2021)

M. Abo-Zahhad, S.M. Ahmed, M. Farrag et al, in *Design and Implementation of Building Energy Monitoring and Management System Based on Wireless Sensor Networks*. Tenth International Conference on Computer Engineering & Systems (ICCES), pp. 230–233 (2015)

K.E.B. Ahmed, R.A. Mokhtar, R.A. Saeed, in *A New Method for Fast Image Histogram Calculation*, International Conference on Computing, Control, Networking, Electronics and Embedded Systems Engineering (ICCNEEE), Khartoum, Sudan (2015), pp. 187–192

Z.E Ahmed, H. Kamrul, R.A. Saeed, S. Khan, S. Islam, M. Akharuzzaman, R.A. Mokhtar, Optimizing energy consumption for cloud internet of things. Front. Phys. **8** (2020). https://doi.org/10.3389/fphy.2020.00358

C. Akanksha, D. Akshay, S. Sandesh et al., IoT based smart building management system using Arduino. Int. Res. J. Eng. Technol. (IRJET) **8**(4), 416–419 (2021)

S. Anjali, S. Arpita, S. Deepa et al, Automatic room light controller with visitor counter (2017). Int. J. Emerg. Technol. (Special Issue CETST-2017) **8**(1), 172–175 (2017)

T. Baykas, M. Kasslin, M. Cummings, H. Kang, J. Kwak, R. Paine, A. Reznik, R. Saeed, S.J. Shellhammer, Developing a standard for TV white space coexistence: technical challenges and solution approaches. IEEE Wirel. Commun. Mag. **19**(2), 10–22 (2012)

M.E.M. Dafalla, R.A. Mokhtar, R.A. Saeed, A. Hesham, S. Abdel-Khalek, M. Khayyat, An optimized link state routing protocol for real-time application over Vehicular Ad-hoc Network. Alexandria Eng. J. (2021)

Energy Saver Identifier (Department of energy, USA) https://www.energy.gov/energysaver/lighting-choices-save-you-money

N. Fazal, A. Noor, A. Rahman et al, Building energy management system based on microcontrollers, in *Emerging Technologies in Computing* (2019). https://doi.org/10.1007/978-3-030-23943-5_24

M.B. Hassan, E.S. Ali, R.A. Mokhtar, R.A. Saeed, B.S. Chaudhari, NB-IoT: concepts, applications, and deployment challenges, in *LPWAN Technologies for IoT and M2MApplications*, eds. by B.S. Chaudhari, M. Zennaro (Elsevier, 2020), ISBN: 9780128188804

M.B. Hassan, A. Sameer, A. Hesham, E.S. Ali, R.A. Mokhtar, R.A. Saeed, An enhanced cooperative communication scheme for physical uplink shared channel in NB-IoT. Wirel. Pers. Commun. **116**(2) (2021)

R. Mokhtar, B.M. Ali, N.K. Noordin, R. Saeed, Y. Abdalla, Distributed cooperative spectrum sensing in cognitive radio networks with adaptive detection threshold. Proc. Asia-Pac. Adv. Netw. **30**, 90–99 (2010)

R. Mokhtar, R.A. Saeed, Conservation of mobile data and usability constraints, in *Cyber Security Standards, Practices and Industrial Applications: Systems and Methodologies, Ch 03*, eds. by Z. Junaid, M. Athar (IGI Global, USA, 2011), pp. 40–55, ISBN13: 978-1-60960-851-4

R. Mokhtar, R.A. Saeed, R. Alsaqour, Y. Abdallah, Study on energy detection-based cooperative sensing in cognitive radio networks. J. Netw. (JNW) **8**(6), 1255–1261 (2013), ISSN 1796-2056. https://doi.org/10.4304/jnw.8.6.1255-1261

R.A. Mokhtar, A.F. Ismail, M.K. Hasan, W. Hashim, H. Abbas, R.A. Saeed, S. Islam, Lightweight handover control function (L-HCF) for

mobile internet protocol version six (IPv6). Indian J. Sci. Technol. **8** (12) (2015). https://doi.org/10.17485/ijst/2015/v8i12/70656

R.A. Mokhtar, R.A. Saeed et al., Cluster mechanism for sensing data report using robust collaborative distributed spectrum sensing. Cluster Comput. (2021)

A.M. Musa, R.A. Mokhtar, R.A. Saeed, H.A lhumyani, S. Abdel-Khalek, A.O.Y. Mohamed, Distributed SC-FDMA sub-carrier assignment for digital mobile satellite. Alexandria Eng. J. **60**(6), 4973–4980 (2021)

N. Nurelmadina, M.K. Hasan, I. Mamon, R.A. Saeed, K. Akram, Z. Ariffin, E.S. Ali, R.A. Mokhtar, S. Islam, E. Hossain, Md.A. Hassan, A systematic review on cognitive radio in low power wide area network for industrial IoT applications. MDPI, Sustainability (2021)

R.A. Saeed, *TV White Space Spectrum Technologies: Regulations, Standards, and Applications* (CRC Press, USA, 2011), ISBN: 9781439848791

R.A. Saeed, R.A. Mokhtar, in *TV White Spaces Spectrum Sensing: Recent Developments, Opportunities and Challenges*, The 6th International Conference SETIT 2012: Sciences of Electronic, Technologies of Information and Telecommunications (SETIT2012), Tunisia (2012), pp. 634–638

R.A. Saeed, R.A. Mokhtar, J. Chebil, A.H. Abdallah, in *TVBDs Coexistence by Leverage Sensing and Geo-location Database*, IEEE International Conference on Computer & Communication Engineering (ICCCE2012a), Malaysia (2012a), pp 33–39

R.A. Saeed, R.A. Mokhtar, in *TV White Spaces Spectrum Sensing: Recent Developments, Opportunities and Challenges*, The 6th International Conference SETIT 2012b: Sciences of Electronic, Technologies of Information and Telecommunications (SETIT2012b), Tunisia (2012b), pp. 634–638

R.A. Saeed, M. Al-Magboul, R.A. Mokhtar, Machine-to-machine communication, in *IGI Global, Encyclopedia of Information Science and Technology*, 3rd Ed (2014), pp. 6195–6206. https://doi.org/10.4018/978-1-4666-5888-2

R.A. Saeed, A.F. Ismail, M.K. Hasan, R. Mokhtar, S.K.A. Salih, W. Hashim, Throughput enhancement for WLAN TV white space in coexistence of IEEE 802.22. Indian J. Sci. Technol. (IJSC) 8(11) (2015). https://doi.org/10.17485/ijst/2015/v8i11/71783

M.M. Saeed, R.A. Saeed, E. Saeid, Survey of privacy of user identity in 5G: challenges and proposed solutions. Saba J. Inf. Technol. Netw. (SJITN) 7(1) (2019a)

M.M. Saeed, R.A. Saeed, E. Saeid, in *Preserving Privacy of Paging Procedure in 5G Using Identity-Division Multiplexing*, 2019 First International Conference of Intelligent Computing and Engineering (ICOICE), IEEE (2019b), pp. 1–6

M.M. Saeed, R.A. Saeed, E. Saeid, in *Identity Division Multiplexing Based Location Preserve in 5G*, 2021 International Conference of Technology, Science and Administration (ICTSA), (2021a), pp. 1-6. https://doi.org/10.1109/ICTSA52017.2021.9406554

R.A. Saeed, M.M. Saeed, R.A. Mokhtar, A. Hesham, S. Abdel-Khalek, Pseudonym mutable based privacy for 5G user identity. J. Comput. Syst. Sci. Eng. **29**(1), 1–14 (2021b)

R. Salih Abdalla, S.A. Mahbub, R.A. Mokhtar, E.S. Ali, R.A. Saeed, *IoE Design Principles and Architecture; Book: Internet of Energy for Smart Cities: Machine Learning Models and Techniques* (CRC Press Publisher, 2020). https://doi.org/10.4018/978-1-7998-5101-1

R. Salih Ahmed, E.S.A. Ahmed, R.A. Saeed, Machine learning in cyber-physical systems in industry 4.0, in *Artificial Intelligence Paradigms for Smart Cyber-Physical Systems*, eds. by A.K. Luhach, A. Elçi (IGI Global, Hershey, PA, 2021), pp. 20–41

Zero-Touch Entrance System and Air Quality Monitoring in Smart Campus Design Based on Internet of Things (IoT)

Sara ALQathami, Shahad ALThiyabi, Sara ALZyadi, Mona ALJuaid, Wejdan AlHarthy, and Rania Mokhtar

Abstract

Humanity is currently witnessing the era of information technology in various forms which impacts all the aspects of daily life. The Internet has become a daily necessity to utmost of the individuals for effective participation and communication among themselves as well as interacting things around them. Consequently, there is serious need to shift from traditional working, living environments into smart environment, by enabling controlling and monitoring the infrastructure, and the environment. Most campus infrastructure still relies on traditional method, where no consideration for automated health environment is given. This study explores the challenges and potentials of the intelligent environment as a new human-technology interaction paradigm. The study proposes a system that provides a way to overcome the health issue triggered by close environment and touching problems and make it more comfortable, smarter, safer, and efficient. This work focuses on two parts: non-touch automatic door based on radio frequency identification technology, and an automated window to provide healthy air quality environment based on sensing and IoT system. The system is designed and simulated using CISCO packet tracer utilizing its real time environment. The results include automated entrance system, safe and healthy room environment.

Keywords

Internet of thing (IoT) • Smart campus • Lighting control • Radio-Frequency identification • Infrastructure • Gas sensing

S. ALQathami · S. ALThiyabi · S. ALZyadi · M. ALJuaid · W. AlHarthy · R. Mokhtar (✉)
Department of Computer Engineering, College of Computers and Information Technology, Taif University, P.O. Box 11099, Taif 21944, Saudi Arabia
e-mail: ramohammed@tu.edu.sa

1 Introduction

The Internet of Things technology has the required capacity to revolutionize the day-to-day lifestyle (Hassan et al. 2021). It can be utilized to make life easier and more efficient in a variety of ways, including for both luxuries, industrial and emergencies cases (Cheng et al. 2021). IoT is now being combined with different technology such as narrow band to provide wide range of application (Nurelmadina et al. 2021; Hassan et al. 2020; Santoso et al. 2018; Kostepen et al. 2020; Eltamaly et al. 2021). IoT also used to automate the periodic and normal duties without human intervention and manual errors, resulting in a more comfortable, safe, and protected human lifestyle. For instance, remote monitoring and managing of equipment and devices, save huge amounts of energy and decrease accidents and health problems (Salih Ahmed et al. 2021). Even though it is still in its early phases, the Internet of Things has infiltrated every aspect of our lives, including education, health, corporate and institutional sector, cities, as well as homes (Salih Abdalla et al. 2020).

Using campus facilities without control and in a bad way, will reflect in human health negatively. Most campus infrastructure still relay on traditional method (Mokhtar and Saeed 2011). Consequently, there's a lot of problems especially under the recent circumstances, so contagious diseases that spreads by touch or due to closed environments and inadequate air quality in the indoor environment impacts terribly to health problems (Saeed et al. 2014; Abbas Alnazir et al. 2021; Dafalla et al. 2021; Musa et al. 2021). Today with the advancements in technology and based on concern for human health, it become serious need to shift from traditional working and living environments into smart environment that is controlled.

Motivated by the huge success of the IoT technology in many areas (Saeed et al. 2021a), this paper introduces model for developing smart campus. The project's goal is to provide an IoT solution for today's challenges and issues. For instance, a smart and healthy (Ahmed et al. 2020) facility,

such as classrooms and laboratories, are designed. IoT solution will be implemented for the case where only authorized students can use such place (Saeed et al. 2015). The solution will incorporate an intelligent room system that will automatically control and monitor the carbon dioxide level in the room, as well as open and close the door.

This intelligent separation system will solve a variety of issues, such as contagious diseases that spreads by touch or due to closed environment. In addition, the quantity of energy utilized in class is precisely controlled (Mokhtar et al. 2015, 2021; Saeed 2011). The study focusses on the present concept of smart building automation system based on Arduino (Table 1).

Several studies utilized IoT for overcoming various issues. The study titled "Smart Home System Using Internet of Things" discusses the implementation of Internet of Things (IoT) technology inside houses to ensure the comfort of the residents, as well as their safety in terms of security, and control of the electronic devices (Saeed and Mokhtar 2012). A Framework for sustainable and data-driven suggested framework that can be applied in universities and/or smart campus (Baykas et al. 2012). The system relays in bigdata technology and sketch a road map toward conversion into smart campus. A hybrid system for renewable energy based on IoT in smart campus was introduced in Ahmed et al. 2015, where an IoT-based architecture is proposed to manage a university campus's small-scale fusion renewable energy model.

2 Smart Entrance and Adequately Ventilated Indoor Space

Primary advice by the world health organization concerning the recent issue of the Coronavirus, is to make the environment safer for the public. The WHO advised in the importance avoiding the 3Cs: that are close, crowded, or with close contact spaces. Today's looking for safe way to return, the WHO recommends incorporating natural ventilation for close spaces (Saeed and Mokhtar 2012; Mokhtar et al. 2013; Saeed et al. 2012). The design of the smart healthcare classroom environment has two main aspects that are safe and secure entrance system and adequately naturally ventilated indoor space (Saeed et al. 2021b). The system design includes zero-touch entrance system and environment monitoring. The zero-touch entrance system is designed based on RFID technology (Mokhtar et al. 2010), and environment monitoring system employs monitoring of the carbon dioxide level (Saeed et al. 2019a). Conceptual model of the system is illustrated below in Fig. 1.

The system model is built with busing gas sensor, and RFID reader devices in addition to servo motor associated with the door and the window units. Two RFID cards are configured for valid and invalid situation.

Partial sector of the campus network is defined for the system, consists of IoT server switch and wireless router. The devices are configured as IoT things and configured to connect to the registration server. Figure 2 illustrates the

Table 1 Comparison of related works

System	Controller/technology	Applications	Merits
Using the IoT for developing smart home system (Santoso et al. 2018)	Arduino IDE	Provide a secure environment which is comfortable and convenient for residents	Energy efficient Flexibility
A framework for sustainable and data-driven smart campus (Kostepen et al. 2020)	Big data	Provide a context for the transformation of a university into smart campus	Time efficient Effort efficient Energy efficient
A fusion renewable energy model for smart campus based on IoT (Eltamaly et al. 2021)	OPNET modeler	Model an architecture that allows the incorporation of HRES in power distribution system	Energy efficient
Smart medical system using NB-IoT technology (Salih Ahmed et al. 2021)	Android mobile	Facilitates the registration of the patients and enables medical staff to complete their work easily	Time efficient Effort efficient
Using BLE and Wi-Fi network for obtaining high-resolution occupancy data (Salih Abdalla et al. 2020)	Interior locating system	Provides appropriate occupancy data version than the traditional positioning systems for operation of the facility	Low cost Energy efficient

Fig. 1 System model
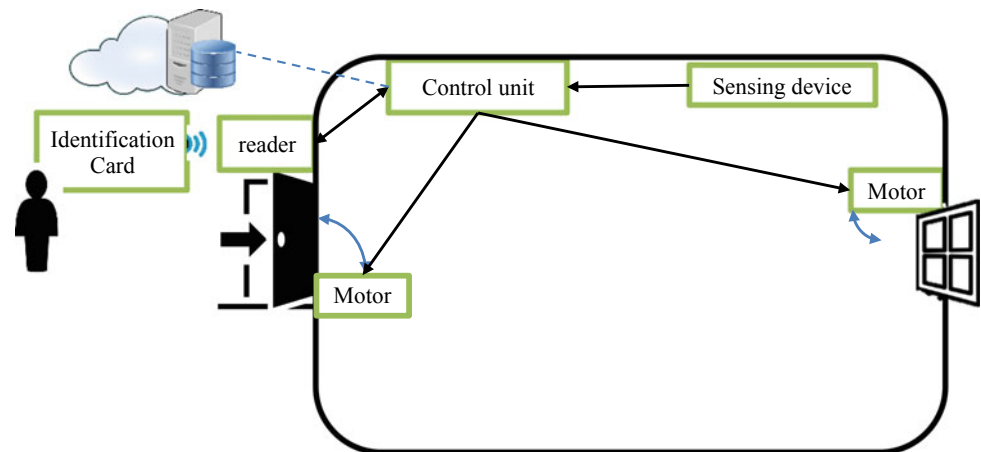
Fig. 2 The block diagram of the system
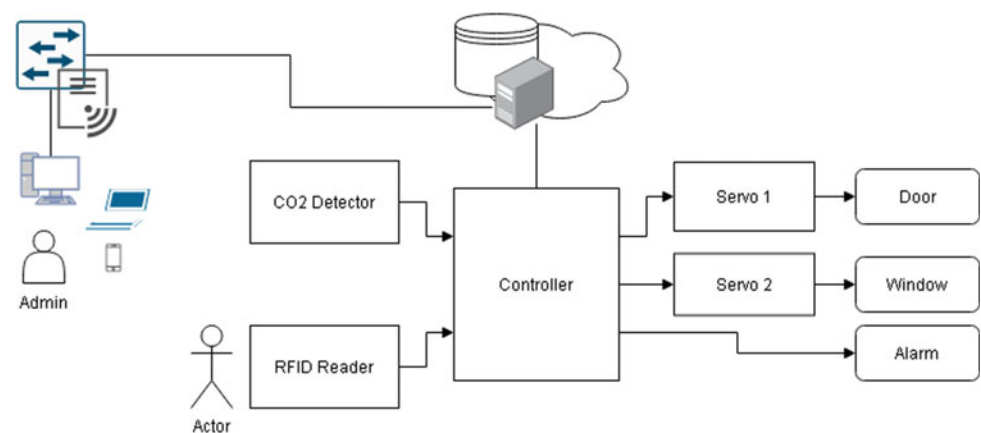
block diagram of the system. The function of the RFID reader is controlling the room access using based on the validity of the user card. The room's door will open/close using a servo motor, the user does not need to touch the door to either open or close it. The RFID reader (Saeed et al. 2021ab) relays in the users' cards configuration at the server, this configuration can be adjusted by the system administrator, from the server itself or any authorized end user device that connected to the network (Saeed et al. 2019b).

To ensure healthy air quality, the sensor is used to test gas in the air and control windows accordingly, the system open the window to refresh the room air.

The CISCO packet tracer simulation is adopted with real-time environment emulator, that provide several environment factors such as time, gases, and sunlight. The system is designed and simulated as shown in Fig. 3. Where the figure Illustrate the system in the logical view mode of the simulation. Figure 4 shows the IoT server configuration.

The simulation devices include RFID reader, RFID cards, gas sensor, door and window units, two servo motors, alarm, LCD, and gas producers. The network section includes a server, switch, wireless router, and two end-user devices: PC and smart phone.

The RFID reader and the sensor are connected to analog ports of the controller, an interrupt is attached to each pin, and an interrupt service routine (ISR) is written for each part to perform the associated controlling functionality based in device reading. The sensor is triggered by air in the environment, particularly CO_2 detector is used to demonstrate this function. The RFID reader remains in waiting status until a card is presented to the reader by a user, then based on the validity of the card the controller together with the IoT server decide the right action for the door. Figure 5 illustrates the flowchart of the system, including setup and main function, and the ISR for air sensor and RFID reader.

3 Results

3.1 Entrance System

Figure 6 illustrates the result for using RFID reader for room access. The reader reads the card and sends the data to the IoT server if the card is identified as valid, the MOU trigger the associated servo motor to rotate 90° to open the door.
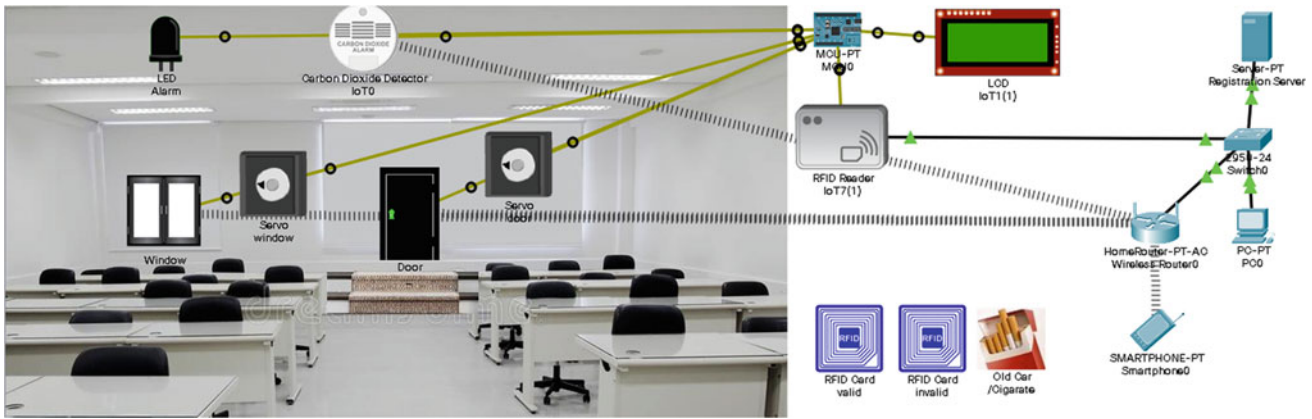
Fig. 3 System design and simulation

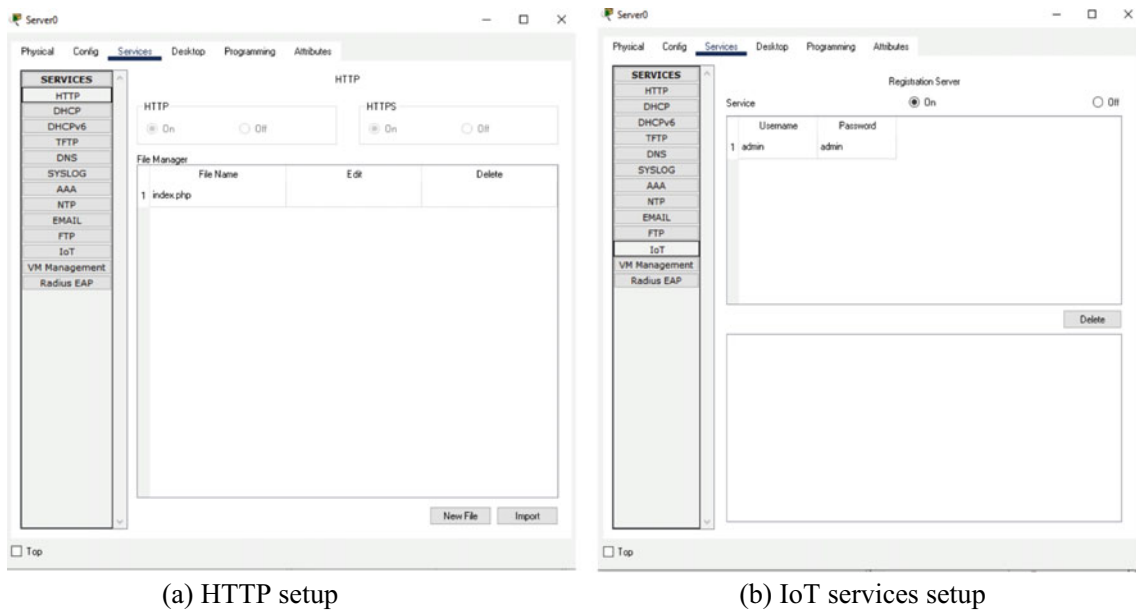(a) HTTP setup   (b) IoT services setup

Fig. 4 IoT server configuration

Otherwise, if the card is not registered in the system and identified as invalid the door will remain close.

The key objective of the entrance system is that the user will not need to touch the door. Modern authentication methods move toward reducing user interaction and relay in biometric feature and/or token method; other objective is the security of facility, and light interaction is needed by the user for the system to perform user authentication.

3.2 Air Quality Monitoring

If the air quality of the room is reduced due to any factor, for example, cigarette smoke, the controller is reading the detector value and will trigger the window associated servo

motor to rotate 90° to open the window until the air quality is reset then it will close it back. The choice of widow opening rather than other method was selected due to recent health advice for COVID-19. Figure 7 illustrates the air quality monitoring, when the level of the carbon dioxide (CO_2) increased due to cigarette smoke, the value is presented in the LCD. When the value exceeds the threshold, the system set ON a LED alarm, and opens the window until the air is refreshed. Figure 8 Illustrates the CO_2 level.

3.3 Remote Monitoring

The administrator can remotely monitor and control all the devices that are connected to the IoT server. Figure 9

Fig. 5 Flowchart
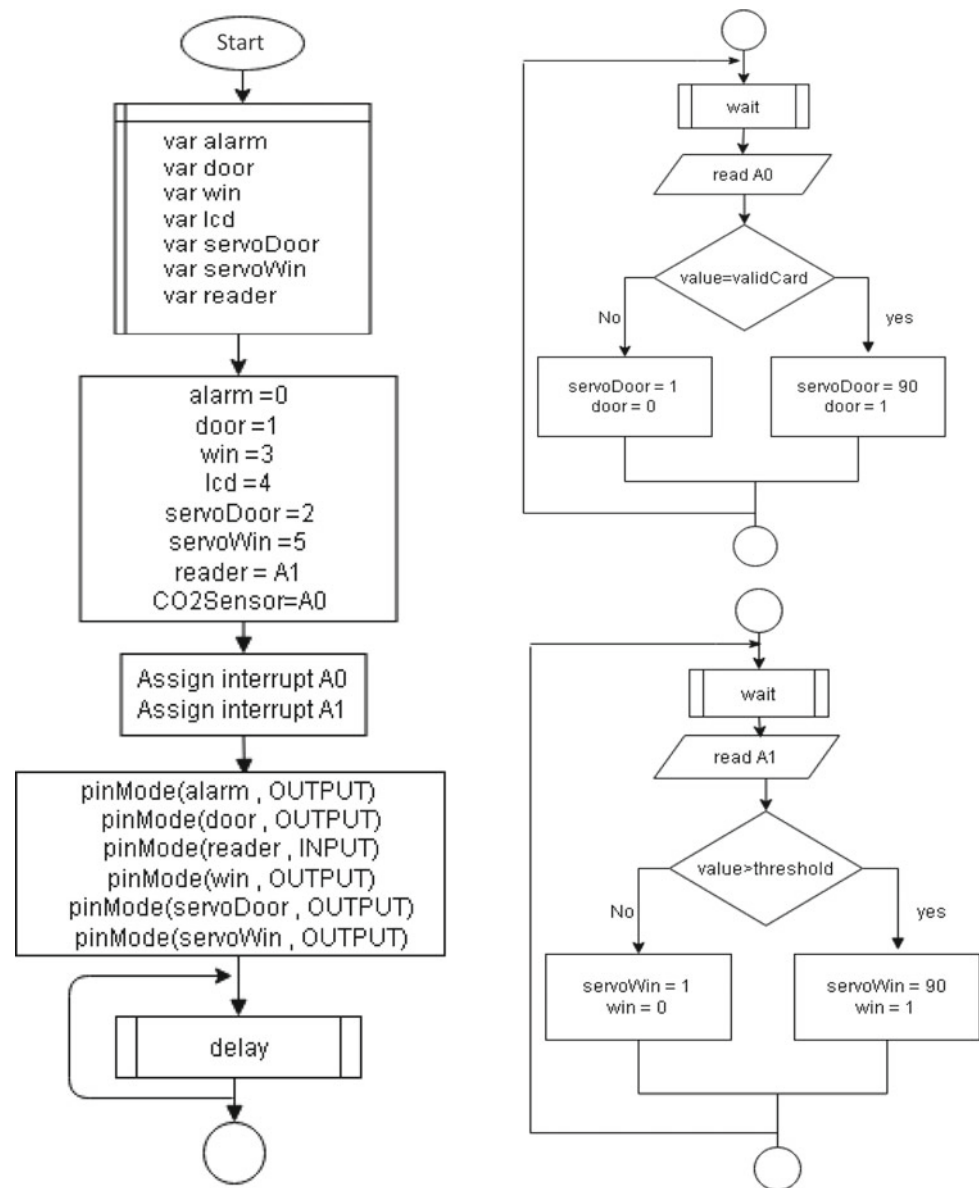
Illustrate the situation where the air quality is low and the system opens the widow as appeared for the administrator. The statues of the devices are accessible through HTTP protocol in server.

4   Discussion

Close area facilities such as classroom laboratories and offices are essential parts of every campus. The environment of such facility should be life friendly and support human safety and health. Recent pandemic of COVID-19 rise attention to many issues such as touch the elevator bottoms or the public doors which are daily life behavior. It also rises attention of important of opening the window for fresh air.

The proposed system tries to overcome these issues by introducing a Zero-Touch Entrance System and Air Quality Monitoring in Smart Campus Design Based on Internet of Things (IoT) (Mokhtar and Saeed 2011). This scheme provides methods for enabling safe and sustainable campus environment. The methodology of the proposed system aims to implement light level of control that has huge impact with respect to human health. The system is useful campus, smart home, and smart building automation.
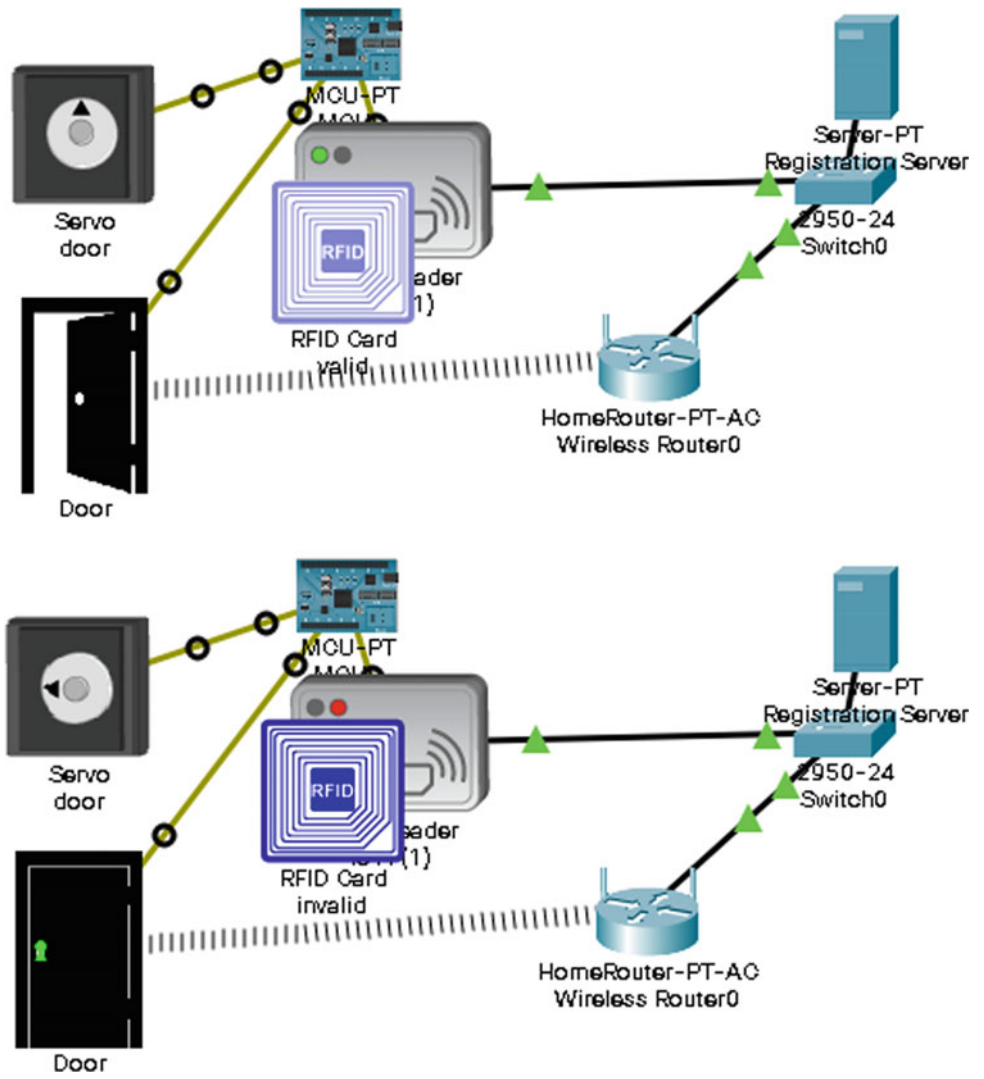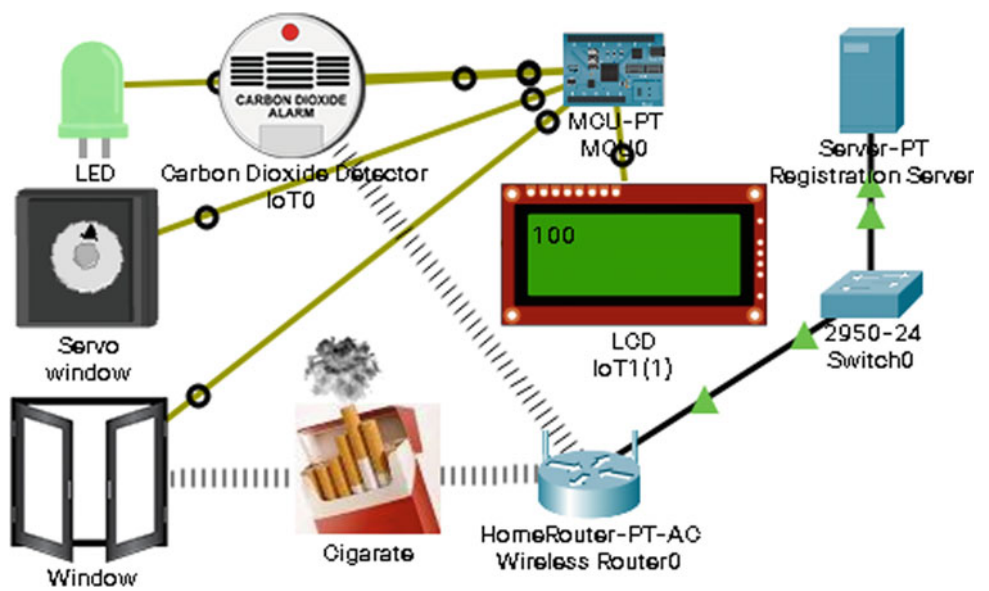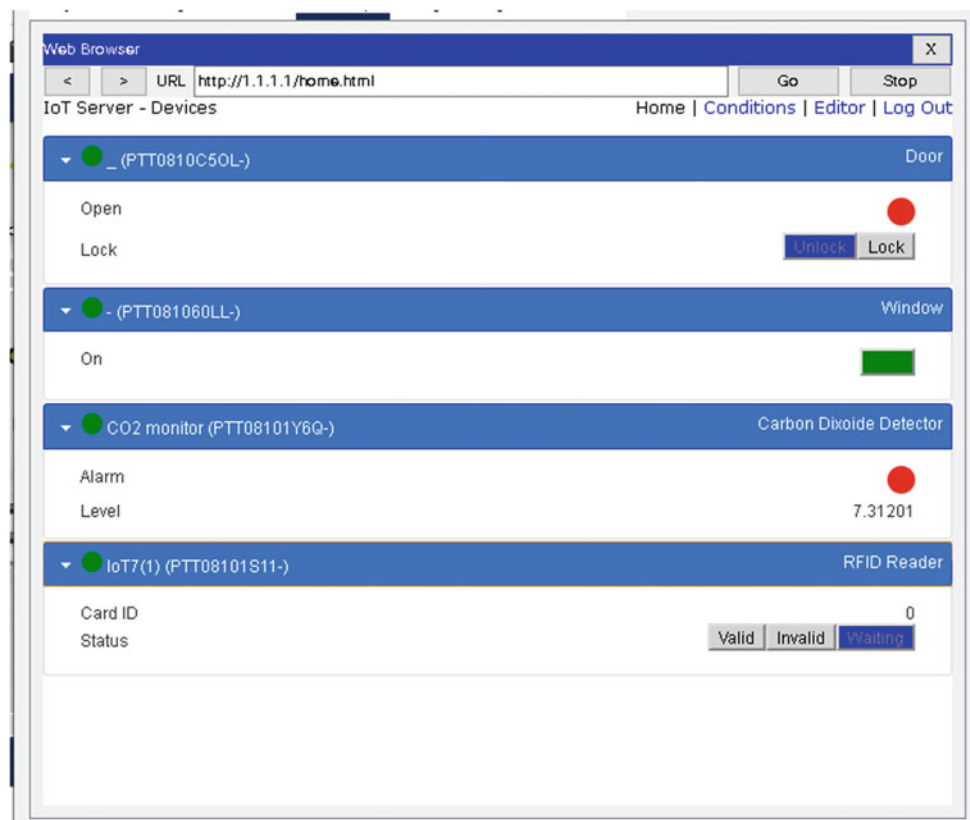
Fig. 6 RFID-controlled door

Fig. 7 Air quality-controlled window

Fig. 8 CO_2 in the environment

Fig. 9 Remote monitoring

5 Conclusions

In this paper, two strategies for helping ensure human health are introduced. The first strategy relay in avoiding touch public door, where an RFID system is implemented to allow access with cards and the movement of the door is done with automated servo motor. The second strategy focuses on air quality of the close facility and automate window system to ensure fresh air for the occupants. The system is designed as local control system as well as IoT-based control and mentoring system. The system supports human health based on recent WHO health advice.

References

R.A. Abbas Alnazir, H.A. Mokhtar, E.S. Ali, R.A. Saeed, S. Abdel-khalek, Quality of services based on intelligent IoT WLAN MAC protocol dynamic real-time applications in smart cities, in *Computational Intelligence and Neuroscience*, vol. 2021, Article ID 2287531, p. 20 (2021)

K.E.B. Ahmed, R.A. Mokhtar, R.A. Saeed, in *A New Method for Fast Image Histogram Calculation*, International Conference on Computing, Control, Networking, Electronics and Embedded Systems Engineering (ICCNEEE), Khartoum, Sudan, (2015), pp. 187–192

Z.E. Ahmed, H. Kamrul, R.A. Saeed, S. Khan, S. Islam, M. Akharuzzaman, R.A. Mokhtar, Optimizing energy consumption for cloud internet of things. Front. Phys. **8** (2020). https://doi.org/10.3389/fphy.2020.00358

T. Baykas, M. Kasslin, M. Cummings, H. Kang, J. Kwak, R. Paine, A. Reznik, R. Saeed, S.J. Shellhammer, Developing a standard for TV white space coexistence: technical challenges and solution approaches. IEEE Wirel. Commun. Mag. **19**(2), 10–22 (2012)

Y. Cheng, X. Zhao, J. Wu, H. Liu, Y. Zhao, M. Al Shurafa, I. Lee, Research on the smart medical system based on NB-IoT technology. Mob. Inf. Syst. (2021)

M.E.M. Dafalla, R.A. Mokhtar, R.A. Saeed, A. Hesham, S. Abdel-Khalek, M. Khayyat, An optimized link state routing protocol for real-time application over vehicular ad-hoc network. Alexandria Eng. J. (2021)

A.M. Eltamaly, M.A. Alotaibi, A.I. Alolah, M.A. Ahmed, IoT-Based hybrid renewable energy system for smart campus. Sustainability. **13**(15), 8555 (2021)

M.B. Hassan, E.S. Ali, R.A. Mokhtar, R.A. Saeed, B.S. Chaudhari, NB-IoT: concepts, applications, and deployment challenges, in *LPWAN Technologies for IoT and M2MApplications*, eds. by B.S. Chaudhari, M. Zennaro (Elsevier, 2020), ISBN: 9780128188804

M.B. Hassan, A. Sameer, A. Hesham, E.S. Ali, R.A. Mokhtar, R.A. Saeed, An enhanced cooperative communication scheme for physical uplink shared channel in NB-IoT. Wirel. Pers. Commun. **116**(2) (2021)

Z. Kostepen, E. Akkol, O. Dogan, S. Bitim, A. Hiziroglu, *A Framework for Sustainable and Data-driven Smart Campus* (2020)

R. Mokhtar, B.M. Ali, N.K. Noordin, R. Saeed, Y. Abdalla, Distributed cooperative spectrum sensing in cognitive radio networks with adaptive detection threshold. Proc. Asia-Pacific Adv. Netw. **30**, 90–99 (2010)

R. Mokhtar, R.A. Saeed, Conservation of mobile data and usability constraints, in *Cyber Security Standards, Practices and Industrial Applications: Systems and Methodologies, Ch 03*, eds. by Z. Junaid, M. Athar (IGI Global, USA, 2011), pp. 40–55, ISBN13: 978-1-60960-851-4

R. Mokhtar, R.A. Saeed, R. Alsaqour, Y. Abdallah, Study on energy detection-based cooperative sensing in cognitive radio networks. J. Netw. (JNW) **8**(6), 1255–1261 (2013), ISSN 1796–2056. https://doi.org/10.4304/jnw.8.6.1255-1261

R.A. Mokhtar, A.F. Ismail, M.K. Hasan, W. Hashim, H. Abbas, R.A. Saeed, S. Islam, Lightweight handover control function (L-HCF) for mobile internet protocol version six (IPv6). Indian J. Sci. Technol. **8**(12) (2015). https://doi.org/10.17485/ijst/2015/v8i12/70656

R.A. Mokhtar, R.A. Saeed et al, Cluster mechanism for sensing data report using robust collaborative distributed spectrum sensing. Cluster Comput. (2021)

A.M. Musa, R.A. Mokhtar, R.A. Saeed, H.A. lhumyani, S. Abdel-Khalek, A.O.Y. Mohamed, Distributed SC-FDMA sub-carrier assignment for digital mobile satellite. Alexandria Eng. J. **60**(6), 4973–4980 (2021)

N. Nurelmadina, M.K. Hasan, I. Mamon, R.A. Saeed, K. Akram, Z. Ariffin, E. Sayed Ali, R.A. Mokhtar, S. Islam, E. Hossain, Md. A. Hassan, A systematic review on cognitive radio in low power wide area network for industrial IoT applications. MDPI, Sustainability (2021)

R.A. Saeed, *TV White Space Spectrum Technologies: Regulations, Standards, and Applications* (CRC Press, USA, 2011), ISBN: 9781439848791

R.A. Saeed, R.A. Mokhtar, in *TV White Spaces Spectrum Sensing: Recent Developments, Opportunities and Challenges*, The 6th International Conference SETIT 2012: Sciences of Electronic, Technologies of Information and Telecommunications (SETIT2012), Tunisia (2012), pp. 634–638

R.A. Saeed, R.A. Mokhtar, J. Chebil, A.H. Abdallah, in *TVBDs Coexistence by Leverage Sensing and Geo-location Database*, IEEE International Conference on Computer & Communication Engineering (ICCCE2012), 3–5 July 2012, Malaysia, pp. 33–39

R.A. Saeed, M. Al-Magboul, R.A. Mokhtar, Machine-to-Machine communication, in *IGI Global, Encyclopedia of Information Science and Technology*, 3rd edn2014)), pp. 6195–6206, https://doi.org/10.4018/978-1-4666-5888-2

R.A. Saeed, A.F. Ismail, M.K. Hasan, R. Mokhtar, K.A. Sajda Salih, W. Hashim, Throughput enhancement for WLAN TV white space in coexistence of IEEE 802.22. Indian J. Sci. Technol. (IJSC), **8**(11) (2015). https://doi.org/10.17485/ijst/2015/v8i11/71783

M.M. Saeed, R.A. Saeed, E. Saeid, Survey of privacy of user identity in 5G:. Saba J. Inf. Technol. Netw. (SJITN) **7**(1) (2019a)

M.M. Saeed, R.A. Saeed, E. Saeid, in *Preserving Privacy of Paging Procedure in 5 th G Using Identity-Division Multiplexing*, 2019 First International Conference of Intelligent Computing and Engineering (ICOICE), IEEE (2019b), pp. 1–6

R.A. Saeed, M.M. Saeed, R.A. Mokhtar, A. Hesham, S. Abdel-Khalek, Pseudonym mutable based privacy for 5G user identity. J. Comput. Syst. Sci. Eng. **29**(1), 1–14 (2021a)

M.M. Saeed, R.A. Saeed, E. Saeid, in *Identity Division Multiplexing Based Location Preserve in 5G*, 2021 International Conference of Technology, Science and Administration (ICTSA), (2021b), pp. 1–6. https://doi.org/10.1109/ICTSA52017.2021.9406554

R. Salih Abdalla,; S.A. Mahbub, R.A. Mokhtar, E.S. Ali, R.A. Saeed, *IoE Design Principles and Architecture; Book: Internet of Energy for Smart Cities: Machine Learning Models and Techniques* (CRC Press Publisher, 2020), https://doi.org/10.4018/978-1-7998-5101-1

R. Salih Ahmed, E.S.A. Ahmed, R.A. Saeed, Machine learning in cyber-physical systems in industry 4.0, in *Artificial Intelligence Paradigms for Smart Cyber-Physical Systems*, ed. by A.K. Luhach, A. Elçi (IGI Global, Hershey, PA, 2021), pp. 20–41

L. Santoso, R. Lim, K. Trisnajaya, A smart home system using Internet of Things. J. Inf. Commun. Convergence Eng. (2018)